DEPARTMENT OF CHEMISTRY, UNIVERSITY OF JYVÄSKYLÄ
RESEARCH REPORT No. 208

MULTIVALENT N-DONOR LIGANDS FOR THE CONSTRUCTION OF COORDINATION POLYMERS AND COORDINATION POLYMER GELS

BY

RAJENDHRAPRASAD TATIKONDA

Academic Dissertation for the Degree of
Doctor of Philosophy

To be presented, by permission of the Faculty of Mathematics and Science of the University of Jyväskylä, for public examination in Auditorium KEM4, on May 18th 2018 at 12 noon.

UNIVERSITY OF JYVÄSKYLÄ

Jyväskylä, Finland
ISBN 978-951-39-7409-1 (print)
ISBN 978-951-39-7410-7 (electronic)
ISSN 0357-346X

Author's address

Rajendhraprasad Tatikonda
Department of Chemistry
P.O. Box 35
FI-40014 University of Jyväskylä
Finland
rp.tatikonda@jyu.fi

Supervisors

Professor Matti Haukka
Department of Chemistry
University of Jyväskylä
Jyväskylä, Finland

Professor Kari Rissanen
Department of Chemistry
Nanoscience Center
University of Jyväskylä

Reviewers

Professor Risto Laitinen
Department of Chemistry
University of Oulu
Oulu, Finland

Docent Pipsa Hirva
Department of Chemistry
University of Eastern Finland
Joensuu, Finland

Opponents

Professor Muriel Hissler
Institute of Chemical Sciences
Université Rennes
Rennes, France

ABSTRACT

Tatikonda, Rajendhraprasad

Multivalent N-donor ligands for the construction of coordination polymers and coordination polymer gels.

Jyväskylä: University of Jyväskylä, 2018, 62 p.
Department of Chemistry, University of Jyväskylä, Research Report No. 208
ISSN 0357-346X
ISBN 978-951-39-7409-1

This work describes the synthesis and characterisation of several multivalent N-donor ligands and their coordination compounds and the use of these ligands in the construction of coordination polymers and coordination polymer gels. The project can be divided into two parts. The first part of the research is focused on the coordination chemistry of ring-substituted biimidazoles in acidic media. The dependence of the formation of ion pairs and zwitterionic, especially zinc and copper containing coordination compounds on the pH of the reaction medium and ring-substituents of the ligand were examined. The second part of the study deals with the preparation of Ag, Zn and Cu coordination polymers (CPs) and coordination polymer gels (CPGs) from geometrically flexible biimidazole- and bipyridine-based ligands. The effect of metal centres and reaction conditions on structural topologies of CPs was studied and presented in publication II. Since the CPGs were obtained by silver coordination, a new photochemical process was developed to form silver nanoparticles (AgNP) on the surface of the coordination polymeric fibers. The method was disclosed in publications III and IV.

In order to explain and combine these different studies into one thesis, the following procedure was followed: first, an introduction to the N-donor ligands, especially biimidazole and bipyridines and their coordination chemistry in acidic and basic media was presented. The later part was focused on general synthetic routes for CPs and possibilities to control their structure with literature examples. The chapter then gives an introduction to the gels, and supramolecular metallogels with examples of recent publications and gel characterisation methods. The introduction ends with the aim of the study.

The second part of the thesis outlines the most significant findings reported in the four original publications. The discussion part begins with a short chapter on the synthesis of a series of N-donor ligands, followed by their coordination chemistry in an acidic medium. The follow-up chapter deals with the construction of CPs and CPGs with semirigid ligands. The final chapter of the discussion ends with the luminescence properties of these CPs and CPGs. At the end of the thesis, these results are briefly summarised with significant findings.

Keywords: semirigid N-donors, ionic, zwitterionic, coordination polymers, coordination polymer gels, *in situ*, self-assembly, X-ray crystallography

TIIVISTELMÄ

Tatikonda, Rajendhraprasad

Monivalenssiset N-donori-ligandit koordinointipolymeerien ja koordinaatio-polymeerigeelien valmistamisessa

Jyväskylä: Jyväskylän yliopisto, 2018, 62 s.
Kemian laitos, Jyväskylän yliopiston tutkimusraporttisarja Nro. 208
ISSN 0357-346X
ISBN 978-951-39-7409-1

Tässä työssä tarkastellaan monihampaisten N-donori-ligandien ja niiden muodostamien koordinaatioyhdisteiden synteesiä ja karakterisointia sekä näiden ligandien käyttöä koordinaatiopolymeerien ja metallogeelien valmistuksessa. Tutkimus jakautuu kahteen pääosaan. Ensimmäisessä osassa keskitytään rengasubstituoitujen bi-imidatsoliyhdisteiden koordinointikemiaan happamissa olosuhteissa. Työssä tutkittiin ioniparien ja kahtaisionisten, erityisesti sinkkiä ja kuparia sisältävien, koordinaatioyhdisteiden muodostumisen riippuvuutta pH:sta ja bi-imidatsoli ligandin renkaan substituentteista. Tutkimuksen toisessa osassa käsitellään Ag, Zn ja Cu koordinointipolymeerien ja koordinointipolymeerigeelien valmistamista käyttäen ligandeina geometrisesti mukautuvien bi-imidatsoli- ja bipyridiinipohjaisia yhdisteitä. Tarkastelun kohteena ovat olleet erityisesti metallikeskusten ja reaktio-olosuhteiden vaikutus koordinaatiopolymeerien rakenteiden topologiaan, jotka on esitelty yksityiskohtaisesti julkaisussa II. Koordinaatiopolymeerigeelien osalta tutkimus keskittyi erityisesti hopeaa sisältävien koordinaatiopolymeerigeelien tarkasteluun. Työn tuloksena kehitettiin uusi valokemiaan perustuva menetelmä hopeananopartikkelien muodostamiseksi koordinaatiopolymeerikuitujen pinnalle. Menetelmä esiteltiin julkaisuissa II ja IV.

Väitöskirjassa N-donoriligandeja, erityisesti bi-imidatsoleja ja bipyridiinejä sekä niiden koordinaatiokemiaa happamissa ja emäksisissä olosuhteissa on esitelty kirjan ensimmäisessä osassa. Merkittävimpänä tekijänä muodostuvien yhdisteiden kannalta esiin nousee happamuudesta riippuva typpiligandin protonaatioaste. Väitöskirjan toisessa osassa keskitytään erityisesti koordinaatiopolymeerien ja niistä koostuvien metallogeelien kemiaan. Tarkastelu painottuu metalli-ionien, vastaionien ja liuottimien roolin selvittämiseen geeliytymisprosessissa.

Väitöskirjan toisessa osassa tehdään yhteenveto neljän alkuperäisjulkaisun keskeisimmistä tutkimusmenetelmistä ja havainnoista. Työn kannalta olennaisimpien ligandien, koordinaatiopolymeerien ja koordinaatio-polymeerigeelien syntetiikka esitellään tässä osiossa. Toisessa osassa

tarkastellaan myös yhdisteiden valokemiallisia ominaisuuksia. Keskeisimpänä kohteena ovat hopeananopartikkelit ja niiden tuottamat luminesoivat geelit. Väitöskirjan yhteenveto-osassa kootaan yhteen keskeisimmät havainnot ja tulokset.

Avainsanat: N-donori ligandit, kahtaisionit, koordinaatiopolymeerit, koordinaatioplymeerigeelit, *in situ*, röntgenkristallografia

PREFACE

This work was carried out at the Department of Chemistry, the University of Jyväskylä during the period of 2013-2018. Research funding was provided by the Department of Chemistry of University of Jyväskylä and Academy of Finland.

First and foremost, my heartfelt thanks and most profound gratitude go to Prof. Matti Haukka for giving me a chance to work under his supervision during my master's studies at the University of Eastern Finland and as a PhD student at the University of Jyväskylä. I also wish to thank my co-supervisor, Prof. Kari Rissanen for his assistance. I am very grateful for the freedom and trust I have received from both during many long years.

Professor Risto Laitinen and Docent Pipsa Hirva are warmly acknowledged for their valuable comments on this thesis. I also thank Matti Nurmia for the language version.

I am also grateful to all members of the Haukka and Rissanen research groups, both past and present. In particular, I would like to thank Elina Laurila, Matti Tuikka, Kalle Kolari, Alexander Chernyshev, Evgeny Bulatov, Margarita Bulatova, Lauri Kivijarvi, and Elmeri Lahtinen for interesting discussions and help. Special thanks also go to Nonappa for his guidance with the scientific writing and microscopy studies.

I want to express my love to my family, especially to my wife Laasya and my daughter Moksha. They deserve a particular note of thanks for their support, care and encouragement for the success of this thesis. I cannot thank enough my parents for all their support and love. I would never have made it here without you.

Jyväskylä, April 2018
Rajendhraprasad Tatikonda

LIST OF ORIGINAL PUBLICATIONS

I. R. Tatikonda, E. Kalenius, and M. Haukka, Synthesis and characterization of Zwitterionic Zn(II) and Cu(II) coordination compounds with ring-substituted 2,2′-biimidazole derivatives, *Inorg. Chim. Acta.* **2016**, 453, 298−304.

II. R. Tatikonda, E. Bulatov, E. Kalenius, and M. Haukka, Construction of coordination polymers from semi-rigid ditopic 2,2′-biimidazole derivatives: synthesis, crystal structures, and characterization, *Cryst. Growth Des.* **2017**, 17, 5918−5926.

III. R. Tatikonda, K. Bertula, Nonappa, S. Hietala, K. Rissanen, and M. Haukka, Bipyridine based metallogels: an unprecedented difference in photochemical and chemical reduction in the *in situ* nanoparticle formation, *Dalton Trans.* **2017**, 46, 2793−2802.

IV. R. Tatikonda, E. Bulatov, Nonappa, and M. Haukka, Self-assembly induced photoluminescence and *in-situ* ultrasmall nanoparticle formation in coordination polymer based metallogels. *Manuscript*

Author's contribution

The author has carried out complete synthetic work and the self-assembly studies in publications **I-IV**. Characterisation of all the compounds, apart from photoluminescence, electron microscopy (SEM and TEM) and rheological measurements has been conducted by the author. The author has written the first manuscript draft of all the publications **I-IV**.

Other related publications, not included in this thesis

V. R. Tatikonda, S. Bhowmik, K. Rissanen, M. Haukka, and M. Cametti, Metallogel formation in aqueous DMSO by perfluorinated decorated terpyridine ligands, *Dalton Trans.* **2016**, 45, 12756−12762.

VI. R. Tatikonda, and M. Haukka, Ruthenium(II) carbonyl compounds with 4´-chloro-2,2´:6´,2´´-terpyridine ligand, *Acta Cryst.* **2017**, E73, 556−559.

VII. E. Laurila, R. Tatikonda, L. Oresmaa, P. Hirva, and M. Haukka, Metallophilic interactions in stacked dinuclear rhodium 2,2´-biimidazole carbonyl complexes, *CrystEngComm.* **2012**, 14, 8401−8408.

VIII. E. Lahtinen, L. Kivijarvi, R. Tatikonda, A. Väisänen, K. Rissanen, and M. Haukka, Selective Recovery of Gold from Electronic Waste Using 3D-Printed Scavengers, *ACS Omega.* ***2017***, 2, 7299−7304.

IX. R. G. eixeira, A. R. Bras, L. Corte-Real, R. Tatikonda, A. Sanches, M. P. Robalo, F. Avecilla, T. Moreira, M. H. Garcia, M. Haukka, A. Preto, A. Valente, Novel ruthenium methylcyclopentadienyl complex bearing a bipyridine perfluorinated ligand shows strong activity towards colorectal cancer cells, *Eur. J. Med. Chem.* **2017**, 143, 503−514.

CONTENTS

ABBREVIATIONS

1D	one-dimensional
2D	two-dimensional
3D	three-dimensional
2,2'-H_2Biim	2,2'-biimidazole
4,4'.H_2Biim	4,4'-biimidazole
2,2'-R_2Biim	1,1'-di(alkyl/aryl)-2,2´-Biimidazole
2,2'-Bipy	2,2'-bipyridine
3,3'-Bipy	2,2'-bipyridine
4,4'-Bipy	4,4'-bipyridine
AgNPs	silver nanoparticles
AFM	atomic force microscope
CPs	coordination polymers
CPGs	coordination polymer gels
DMSO	dimethyl sulfoxide
DMF	*N,N'*-dimethylformamide
FTIR	Fourier transform infrared spectroscopy
LMWG	low molecular weight gelator
MGC	minimum gelation concentration
MOFs	metal-organic frameworks
NMR	nuclear magnetic resonance
NEPs	negative electrostatic potentials
SEM	scanning electron microscope
TEM	transmission electron microscope
T_{gel}	gel-sol phase transition temperature
UV-Vis	ultraviolet-visible spectroscopy
XRPD	X-ray powder diffraction
XRD	X-ray diffraction

1 INTRODUCTION

1.1 Coordination compounds

1.1.1 *N*-donor ligands

N-donor ligands are among the most widely used donors in coordination chemistry together with P, S, and O donors. The nitrogen atoms of the donor molecules possess a lone pair of electrons (Lewis base) which can form complexes with metal atoms (Lewis acid). These *N*-donor ligands occur in different forms: aliphatic, aromatic, and heterocyclic. Simple *N*-donors based on amine, amide, imide, and imine structures have been extensively developed over several decades to control the stability and reactivity of the resulting metal complexes.[1-5] This thesis examines *N*-containing heterocyclic compounds which can act as polydentate ligands in metal complexation. Imidazole, pyridine, and their derivatives are most widely used ligands in coordination chemistry of *N*-containing heterocyclic compounds.[6-8]

Biimidazole (H_2Biim) and Bipyridines (Bipy) are biaryl molecules composed of two imidazole or pyridine rings that exist in different forms (2,2′-Bipy, 3,3′-Bipy, 4,4′-Bipy, 2,2′-H_2Biim and 4,4′-H_2Biim) depending on their connectivity.[9-12] In coordination chemistry they mostly act as spectator ligands, which normally do not interfere with the reaction scenarios occurring at the metal centres. The bidentate chelate nature of 2,2′-H_2Biim and 2,2′-Bipy provides greater complex stability by forming a 5-membered chelate ring.[13] Bipy is considered as a parent compound of a series of classical chelating polydentate *N*-donor ligands. 2,2′-Bipy has proven to be one of the most versatile ligand in coordination chemistry owing its ability to coordinate to most metals in the periodic table. 4,4′-Bipy is an example of a prototypical ligand and an attractive building block for creating various architectures of metal−organic networks with different dimensionalities. 4,4′-Bipy acts not only as a linear spacer between metal ions but it can also function as a H-bond acceptor.[14-17]

Due to greater *N*,*N*′-distance in 2,2′-H_2Biim than in 2,2′-Bipy, the bite angle (*N*−M−*N*′) of 2,2′-H_2Biim complexes is substantially diminished from that of 2,2′-Bipy complexes (Fig. 1).[18,19] 2,2′-H_2Biim forms complexes with large M−N bond lengths compared with 2,2′-Bipy. Due to such architecture 2,2′-H_2Biim is able to form complexes even with large metal atoms and the formation constants for 2,2′-H_2Biim are higher than those for 2,2′-Bipy.

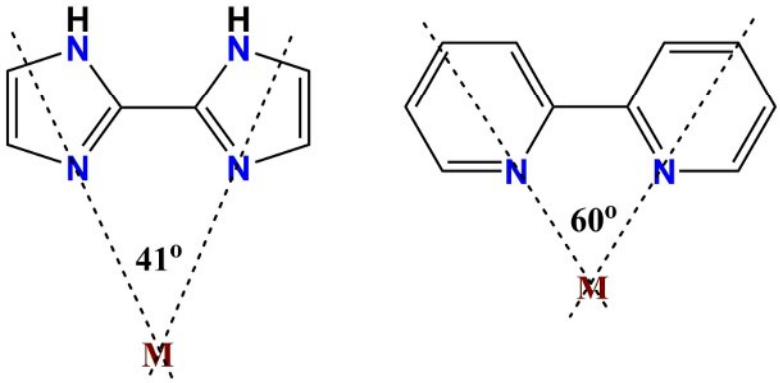

FIGURE 1 The difference in bite angles for 2,2′-H_2Biim and 2,2′-Bipy.[18]

The ring substituents on H_2Biim and Bipy have a strong impact on physical and chemical properties of these molecules. The strength of the coordination bond is affected by the nature of ring-substituents.[20-23] The direction of the migration of electron density between the ring and the substituents influences the availability of non-bonding pairs of electrons at the nitrogen atom for metal coordination. The electron withdrawing groups lower the electron density on the ring, which weakens the co-ordination bond; electron donating groups cause a migration of electrons towards the ring, which enhances the coordination-bond strength.

1.1.2 Effect of pH on coordination chemistry of H_2Biim and Bipy

In coordination chemistry, 2,2′-H_2Biim bonds to metals in a bidentate manner through the pyridine-like nitrogen atoms in a strictly planar coordination geometry. When hydrogen atoms are replaced with bulkier groups (R_2Biim; R= alkyl or aryl), the ligand loses its coplanarity between imidazole rings and behaves as a bidentate bridging ligand to generate dinuclear,[24,25] oligonuclear or polynuclear[26,27] complexes depending on the metal atom. The denticity of biimidazole ligand can also vary from zero to tetra depending on the level of protonation or deprotonation (Fig. 2).

Deprotonation of H_2Biim generates mono- ($HBiim^-$) and di-anions ($Biim^{2-}$), which act as tri- (**a**)[28] or tetradentate (**b** & **c**)[29-33] ligands in metal coordination. In the case of di-anions, bis-chelating-bridging (**b**)[31-33] or chelating-bridging (**c**)[32,33] between pairs of metal ions is feasible. Generally, anionic forms have been utilised as bridged ligands for the synthesis of homo- or hetero- multinuclear compounds (Fig. 3).[29,33] Heteronuclear compounds derived from $Biim^{-2}$ have been studied as homogenous catalysts. However, only one of the metal centres shows catalytic activity while others predict molecular architecture and support catalytic activity of the metal centre by donating or accepting electron density.[33] Mono- (H_3Biim^+) and di-cationic (H_4Biim^{2+}) forms are observed in acidic media, where H_3Biim^+ acts as monodentate (**d**)[34] ligand and H_4Biim^{2+} does not participate in metal coordination.[35] Except di-anion ($Biim^{2-}$), all other forms act as H-bond donors and have been widely studied as anion sensors.

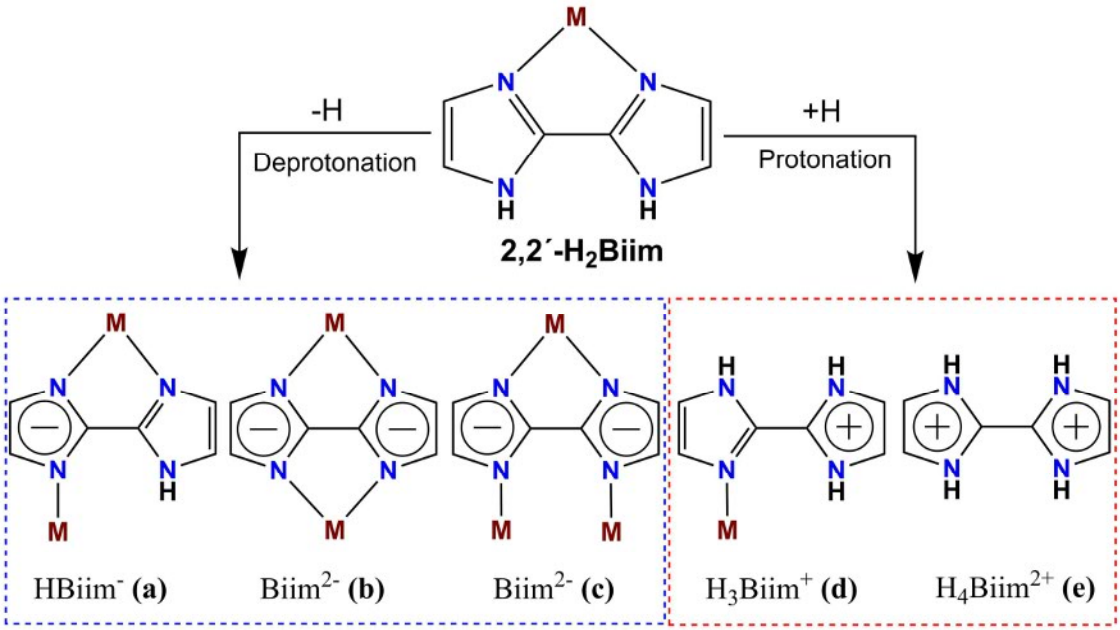

FIGURE 2 Effect of pH on coordination chemistry of 2,2′-H_2Biim.

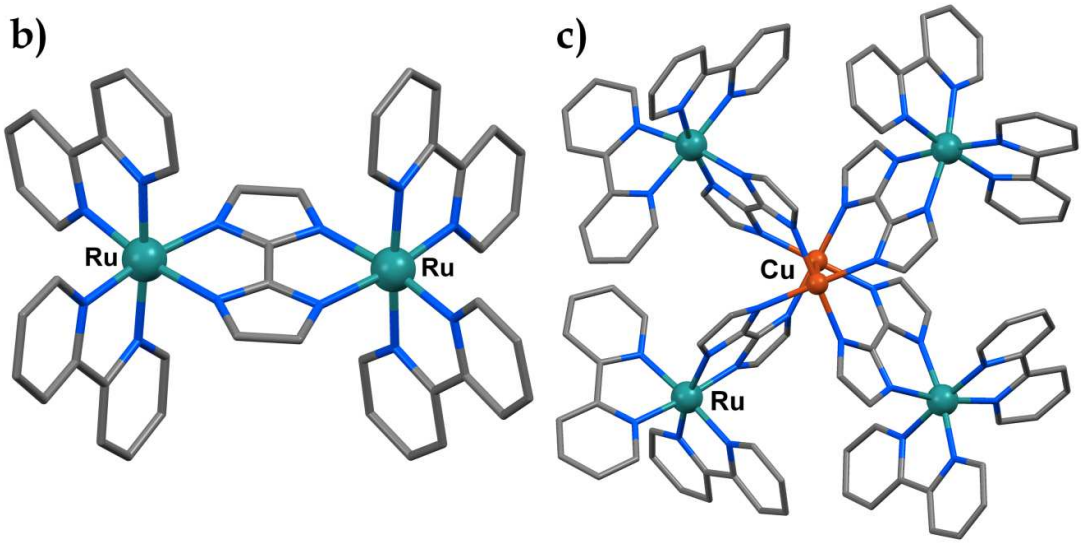

FIGURE 3 Coordination modes of $Biim^{-2}$ as bis-chelating in homodinuclear (**b**) and chelating-bridging in heteromultinuclear (**c**) compounds.[29,33]

In supramolecular chemistry, Bipy is often used as hydrogen/halogen bond acceptor; in acidic conditions bipy nitrogen atoms undergo protonation to generate bipyridinium dications. These dications act as H-bond donors and exist in the form of salts by forming intermolecular H-bonds with anions. They are also found as linkers in many organic-inorganic hybrid materials, especially with metal dianions (MX_n^{2-}; Fig. 4) and with polyoxymetallates (POMs).[36-40]

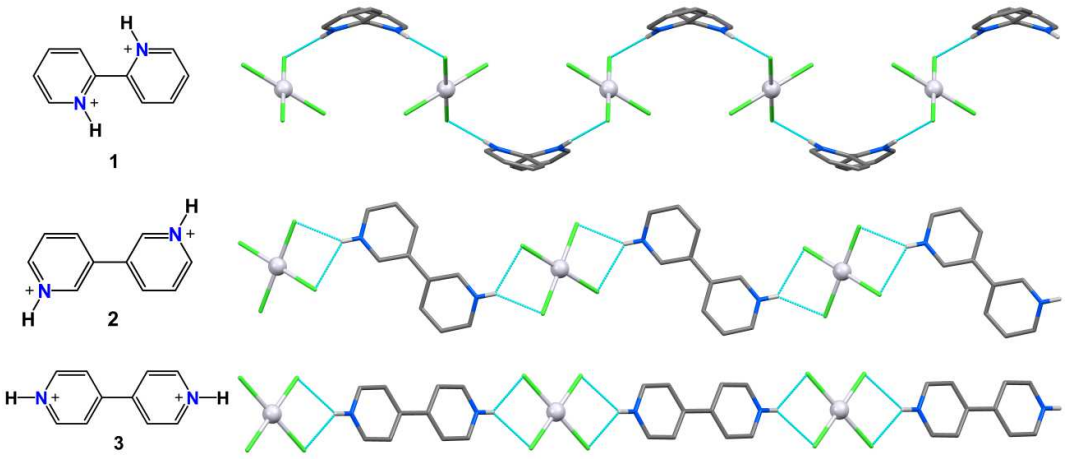

FIGURE 4 Dicationic species of bipy derivatives and their salts with $PtCl_4^{2-}$.[39]

1.1.3 Coordination polymers

1.1.3.1 Background

The term ''Coordination Polymers (CPs)'' was first used by J. C. Bailer in 1964, when he compared organic polymers with coordination compounds that can be considered polymeric species.[41] CPs are defined as infinite systems built from metal ions (nodes) and organic ligands (linkers) as main elementary units linked via coordination bonds.[42] However, coordinate bonds are not the only interactions in these compounds. Weaker non-covalent interactions such as hydrogen bonds, π···π stacking or van der Waals interactions may also influence the formation of CPs. They can provide various frameworks that can develop into one-, two- and three-dimensional networks (Fig. 5).[43-45] The solid-state structure of CPs can only be determined by X-ray crystallographic methods, which confirm that CPs have structural diversity and porosity. The solid products are generally insoluble or degrade upon dissolution; characterizations in solution only prove the existence of oligomeric fragments.

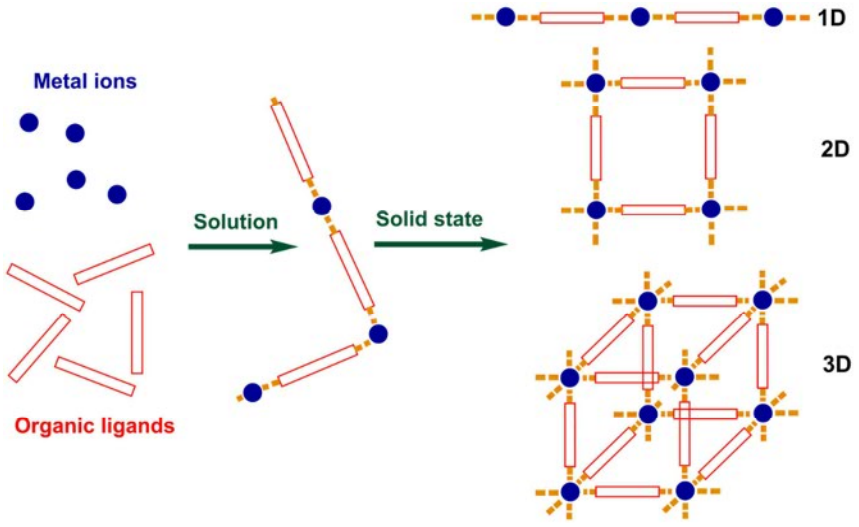

FIGURE 5 Schematic illustration of the formation of CPs from their building blocks.[45]

1.1.3.2 Synthesis of CPs

For the chemist, coordination-polymer network synthesis could be considered as ''construction of games''. Four synthetic strategies are known from the literature for obtaining coordination polymers.[43] Improvement of synthesis is essential for getting good quality crystals for X-ray diffraction measurements.

- *Saturation method:* Self-assembly allows crystal formation when different reagents are mixed together. Molecular recognition allows the construction of products. This technique needs favourable conditions. One of them is crystal growth in saturated solutions by slow evaporation. Furthermore, solubility increases with temperature and crystals can appear during the cooling step.
- *Diffusion method:* This is preferred for single crystals for X-ray diffraction, especially when the products are poorly soluble. The principle of this method is to slowly bring the different species into contact. This can happen via solvent liquid (vapour) diffusion where the first solvent contains the product and the other one is a precipitating solvent. Crystal growth occurs with slow diffusion of precipitating solvent into the first solvent. Another approach is a slow diffusion of reactants. This technique is similar to the above one, the only difference being that the reactants are dissolved into two separate solvents and layered on top of each other.
- *Hydro (Solvo) thermal methods*: These methods are originally used for the synthesis of zeolites and adopted for the formation of CPs. Usually these reactions are performed in an autoclave under autogenous pressure at temperatures usually between 120−260°C. The solubility difference between organic and inorganic components in the same solvent often acts as a barrier for the formation of single crystals. The crystallisation technique is a non-equilibrium synthesis and may lead to metastable products. This can be influenced mainly by the cooling rate at the end of the reaction.
- *Microwave and Ultrasonic methods* are so far less used for the formation of CPs. These methods are also based on the changes of solubility of the involved species to crystallize the products.

CPs have attracted increasing attention since the early 1990s, not only due to their fascinating structures and potential applications in various fields. The use of metal atoms in CPs offers several advantages over purely organic polymers organised by non-covalent interactions. Metal-ligand (coordinative) bonds are stronger than hydrogen bonds and have more directionality than other weak interactions. A final goal is to design properties of the CPs for applications such as drug delivery, conductivity, magnetic, luminescence, non-linear optical or porous materials.[46-48] Chiral CPs are expected to play a crucial role in optical devices; they can also be used to separate enantiomers. The electrical conductivity of CPs is one of the most important research areas in material science; it depends on the interactions between the metal d-orbitals and the π* orbitals of the bridging ligand. CPs with ligand-supported Ag···Ag interactions may exhibit semiconductivity; with unsupported Ag···Ag interactions they show a weak semiconductivity.[49,50] The metal coordination to the organic ligand may affect the emission wavelength of the organic material and

show a high thermal stability. The combination of organic spacers and metal centres in CPs is seen as an efficient method to obtain new types of luminescent materials for applications as LEDs (light-emitting diodes). CPs that show non-centrosymmetric structures could be used as NLO (non-linear optical) materials for frequency conversion and intensity modulation of light. Special interest is directed to coordination polymers with porous structures. Due to adjustable pore size and vast surface area, they could have promising applications in size-selective sorption, molecular recognition, gas storage, and catalysis.[51-53]

The final structure of a CP is influenced by several factors, such as the structure of organic ligand, nature of metal, metal-to-ligand ratio, possible counterions and the reaction solvent used. Organic ligands act as bridges between the metal centres, and for possible infinite expansion ligand molecules must be polydentate. In particular, size (distance between coordination functions) and shape (rigid or non-rigid) of the ligand can dramatically change the final structure of the CP. The structure of the CPs also depends on the size, hardness/softness, and various coordination geometries of the metal atoms. The positive charges on metal ions obtained by ligation of neutral ligands need to be counterbalanced with the presence of counter ions in the structure. They can influence the overall structure by participating in weak interactions or acting as guest molecules in void spaces. Finally, solvent molecules may co-crystallise by filling voids as guest molecules and increasing the number of possible weak interactions in the final solid-state structure. They may play a crucial role in the construction of highly porous materials and act as reversible guest molecules.

The structural diversity along with exciting applications motivated this work on CPs with late transition metals (Ag, Cu, and Zn). These metals are widely used in coordination chemistry because of their low oxidation states and versatile coordination geometries.

1.1.3.3 Silver-based coordination polymers

Due to their soft acceptor feature along with flexible coordination spheres, Ag(I) ions have been widely used in coordination chemistry. This metal can be coordinated by a variety of ligands with heteroatoms such as oxygen, sulphur, phosphorus and nitrogen to generate a number of topologies, which are interesting from the structural point of view in crystal engineering.

Ag(I) ions are known to have coordination geometries from linear to octahedral, which are dependent, not only on the type of ligand and the reaction conditions, but also on the electronic requirements that can directly contribute to the assembly and stability of the resulting supramolecular framework. This is why Ag(I)- based coordination polymers have attracted our attention, not only due to their interesting structural topologies,[54,55] but also their outstanding functional properties such as photoluminescence, porosity, conductivity, magnetism, and supramolecular chirality.[56-58] Silver and its coordination compounds are highly toxic to microorganisms, showing strong biocidal effects on bacteria species, including E. coli.[59-61]

1.1.3.4 Copper-based coordination polymers

Copper forms a rich variety of coordination compounds with +1 and +2 oxidation states, which are often respectively called cuprous and cupric. Cu(I)-based networks are attractive as they readily coordinate with *N*-donor ligands. Many coordination compounds are derived from CuX (X= Cl, Br or I); they are mainly neutral as halide counter anions are generally strongly coordinated to the Cu(I).[62-68] These coordination polymers are found to be quite stable, as there are no counter anions in the coordination polymer network. Furthermore, combinations of CuX with bridging ligands mostly result in the formation of 1D or 2D CP networks through the linking of $(CuX)_n$ chains or $(Cu_2X_2)_n$ rings by the ligand.[64-67]

The structural diversity of the Cu(II) complexes is largely related to their d^9 system. It enables a variety of coordination polyhedra with significantly different geometries: tetrahedral,[69] square planar,[70] trigonal bipyramidal/planar,[71,72] square pyramidal,[73,74] octahedral[75,76] or mixed geometries[77,78] can be found in the compounds. The coordination sphere of Cu(II) is usually occupied by two to four *N*-donor groups, the other positions being occupied with halides, counter anions or solvent molecules. When bifunctional ligands are used, the copper cation is coordinated with both ligand functions. Coordination compounds derived from paramagnetic Cu(II) ions have great importance for the development of magnetic materials such as molecular-based magnets.[79,80]

1.1.3.5 Zinc based coordination polymers

Zinc is particularly studied in the construction of coordination polymers due to its lability associated with its spherical d^{10} electron configuration. The flexible coordination environment of Zn allows a wide variety of structures ranging from 1D chains to robust and porous 3D networks with potential applications. Due to the flexible coordination environment, the geometry around the zinc atom can be tetrahedral, trigonal bipyramidal, square pyramidal or octahedral.[81-83]

As discussed, the structure of the CP is strongly influenced by bridging ligands. The structure prediction is easy with rigid ligands compared to non-rigid ones because of the flexibility and different confirmations of the latter. Nowadays there is increasing attention towards non-rigid ligands in constructing extended networks with useful properties. Xian-He Bu and co-workers demonstrated the importance of non-rigid bridging ligands in the construction of CPs with different dimensions and pore sizes.[84] They have used 3 ditopic ligands (**4**−**6**), which are very similar in structure but differ in size by one CH_2 group in the spacer. The different pore sizes in CPs were explained with the length of the ligand; the pore size is directly proportional to the length of the ligand (Fig. 6).

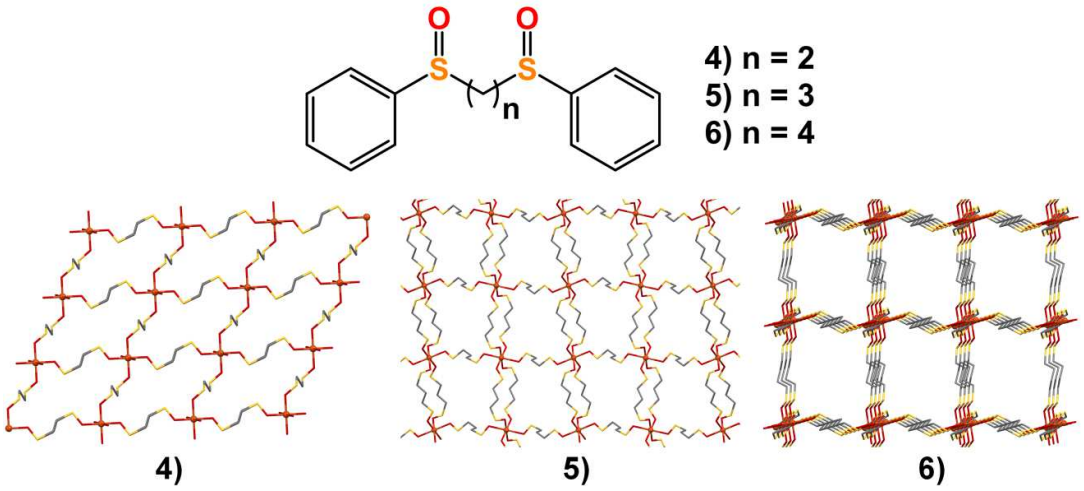

FIGURE 6 Size of the cavities increases with the length of the ligand from **4** to **6**.[84]

It is well known that the dimensionality of the CP depends on the molar ratio of metal to ligand, and also on the coordination geometry of the metal ion. Mirkin and co-workers synthesised a series of CPs from the reaction of silver with several flexible pyridyl-type ligands at different molar ratios (Fig. 7).[85,86] The reaction of **8** with silver ion gave 1D and 2D CPs respectively at 1:1 and 1:2 molar ratios of Ag to ligand.[86] The reaction of **7** with silver at 1.5: 1 molar ratio resulted in the formation of macrocyclic cages along the polymer backbone.[85] In CP synthesis 7 acts as a bis-bidentate ligand to link two Ag ions with sulphur and nitrogen donor atoms, while 8 acts as a bis-monodentate ligand with a linear conformation to link two Ag ions.

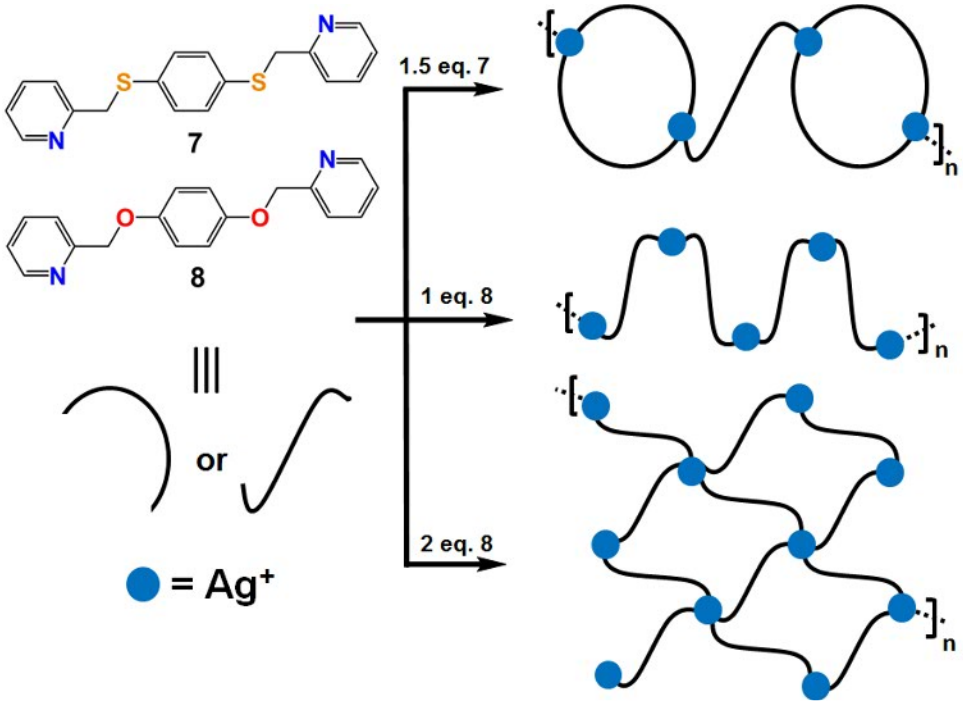

FIGURE 7 Schematic representation of the stoichiometric control in the synthesis of CPs.[85,86]

Flexible ligands can adopt different conformations under different conditions, especially at different temperatures. In 2007, Yu-Bin Dong, Bo Tong and co-workers demonstrated that the conformation of a flexible ligand and consequently the structural topologies of the MOFs could be controlled with the temperature.[87] The reaction of $AgSbF_6$ with **9** at 0°C and 30°C resulted respectively in 3D and 2D CP networks. Changing the counterion from SbF_6 to BF_4, gave respectively 2D and 1D CP networks.

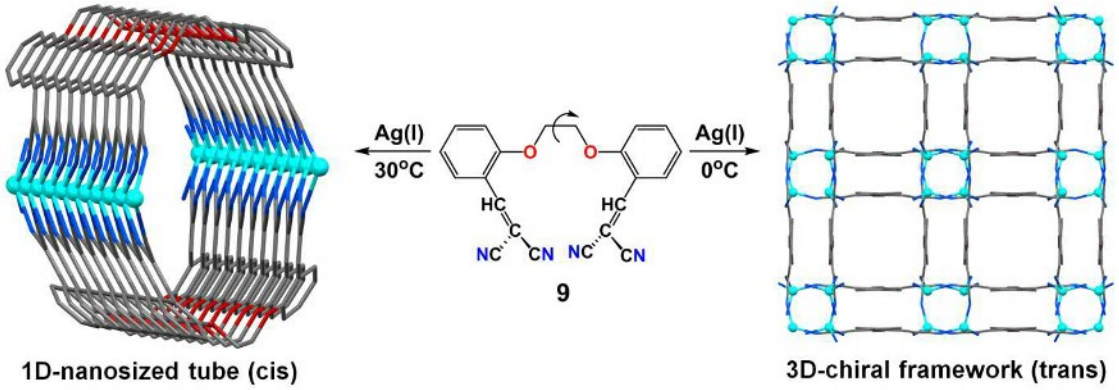

FIGURE 8 The effect of temperature on the structure of CP.[87]

Myongsoo Lee and co-workers reported anion-directed self-assembled silver CPs (Fig. 9). In their study they synthesised a conformationally flexible, bent-shaped bipyridine ligand containing a dendritic aliphatic side chain (**10**). The ligand was used as bridging ligand for the synthesis of silver CPs through self-assembly by changing the counter anion. They proved that the structure of the CP highly depends on the size of counter anion.[88,89] As the size of the counter anion was increased, the structure of CP changed from a folded helical chain (NO_3^- or BF_4^-) to unfolded zigzag conformation ($C_3F_7COO^-$) via a dimeric cycle ($CF_3SO_3^-$).

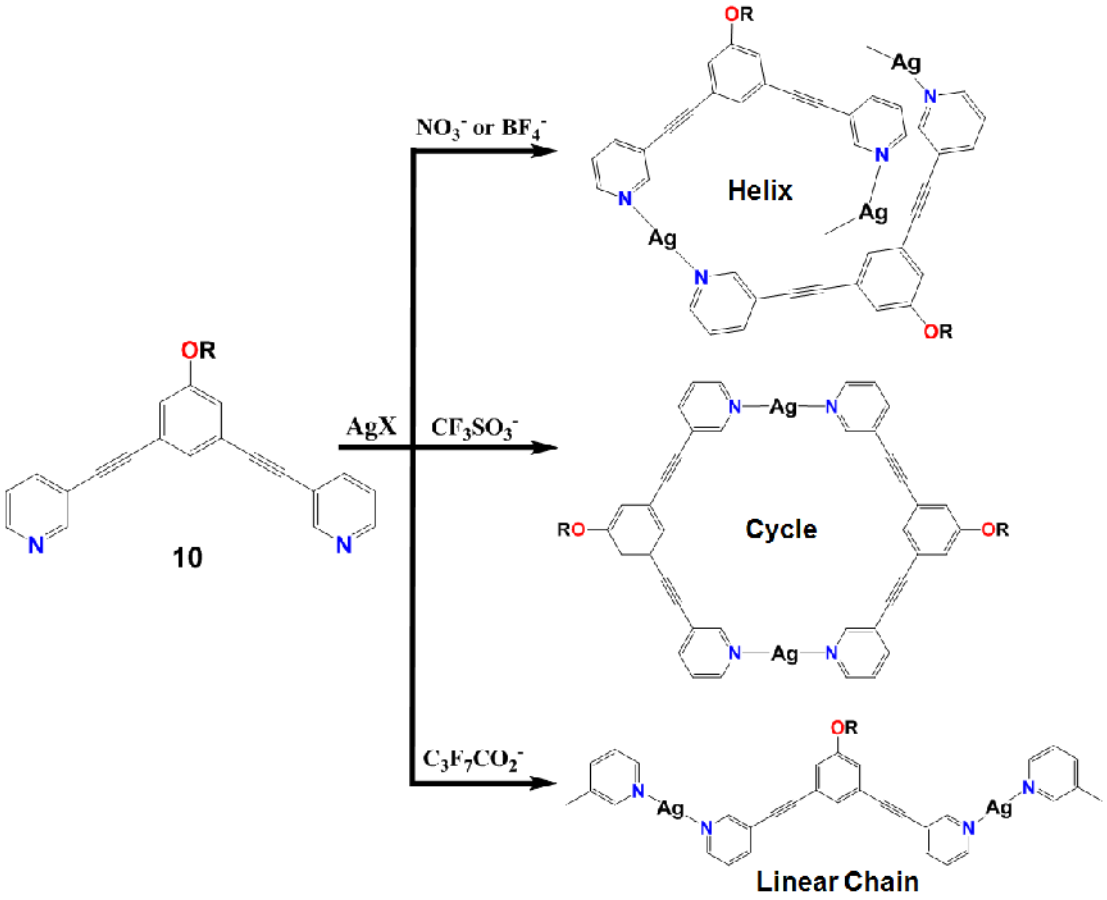

FIGURE 9 Effect of counter anion on self-assembled silver CPs.[88]

The groups of Yaghi and Li individually reported the synthesis of a series of Cu(I) CPs from the reaction of CuX_2 (X= Cl, Br or I) and 4,4'-bipy via hydrothermal or slow diffusion methods.[90,91] In these reaction conditions, copper was reduced from Cu(II) to Cu(I). The reaction of CuX_2 with 4,4'-bipy at 1:1 and 1:2 ratio of copper to ligand resulted respectively in 2D and 3D coordination networks. In a 2D layered network the ligand was bridged between the $(Cu_2X_2)_n$ ribbons (Fig. 10a). All Cu(I) atoms in the $(Cu_2X_2)_n$ ribbon are 3-fold coordinated to X and all X atoms also bridge to three copper metal centres. Each 4,4'-bipy binds to two different copper atoms of two individual ribbons to complete the fourth coordination of Cu(I) with a preferred tetrahedral geometry. The 3D coordination network (Fig. 10b) consisted of four interlocking planar lattices. Each copper atom is ligated by two bridging 4,4'-bipy ligands and two bridging chlorido ligands. The copper atoms are asymmetrically bridged by two chlorido ligands to form a Cu_2X_2 ring.

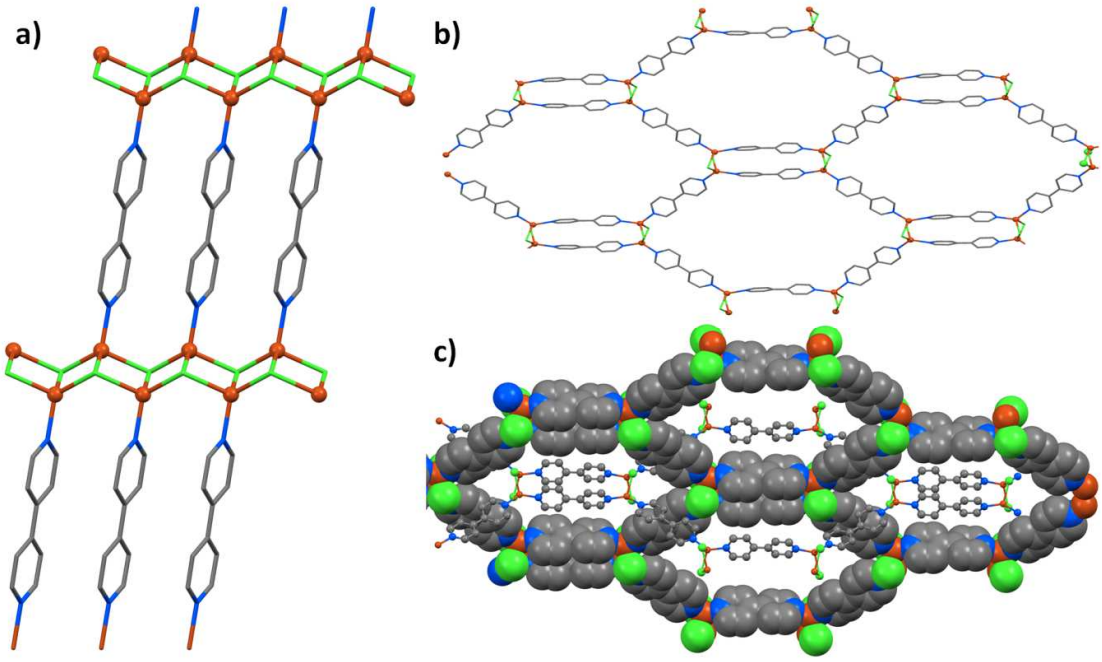

FIGURE 10 a) 2D structure of $[(CuCl)_2(4,4´\text{-bipy})]_n$, b) structure of the interlocking planar net in 3D network of $[CuCl(4,4'\text{-bipy})]_n$ and c) two perpendicular interlocking nets in 3D network shown at 90°.[90,91]

1.2 Gels

1.2.1 Definition, classification, and formation

Gel materials play an essential role in people's everyday life. Right from the beginning of a human life gels afford convenience to every family using disposable diapers for their babies. The most important ingredient here is a superabsorbent polymer and when contacted with urine, a hydrogel is formed that absorbs the liquid.[92]

Despite being known and studied since the nineteenth century, gels have been notoriously hard to define. In 1923, Dorothy Jordon-Lloyd already stated that the gel is one which is easier to recognise than to define.[93] Almost 50 years later (1974), one of the most important and comprehensive definition for gel was introduced by Paul John Flory. He described a gel as a two-component colloidal dispersion exhibiting a continuous microscopic structure with macroscopic dimensions, which is permanent on the time scale of analytic experiments and is solid-like in its rheology behaviour below a certain stress limit, despite being mostly liquid.[94] Not all gel systems are colloidal in nature, and one can consider that all gels consist of a solid three-dimensional matrix constructed by crosslinking of polymeric strands of (macro) molecules by physical or chemical forces in the presence of bulk gas or liquid phases.[95] The viscoelastic, solid-like macroscopic appearance of a gel is the result of the entrapment of bulk gas or liquid phase (solvent) in the interstices of a 3D elastic network of gelator molecules through surface tension and capillary forces.[96]

Gels can be classified by different criteria (Fig. 11).[97] Basically, they can be classified either according to their source (natural or artificial) or based on the nature of liquid phase (solvent). Regarding the liquid phase, when water is used as a solvent the gel is called hydrogel,[98] and if the liquid phase is an organic solvent, then the system is called organogel.[99] If a gelator can form a gel in both groups of solvents, it is called amphiphilic.[100] Additionally, a special case exists where the solution is a mixture of organic solvent and water.[101-104] There are also aerogels and xerogels, where aerogels can be obtained when the liquid medium is replaced with air and xerogels are formed from gels by drying.[105]

Another way of distinguishing between gels is to analyse their driving force for molecular aggregation. Based on the type of interactions, they classified as chemical gels and physical gels. In chemical gels, the gelator molecules are held together by strong chemical bonds (covalent bonds) to form a 3D network which makes them robust and tolerant of physical deformation.[106] Physical gels that can be derived from macromolecules or low molecular-weight compounds are called supramolecular gels. In physical gels, the small gelator molecules are self-assembled by one or a combination of several non-covalent interactions such as hydrogen bonding, van der Waals forces, π-π stacking, F-F interactions and metal coordination...etc.[107-109]

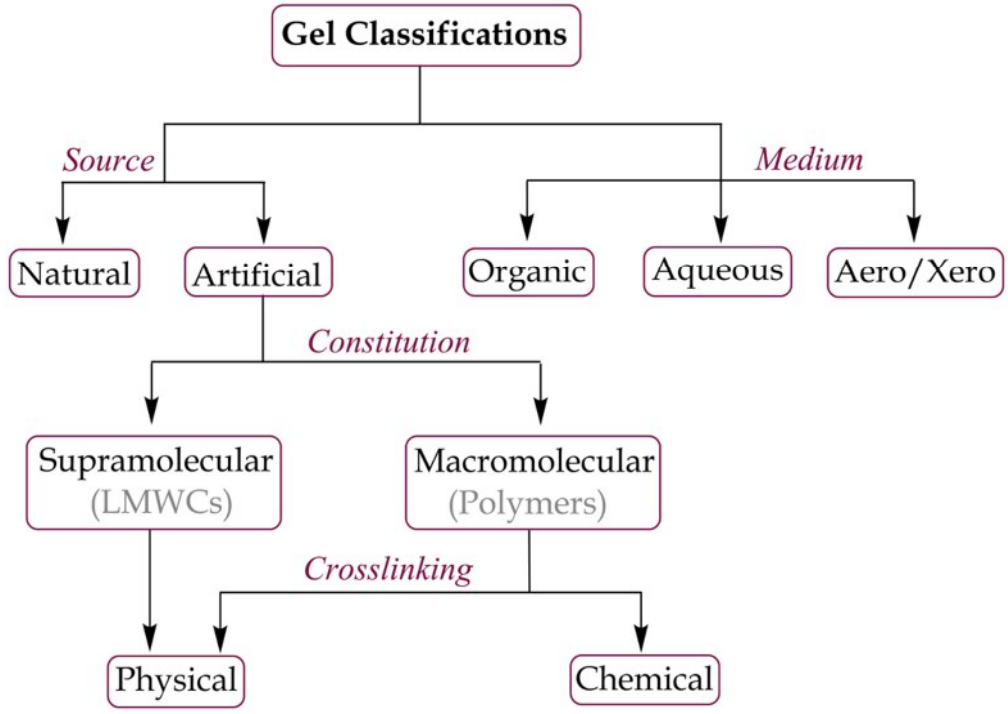

FIGURE 11 Classification of gels.[97]

The difference between chemical and physical gels can be clarified by comparing their thermoreversibility. Most of chemical gels are thermoirreversible, and they cannot be redissolved due to their formation by chemical bonds. Physical gels are thermoreversible due to the presence of non-covalent interactions. They can be liquefied by heating to their sol-to-gel transition temperature (T_{gel}), which results in the collapse of their 3D network, which is reformed upon cooling.[110]

1.2.2 Supramolecular metallogels

There has recently been increasing interest in the investigation of supramolecular metallogels.[111,112] In a simplified way, metallogels could be described as gels which contain both LMW ligands and metal ions. Metal-ligand coordination is considered the primary driving force to build up metallosupramolecular gels. Metallogels have been used to prepare materials with very attractive properties such as luminescence, magnetism, catalytic, conductivity and antibacterial, etc.[113-116] Usually, supramolecular gels were prepared in two ways: One case is *in situ* gelation,[117] where rational amounts of LMW ligand and metal ions are dissolved in a suitable solvent (water or organic solvent or an aqueous-organic mixture) through heating or sonication and resting for few minutes leads for gelation. In the second case, the metal-ligand complex/ polymer is premade (e.g. in solution) as a gelator.[118]

Metallogels are broadly divided into two categories: as discrete metal complex gels and coordination polymer gels (CPGs).[119-122] In discrete metal complex gels, the gelator molecules are self-assembled through several non-covalent interactions resulting in a fibrous network. CPGs belong to another category where metal ions act as nodes and LMW ligands as linkers. Therefore, the combination of metal ions and LMW ligands results in a coordination polymer (CP) network (1D/2D/3D), which immobilizes the solvent within it. The structure of the CP network is strongly dependent on the geometry of metal ions and the conformation and binding sites of LMW ligands. For this purpose, a variety of different ligands has been developed and studied for supramolecular metallogelation. Among them, pyridine (py),[123-125] bipyridine (bipy)[126,127] and terpyridines (tpy)[128-131] and their derivatives are particularly popular and have been extensively studied.

You and co-workers reported the metallogelation ability of simple imidazole-containing ligands (Fig. 12).[132] Optically transparent metallogels were prepared upon addition of aqueous solution of $AgNO_3$ to the solution of **11** or **12** in MeOH at a 1:1 ratio of $AgNO_3$ to ligand. The formation of helical chiral nanotubular structures in the gel state was revealed by using tapping-mode AFM microscopy. This was further explained by observing a strong cotton effect in the CD spectra, which is absent for free ligands. The Ag(I) ions coordinate to the imidazole nitrogen atoms in a linear geometry to form extended structures. The bent shape of the ligands and the directional metal-ligand interactions lead to the formation of helical structures in both right- and left-handed chirality.

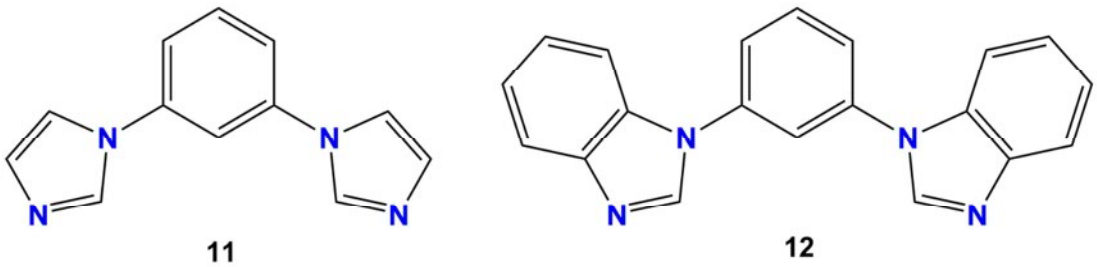

FIGURE 12 Chemical structures of imidazole-based gelators.[132]

Jung and co-workers reported a coordination polymer gel (CPG) from a tetrazole-based ligand (**13**) and Ag(I) ions in an aq.NaOH solution (pH= 10).[133] No gelation was observed in acidic or neutral conditions because of the protonated nitrogen atoms of the tetrazoles. They also reported the effect of counter anions towards gelation, and no gelation was observed for CH_3COO^- or SO_4^{-2} because of higher Hofmeister effect, which induces the formation of solid products. They also reported *in situ* formation of AgNPs within the gel matrix. It was found that the particle size is related to the concentration of silver salt in CPGs. CPGs prepared from 3 and 5 equivalents of $AgClO_4$ showed large nanoparticles ranging from 2−5 nm. The presence of AgNPs was confirmed by observing surface plasmon resonance at 450 nm in UV-Vis absorption spectra. They also observed the catalytic activity of these AgNPs in the reduction of 4-nitrophenol into 4-aminophenol by $NaBH_4$ in an aqueous solution. The catalytic reduction was monitored with the help of UV-Vis spectroscopy. During the reduction, the peak at 317 nm (4-nitrophenol) was shifted to 400 nm due to the formation of 4-nitrophenolate as an intermediate. With time, the disappearance of the 400 nm peak with the appearance of a new peak at 300 nm was observed, which was attributed to 4-aminophenol.

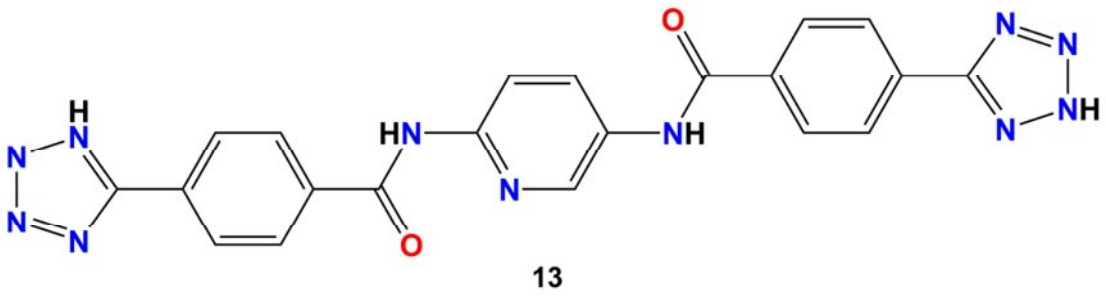

13

FIGURE 13 Chemical structure of tetrazole-based ligand.[133]

Liu and co-workers synthesised a pyridine based ligand, N,N´-bis(pyridyl-4-methyl)-N-fluorenyl-9-methoxycarbonyl(Fmoc)-L-glutamate (4MPFG; **14**) which yielded no gelation without metal coordination. Complexing it with $AgNO_3$ in a mixture of water and ethanol (1:1, v/v) forms CPG.[134] The self-assembly behaviour of metallogels was largely dependent on their concentration. At lower concentration, metallogels self-assembled to form nanotubes with an outer diameter from ~100 to 150 nm and inner diameter ~20 nm. Upon increasing the concentration of metallogel, the transition of the self-assembled nanostructures from nanotubes to nanofibers was observed. These formed nanomaterials were also studied for their antibacterial activity.

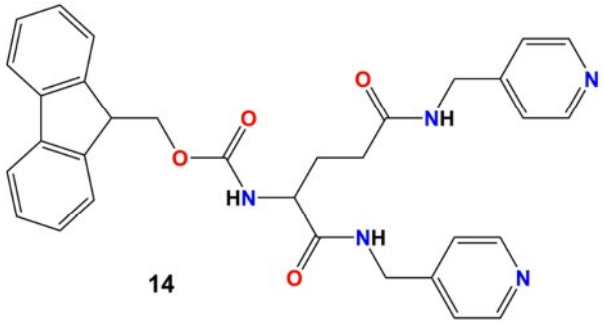

FIGURE 14 Chemical structure of 4MPFG gelator. [134]

The groups of Bian and Gao reported an example of binapthylbisbipyridine-based ligand (**15**), which is capable of forming CPG with Ag(I) in a 1:1 stoichiometry in CH_3CN.[135] The silver coordination to 15 is capable of forming nanotubular helices. The formed CPs were self-assembled into an entangled fibrous network capable of holding solvent molecules. The effect of various anions on gel stability and the morphology of the CPGs were studied. More interesting is their follow up paper,[136] where the same ligand is found able to form dinuclear heterochiral metallocycles containing two ligand molecules and two silver (I) cations. These metallocycles are self-assembled into the 3D network by using non-covalent interactions to hold the solvent molecules.

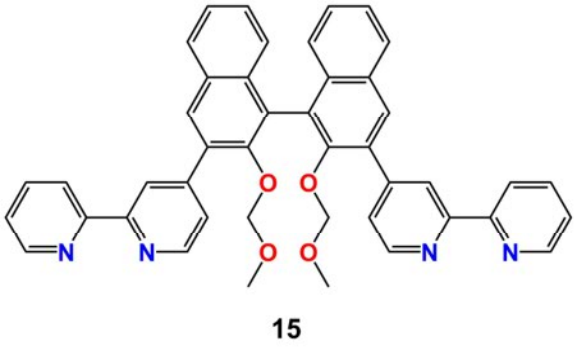

FIGURE 15 Chemical structure of binapthylbisbipyridine gelator.[135,136]

Shinkai and co-workers reported the first redox-responsive metallogel from the reaction of Cu(I) with 2,2´-bipyridine derivative bearing two cholesteryl groups (**16**).[137] It was found that the gel stability was highly dependent on the metal-ligand molar ratio; a stable gel was formed from 1:2 of Cu(I) and 16. A thermochromic sol-gel transition behaviour of this complex was reported in 1-butyronitrile with a colour change from reddish brown (solution) to greenish blue (gel) which is unusual for Cu(I) complexes. They also studied reversible sol-gel phase transitions upon addition of oxidizing and reducing reagents; this transition was attributed to the redox state of the copper ion. In conclusion, they stated that the chromatic change in the complex was induced by a sol-gel phase transition associated with deformation of the coordination complex in the specific cholesteric gel fibril, attributed to the redox state of the copper playing a critical role in the gel stability.

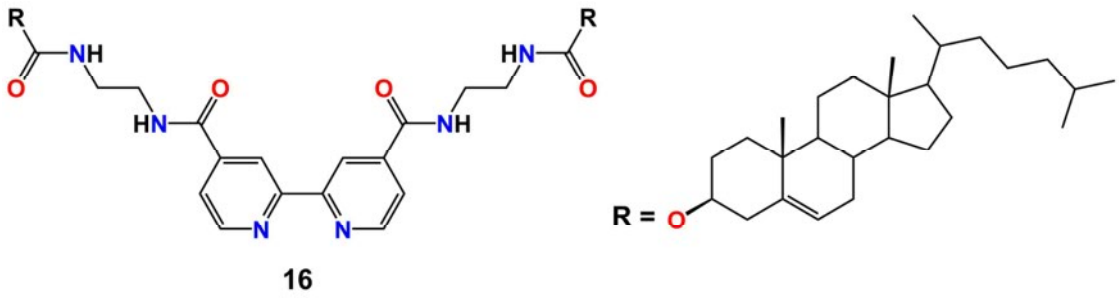

FIGURE 16. Structure of cholesteryl 2,2′-bipyridine-based gelator.

Xu and co-workers reported a ruthenium-based fluorescent supramolecular metallohydrogel.[138] They synthesised a ruthenium (II) tris(bipyridine) complex (**17**) from the reaction of Ru(II)(bipy)$_2$(4,4´-dicarboxyl-2,2´-bipy) with tripeptide. They studied the hydrogelation ability of **17** at different pH's with various concentrations. For example, at pH = 1 it forms a firm gel at a concentration of 0.4% (w/v) and at pH = 7 it forms firm gel at a concentration of 0.8% (w/v). These results could be explained with the degree of protonation on carboxylic groups of **17**, where low pH decreases the solubility of **17** and thus favours the formation of the hydrogel at a lower concentration. They have shown that the self-assembly of **17** results in nanofibers resulting from 1D intermolecular interactions. Upon oxidation of Ru(II) to Ru(III), the nanofibers of **17** break down to turn the hydrogel into a solution.

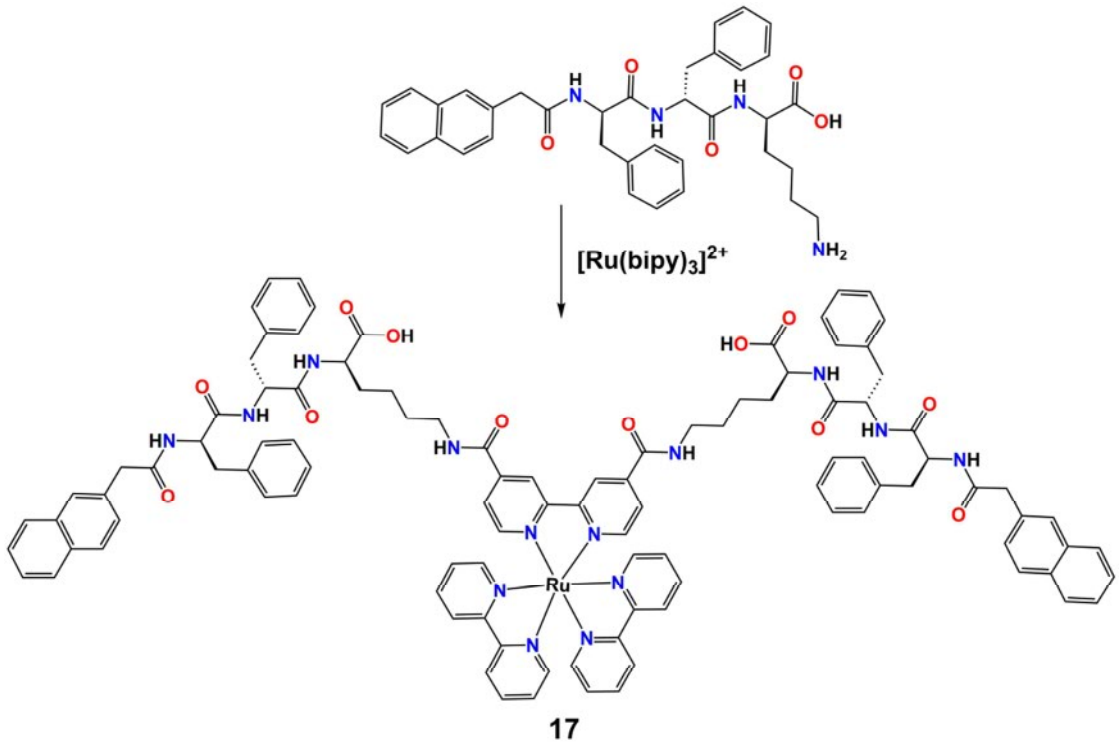

FIGURE 17 Molecular structure of the metallo-hydrogelator (**17**).[138]

The hydrogelation ability of a series of amino-terpyridine ligands (**18**−**20**) in the presence of divalent metal ions was reported by Rissanen group.[139] All gelation experiments were carried out in an aqueous solution of 0.15−0.2 N HCl and a metal-to-ligand ratio equal to 1 was employed. Metallogels of **18** with Cu(II), Zn(II), and Cd(II), and of **19** with Zn(II), Cd(II), and Hg(II) were reported. In the case of **20**, gelation was found to be highly cation-specific; a gel forms upon complexation with Hg(II). In conclusion, it was stated that the hydrogelation critically depends on the metal ions and also on minor changes in the ligand structure. Interestingly, in their follow-up paper they also reported a pyrophosphate (ppi) detection ability of a hydrogel derived from **18** and Zn(II). A gel-coated paper strip was able to sense ppi through fluorescence.[140]

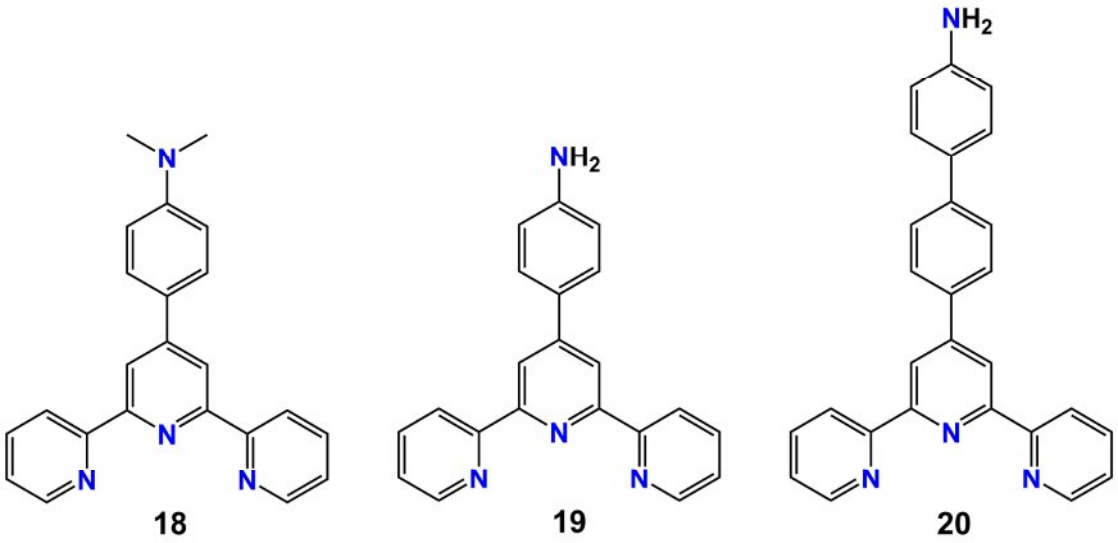

FIGURE 18. Chemical structure of the amino-terpyridine ligands.[139]

Maji and co-workers have reported the rational design and synthesis of a series of new bi- (**21**),[141] tri-,[142] and tetrapodal terpyridine-based LMWGs[143]. These LMWGs can form an opaque gel in a mixture of $CHCl_3$:THF (2:1) without metal coordination and show blue emission. They explained that the LMWGs upon coordination to Eu^{3+} and Tb^{3+} in the same solvent mixture results in the formation of CPGs which showed respectively pink and green emissions. Bimetallic CPGs that could be obtained by controlling the stoichiometry of LMWG/Eu^{3+}/Tb^{3+} show tunable emission. The bimetallic CPG with a stoichiometry of LMWG:Tb:Eu = 1:1:1.2 showed a strong greenish yellow emission; white light emission was observed for LMWG:Tb:Eu = 1:1:2 bimetallic CPG. Furthermore, the coordination-driven self-assembly of tripodal LMWG with Zn^{2+} led to the formation of CPG in a mixture of H_2O:MeOH (4:6), which exhibited sheet-like morphology.

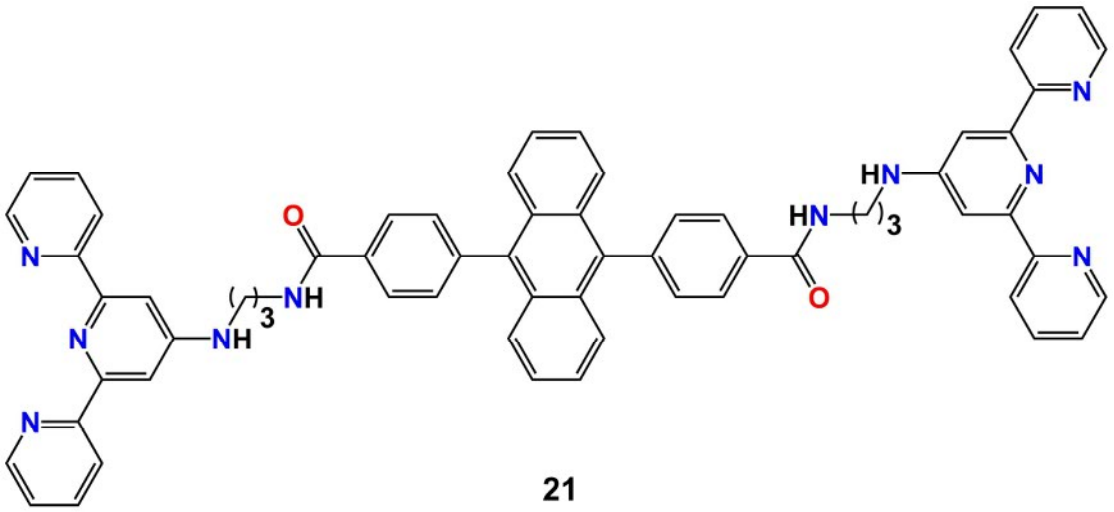

21

FIGURE 19 Chemical structure of bipodal LMWG.[141]

1.2.3 Methods of gel study and characterization

The characterisation of gels is essential to obtain measurable values for comparison. The values obtained open ways to practical applications.

Minimum gelation concentration (MGC)

The MGC defines the lowest amount of gelator needed for the gelation of a specific volume of solvent. Below MGC, a gelator is not able to build up a sufficient 3D network structure to entrap the solvent molecules. That can be confirmed by the inversion of the test tube; the material is classified as a gel when no gravitational flow occurs. Usually, MGC is determined in wt% (w/v). When the MGC is less than 1 wt%, the gelators are described as supergelators.[144]

Temporal stability

The temporal stability of a gel is defined as a time period between the gel formation and gel destruction. Gel destruction can happen either by phase separation or crystallisation inside the gel material.

Thermal stability (T_{gel})

It can be described as the gel-sol phase transition temperature (T_{gel}). It can be obtained by a number of different characterisation methods. The following two are most common ones.

The ***"Dropping ball method"*:**[145] A small ball is placed in the middle of the gel surface and the temperature is slowly raised until the gel transforms into a solution and the ball touches the bottom of the vial. It is essential to have an inert ball (no reaction with gel) and not too heavy or too light one to avoid dunking or floating of the ball in the gel.

The ***"Inverse flow method"*:** Measurements are taken in a sealed vial containing the gel. The vial is immersed in a thermostatic oil bath upside-down and the temperature is slowly raised until the gel matrix breaks down.

Temperature-dependent ^{1}H NMR spectroscopy

The ^{1}H NMR spectra can provide an insight into the stabilisation of the gelator network by the involved protons. For this gel has to be prepared from deuterated solvents and NMR spectra have to be measured at different temperatures below and above T_{gel}. The signals observed in ^{1}H NMR spectra belong to gelator molecules dissolved in the immobilised solvents. While increasing the temperature, the number of dissolved molecules increases leading to a growth in signal intensity and multiplicity. With increasing temperature the signals can shift either to up- or downfield, and the point of inflection of a plot of shift *Vs* temperature corresponds to T_{gel}. NMR spectroscopy gives useful information on π−π stacking, hydrogen bonding and even metal coordination in metallogels.[146,147]

Morphological characterization

Scanning electron microscopy (SEM), transmission electron microscopy (TEM) and atomic force microscopy (AFM) are proven tools for microscopic morphologies of dried gels.[148,149] These techniques enable a study of the gel structures and changes in their morphology caused by changes of solvent or gelation concentration. The high-resolution images also make visible the inclusion of particles or crystals or the formation of nanoparticles.

For SEM, TEM and AFM measurements dried samples (xerogels) must be prepared. Xerogels are generally prepared by freeze-drying a gel before the solvent is removed by vacuum to preserve the internal 3D network structure. This is a crucial step of the whole measurement. For SEM measurement, xerogels have to be coated with gold prior to imaging. A copper grid is used to prepare the TEM samples by drop-casting method. The high resolution of TEM enables imaging single fibres of the 3D network, while SEM images show the assembly of the fibres. There are other techniques called cryo-SEM and cryo-TEM which allow studying gel matrices without drying.

Rheological properties

Another important characteristic of a gel is mechanical stability which can be assessed by rheology. Rheology is defined as the science dealing with the deformation and flow of matter (gel) under the effect of an applied stress.[150] In rheological experiments, the gel is subjected to an oscillatory stress and its response is measured in terms of elastic (storage, G′) and loss (viscous, G″) moduli. This technique gives information on the lifetime of the non-covalent bonds between gelator molecules and allows us to differentiate hard gels (G′>>G″ at all frequencies) and soft gels, where G′>G″ at high frequencies and G′<G″ at low frequencies.

Rheology studies may also be complemented with microscopy techniques such as scanning electron microscopy (SEM) or transmission electron microscopy (TEM) to relate the viscoelastic properties of the gel with the morphology of the fibre network.

X-ray diffraction

X-ray diffraction is an important method to have an insight on the modes of molecular packing and related physical and chemical properties of the gel. Nowadays, single-crystal X-ray diffraction is very commonly used for structure determination. However, the difficulty in obtaining single crystals limits the use of this method. As a result, powder X-ray diffraction of lyophilised gels is commonly used to gather some information on the structure of a gel and organisation of the fibres.[151]

Other physical methods

Besides the techniques referred to above, some other physical methods, such as UV-Vis, Infrared (IR), and Raman spectroscopies may also provide information about the molecular arrangements in supramolecular gels. UV-Vis technique is used for investigating π−π interactions, metal coordination in the process of gelation and also to detect metal nanoparticles.[152] IR spectroscopy is commonly used for identifying the chemical structure of a substance. In gel structure investigations, it is most useful in the study of molecular aggregates; particularly in detecting hydrogen-bonding interactions.[153] NMR may also be helpful for this purpose; although very broad signals are obtained in a gel phase due to the large correlation time and very short relaxation time.

1.3 Aims of the study

The aim of this work is to synthesise multidentate ditopic *N*-donor ligands from biimidazole or bipyridines. These ditopic ligands were employed as bridging ligands in the construction of CPs and coordination polymer gels (CPGs). In addition, this study also deals with the effect of pH on metal coordination into the ring-substituted biimidazoles. The more detailed goals of the study are as follows:

- Studying the importance in ring-substituents on biimidazole ligands for zwitterionic coordination-compound formation in acidic media.
- The possibilities to control the structure of coordination polymers by varying metal centres and reaction conditions. This study also deals with the competition between the imidazole and pyridine nitrogen atoms in metal coordination.
- Use of pyridine and bipyridine derivatives as low molecular-weight ligands for the construction of silver coordination polymer gels (CPGs).
- Studying *in situ* formed silver nanoparticles (AgNPs) in terms of size and distribution by photo- and chemical reduction.

2 RESULTS AND DISCUSSION

2.1 Synthesis of N-donor ligands

(Paper I): Ring-substituted 2,2′-biimidazole (**L1−L3**) ligands were synthesised by following a modified literature procedure.[154] The ligand synthesis involves direct lithiation followed by subsequent formylation with DMF in THF solution.

(Paper II): Ditopic biimidazole derivatives (**L4 & L5**) were synthesised by adopting the literature procedure.[155] 2,2′-H_2Biim undergo electrophilic substitution with 3- or 4-chloromethyl pyridine under basic conditions to furnish **L4** and **L5** respectively. The ligand has four binding sites for metal coordination; two come from the biimidazole ring and other two from pyridine rings.

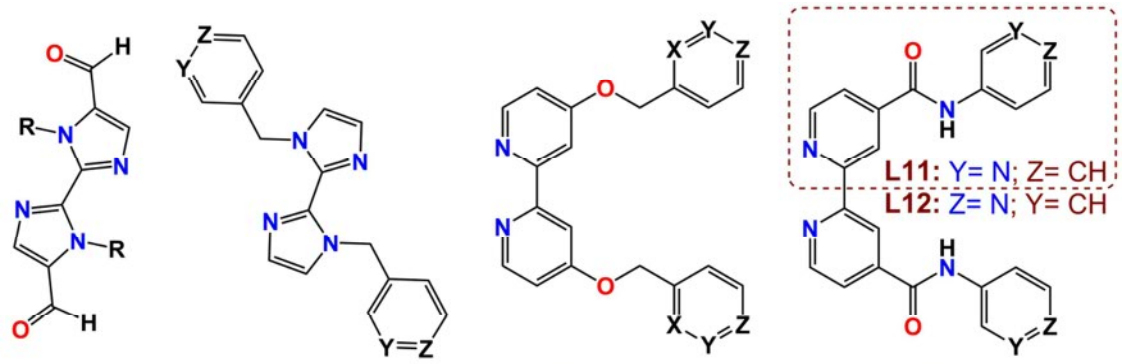

FIGURE 20 Chemical structure of ligands (**L1−L12**) used in the thesis.

(Paper III and IV): Bipyridine-based semirigid ligands (**L6−L10**) were synthesised based on modified literature procedures.[156,157] Synthesis of **L6−L8** was involved in etherification of 4,4´-dihydroxy-2,2´-bipyridine with 2-, 3-, or 4-chloromethyl pyridine in the presence of potassium carbonate. **L9** and **L10** are quite similar to **L7** and **L8** except for the spacer between bipy and py units, which is an amide. These lig-

ands were synthesised by amidation of 4,4′-dicarboxy-2,2′-bipyridine with corresponding aminopyridines in the presence of EDC (N-ethyl-N′-(3-dimethylaminopropyl) carbodiimide) in a DMF solution.

Ligands **L11** and **L12** synthesis was carried out by following the literature procedure where isonitinoyl chloride was treated with corresponding aminopyridines in the presence of triethyl amine.[158]

Generally, the purity of the products (**L1−L12**) was good, although in some cases they were recrystallized from suitable solvents. These products were characterized with 1D (^{1}H, ^{13}C), 2D (^{1}H-^{1}H COSY, HMQC, HMBC and ^{1}H-^{15}N-COSY) NMR spectroscopy, mass spectroscopy and single-crystal X-ray crystallography.

2.2 Ionic and zwitterionic coordination compounds

Binuclear Zn(II) and mononuclear Cu(II) coordination compounds were obtained from the reaction of metal chlorides (MCl_2) with ligands L1−L3 at 1:1 molar ratio. These reactions were performed in a methanol solution at pH= 7 (neutral). The coordination behaviour of the ligand differed with the nature of the metal ion, the ligand being involved in bridging coordination[159] with zinc (**22**) and chelated[160] with copper (**23**; Fig. 21).

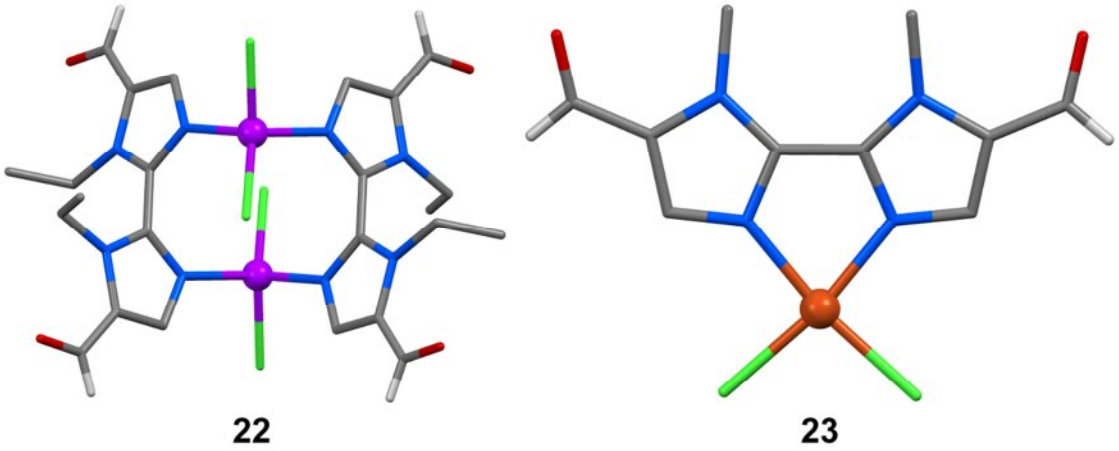

FIGURE 21 X-ray structure of binuclear Zn (**22**) and mononuclear Cu (**23**) coordination compounds.

When the reaction of MCl_2 with L1−L3 was performed in methanolic HCl solution (pH= 3−4), either ion pairs or zwitterionic coordination compounds were obtained depending on the level of protonation (Scheme 1). Similar results were also obtained while dissolving binuclear zinc or mononuclear copper coordination compounds into the methanolic solution by adding a few drops of conc. HCl. In addition to protonation, aldehyde groups from the ligand were involved in acetal formation; this was found to be crucial for zwitterionic coordination compound formation. The ion pairs (**24 & 25**) were obtained only when the ligand had a methyl group as N-substituent (Fig. 22). During ion pair formation from neutral coordination com-

pounds, both metal-nitrogen bonds were broken and protonated. In the crystal packing, the cationic ligand (H_2L1^{+2}) was involved in intermolecular H-bonding with MCl_4 anion with $R^2_2(9)$ and $R^4_2(8)$ synthons.

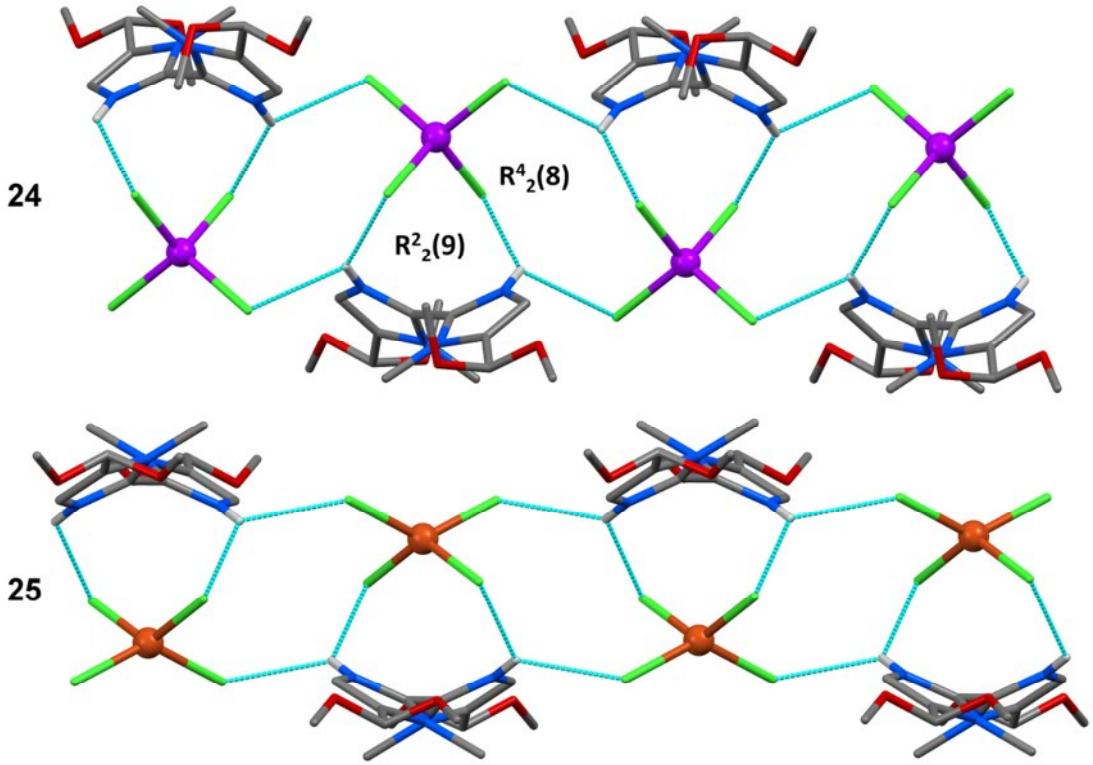

FIGURE 22 Crystal packing of ion pairs obtained from Zn (**24**) and Cu (**25**) with protonated ligand **L1** in an acidic medium.

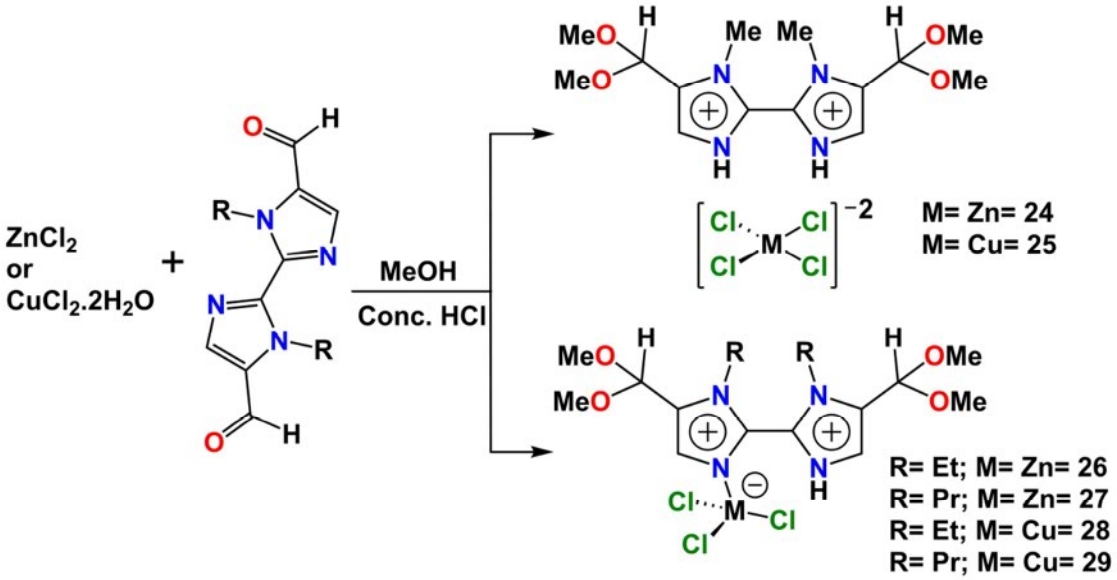

SCHEME 1 Synthesis of ionic and zwitterionic Zn(II) and Cu(II) coordination compounds in an acidic medium.

Zwitterionic coordination compounds (**26**−**29**) were obtained by single metal-nitrogen bond cleavage when the ligand had a longer alkyl chain as *N*-substituent (R= Et or Pr). In the crystal packing, the molecule was involved in intermolecular H-bonding to form a dimer with the $R^2_2(14)$ synthon (Fig. 23). In solution, zwitterionic coordination compounds were found to be unstable and decomposed to form free neutral ligand and $HZnCl_3$ salt; this was confirmed by observing a single peak for biimidazole protons in ^1H NMR and from molar-conductivity experiments. Similar results were also obtained while changing MCl_2 to MBr_2.

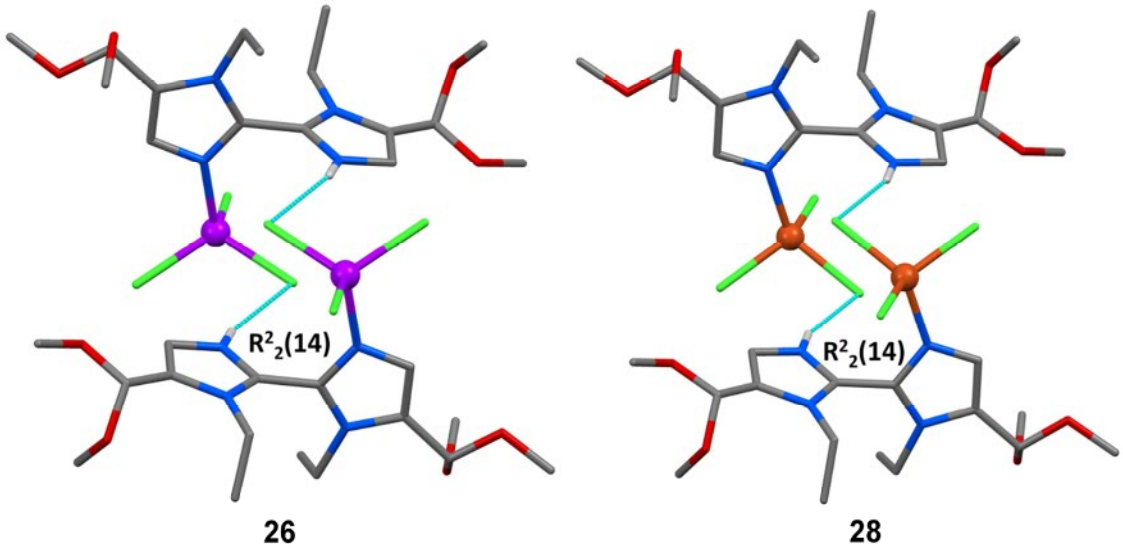

FIGURE 23 Intermolecular H-bonding in zwitterionic Zn (**26**) and Cu (**28**) coordination compounds from **L2**.

The importance of the aldehyde group at the ligand was elucidated by performing the reaction between R_2Biim (without ring-substituent, R= Et or Pr) and MCl_2 in acidic medium. All these reactions resulted only in the formation of ion pairs. Therefore, for zwitterionic coordination compound formation a low enough pH (3−4), an aldehyde group as ring-substituent and longer alkyl substituents are required.

2.3 Coordination polymers

Ligands **L4**−**L12** (see Fig. 20) were synthesised and used as semirigid ligands for the construction of CPs with different structural topologies. **L4** and **L5** are biimidazole derivatives with four binding sites: two imidazole nitrogen (N_{Im}) atoms and two pyridine nitrogen (N_{Py}) atoms. The coordination ability of N_{Im} differs from that of N_{Py}, which can be explained by negative electrostatic potentials (NEPs) of donor atoms. The NEPs associated with the N_{Py} (−182 kJ/mol) are higher than those of N_{Im} (−128 kJ/mol) which makes them more prone to metal coordination, as well as hydrogen/halogen bonding acceptors.[161,162]

Ligands **L6−L10** are 2,2′-bipy derivatives with flexible pyridine arms at 4, 4′ position. In **L6−L8**, the bipy is connected to pyridyl groups with an ether linkage; they differ in the position of nitrogen atom at the pyridine ring. In ligands **L9** and **L10**, the bipy is connected to pyridine groups through an amide linkage, and they also differ in the position of nitrogen atom at the pyridine ring. In CPs synthesis, the bipy nitrogen (N_{bipy}) atoms are assumed to be involved in the chelation with the metal, leaving the pyridine nitrogen (N_{Py}) atoms free to act as a bridge between the metals.

Ligands **L11** and **L12** are pyridine derivatives where two pyridine units are connected with an amide group. They also differ in the position of the nitrogen atom at the pyridine group.

2.3.1 Zinc and Copper coordination polymers from L4 and L5

The reaction of $ZnCl_2$ with L4 and L5 at 1:1 molar ratio gave two distinct 1D-CPs (Fig. 24). The coordination geometry around the metal in both cases is a slightly distorted tetrahedral with the N_2Cl_2Zn binding set. In both cases, ligand (L4 or L5) was observed as bidentate bridging ligand through either N_{Im} or N_{Py} atoms. Ligand L4 was coordinated to the metal through N_{Im} (**30**) atoms while N_{Py} atoms are free of coordination; the situation is vice versa for ligand L5 (**31**) in metal coordination.

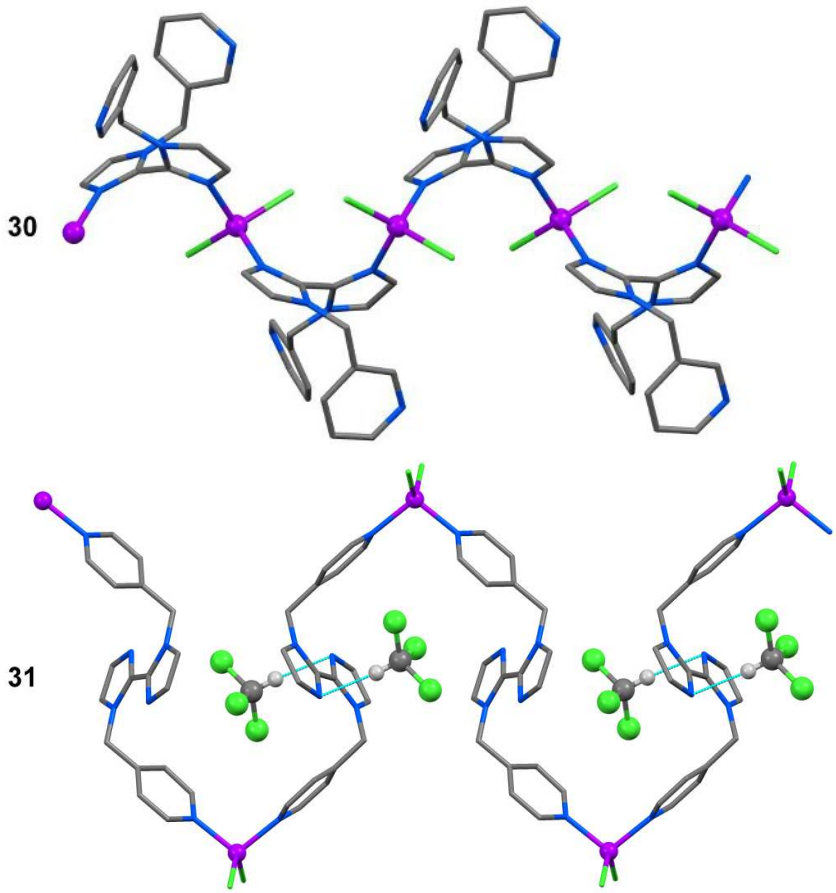

FIGURE 24 X-ray structure of 1D-Zn-CPs from ligands L4 (**30**) and L5 (**31**).

The 2D paramagnetic copper(II) CP resulted from the reaction of $CuCl_2.2H_2O$ with L4 (1:2) in methanol solution (**32**). The coordination geometry around the metal is square pyramidal with an N4ClCu binding set. Similar to zinc CP, L4 is acting as bidentate bridging ligand through its N_{Py} atoms and N_{Im} atoms are free of coordination. When the reaction was performed with ligand L5 in a mixture of DMSO and water (v/v 1:1), it resulted in two individual 1D and 3D Cu(I) CPs through the linking of $(Cu_2Cl_2)_n$ rings. The reduction of copper in a mixture of DMSO and water is not known in the literature. The coordination geometry around the Cu(I) is distorted tetrahedral with the N2Cl2Cu binding set. In 1D-CP (**33**), the metal-to-ligand ratio was 1:1 and only N_{Py} was involved in metal coordination. The 3D-CP (**34**) was obtained as a by-product along with 33 and no rational route could be found to produce a pure form of it. In 34, L5 was observed as tetradentate where all the nitrogen atoms (N_{Im} and N_{Py}) are involved in metal coordination.

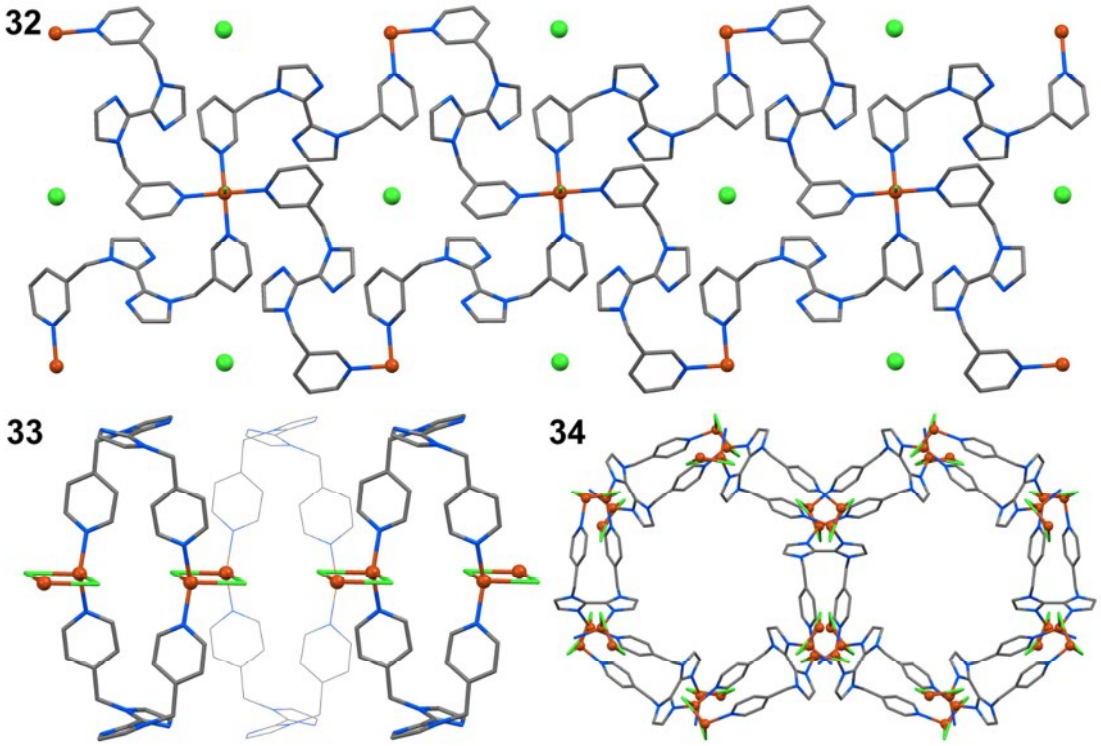

FIGURE 25 X-ray structures of Cu-CPs with L4 (**32**) and L5 (**33** & **34**).

2.3.2 Silver(I) CPs from L4, L5, and L11

The soft nature of silver along with its flexible coordination sphere allows us to synthesise CPs with different structural topologies. The dimensionality of CP was found to be dependent on the reaction solvent used. The reaction of $AgClO_4$ with L4 (**35**) or L5 (1:1) in dry acetonitrile gave two structurally similar 2D CPs where all the nitrogen atoms (N_{Im} and N_{Py}) from the ligand were involved in coordination. The coordination environment around the metal was tetrahedral with an N4Ag biding set. When the reaction solvent was changed to a mixture of water and acetonitrile (v/v

2:8), only N_{Py} atoms participated in coordination to result in 1D-CP (**36**). The coordination sphere around the metal was linear with an N2Ag binding set.

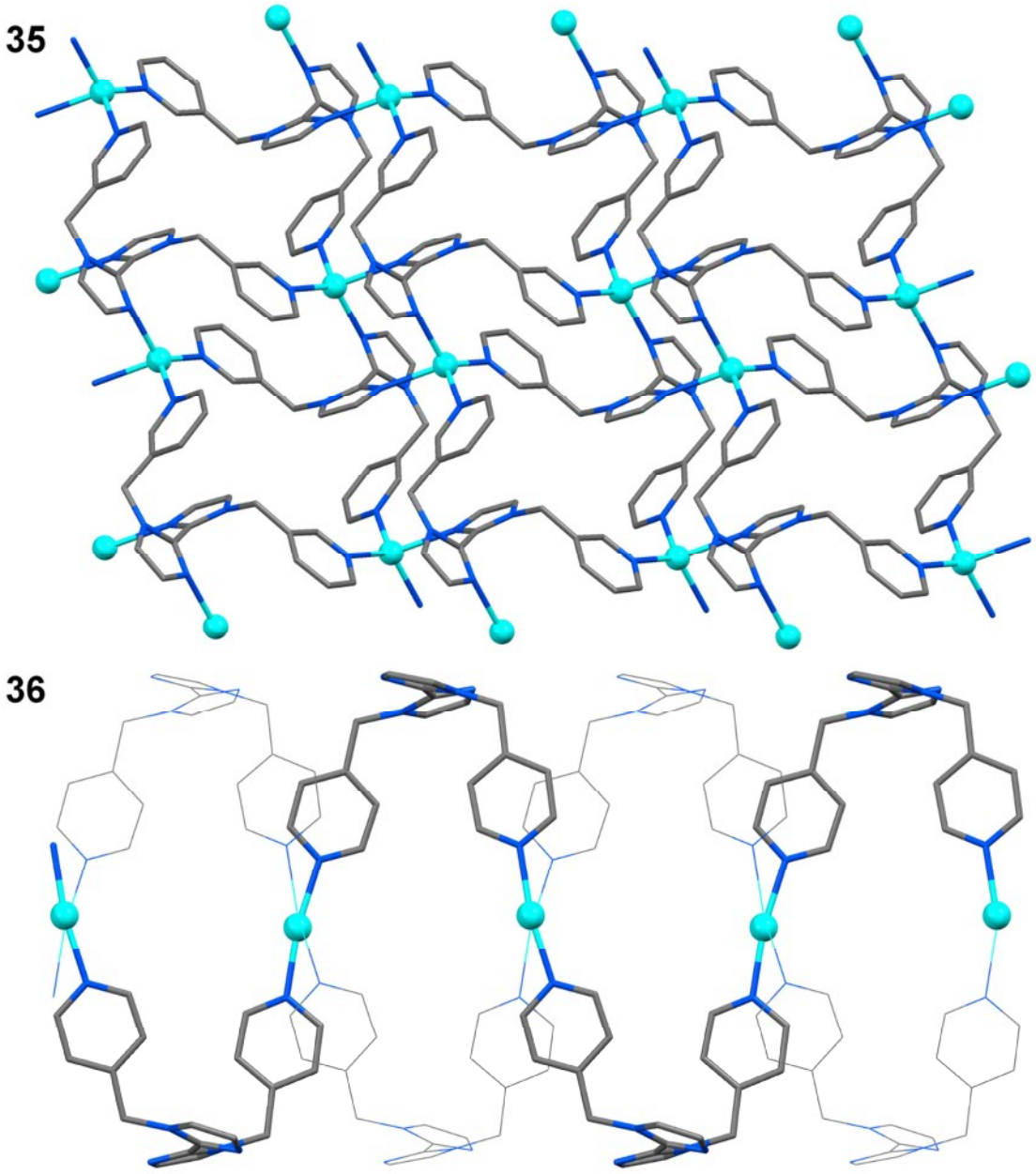

FIGURE 26 X-ray structures of 2D- and 1D-Ag-CPs from L4 (**35**) and L5 (**36**).

The reaction of AgOTf with **L11** at 1:2 molar ratio resulted in a 2D CP (**37**).[163] In its crystal structure each silver atom is coordinated by four individual ligand molecules to furnish a 2D layered structure. The voids in the crystal packing were occupied with the counterions by forming H-bonds with the amide protons (Fig. 27). Similar 2D CPs were obtained from other silver salts (AgX; X= ClO_4^-, BF_4^-, and PF_6^-).

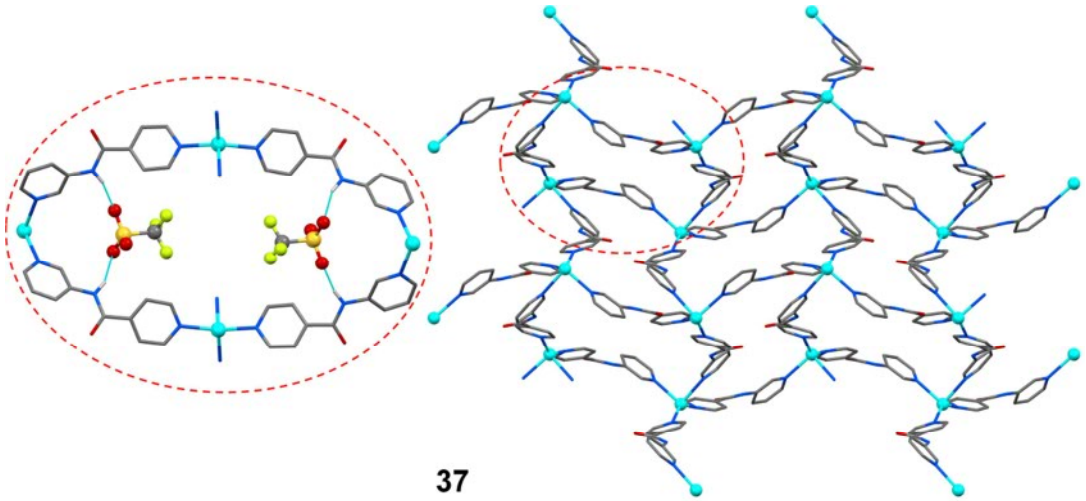

FIGURE 27 X-ray structure of 2D-Ag-CP from **L11**.

The reaction of AgOAc with **L11** (1:1) resulted in ladder-type 1D-CP (**38**), where the coordination geometry around the metal is tetrahedral with an N2O2Ag binding set. In its crystal structure two acetate anions are bridging two silver atoms to form a ring (Fig. 28). These 1D CPs are further extended to the 2D structure via intermolecular H-bonding between an amide proton and an oxygen atom from each carboxylate anion (Fig. 28). A similar structure was obtained from the reaction of AgOAc with **L12**.

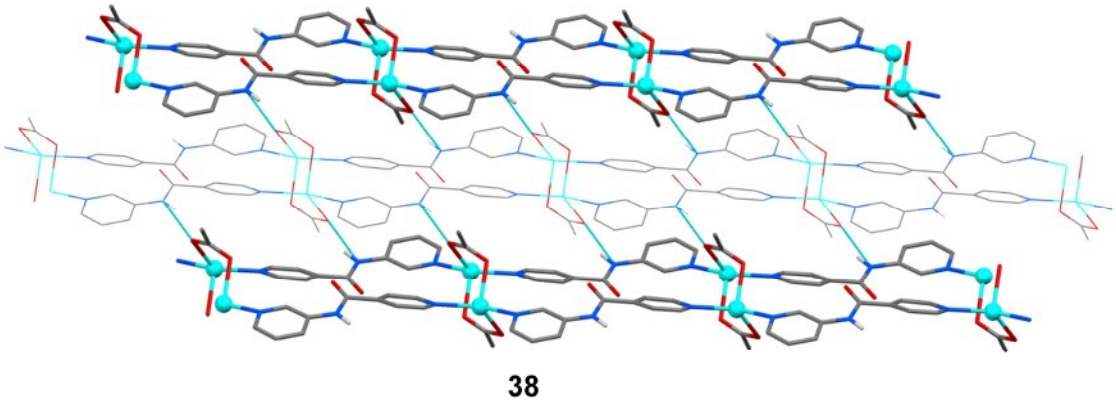

FIGURE 28 1D-ladder Ag-CP from **L11** displaying the role of counter anion acetates as bridging ligands.

2.3.3 X-ray powder diffraction (XRPD)

The bulk-phase purity of zinc, copper, and silver CPs derived from L4 and L5 as confirmed by X-ray powder diffraction. The XRPD measurements were performed on a Panalytical XPert Pro MPD diffractometer operating at the Cu Kα wavelength (1.54184 Å). In all cases, the single-crystal X-ray diffraction results were well matched with the simulated patterns (Fig. 29).

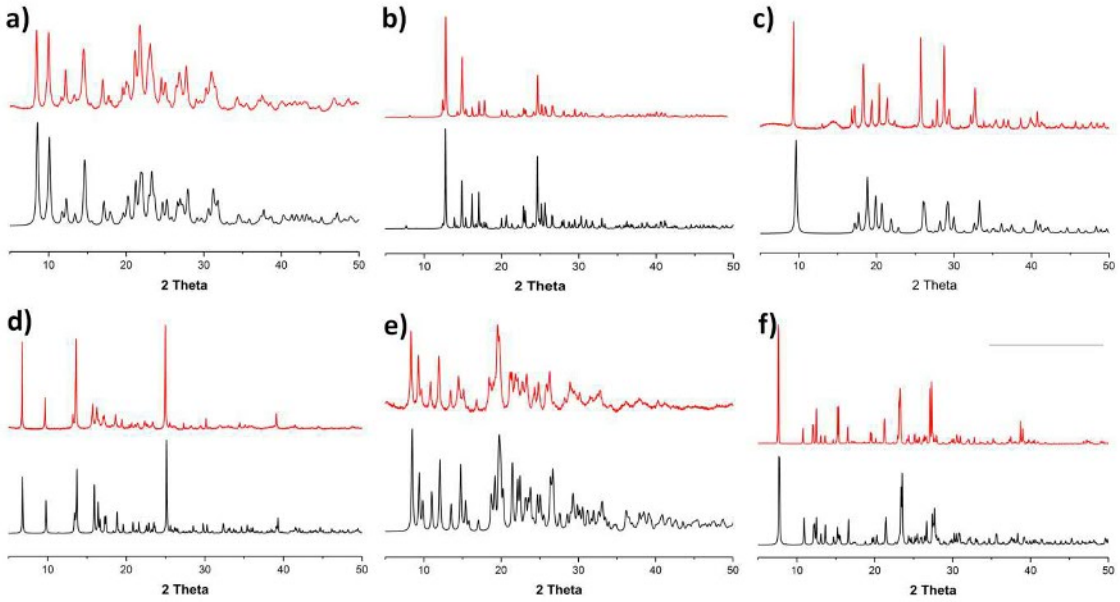

FIGURE 29 The XRPD patterns for **30** (a), **31** (b), **32** (c), **33** (d), **35** (e), and **36** (f) (red- experimental & black-simulated).

2.4 Self-assembly and solid-state studies

2.4.1 Metallosupramolecular gelation

In initial gelation experiments from **L6**−**L10** without metal coordination, only **L7** resulted in a supramolecular gel from the mixture of DMSO/water (8:2 v/v). The hydrogelation ability of **L12** has been reported in the literature.[164] The gel obtained from L7 was found to be unstable and collapsed by standing at room temperature for several hours. During metallogelation experiments from **L6**−**L12**, all ligands except **L6** were able to form CPGs in a mixture of DMSO and water (Table 1, Fig. 30). No metallogelation was observed in pure organic or aqueous solutions. Metallogelation was found to be cation-specific; only silver was able to form metallogels. All these gels derived from ligands **L7**−**L12** can be called as "supergelators" since they can form a gel at lower than 1 w/v%.

TABLE 1 List of silver salts tested for gelation (Note: G= gel, G*= gels are unstable and collapsed upon standing at room temperature for an hour, P= precipitate)

Ligand	DMSO/Water (v/v)	NO_3	ClO_4	OTf	BF_4	PF_6	OAc
L7	7:3	G	G	G	G	G	G
L8	7:3	G	G*	G*	G*	G*	G*
L9	7:3	G	G	G	G	G	G
L10	7:3	G*	G*	G*	G	G*	G
L11	2:8	G	G*	G*	G	G	G
L12	8:8	P	P	G	G	P	G*

All these CPGs were prepared in an *in situ* manner. In a typical gelation experiment, an appropriate amount of a bipy derivative (L7−L10) was dissolved in DMSO upon heating and an equimolar amount of silver salt solution in water was added to reach a final volume of 1.0 mL. The resulting mixture was then heated to obtain a clear solution which was then cooled down to room temperature to afford a CPG. The visual appearance and MGC of these CPGs were found to be related to the volume of cosolvent in a mixture. The CPGs turn from transparent to translucent and MGC drops from 0.6 to 0.4 w/v% while changing the mixture from 8:2 to 6:4 (v/v) of DMSO/water. Pyridine derivatives (L11 and L12) were also able to produce CPGs upon silver coordination (1:2 of silver: ligand) in a mixture of DMSO and water (v/v 2:8 and 3:7). Increasing the volume of DMSO in a mixture results in either a precipitate or single crystals (See Figs. 27, 28).

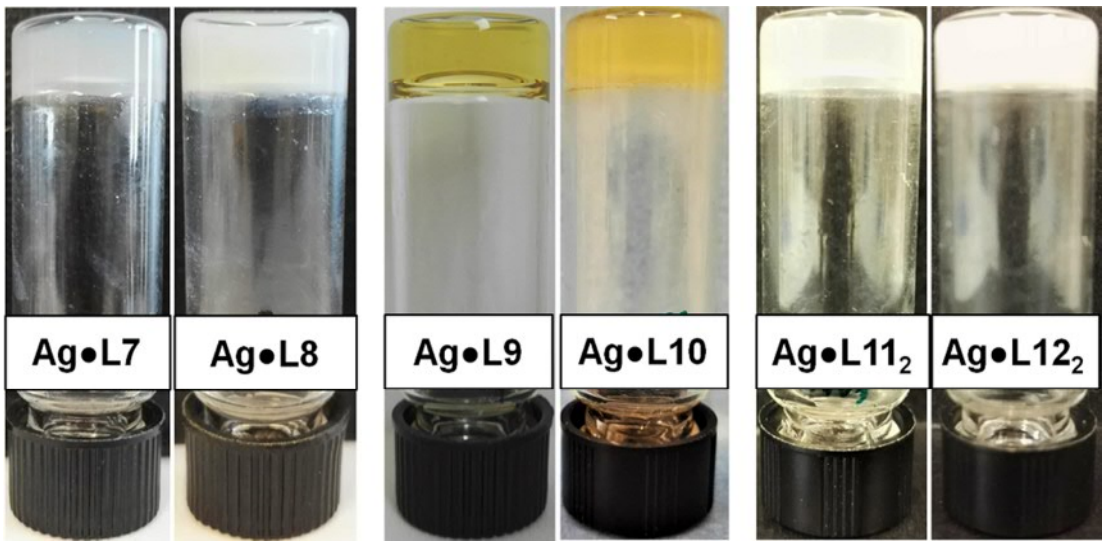

FIGURE 30 Photographs of the Ag-CPGs obtained from ligands **L7−L12** in a mixture of DMSO and water.

2.4.2 NMR studies

In this work, one-dimensional (1D; ^{1}H, ^{13}C) and two-dimensional (2D; COSY, HMQC, and HMBC) NMR spectroscopies were utilised to characterise newly synthesised organic compounds, as well as their coordination compounds in solution (See ESI of paper II-IV).

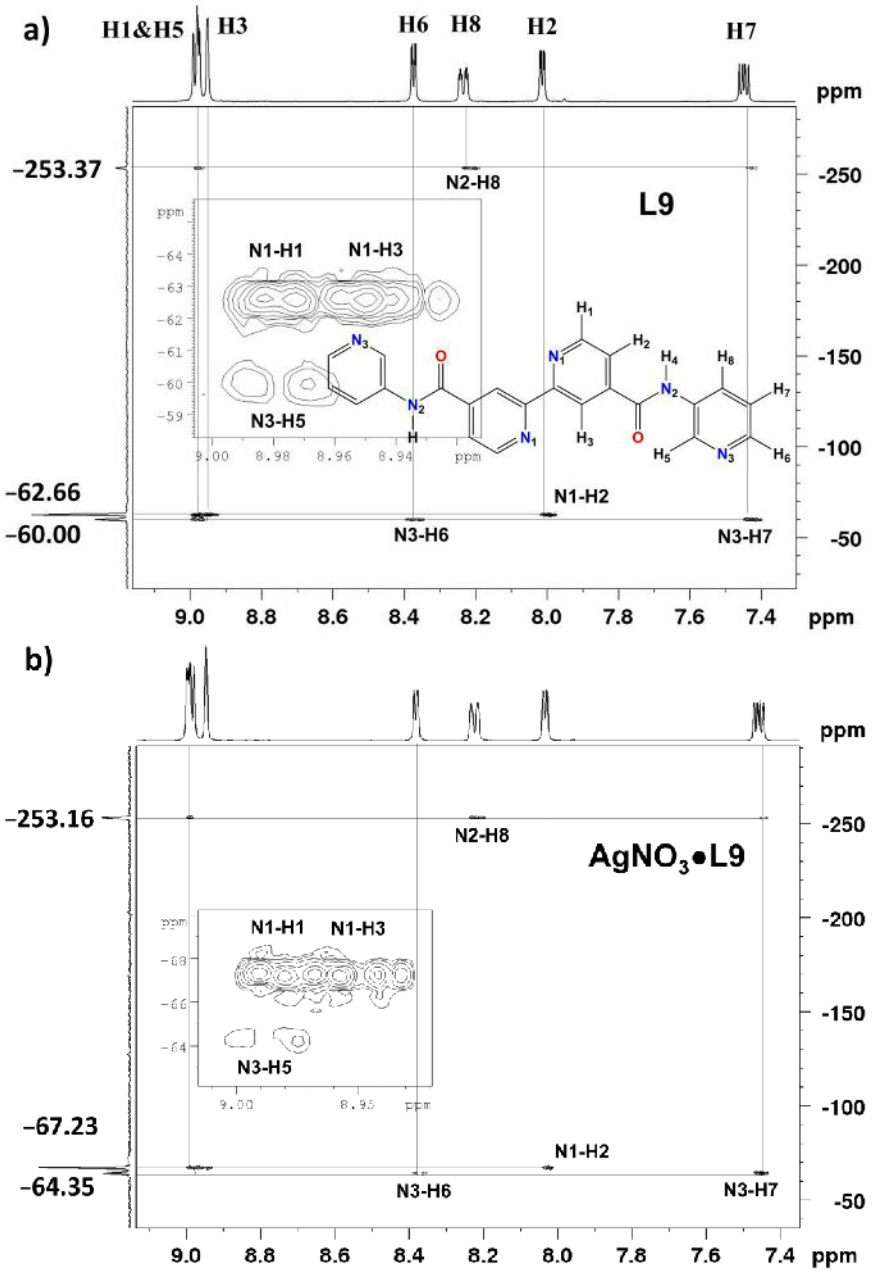

FIGURE 31 ^{1}H-^{15}N 2D correlated spectra of **L9** (a) and **$AgNO_3$•L9** (b) at 70°C in DMSO-*d6*.

Figs. 29 and 30 show $^{1}H-^{15}N$ COSY spectra of ligand **L9**, **L11** and their silver coordination compounds in DMSO-d_6. Upon metal complexation, significant changes in the chemical shift values of nitrogen atoms were observed. For ligand **L9**, the signals from bipyridine nitrogen atoms (N1) and pyridine nitrogen atoms (N3) were shifted upfield by 4.57 and 4.35 ppm, respectively (Fig. 31). This is evidence that all nitrogen atoms from bipyridine and pyridine rings are involved in metal coordination. Similarly, for L11 signals from both pyridine nitrogen atoms (N1 and N3) were shifted to upfield by 6.84 and 10.62 ppm, respectively (Fig. 32).

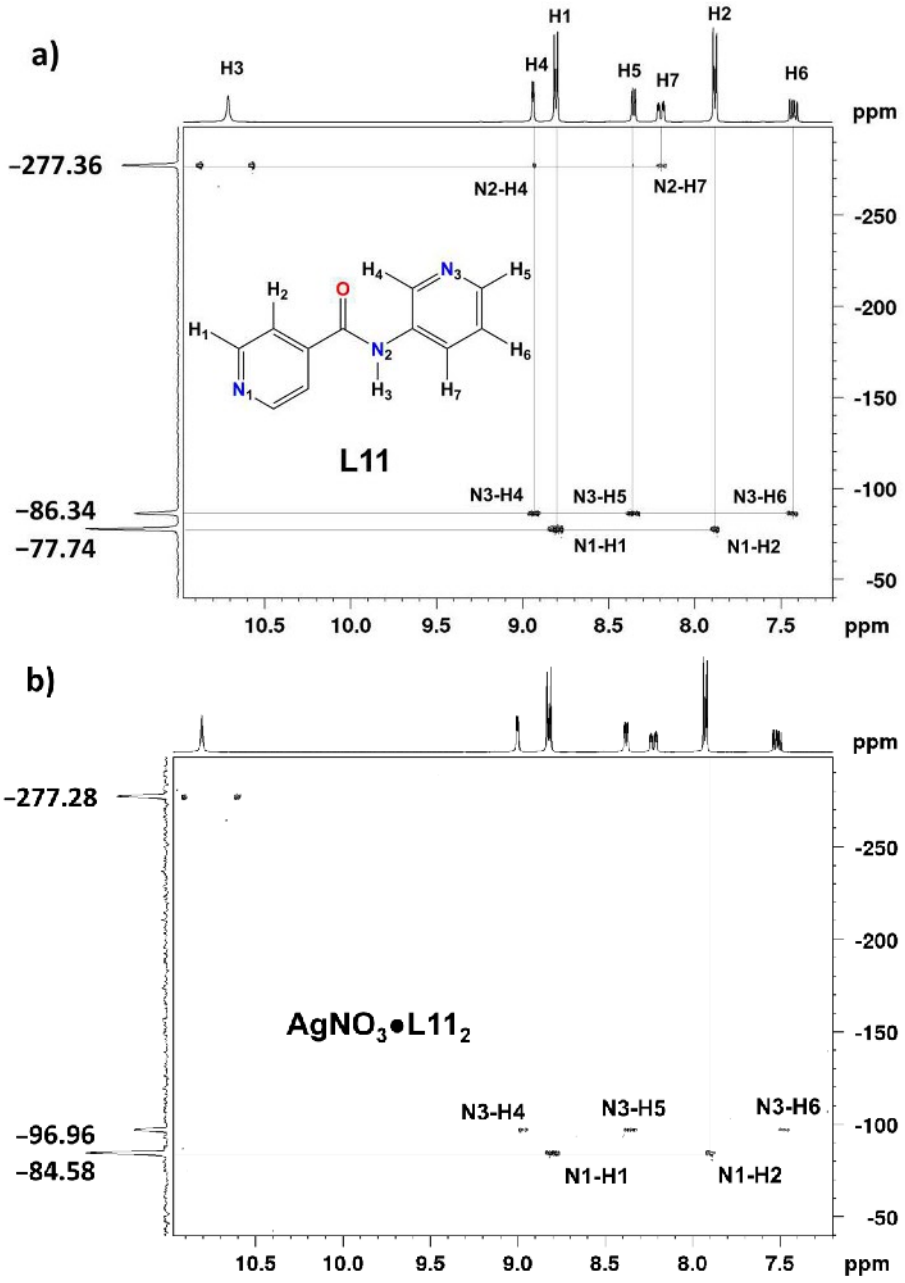

FIGURE 32 ^{1}H-^{15}N 2D correlated spectra of **L11** (a) and **$AgNO_3$•L11$_2$** (b) at 30°C in DMSO-*d6*.

Variable-temperature measurements of the **$AgNO_3$•L9** in solution reveals that the changes in chemical shift values of protons of amide groups suggest a participation of these molecules in intermolecular H-bonding with the counter anion (Fig. 33). The presence of H-bonding with the counter anions can also be seen in the solid-state structure of silver CPs with ligand L11 **(37 & 38)**.

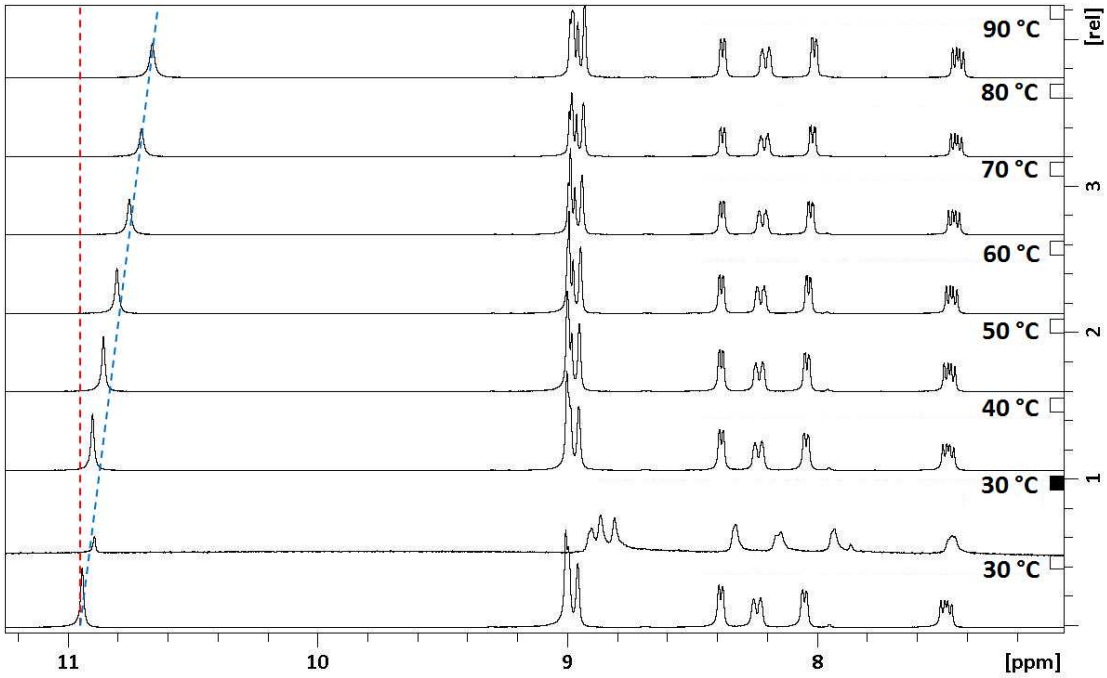

FIGURE 33 ^{1}H NMR sub spectra of **AgNO$_3$●L9** in DMSO-d_6 at different temperatures (30−90°C).

Based on the molar ratio of bipyridine ligands (L7−L10) to AgX (1:1) and the NMR spectral analysis, the complexes were confirmed as coordination polymers where the silver cation is tetrahedrally coordinated by one chelating bipyridine unit and two bridging pyridine rings from adjacent ligands (Fig. 34).

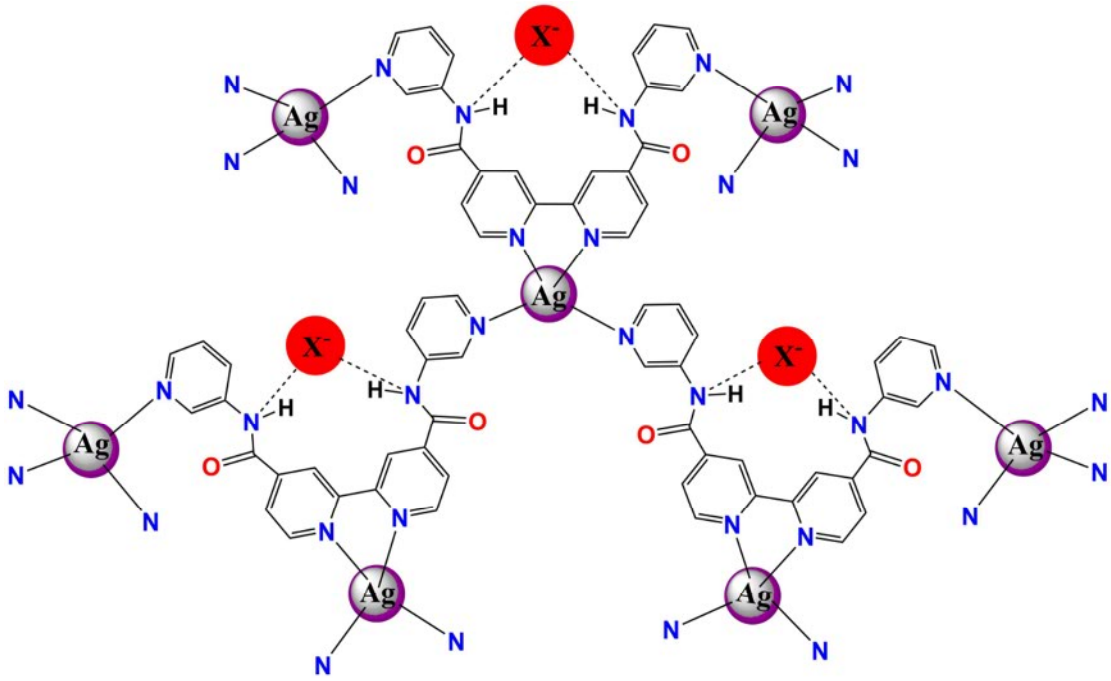

FIGURE 34 The proposed structure of the metallosupramolecular polymer **AgX●L9** (X$^-$= NO_3^-, ClO_4^-, OTF^-, BF_4^-, and PF_6^-).

2.4.3 Rheological studies

The mechanical properties of the **$AgNO_3$●L7** and **$AgNO_3$●L8** gels (paper III) were studied by frequency-sweep measurements (Fig. 35). These experiments revealed that the elastic modulus G′ was higher than the loss modulus G″ for both gels. Interestingly, the **$AgNO_3$●L8** gels are somewhat stronger than the **$AgNO_3$●L7** gels. No significant changes in G′ values (100 Pa) for **$AgNO_3$●L7** gels were observed upon changing the DMSO/H_2O ratio. However, **$AgNO_3$●L8** gels showed higher G′ values (800−1000 Pa) compared to those of **$AgNO_3$●L7** gels at 8:2 (v/v) DMSO: H_2O ratio.

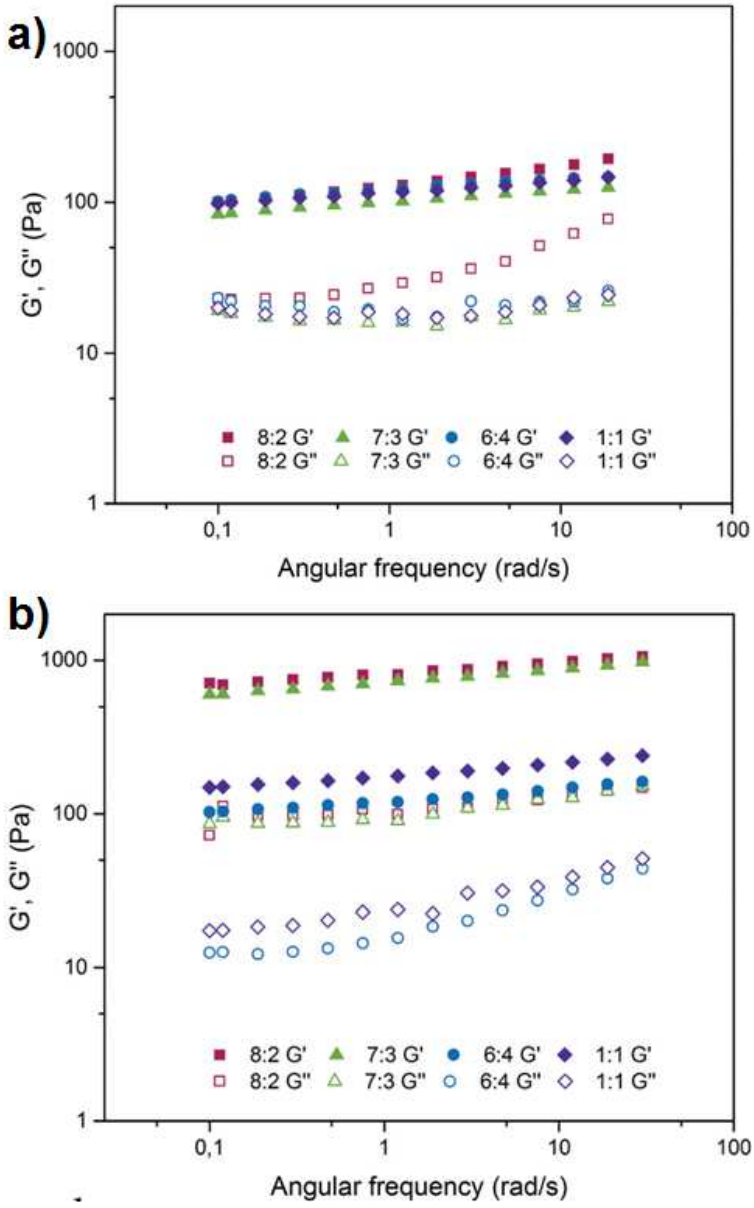

FIGURE 35 Frequency-sweep experiments for 0.6 w/v% **$AgNO_3$●L7** (a) and **$AgNO_3$●L8** (b) gels formed in DMSO/H_2O mixture.

2.4.4 Morphology of the gels (SEM & TEM)

SEM and TEM measurements were used to study the morphological features of metallogels. The unstable gelation behaviour of **L7** is due to the formation of microcrystalline aggregates (Fig. 36a), as revealed by SEM. Typically, a fibrous network was detected in dried CPGs (xerogels) by SEM and TEM. Fig. 36b,d shows a thin nanofibrillar network in **$AgNO_3$●L7** and thick highly entangled nanofibers in **$AgNO_3$●L8**.

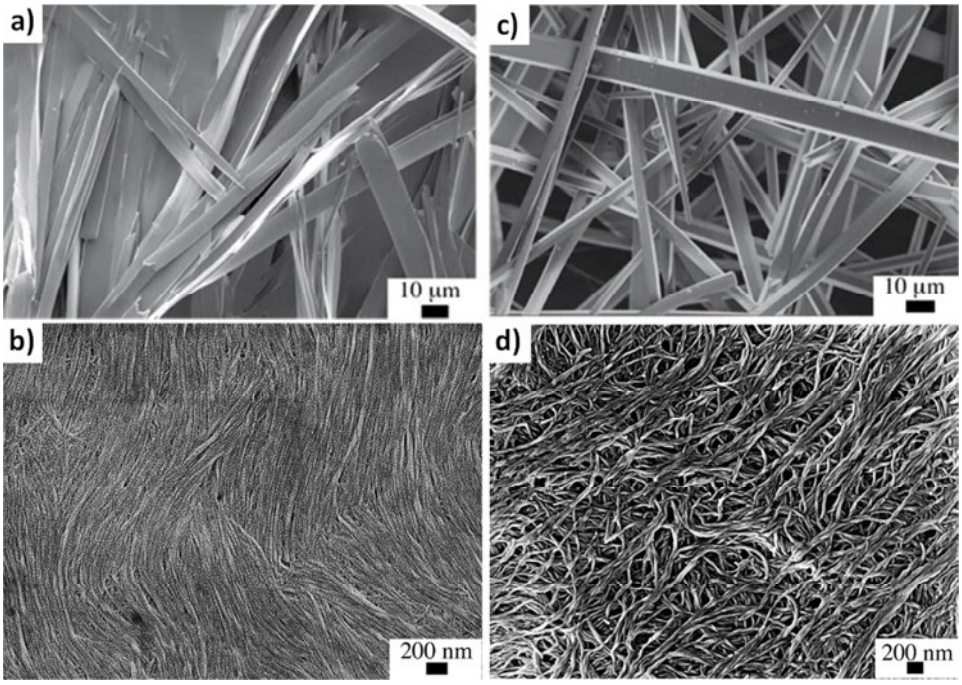

FIGURE 36 SEM micrographs of xerogels derived from 0.6 w/v% of (a) **L7**, (b) **$AgNO_3$●L7**, (c) **L8,** (d) **$AgNO_3$●L8**.

The size, shape, and distribution of silver nanoparticles (AgNPs) over gel networks was studied by TEM. It was observed that the size and shape of the AgNPs are related to the rate of reduction. Usually, the photoreduction was known to be slower than the chemical reduction. When exposing CPGs prepared from bipyridyl ether derivatives (**L7** and **L8**) to daylight, a gradual colour change from colourless to brown was observed for **$AgNO_3$●L7** (Fig. 37a), while **$AgNO_3$●L8** gels were found to be resistant for daylight reduction. Surprisingly, the photoreduced gels were found to be stable for more than a year. This might be due to the gelation ability of the ligand itself. In the case of CPGs obtained from pyridyl and bipyridyl amide derivatives (**L9−L12**), AgNP formation was observed without any stimuli (reduction under darkness). This could be explained by the reduction capability of aq. DMSO solvent or the amide functionality of the ligand. A TEM image of photoreduced **$AgNO_3$●L7** gel shows 3−4 nm (Fig. 37b) highly monodispersed AgNPs on the gel network fibres. Similarly, ~2 nm (Fig. 37c,d) monodispersed AgNPs were observed in **$AgNO_3$●L9** and **$AgNO_3$●$L11_2$** gels.

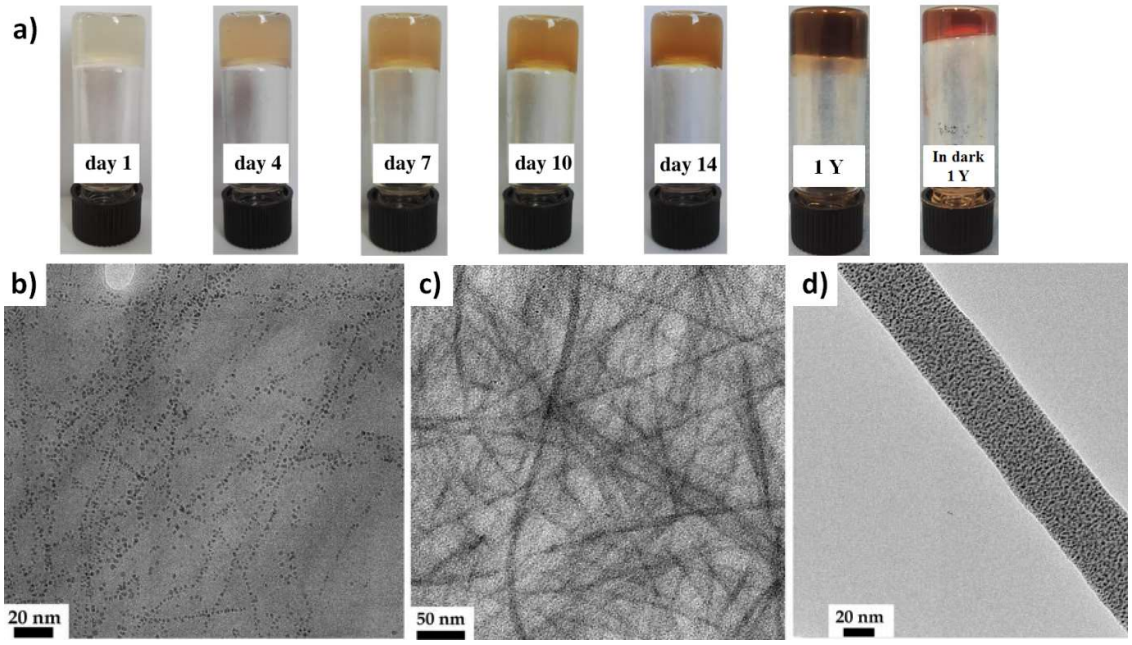

FIGURE 37 Photographs showing visual colour change of **$AgNO_3$●L7** gel upon exposure to daylight or in dark (a) and TEM micrographs of photochemically reduced **$AgNO_3$●L7** (b), **$AgNO_3$●L9** (c), and **$AgNO_3$●$L11_2$** (d) gels.

To compare size and distribution of these photochemically obtained *in situ* AgNPs, chemical reduction experiments with $NaBH_4$ of the **$AgNO_3$●7** gel were conducted. The chemical reduction resulted in about 20 nm (Fig. 38a) polydisperse nanoparticles. When photochemically inactive **$AgNO_3$●8** gel was subjected to chemical reduction, it resulted in much larger AgNPs (>50 nm) with either cuboctahedron or prismatic shape (Fig. 38b).

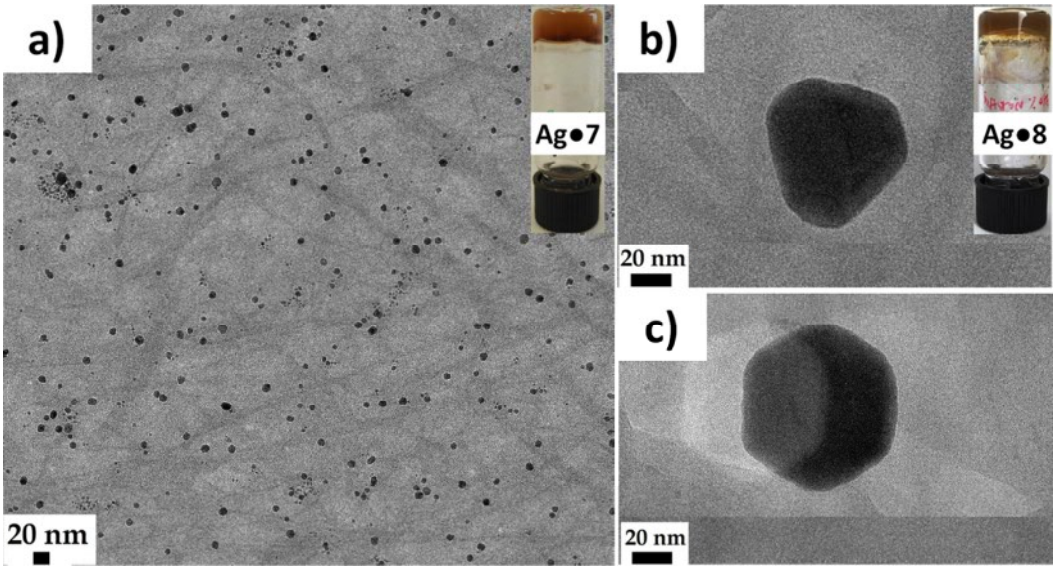

FIGURE 38 TEM micrographs of $NaBH_4$-mediated chemically reduced **$AgNO_3$●7** (a) and **$AgNO_3$●8** (b & c) gels.

2.4.5 UV-Vis spectroscopy

In situ nanoparticle formation in supramolecular CPGs (Papers III and IV) upon exposing to daylight or chemical reduction or without any stimuli was confirmed using UV-Vis spectroscopy, which revealed as characteristic surface-plasmon resonance around 430−450 nm (Fig. 39). No surface-plasmon resonance was observed in freshly prepared gels.

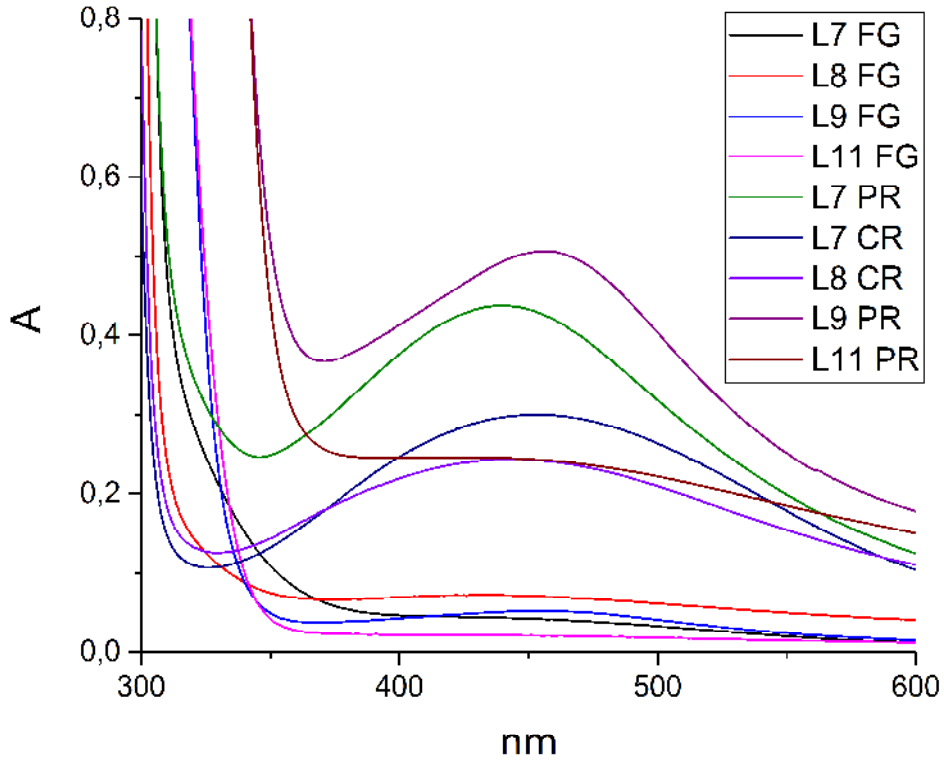

FIGURE 39 UV-Vis spectra of freshly prepared (FG), photo reduced (PR) and chemically reduced (CR) metallogels in DMSO.

2.5 Luminescence studies

2.5.1 Photoluminescence in solid state

Photoluminescence properties of semirigid biimidazole ligands (L4 and L5) and their silver and zinc CPs were studied in the solid state; the spectra obtained are presented in Fig. 40. The free ligands L4 and L5 display fluorescence with emission maxima at 495 nm (excitation at 450 nm) and 410 nm (excitation at 350 nm) respectively. It should be stated that fluorescence emission of L4 and L5 in the solid state depends on the excitation wavelength and shows additional emission peaks in the UV range. Similar dual fluorescence can be seen in the literature for biimidazoles and N-substituted biimidazoles.[165]

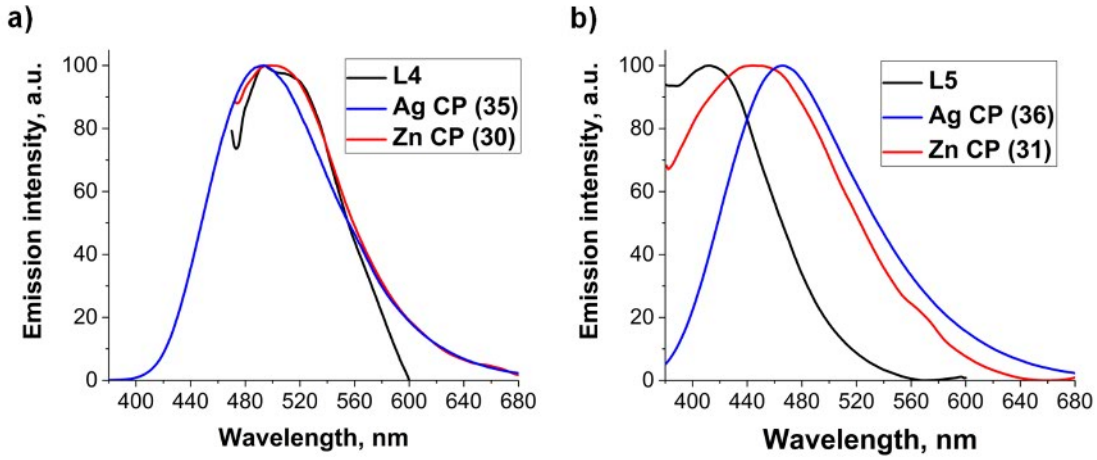

FIGURE 40 Photoluminescence spectra of **L4**, **L5** and their silver and zinc CPs in solid state.

No fluorescence was observed for silver CPs (**35** and **36**), but they exhibited intense phosphorescence with emission maxima at 490 nm (excitation at 280 nm) and 465 nm (excitation at 250 nm), respectively. The absence of fluorescence can be explained with the heavy-atom effect of the metal centre. The ability of Ag(I) ions to promote intersystem crossing to the triplet excited states within CPs is well known in the literature.[166]

Zinc CPs (**30** and **31**) possess fluorescence emission with maxima at 495 nm (excitation at 450 nm) and 445 nm (excitation at 370 nm), respectively. Apart from fluorescence, both CPs display weak phosphorescence emission at 520 nm.

2.5.2 Luminescence of metallogels

The luminescence properties of CPGs derived by silver coordination to the ligands **L9−L12** were investigated. All the gels obtained displayed weak emission in the visible range upon excitation at 300 nm (Fig. 41a). Temperature-dependent emission spectra of metallogels revealed that the luminescence intensity decreased upon heating and completely disappeared upon dissolution of the gels (Fig. 41c and 41d). This phenomenon is called aggregation-induced emission (AIE). The emission spectra of all the gels displayed additional emission bands at 362 and 393 nm, which is attributed to solvent admixture; the emission intensity depended on the transparency of the metallogel.

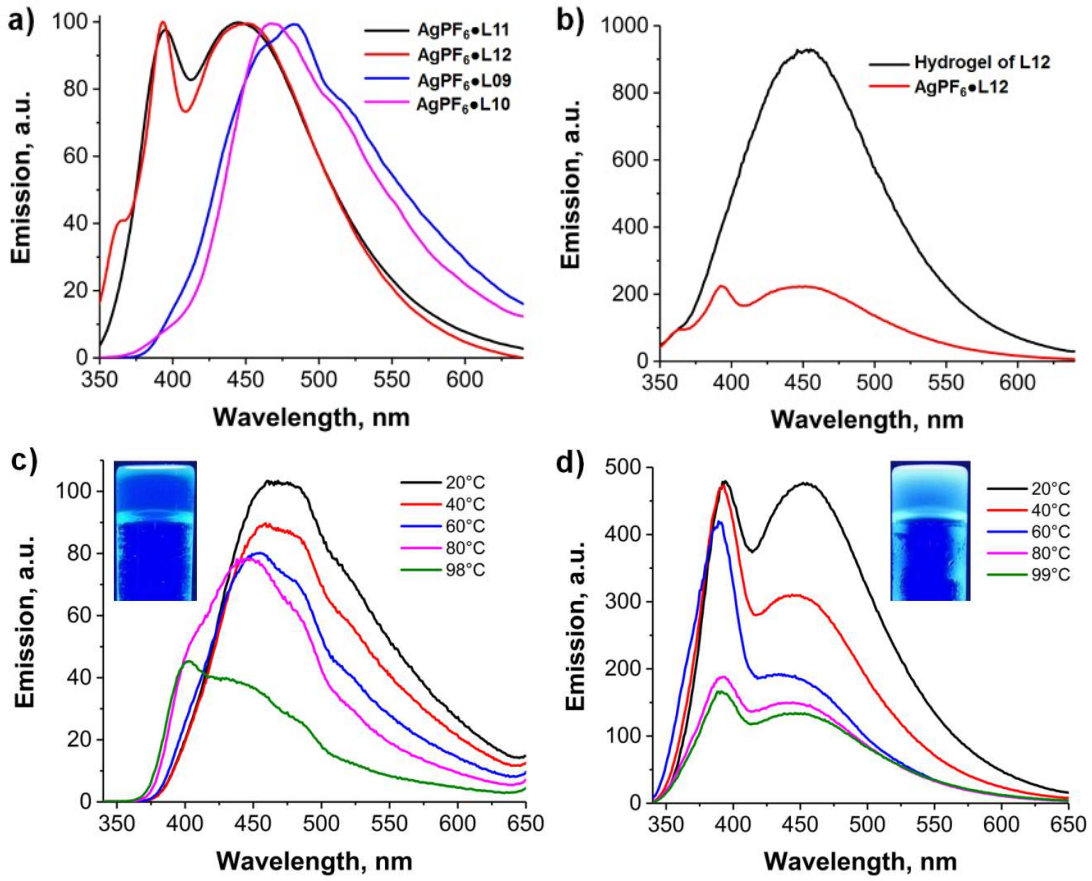

FIGURE 41 a) Normalized emission spectra of metallogels. b) Emission spectral comparison of ligand 12 and its metallogel. c & d) Temperature-dependent emission spectra of **$AgPF_6$•9 (c;** in 7:3 of DMSO: water (v/v) at 0.6 wt%) and **$AgPF_6$•11_2 (d;** in 3:7 of DMSO: water at 0.8 wt%) gels.

Comparison of emission spectra of hydrogels derived from L12 with its CPG (Fig. 41b) reveals the same emission wavelength, even though the emission intensity of the CPG is several orders of magnitude lower. From this the preliminary assignment for the luminescence of the metallogels can be made to intraligand π*−π or π*−n transitions. Based on literature evidence, the lower emission intensity of metallogels could be explained as due to Ag(I) singlet-triplet transitions or suppressed vibrational relaxation due to the increased rigidity of the polymer.[167,168] CPGs of L9 and L10 display red-shift emission compared to pure solid ligands; this is due to the chelation of silver atoms by bipyridyl moieties of the ligand.

3 SUMMARY AND CONCLUSIONS

In summary, this thesis describes the synthesis and characterisation of multivalent N-donor ligands from biimidazole and bipyridines and their coordination compounds with late transition metals (Cu, Zn, and Ag) in neutral and acidic media.[I–IV]

In the first part of the project, the coordination chemistry of ring- (aldehyde) and N-substituted (alkyl) 2,2′-biimidazole (**L1−L3**) ligands were investigated with zinc and copper in neutral and acidic media.[I] In the neutral medium, mononuclear copper and binuclear zinc coordination compounds were obtained. When the reaction was performed in an acidic medium (pH= 3−4), the formation of ion pairs and surprisingly, zwitterionic coordination compounds were observed. In zwitterionic coordination compounds the ligand was monodentate; its formation mainly relies on the combination of pH together with ring- and N-substituents. In ion pairs, the ligand was double-protonated and involved in intermolecular H-bonding with metal dianions (MCl_4^{2-}, M= Zn or Cu). Upon dissolution, these zwitterionic compounds are decomposed to form a neutral ligand and $HZnCl_3$ salt. All these coordination compounds were primarily characterised with single-crystal X-ray diffractometer.

The second part of the research was devoted to possibilities to control the structure of CPs by varying metal centres and reaction conditions.[II] Two semirigid ditopic biimidazole (**L4** and **L5**) ligands were employed as linkers, where they showed two sets of binding sites (N_{Im} and N_{Py}) for metal coordination. The competition between N_{Im} and N_{Py} atoms in metal coordination was explained by considering negative electrostatic potential values (NEPs) associated with the N_{Im} and N_{Py} atoms. The high NEPs of N_{Py} (−182 kJ/mol) makes them more prone to metal coordination than the low NEPs of N_{Im} (−128 kJ/mol). These results are found to be in good agreement with the Aakeröy study, where these ligands were used as halogen/hydrogen bond donors. The effect of reaction solvent on the coordination geometry of silver (linear and tetrahedral) atoms was observed to result in two CPs with different dimensionalities. Surprisingly, the reduction of Cu(II) to Cu(I) in a mixture of water and DMSO was observed to give CPs with different structural topologies.

The third part of the project delt with the synthesis of several bipyridine- and pyridine-based ligands (**L6−L12**). These ligands either differ in the spacer between bipyridine and pyridine rings or in the position of the nitrogen atom at the pyridine ring. In this study, they were used as low molecular-weight ligands to form CPGs by

silver coordination.[III, IV] Metallogelation was observed only in a mixture of water and DMSO/DMF at different ratios (v/v). The study also revealed the effect of photo- and chemical reduction on the size and distribution of *in situ* formed silver nanoparticles (AgNPs) on the gel network.[III] AgNP formation without any stimuli was studied for CPGs derived from ligands L9−L12; it was explained by considering the reduction capability of the solvent mixture or the amide spacer in the ligand structure.[IV] AgNP formation was confirmed with UV-Vis spectral measurements by observing surface-plasmon resonance around 450 nm. Size, shape and distribution of AgNPs in gel samples were also studied with HR-TEM imaging. The aggregation-induced emission (AIE) properties of CPGs obtained from ligands L9−L12 were studied in detail. All gelation experiments with other transition metals were led to negative results; this suggested that gelation is cation-specific.

REFERENCES

1. Olson, D. C.; Vasilevkis, *J. Inorg. Chem*. **1971**, *10*, 463−470.
2. Blackman, A. G. *Polyhedron*. **2005**, *24*, 1−39.
3. Albrecht, M.; Janser, I.; Fröhlich, R. *Chem. Commun*. **2005**, 157−165.
4. Petrovic, D.; Bannenberg, T.; Randoll, S.; Jones, P. G.; Tamm, M. *Dalton Trans*. **2007**, 2812−2822.
5. Savastano, M.; Bazzicalupi, C.; Giorgi, P.; Bianchi, A. *Molecules*. **2017**, *22*, 816.
6. Gupta, P.; Gupta, J. K. *Int. J. Modern Chem*. **2015**, *7*, 60−80.
7. Barnett, S. A.; Champness, N. R. *Coord. Chem. Rev*. **2003**, *246*, 145−168.
8. Kharisov, B. I.; Martinez, P. E.; Jimenez-Perez, V. M.; Kharissova, O. V.; Martinez, B. N.; Perez, N. *J. Coord. Chem*. **2010**, *63*, 1−25.
9. Murata, T.; Morita, Y.; Nishimura, Y.; Nakasuji, K. *Polyhedron*, **2005**, *24*, 2625−2631.
10. Murata, T.; Yakiyama, Y.; Nakasuji, K.; Morita, Y. *Cryst. Growth Des*. **2010**, *10*, 4898−4905.
11. Kaes, C.; Katz, A.; Hosseini, M. W. *Chem. Rev*. **2000**, *100*, 3553−3590.
12. Constable, E. C.; Housecroft, C. E. *Coord. Chem. Rev*. **2017**, *350*, 84−104.
13. Buist, D.; Williams, N. J.; Reibenspies, J. H.; Hancock, R. D. *Inorg. Chem*. **2010**, *49*, 5033−5039.
14. Metrangolo, P.; Meyer, F.; Pilati, T.; Resnati, G.; Terraneo, G. *Angew. Chem. Int. ed*. **2008**, *47*, 6114−6127.
15. Nichol, G. S.; Clegg, W. Cryst. *Growth Des*. **2009**, *9*, 1844−1850.
16. Takemura, A.; McAllister, L. J.; Karadakov, P. B.; Pridmore, N. E.; Whitwood, A. C.; Bruce, D. W. *CrystEngComm*. **2014**, *16*, 4254−4264.
17. Tothadi, S. *CrystEngComm*. **2014**, *16*, 7587−7597.
18. Goulle, V.; Thummel, R. P. *Inorg. Chem*. **1990**, *29*, 1767−1772.
19. Li, J.; Widlicka, D. W.; Fichter, K.; Reed, D. P.; Weisman, G. R.; Wong, E. H.; DiPasquale, A.; Heroux, K. J.; Golen, J. A.; Rheingold, A. L. *Inorg. Chim. Acta*. **2010**, *364*, 185−194.
20. Tsai, C. S. *Can. J. Chem*. **1967**, *45*, 2862−2864.
21. a) Sato, Y.; Takizawa, S.-Y.; Murata, S. *Eur. J. Inorg. Chem*. **2015**, 5495−5502. b) Kim; M.; Oh, S.; Kim, J.; Park, K.-M.; Kang, Y. *Dyes Pigm*. **2017**, *146*, 386−391.
22. Apen, P. G.; Rasmussen, P. G. *J. Am. Chem. Soc*. **1991**, *113*, 6178-6187.
23. A) Rasmussen, P. G.; Bailey, O. H.; Bayon, J. C. *Inorg. Chem*. **1984**, *23*, 338-343. B) Mijangos, E.; Costa, J. S.; Roubeau, O.; Teat, S. J.; Gamez, P.; Reedijk, J.; Gasque, L. *Cryst. Growth Des*. **2008**, *8*, 3187-3192.
24. Sabiah, S.; Lee, C.-S.; Hwang, W.-S.; Lin, I. J. B. *Organometallics*. **2010**, *29*, 290−293.

25. a) Gulbransen, J. L.; Fitchett, C. M. *CrystEngComm*. **2014**, *14*, 5394−5397. b) Ferguson, J. L.; Fitchett, C. M. *Cryst. Growth Des*. **2015**, *15*, 1280−1288.
26. Laurila, E.; Oresmaa, L.; Kalenius, E.; Hirva, P.; Haukka, M. *Polyhedron*. **2013**, *52*, 1231−1238.
27. Yang, L.-N.; Zhi, Y.-X.; Hei, J.-H.; Li, J.; Zhang, F.-X.; Gao, S.-Y. *J. Coord. Chem*. **2011**, *64*, 2912−2922.
28. Wang, J.-L.; Zhang, L.-C.; Li, X.-H.; You, C.-C.; Zhu, Z.-M. *Transition Met. Chem*. **2012**, *37*, 303−307.
29. Majumdar, P.; Peng, S.-M.; Goswami, S. J. Chem. Soc., *Dalton Trans*. **1998**, 1569−1574.
30. Das, A.; Mobin, S. M.; Lahiri, G. K. *Dalton Trans*. **2015**, *44*, 13204−13219.
31. Rommel, S. A.; Sorsche, D.; Schonweiz, S.; Kubel, J.; Rockstroh, N.; Dietzek, B.; Streb, C.; Rau, S. *J. Organomet. Chem*. **2016**, *821*, 163−170.
32. Kaiser, S. W.; Saillant, R. B.; Butler, W. M.; Rasmussen, P. G. *Inorg. Chem*. **1976**, *15*, 2688−2694.
33. Kamar, K. K.; Falvello, L. R.; Fanwick, P. E.; Kim, J.; Goswami, S. *Dalton Trans*. **2004**, 1827−1831.
34. Li, Y.-P.; Yang, P. *Chin. J. Chem*. **2010**, *28*, 759−765.; *Inorg. Chem. Commun*. **2011**, *14*, 545−549.
35. Martinez-Lillo, J.; Armentano, D.; De Munno, G.; Marino, N.; Lloret, F.; Julve, M.; Faus, J. *CrystEngComm*. **2008**, *10*, 1284−1287.
36. Lewis, G. R.; Orpen, A. G. *Chem. Commun*. **1998**, *0*, 1873−1874.
37. Gillon, A. L.;Orpen, A. G.; Starbuck, J.; Wang, X.-M.; Rodriguez-Martin, Y.; Ruiz-Perez, C. *Chem. Commun*. **1999**, 2287−2288.
38. Dolling, B.; Gillon, A. L.; Orpen, A. G.; Starbuck, J.; Wang, X.-M. *Chem. Commun*. **2001**, 567−568.
39. Angeloni, A.; Crawford, P. C.; Orpen, A. G.; Podesta, T. J.; Shore, B. J. *Chem. Eur. J*. **2004**, *10*, 3783−3791.
40. Atencio, R.; Briceno, A.; Galindo, X. *Chem. Commun*. **2005**, 637−639.
41. Bailer, J. C. J. In *Preparative InorganicReactions, Ed*. W. L. Jolly, InterscicencePublishers, John Wiley & Sons, Newyork: **1964**, *vol 1*, pp.1−27.
42. Connelly, N. G.; Damhus, T.; Hartshorn, R. M.; Hutton, A. T. *Nomenclature of Inorganic Chemistry IUPAC Recommendations* **2005**.
43. Robin, A. Y.; Fromm, K. M. *Coord. Chem. Rev*. **2006**, *250*, 2127−2157.
44. Fromm, K. M.; Sague, J. L.; Mirolo, L. *Macromol. Symp*. **2010**, *291*, 75−93.
45. Sanchez-Serratos, M.; Alvarez, J. R.; Gonzalez-Zamore, E.; Ibarra, I. A. *J. Mex. Chem. Soc*. **2016**, *60*, 43−57.
46. Chen, C.-T.; Suslick, K. S. Coord. Chem. Rev. 1993, 128, 293−322.
47. Janiak, C. Dalton Trans. 2003, 2781−2804.
48. Moulton, B.; Ma, Z. Coord. Chem. Rev. 2011, 255, 1623−1641.

49. Rao, C. N. R.; Ranganathan, A.; Pedireddi, V. R.; Raju, A. R. *Chem. Commun*. **2000**, 39−40.
50. Su, W.; Hong, M.; Weng, J.; Caro, R.; Lu, S. *Angew. Chem. Int. Ed*. **2000**, *39*, 2911−2914.
51. Noro, S.-I.; Kitaura, R.; Kitagawa, S. *Angew. Chem. Int. Ed*. **2004**, *43*, 2334−2375.
52. Janiak, C.; Vieth, J. K. *New. J. Chem*. **2010**, *34*, 2366−2388.
53. Lin, Z.-J.; Lu, J.; Hong, M.; Cao, R. *Chem. Soc. Rev*. **2014**, *43*, 5867−5895.
54. Hong, M.-C.; Chen, L. Ed. Design and Construction of CPs; Chapters 1 and 5; *John wiley & Sons, Inc*., Hoboken, New Jersey, USA.
55. Khlobystov, A. N.; Blake, A. J.; Champness, N. R.; Lemenovskii, D. A.; Majouga, A. G.; Zyk, N. V.; Schroder, M. *Coord. Chem. Rev*. **2001**, *222*, 155−192.
56. Yamada, S.; Ishida, T.; Nogami, T. *Dalton Trans*. **2004**, 898−903.
57. Wang, R.; Xu, L.; Li, X.; Li, Y.; Shi, Q.; Zhou, Z.; Hong, M.; Chan, A. S. C. *Eur. J. Inorg. Chem*. **2004**, 1595−1599.
58. Zhang, J.-P.; Horike, S.; Kitagawa, S. *Angew. Chem. Int. Ed*. **2007**, *46*, 889−892. *J. Am. Chem. Soc*. **2008**, *130*, 907−917.
59. Tabacaru, A.; Pettinari, C.; Marchetti, F.; Di Nicola, C.; Domasevitch, K. V.; Galli, S.; Masciocchi, N.; Scuri, S.; Grappasonni, I.; Cocchioni, M. *Inorg. Chem*. **2012**, *51*, 9775−9788.
60. Fromm, K. M. *Appl. Organometal. Chem*. **2013**, *27*, 683−687.
61. Cardoso, J. M. S.; Galvao, A. M.; Guerreiro, S. I.; Leitao, J. H.; Suarez, A. C.; Carvalho, M. F. N. N. *Dalton Trans*. **2016**, *45*, 7114−7123.
62. Graham, P. M.; Pike, R. D.; Sabat, M.; Bailey, R. D.; Pennington, W. T. *Inorg. Chem*. **2000**, *39*, 5121−5132.
63. Pedireddi, V. R.; Shimpi, M. R.; Yakhmi, J. V. *Macromol. Symp*. **2006**, *241*, 83−87
64. Hu, S.; Zhou, A.-J.; Zhang, Y.-H.; Ding, S.; Tong, M.-L. *Cryst. Growth Des*. **2006**, *6*, 2543−2550.
65. Tzeng, B.-C.; Chang, T.-Y. *Cryst. Growth Des*. **2009**, *9*, 5343−5350.
66. Li, B.; Peng, Y.; Li, G.; Hua, J.; Yu, Y.; Jin, D.; Shi, Z.; Feng, S. *Cryst. Growth Des*. **2010**, *10*, 2192−2201.
67. Zhang, Z.; Liu, J.; Li, Y.; Yao, S.; Wang, E.; Wang, X. *J. Solid State Chem*. **2010**, *183*, 228−233.
68. Knorr, M.; Bonnot, A.; Lapprand, A.; Khatyr, A.; Strohmann, C.; Kubicki, M. M.; Rousselin, Y.; Harvey, P. D. *Inorg. Chem*. **2015**, *54*, 4076−4093.
69. Benson, E. E.; Rheingold, A. L.; Kubiak, C. P. *Inorg. Chem*. **2010**, *49*, 1458−1464.
70. Kounavi, K. A.; Kitos, A. A.; Moushi, E. E.; Manos, M. J.; Papatriantafyllopoulou, C.; Tasiopoulos, A. J.; Perlepes, S. P.; Nastopoulos, V. *CrystEngComm*. **2015**, *17*, 7510−7521.
71. Du, M.; Bu, X.-H.; Guo, Y.-M.; Liu, H. *Inorg. Chem*. **2002**, *41*, 4904−4908.

72. Balamurugan, R.; Palaniandavar, M.; Gopalan, R. S. *Inorg. Chem.* **2001**, *40*, 2246−2255.
73. Jayamani, A.; Sengottuvelan, N.; Kang, S. K.; Kim, Y.-I. *Polyhedron*. **2015**, *98*, 203−216.
74. Noro, S.-I.; Kitaura, R.; Kondo, M.; Kitagawa, S.; Ishii, T.; Matsuzaka, H.; Yamashita, M. *J. Am. Chem. Soc.* **2002**, *124*, 2568−2583.
75. Hu, F.; Yin, X.; Mi, Y.; Li, W.; Tang, X.; Ma, Z. Inorg. *Chem. Commun*. **2010**, *13*, 720−723.
76. Carlucci, L.; Ciani, G.; Moret, M.; Proserpio, D. M.; Rizzato, S. *Angew. Chem. Int. ed*. **2000**, *39*, 1506−1510.
77. Lane, A. C.; Barnes, C. L.; Antholine, W. E.; Wang, D.; Fiedler, A. T.; Walensky, J. R. *Inorg. Chem*. **2015**, *54*, 8509−8517.
78. Zhou, X.-P.; Li, D.; Zheng, S.-L.; Zhang, X.; Wu, T. *Inorg. Chem*. **2006**, *45*, 7119−7125.
79. Rentschler, E.; Gatteschi, D.; Cornia, A.; Favretti, A. C.; Barra, A.-L.; Shchegolikhina, O. I.; Zhdanov, A. A. *Inorg. Chem*. **1996**, *35*, 4427−4431.
80. Mrozinski, J. *Coord. Chem.Rev*. **2005**, *249*, 2534−2548.
81. Erxleben, A. *Coord. Chem. Rev*. **2003**, *246*, 203−228.
82. Hu, C.; Englert, U. *CrystEngComm*. **2001**, *23*, 1-5.
83. Guo, F. *Inorg. Chim. Acta*. **2013**, *399*, 79-84.
84. Bu, X.-H.; Chen, W.; Lu, S.-L.; Zhang, R.-H.; Liao, D.-Z.; Bu, W.-M.; Shionoya, M.; Brisse, F.; Ribas, J. *Angew. Chem. Int. Ed*. **2001**, *40*, 3201−3203.
85. Oh, M.; Stern, C. L.; Mirkin, C. A. *Chem. Commun*. **2004**, 2684−2685.
86. Oh, M.; Stern, C. L.; Mirkin, C. A. *Inorg. Chem*. **2005**, *44*, 2647−2653.
87. Dong, Y.-B.; Jiang, Y.-Y.; Li, J.; Ma, J.-P.; Liu, F.-L.; Tang, B.; Huang, E.-Q.; Batten, S. R. *J. Am. Chem. Soc*. **2007**, *129*, 4520−4521.
88. Kim, H.-J.; Zin, W.-C.; Lee, M. *J. Am. Chem. Soc*. **2004**, *126*, 7009−7014.
89. Kim, H.-J.; Lee, J.-H.; Lee, M. *Angew. Chem. Int. Ed*. **2005**, *44*, 5810−5814.
90. Lu, J. Y.; Cabrera, B. R.; Wang, R.-J.; Li, J. *Inorg. Chem*. **1999**, *38*, 4608−4611.
91. Jalbout, A. F.; Li, X.-H.; Hassan, M. R.; Golzar Hossain, G. M. *Transition Met. Chem*. **2008**, *33*, 597−603.
92. Sires, U. I.; Mallory, S. B. Postgrad. Med. J. 1995, 98, 79−84.
93. Lloyd, D. J. In *Colloidal Chemistry*: *Theoretical and Applied*; Alexander, J. (Ed.); *The chemical Catalog Co*.: Newyork, **1926**; pp 767−782.
94. a) Flory, P. J. *Faraday Discuss. Chem. Soc. Rev*. **1974**, *57*, 7−18. b) Almdal, K.; Dyre, J.; Hvidt, S.; Kramer, O. *Polym Gels Netw*. **1993**, *1*, 5−17.
95. Fialkowski, M.; Bishop, K. J. M.; Klajn, R.; Smoukov, S. K.; Campbell, C. J.; Grzybowski, B. A. *J. Phys. Chem.* **B 2006**, *110*, 2482−2496.
96. Pappas, C. G.; Sasselli, I. R.; Ulijn, R. V. *Angew. Chem. Int. Ed*. **2015**, *54*, 8119−8123.

97. Sangeetha, N. M.; Maitra, U. *Chem. Soc. Rev*. **2005**, *34*, 821−836.
98. a) Estroff, L. A.; Hamilton, A. D. *Chem. Rev*. **2004**, *104*, 1201−1217. b) Du, X.; Zhou, J.; Shi, J.; Xu, B. *Chem. Rev*. **2015**, *115*, 13165−13307.
99. Terech. P.; Weiss, R. G. *Chem. Rev*. **1997**, *97*, 3133−3159.
100. Anac, I.; Aulasevich, A.; Junk, M. J. N.; Jakubowicz, P.; Roskamp, R. F.; Menges, B.; Jonas, U.; Knoll, W. *Macromol. Chem. Phys*. **2010**, *211*, 1018−1025**.**
101. Applegarth, L.; Clark, N.; Richardson, A. C.; Parker, A. D. M.; Radosavljevic-Evans, I.; Goeta, A. E.; Howard, J. A. K.; Steed, J. W. *Chem. Commun*. **2005**, 5423−5425.
102. Khatua, S.; Stoeckli-Evans, H.; Harada, T.; Kuroda, R.; Bhattacharjee, M. *Inorg. Chem*. **2006**, *45*, 9619−9621.
103. Adarsh, N. N.; Dastidar, P. *Cryst. Growth Des*. **2011**, *11*, 328−336.
104. Ghosh, D.; Lebedyte, I.; Yufit, D. S.; Damodaran, K. K.; Steed, J. W. *CrystEngComm*. **2015**, *17*, 8130−8138.
105. Primo, A.; Liebel, M.; Quignard, F. *Chem. Mater*. **2009**, *21*, 621−627.
106. Gronwald, O.; Shinkai, S. *Chem. Eur. J*. **2001**, *7*, 4328−4334.
107. Kotova, O.; Daly, R.; Das Santos, C. M. G.; Boese, M.; Kruger, P. E.; Boland, J. J.; Gunnlaugsson, T. *Angew. Chem. Int. Ed*. **2012**, *51*, 7208−7212.
108. Fages, F. *Angew. Chem. Int. ed*. **2006**, *45*, 1680−1682.
109. Arnedo-Sanchez, L.; Nonappa. N.; Bhowmik, S.; Hietala, S.; Puttreddy, R.; Lahtinen, M.; De Cola, L.; Rissanen, K. *Dalton trans*. **2017**, *46*, 7309−7316.
110. De Loos, M.; Feringa, B. L.; Van Esch, J. H. *Eur. J. Org. Chem*. **2005**, 3615−3631.
111. Xing, B.; Choi, M.-F.; Xu, B. *Chem. Eur. J*. **2002**, *8*, 5028−5032.
112. Jung, J. H.;, Lee, J. H.; Silverman, J. R.; John, G. *Chem. Soc. Rev*. **2013**, *42*, 924−936.
113. Diaz, D. D.; Kuhbeck, D.; Koopmans, R. J. *Chem. Soc. Rev*. **2011**, *40*, 427−448.
114. Tam, A. Y.-Y.; Yam, V. W.-W. *Chem. Soc. Rev*. **2013**, *42*, 1540−1567.
115. Lin, Q.; Lu, T.-T.; Zhu, X.; Sun, B.; Yang, Q.-P.; Wei, T.-B.; Zhang, Y.-M. *Chem. Commun*. **2015**, *51*, 1635−1638.
116. Sutar, P.; Maji, T. K. *Chem. Commun*. **2016**, *52*, 8055−8074.
117. Haring, M.; Diaz, D. D. *Chem. Commun*. **2016**, *52*, 13068−13081.
118. Tam, A. Y.-Y.; Wong, K. M.-C.; Yam, V. W.-W. *Chem. Eur. J*. **2009**, *15*, 4775−4778.
119. Zhang, J.; Su, C.-Y. *Coord. Chem. Rev*. **2013**, *257*, 1373−1408.
120. Brassinne, J.; Fustin, C.-A.; Gohy, J.-F. *J Inorg Organomet Polym*. **2013**, *23*, 24−40.
121. Dastidar, P.; Ganguly, S.; Sarkar, K. *Chem. Asian. J*. **2016**, *11*, 2484−2498.
122. Fang, W.; Liu, C.; Chen, J.; Lu, Z.; Li, Z.-M.; Bao, X.; Tu, T. Chem. Commun. 2015, 51, 4267−4270.
123. Escuder, B.; Rodriguez-Llansola, F.; Miravet, J. F. *New. J. Chem*. **2010**, *34*, 1044−1054.
124. Cametti, M.; Cetina, M.; Dzolic, Z. *Dalton Trans*. **2015**, *44*, 7223−7229.

125. Kelly, N.; Gloe, K.; Doert, T.; Hennersdorf, F.; Heine, A.; Marz, J.;m Schwarzenbolz, U.; Weigand, J. J.; Gloe, K. *J. Organomet. Chem*. **2016**, *821*, 182−191.
126. He, Y.; Bian, Z.; Kang, C.; Cheng, Y.; Gao, L. *Chem. Commun*. **2010**, *46*, 3532−3534.
127. Li, Y.; Tam, A. Y.-Y.; Wong, K. M.-C.; Li, W.; Wu, L.; Yam, V. W.-W. *Chem. Eur. J*. **2011**, *17*, 8048−8059.
128. Beck, J. B.; Rowan, S. J. *J. Am. Chem. Soc*. **2003**, *125*, 13922−13923.
129. Tan, X.; Chen, X.; Zhang, J.; Su, C.-Y. *Dalton Trans*. **2012**, *41*, 3616−3619.
130. Yu, X.; Wang, Z.; Li, Y.; Geng, L.; Ren, J.; Feng, G. *Inorg. Chem*. **2017**, *56*, 7512−7518.
131. Chan, M. H.-Y.; Ng, M.; Leung, S. Y.-L.; Lam, W. H.; Yam, V. W.-W. *J. Am. Chem. Soc*. **2017**, *139*, 8639−8645.
132. Zhang, S.; Yang, S.; Lan, J.; Yang, S.; You, J. *Chem. Commun*. **2008**, 6170−6172
133. Lee, J. H.; Kang, S.; Lee, J. Y.; Jung, J. H. *Soft Matter*. **2012**, *8*, 6557−6563.
134. Qin, L.; Wang, P.; Guo, Y.; Chen, C.; Liu, M. *Adv. Sci*. **2015**, *2*, 1500134.
135. He, Y.; Bian, Z.; Kang, C.; Gao, L. *Chem. Commun*. **2010**, 46, 5695−5697.
136. He, Y.; Bian, Z.; Kang, C.; Gao, L. *Chem. Commun*. **2011**, *47*, 1589−1591.
137. Kawano, S.-I.; Fujita, N.; Shinkai, S. *J. AM. Chem. Soc*. **2004**, *126*, 8592−8593.
138. Zhang, Y.; Zhang, B.; Kuang, Y.; Gao, Y.; Shi, J.; Zhang, X. X.; Xu, B. *J. Am. Chem. Soc*. **2013**, *135*, 5008−5011.
139. a) Ghosh, B. N.; Bhowmik, S.; Mal, P.; Rissanen, K. *Chem. Commun*. **2014**, *50*, 734−736. b) Bhowmik, S.; Ghosh, B. N.; Rissanen, K. *Org. Biomol. Chem*. **2014**, *12*, 8836−8839.
140. Bhowmik, S.; Ghosh, B. N.; Marjomäki, V.; Rissanen, K. *J. Am. Chem. Soc*. **2014**, *136*, 5543−5546.
141. Sutar, P.; Suresh, V. M.; Maji, T. K. *Chem. Commun*. **2015**, *51*, 9876−9879.
142. Sutar, P.; Maji, T. K. *Chem. Commun*. **2016**, *52*, 13136−13139.; *Inorg. Chem*. **2017**, *56*, 9417−9425.
143. Suresh, V. M.; De, A.; Maji, T. K. *Chem. Commun*. **2015**, *51*, 14678−14681.
144. Mukhopadhyay, S.; Maitra, U.; Ira.; Krishnamoorthy, G.; Schmidt, J.; Talmon, Y. *J. Am. Chem. Soc*. **2004**, *126*, 15905−15914.
145. Takahashi, A.; Sakai, M.; Kato, T. *Polym. J*. **1980**, *12*, 335−341.
146. Allix, F.; Curcio, P.; Pham, Q. N.; Pickaert, G.; Jamart-Gregoire, B. *Langmuir*. **2010**, *26*, 16818−16827.
147. Xue, M.; Lu, Y.; Sun, Q.; Liu, K.; Liu, Z.; Sun, P. *Cryst. Growth Des*. **2015**, *15*, 5360−5367.
148. Kikuchi, J.; Yasuhara, K. In *Supremolecular Chemistry: From molecules to Nanomaterials*; Steed, J. W.; Gale, P. A. (Eds.), Wiley&Sons Ltd.: Chichester, UK, 2012; Vol. 7, pp 633−646.

149. Friedrich, H.; Frederik, P. M.; With, G. D.; Sommerdijk, N. A. J. M. *Angew. Chem. Int. Ed*. **2010**, *49*, 7850−7858.
150. Sollich, P.; *Phys. Rev. E*. **1998**, *58*, 738−759.
151. Ostuni, E.; Kamaras, P.; Weiss, R. G. *Angew. Chem. Int. Ed*. **1996**, *35*, 1324−1326.
152. Amendola, V.; Meneghetti, M. J. Phys. Chem. C 2009, 113, 4277−4285.
153. Mansur, H. S.; Orefice, R. L.; Mansur, A. A. P. *Polymer*. **2004**, *45*, 7193−7202.
154. Whitten, J. P.; Matthewes, D. P.; McCarthy, J. R. *J. Org. Chem*. **1986**, *51*, 1891−1894.
155. Aakeröy, C. B.; Wijeyhunga, T. K.; Desper, *J. Mol. Struct*. **2014**, *1072*, 20−27.
156. a) Cabrera, P. J.; Yang, X.; Suttil, J. A.; Brooner, R. E. M.; Thompson, L. T.; Sanford, M. S. *Inorg. Chem*. **2015**, *54*, 10214−10223. b) Tatikonda, R.; Bhowmik, S.; Rissanen, K.; Haukka, M.; Cametti, M. *Dalton trans*. **2016**, *45*, 12756−12762.
157. Zhang, Y.; Zhou, R.; Shi, J.; Zhou, N.; Epstein, I. R.; Xu, B. *J. Phys. Chem*. **B 2013**, *117*, 6566−6573.
158. Gardner, T. S.; Wenis, E.; Lee, J. *J. Org. Chem*. **1954**, *19*, 753−757.
159. Sang, R.; Xu, l. *Inorg. Chem*. **2005**, *44*, 3731−1337.
160. Atencio, R.; Ramirez, K.; Reyes, J. A.; Gonzalez, T.; Silva, P. *Inorg. Chim. Acta*. **2005**, *358*, 520−526.
161. Aakeröy, C. B.; Wijethunga, T. K.; Desper, J. *New. J. Chem*. **2015**, *39*, 822−828.
162. Aakeröy, C. B.; Wijethunga, T. K.; Desper, J.; Moore, C. *J. Chem. Crystallogr*. **2015**, *45*, 267−276.
163. Uemura, K. *Inorg. Chem. Commun*. **2008**, *11*, 741−744.
164. Kumar, D. K.; Jose, D. A.; Dastidar, P.; Das, A. *Langmuir*. **2004**, *20*, 10413−10418.
165. Shi, Z.; Peng, J.; Zhang, Z.; Yu, X.; Alimaje, K.; Wang, X. *Inorg. Chem. Commun*. **2013**, *33*, 105−108
166. Xiao, Y.-H.; Huang, J.; Deng, Z.-P.; Huo, L.-H.; Gao, S. *J. Solid State Chem*. **2017**, *251*, 255−265.
167. Wilson, J. A.; LaDuca, R. L. *Inorg. Chim. Acta*. **2013**, *403*, 136−141.
168. Beard, T. A.; Wilson, J. A.; LaDuca, R. L. *Inorg. Chim. Acta*. **2017**, *466*, 30−38.

ORIGINAL PAPERS

I

SYNTHESIS AND CHARACTERIZATION OF ZWITTERIONIC ZN(II) AND CU(II) COORDINATION COMPOUNDS WITH RING-SUBSTITUTED 2,2´-BIIMIDAZOLE DERIVATIVES

by

Rajendhraprasad Tatikonda, Elina Kalenius, & Matti Haukka

Inorg. Chim. Acta., **2016**, *453*, 298−304

Inorganica Chimica Acta 453 (2016) 298–304

Contents lists available at ScienceDirect

Inorganica Chimica Acta

journal homepage: www.elsevier.com/locate/ica

Research paper

Synthesis and characterization of Zwitterionic Zn(II) and Cu(II) coordination compounds with ring-substituted 2,2′-biimidazole derivatives

Rajendhraprasad Tatikonda, Elina Kalenius, Matti Haukka *

Department of Chemistry, University of Jyväskylä, P.O. Box 35, FI-40014 University of Jyväskylä, Finland

ARTICLE INFO

Article history:
Received 29 March 2016
Received in revised form 16 July 2016
Accepted 8 August 2016
Available online 9 August 2016

Keywords:
Zinc
Copper
Biimidazole
Crystal structures
Zwitterionic and non-coordinated compounds

ABSTRACT

Zwitterionic coordination compounds with strongly asymmetrical charge distribution were synthesized and characterized. Ring-substituted biimidazoles were used as the primary ligands for Zn and Cu compounds. Formation of Zwitterionic coordination compound was found to be strongly dependent on the pH of the reaction medium as well as on the ring and nitrogen substituents of the ligand. Reaction of the Df-R_2biim (Df-R_2biim = 2,2′-bi-1R-imidazole-5,5′-dicarboxaldehyde, R = Me, Et or Pr) with $ZnCl_2$ in neutral conditions led to binuclear compounds $[Zn_2Cl_4(Df\text{-}R_2biim)_2]$ with two bridging ligands (**1a–c**). Reaction with $CuCl_2{\cdot}2H_2O$ gave neutral mononuclear compound $[CuCl_2(Df\text{-}Me2biim)]$ (**1d**) with chelating biimidazole ligand. In acidic conditions (pH = 3–4) the imidazole nitrogens were either fully or partially protonated, which prevented the bidentate coordination of the ligands. Furthermore, aldehyde substituents of Df-R_2biim ligands were involved in acetal formation with methanol solvent. Under acidic conditions the primary products were either ion pairs $[MCl_4][C_{14}H_{24}N_4O_4]{\cdot}$(M = Zn **3a**, M = Cu **3b**) with fully protonated H_2L^{2+} counter cation or desired Zwitterionic coordination compounds $[ZnCl_3(C_{16}H_{27}N_4O_4)]$ (**2a**), $[ZnCl_3(C_{18}H_{31}N_4O_4)]$ (**2b**), $[CuCl_3(C_{16}H_{27}N_4O_4)]$ (**2c**), or $[CuCl_3(C_{18}H_{31}N_4O_4)]$ (**2d**) with partially protonated monodentate HL^+ ligand. Zwitterions were obtained only with ligands having both aldehyde groups as ring-substituents and longer alkyl chains (ethyl or propyl) as *N*-substituents. In other cases ion pairs were formed as final products. Zwitterions were found to decompose in alcoholic solutions. In methanol solution, Zwitterionic compounds released neutral ligand and $HZnCl_3$. All main products were characterized by NMR, elemental analysis and single-crystal X-ray diffraction.

1. Introduction

Imidazole is an important aromatic N-heterocyclic compound because of its significant role in biosystems and its versatile coordination ability [1]. The 2,2′-biimidazole molecule, H_2biim, is one of the most useful dimeric analogue of imidazole and well known ligand for transition metals. Compounds containing H_2biim moiety have been the focus of several investigations due to their biological and catalytic activity [2]. anti-protozoal [2a], anti-tuberculosis [2b], anti-cancer [2c], and cardiotonic [2d], properties are examples of pharmacological functionalities of biimidazole based compounds. The conjugate polymers of imidazole and biimidazole containing metal compounds exhibit outstanding sensing properties to metal ions, anions, nitric oxide and amino acids [3]. In H_2biim, two imidazole rings are capable to adopt coplanar orientation when the ligand reacts with a metal cation. This favors chelation as the primary coordination mode [4]. However, few exceptions, where H_2biim behaves as a bridging ligand in binuclear and polynuclear compounds, are also known [5]. If the N–H hydrogens are replaced with bulkier groups, chelation is less likely. Therefore, *N*-substituted R_2biim moieties are more commonly acting as bridging ligands in binuclear [6], oligonuclear or polynuclear [7] compounds. So far, only few literature precedence exist of mononuclear compounds where 1,1′-dimethyl-2,2′-biimidazole, Me_2biim involved in chelation with the metal ion [8].

Coordination modes of unsubstituted biimidazole vary from monodentate to tetradentate depending on the reaction conditions and level of protonation (Fig. 1). In neutral medium the most common coordination mode of H_2biim is bidentate chelating bonding (Fig. 1a) [9]. In this mode the protonated nitrogens are available for H-bonding as H-bond donors [9]. Removal of N-H protons produces typically tridentate (mono-deprotonated biimidazole, $Hbiim^-$) [10], or tetradentate (fully deprotonated biimidazole,

* Corresponding author.
E-mail address: matti.o.haukka@jyu.fi (M. Haukka).

http://dx.doi.org/10.1016/j.ica.2016.08.015
0020-1693/

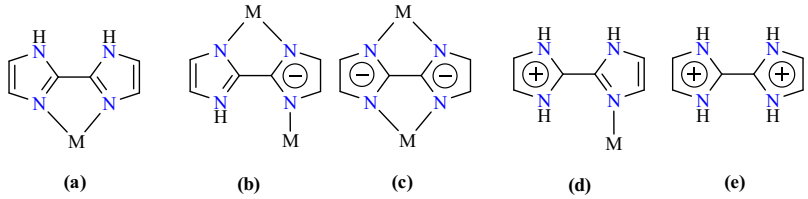

Fig. 1. Coordination mode of H_2biim (a) chelating, (b, c) chelating-bridging, and (d, e) monodentate and ionic.

biim^{-2}) [11] ligands (Fig. 1b,c). Basic medium usually favors these two coordination modes. In acidic medium biimidazole can be protonated to H_3biim$^+$ or H_4biim^{2+}. The cationic H_3biim$^+$ (Fig. 1d) [12] favors monodentate coordination. In H_4biim^{2+} (Fig. 1e) [13] there are no available nitrogens for coordination and therefore H_4biim^{2+} is usually acting as counter cation in ionic systems.

The ring substituents (Fig. 2) have strong impact on physical and chemical properties of the biimidazole molecule. Ring substitution opens up a route for fine-tuning the properties of the ligand. However, only limited number of such biimidazole derivatives have been synthesized and structurally characterized and even fewer of those have been used as ligands in metal compounds [14,15].

This paper describes the synthesis and structural characterization of a series of zinc and copper coordination compounds with ring-substituted Df-R_2biim (2,2′-bi-1R-imidazole-5,5′-dicarboxaldehyde, R = Me, Et or Pr) derivatives. The goal was to use different ring substituents and the level of protonation as tools for preparation of polar and especially Zwitterionic coordination compounds. The products were characterized by NMR, IR, elemental analysis, molar conductivity and single crystal X-ray crystallography. The potential reaction route to Zwitterionic products is also briefly discussed.

2. Experimental section

2.1. General considerations

R_2biim and ring-substituted 2,2′-biimidazole derivatives, 2,2′-bi-1alkyl-imidazole-5,5′-dicarboxaldehyde (Df-R_2biim) were synthesized by following literature methods (see ESI) [16,17]. All other chemicals were obtained from commercial source. The NMR spectra (^{1}H and ^{13}C) of ligands were recorded on Bruker Avance DRX 400 NMR spectrometer and chemical shifts were expressed in ppm. Elemental analyses were performed on VarioEL elemental analyzer. Molar conductivity experiments were performed by using handylab LF11 manufactured by Scott.

2.2. Synthesis

2.2.1. Synthesis of binuclear Zn(II) and mononuclear Cu(II) coordination compounds with Df-R_2biim (R = Me, Et or Pr) (**1a–f**)

A mixture of metal chloride ($ZnCl_2$ or $CuCl_2{\cdot}2H_2O$) and Df-R_2biim (1:1) in methanol was stirred for 30 min to produce binuclear Zn(II) (white precipitate) and mononuclear Cu(II) compounds (blue precipitate). The compound was collected through filtration, washed with cold methanol and dried under vacuum. X-ray quality crystals were obtained with solvent diffusion process of methanolic metal solution to the ligand solution in chloroform. The yield was calculated based on metal salt.

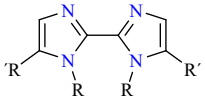

R = Hydrogen or alkyl
R′ = Nitro, Cyano, Aldehyde or Alkyl group

Fig. 2. Ring-substituted (R′) and *N*-substituted (R) 2,2′-Biimidazole.

*2.2.1.1. $[Zn_2Cl_4(C_{10}H_{10}N_4O_2)_2]$ **1a**.* Yield: 82%. ^{1}H NMR (δ, 400 MHz, DMSO-D6): 4.18 (s, 12H), 8.10 (s, 4H), 9.86 (s, 4H). ^{13}C NMR (δ, 100 MHz, DMSO-D6): 34.35, 132.63, 141.94, 142.02, 180.96. Anal. Calcd for $C_{20}H_{20}N_8O_4Zn_2Cl_4{\cdot}CH_3OH$ (741.038): C, 34.04; H, 3.26; N, 15.12. Found: C, 33.84; H, 3.34; N, 14.80. IR (ν, cm^{-1}): 1686 (CO).

*2.2.1.2. $[Zn_2Cl_4(C_{12}H_{14}N_4O_2)_2]$ **1b**.* Yield: 80%. ^{1}H NMR (δ, 400 MHz, DMSO-D6): 1.33 (t, 12H), 4.69 (q, 8H), 8.13 (s, 4H), 9.84 (s, 4H). ^{13}C NMR (δ, 100 MHz, DMSO-D6): 16.12, 41.81, 131.99, 141.30, 143.08, 180.53. Anal. Calcd for $C_{24}H_{28}N_8O_4Zn_2Cl_4$ (765.102): C, 37.68; H, 3.69; N, 14.65. Found: C, 37.22; H, 3.76; N, 14.27. IR (ν, cm^{-1}): 1686 (CO).

*2.2.1.3. $[Zn_2Cl_4(C_{14}H_{18}N_4O_2)_2]$ **1c**.* Yield: 87%. ^{1}H NMR (δ, 400 MHz, DMSO-D6): 0.79 (t, 12H), 1.66-1.75 (m, 8H), 4.69 (t, 8H), 8.14 (s, 4H), 9.84 (s, 4H). ^{13}C NMR (δ, 100 MHz, DMSO-D6): 10.58, 23.75, 47.46, 132.22, 141.56, 142.95, 180.64. Anal. Calcd for $C_{28}H_{36}N_8O_4Zn_2Cl_4$ (821.209): C, 40.95; H, 4.42; N, 13.64. Found: C, 40.68; H, 4.38; N, 13.34. IR (ν, cm^{-1}): 1682 (CO).

*2.2.1.4. $[CuCl_2(C_{10}H_{10}N_4O_2)]$ **1d**.* Yield: 74%. Anal. Calcd for $C_{10}H_{10}N_4O_2CuCl_2$ (352.664): C, 34.06; H, 2.86; N, 15.89. Found: C, 34.12; H, 2.92N, 16.02. IR (ν, cm^{-1}): 1686 (CO).

*2.2.1.5. $[CuCl_2(C_{12}H_{14}N_4O_2)]$ **1e**.* Yield: 78%. Anal. Calcd for $C_{12}H_{14}N_4O_2CuCl_2$ (380.717): C, 37.86; H, 3.71; N, 14.72. Found: C, 37.56; H, 3.66; N, 14.44. IR (ν, cm^{-1}): 1687 (CO).

*2.2.1.6. $[CuCl_2(C_{14}H_{18}N_4O_2)]$ **1f**.* Yield: 77%. Anal. Calcd for $C_{14}H_{18}N_4O_2CuCl_2$ (408.770): C, 41.14; H, 4.44; N, 13.71. Found: C, 40.80; H, 4.42; N, 13.86. IR (ν, cm^{-1}): 1686 (CO).

2.2.2. Synthesis of Zwitterionic coordination compounds **2a–d**

A binuclear (**1b** or **1c**, 0.1 mmol) or mononuclear (**1e** or **1f**, 0.1 mmol) coordination compounds were dissolved in 2 mL of methanol by adding 5–6 drops of Conc. HCl (pH = 3–4). The resulting solution was filtered off and the final crystalline product was obtained by slow evaporation of the solvent. After couple of days, colorless crystals for Zn^{2+} or blue colored crystals for Cu^{2+} were formed in filtrate at room temperature. During the reaction aldehyde groups from the ligand was involved in acetal formation in presence of methanolic HCl solutions. The yield was calculated based on metal salt.

*2.2.2.1. $[ZnCl_3(C_{16}H_{27}N_4O_4)]$ (**2a**).* Yield: 62%. Anal. Calcd for $C_{16}H_{27}N_4O_4ZnCl_3{\cdot}CH_3OH$ (543.191): C, 37.59; H, 5.75; N, 10.31. Found: C, 37.36; H, 5.49; N, 10.45.

*2.2.2.2. [$ZnCl_3(C_{18}H_{31}N_4O_4)$] (**2b**).* Yield: 60%. Anal. Calcd for $C_{18}H_{31}N_4O_4ZnCl_3{\cdot}CH_3OH$ (571.244): C, 39.95; H, 6.18; N, 9.81. Found: C, 39.69; H, 5.96; N, 9.88.

*2.2.2.3. [$CuCl_3(C_{16}H_{27}N_4O_4)$] (**2c**).* Yield: 58%. Anal. Calcd for $C_{16}H_{27}N_4O_4CuCl_3$ (509.32): C, 37.73; H, 5.34; N, 11.00. Found: C, 37.62; H, 5.39; N, 11.02.

*2.2.2.4. [$CuCl_3(C_{18}H_{31}N_4O_4)$] (**2d**).* Yield: 57%. Anal. Calcd for $C_{18}H_{31}N_4O_4CuCl_3$ (537.37): C, 40.23; H, 5.81; N, 10.43. Found: C, 40.42; H, 5.92; N, 10.39.

2b1 is hydrolyzed product of **2b**, where acetal groups are hydrolyzed back to aldehyde. Compound **5** was synthesized following the same procedure but using HBr instead of HCl. Compound 2b1 and **5** was characterized only by single-crystal X-ray crystallography (For single crystal X-ray structure see ESI).

*2.2.3. Synthesis of Cu(II) and Zn(II) ion pairs with Df-Me_2biim (**3ab**)*

Syntheses of ionic compounds were carried out by dissolving binuclear [Zn_2Cl_4(Df-Me_2Biim)$_2$] (**1a**, 0.1 mmol) or mononuclear [$CuCl_2$(Df-Me_2Biim)] (**1d**, 1 mmol) in 2 mL of methanol. The solution was made acidic by adding 5–6 drops of Conc. HCl. After couple of days, colorless or blue crystals were obtained in filtrate. The aldehyde group from the ligand was involved in acetal formation.

*2.2.3.1. [$ZnCl_4$][$C_{14}H_{24}N_4O_4$] (**3a**).* Yield: 64%. Anal. Calcd for $C_{14}H_{24}N_4O_4ZnCl_4$: C, 32.36; H, 4.66; N, 10.78. Found: C, 32.99; H, 4.72; N, 11.85.

*2.2.3.2. [$CuCl_4$][$C_{14}H_{24}N_4O_4$] (**3b**).* Yield: 54%. Anal. Calcd for $C_{14}H_{24}N_4O_4CuCl_4$: C, 32.48; H, 4.67; N, 10.82. Found: C, 33.10; H, 4.80; N, 10.98.

Ion pairs ($[ZnCl_4]^{-2}[C_{10}H_{16}N_4]^{2+}$: **4a** and $[ZnCl_4]^{-2}[C_{12}H_{20}N_4]^{2+}$: **4b**) were synthesized from the reaction of $ZnCl_2$ with R_2Biim (R = Et or Pr) in acidic medium (pH = 3–4). These compounds were characterized only by single crystal X-ray crystallography (see ESI).

2.3. X-ray crystallography

2.3.1. X-ray structure determination

The crystals of **1**–**5** were immersed in cryo-oil, mounted in a MiTeGen loop and measured at 120–123 K. The X-ray diffraction data were collected on an Agilent Technologies Supernova or a Bruker AXS Kappa Apex diffractometer using Mo Kα or Cu Kα radiation. The *CrysAlisPro* [18] or *Denzo-Scalepack* [19] program packages were used for cell refinements and data reductions. Structures were solved by charge flipping method using *SUPERFLIP* [20] program or by direct methods using *SHELXS-2014* [21] program. An analytical, Gaussian, or multi-scan (*CrysAlisPro* [18], *SADABS* [22]) absorption correction was applied to all data. Structural refinements were carried out using *SHELXL-2014* [21] or SHELXL-97 [21] software. In structure **2b1**, carbon atoms of some of the alkyl substituents (C9–C14) were slightly disordered but no disorder model was used in the final structure refinement. In **4a**, one of the ethyl substituents (C9C, C10C/C9D C10D) was disordered over two sites with occupancy ratio of 0.48/0.52. The carbon atoms of these disordered groups were restrained with effective standard deviation 0.01 so that their U_{ij} components approximate to isotropic behavior. In structure **5**, two of alkoxy groups (C13–C15B) were disordered over two sites with occupancy ratio of 0.57/0.43. Also, Br2 atom was slightly disordered but no disorder model was used for the final structure refinement. Hydrogen atoms were either placed in calculated positions or located from the difference Fourier map. In all cases hydrogen atoms were refined using riding model. The crystallographic details of **1b**, **1d**, **2a**, **2b**, **2c**, **3a**, and **3b** are summarized in Table S1. Crystallographic details of all other structures (**4** and **5**) are given in Table S3. Graph sets for intermolecular H-bonding were analyzed by using Mercury [23].

3. Results and discussion

A series of ring-substituted 2,2′-biimidazole derivatives were synthesized by adopting literature procedure [17]. The ligand synthesis method was slightly modified by increasing the reaction time and molar amounts of reagents used to improve the yields and selectivity towards 2,2′-Bi-1R-imidazole-5,5′-dicarboxaldehydes (Df-R_2biim) (see ESI). The ligands (Df-R_2biim) synthesis involves direct lithiation followed by subsequent formylation with DMF in THF solution.

Reaction of Df-R_2biim with $ZnCl_2$ and $CuCl_2{\cdot}2H_2O$ in methanolic solution produced neutral binuclear Zn(II) (**1a**–**c**) [23] and mononuclear Cu(II) (**1d**) compounds (Scheme 1). Reaction of Df-R_2biim with Zn^{2+} led to binuclear compounds with bridging Df-R_2biim ligands linking two tetrahedral Zn centers together. With Cu^{2+} Df-Me_2Biim formed mononuclear square planar structure, where the imidazole derivative was chelating (**1d**). Unlike in structures **1a**–**1c**, the imidazole rings in the chelating **1d** structure were nearly coplanar.

Reaction of Cu^{2+} with ethyl and propyl substituted ligands gave solid products but no X-ray quality crystals could be obtained. These products were characterized only by elemental analysis. Because of the lack of crystal structures, detailed geometries of products **1e** and **1f** could not be confirmed. Based on literature and obtained results, it can be assumed that the structure of **1e** and **1f** could resemble either mononuclear copper compound **1d** or a binuclear zinc compound **1a**–**c** [6,24].

When the compounds **1a**–**1f** were redissolved in methanol by adding few drops of concentrated HCl (pH = 3–4), either one or both metal-nitrogen bonds were broken and protonated. This led to two types of new products i.e. Zwitterionic (**2a**–**d**) coordination compounds (Scheme 1) or ion pairs of the type $[MCl_4]^{2-}[C_{14}H_{24}N_4O_4]^{2+}$ (**3a,b**) or $[MCl_4]^{2-}[H_2R_2biim]^{2+}$ (**4a,b**) depending on the substituents of the biimidazole ligand. Formation of Zwitterionic coordination compounds required low enough pH (3–4) to protonate one of the biimidazole nitrogens. In addition, the biimidazole ligand had to have aldehyde group as ring-substituents and longer alkyl chain (ethyl or propyl) as *N*-substituents. The aldehyde groups were involved in acetal formation during the reaction and this was found to be crucial step to obtain Zwitterionic coordination compounds even if the detailed mechanism is not clear. On the other hand, aldehyde group alone was not enough to get Zwitterionic compounds (**3a,b**). The ligand also had to have longer chain alkyl groups as ring-substituents (Fig. 3).

If either aldehyde group or longer chain alkyl group was missing, only ion pairs were obtained (**3a,b** and **4a,b**). Interestingly, the acetal formation was found to be reversible. When the acetal containing Zwitterion compound **2b** was recrystallized from acetonitrile, the acetal groups were hydrolyzed back to aldehyde (**2b1**) due to residual water of the solvent.

The reaction of $ZnCl_2$ with Df-Et_2Biim was also performed in methanolic HBr solution. In this reaction, the formation of the Zwitterionic compound was accompanied by exchange of Cl ligands with Br (**5**).

3.1. Molar conductivity

The stability of the Zwitterions in solution was studied by dissolving compounds **2a** and **2b** in methanol and measuring the conductivity of the solutions ($5{\cdot}10^{-4}$ M). The conductivities of the solutions of **2a** and **2b** were found to be 52.4 and 52.7 μS/cm at 21 °C respectively. Such values fall into the range of typical 1:1

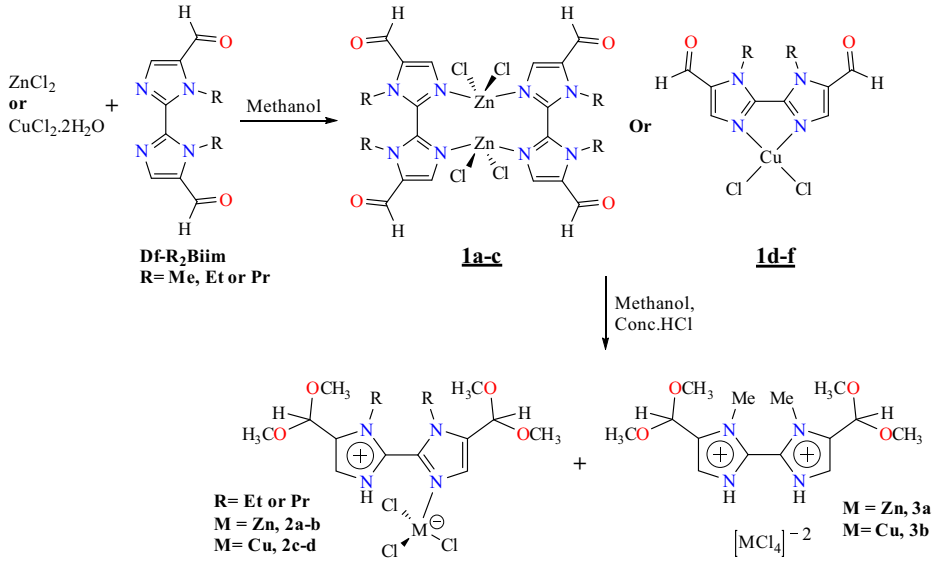

Scheme 1. Synthesis of Zn(II) and Cu(II) compounds in neutral and acidic medium.

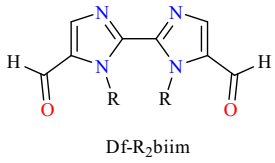

Fig. 3. Ligand required for the Zwitterion formation (R = Et, Pr).

electrolytes (the molar conductivity of $5{\cdot}10^{-4}$ M KCl solution in methanol was found as 52.7 μs/cm at 21 °C) [25] indicating that the Zwitterions were decomposed. It is expected that the proton of the biimidazole is migrated to Zn, which results in release of neutral biimidazole compounds with acetal substituents and $HZnCl_3$ salt (Scheme 2).

The proposed decomposition route was further supported by ^{1}H NMR and mass spectrometric analysis. In ^{1}H NMR only one ring proton signal was observed at δ 7.65 ppm. Mass spectra confirmed the decomposition ($[C_{16}H_{27}N_4O_4]^+$ at m/z_{exp} 339.1892, m/z_{theor} 339.2027; $[C_{18}H_{31}N_4O_4]^+$ at m/z_{exp} 367.2305, m/z_{theor} 339.234 and $[ZnCl_3]^-$ at m/z_{exp} 168.7905, m/z_{theor} 168.8363).

3.2. Crystal structures

The molecular structures with the numbering schemes are shown in Figs. 4–7. Crystallographic data and selected bond distances, angles are summarized in the Supplementary Tables S1, S2 and S3.

3.2.1. $[Zn_2Cl_4(Df\text{-}Et_2Biim)_2]$ (**1b**)

As in the case of known $[Zn_2Cl_4(Me_2Biim)_2]$ structure [24], the zinc atoms in **1b** are centrosymmetrycally double-bridged by two biimidazolic nitrogens to form a binuclear compound. The planes of the imidazole rings of the ligands are nearly perpendicular with the angle of 85.67°. In **1b**, the typical tetrahedral coordination sphere of the Zn atoms are completed by two chlorido ligands. The Zn–N [Zn1–N2 = 2.064(5) Å, Zn1–N4 = 2.053(2) Å], Zn–Cl [Zn–Cl1 = 2.219(3) Å, Zn1–Cl2 = 2.207(5) Å] distances indicate slight asymmetry in the structure and Zn–N bond distances are almost identical to the $[Zn_2Cl_4(Me_2Biim)_2]$ structure. The Zn1–N4 bond length (2.053(2) Å) remains practically unchanged during conversion from the binuclear **1b** to Zwitterionic **2a** and Zn1–N2 bond (2.064(5) Å) opens up allowing a third chloride ligand entering the coordination sphere of Zn.

3.2.2. $[CuCl_2(Df\text{-}Me_2Biim)]$ (**1d**)

The copper atom in this molecule is tetra-coordinated with square planar geometry and surrounded by two chlorido ligands and two nitrogen atoms from the chelating ligand. The bite angle [N2–Cu1–N2] of the chelating biimidazole ligand is 78.96° and the imidazole rings of the ligand are almost coplanar. The angle between the planes of the rings is only about 5.9°. The Cu–N distances (1.988(2) and 2.2261(6) Å) are in the range of typical Cu–N_{im} (1.94–2.03 Å) distances [6,26].

3.2.3. $[ZnCl_3(C_{16}H_{27}N_4O_4)]$ (**2a**)

The coordination geometry around zinc atom is slightly distorted tetrahedron consisting of three chlorido ligands and one nitrogen atom from the singly protonated biimidazole ligand, $[C_{16}H_{27}N_4O_4]^+$. The Zn–Cl bond lengths [Zn1–Cl1 = 2.242(3) Å, Zn1–Cl2 = 2.260(4) Å and Zn1–Cl3 = 2.270(6) Å] show again slight asymmetry of the structure. The angle between the planes of the two-imidazole rings is about 89.3°. In 2a, the intermolecular

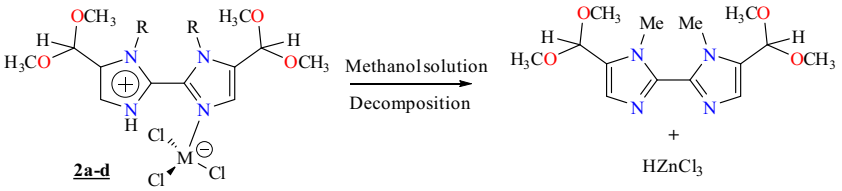

Scheme 2. Decomposition of the Zwitterionic compound in methanolic solution.

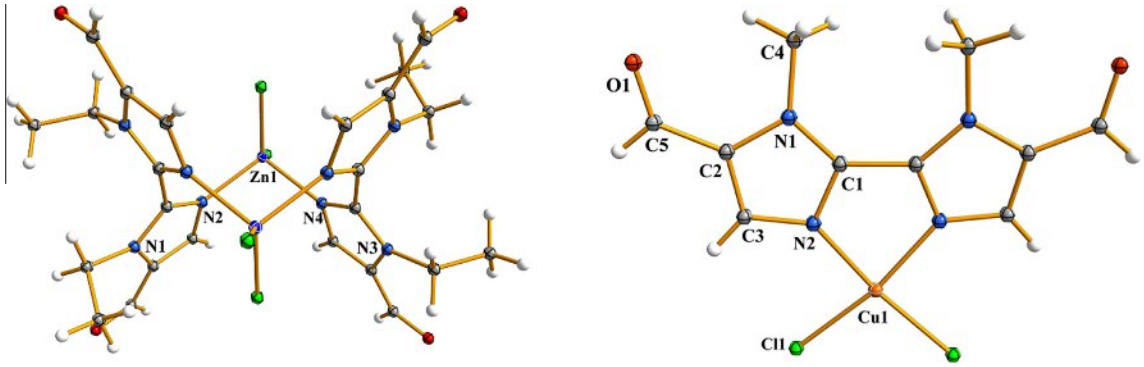

Fig. 4. Molecular structure of **1b** (Left) and **1d** (right). Thermal ellipsoids are drawn at the 50% probability level.

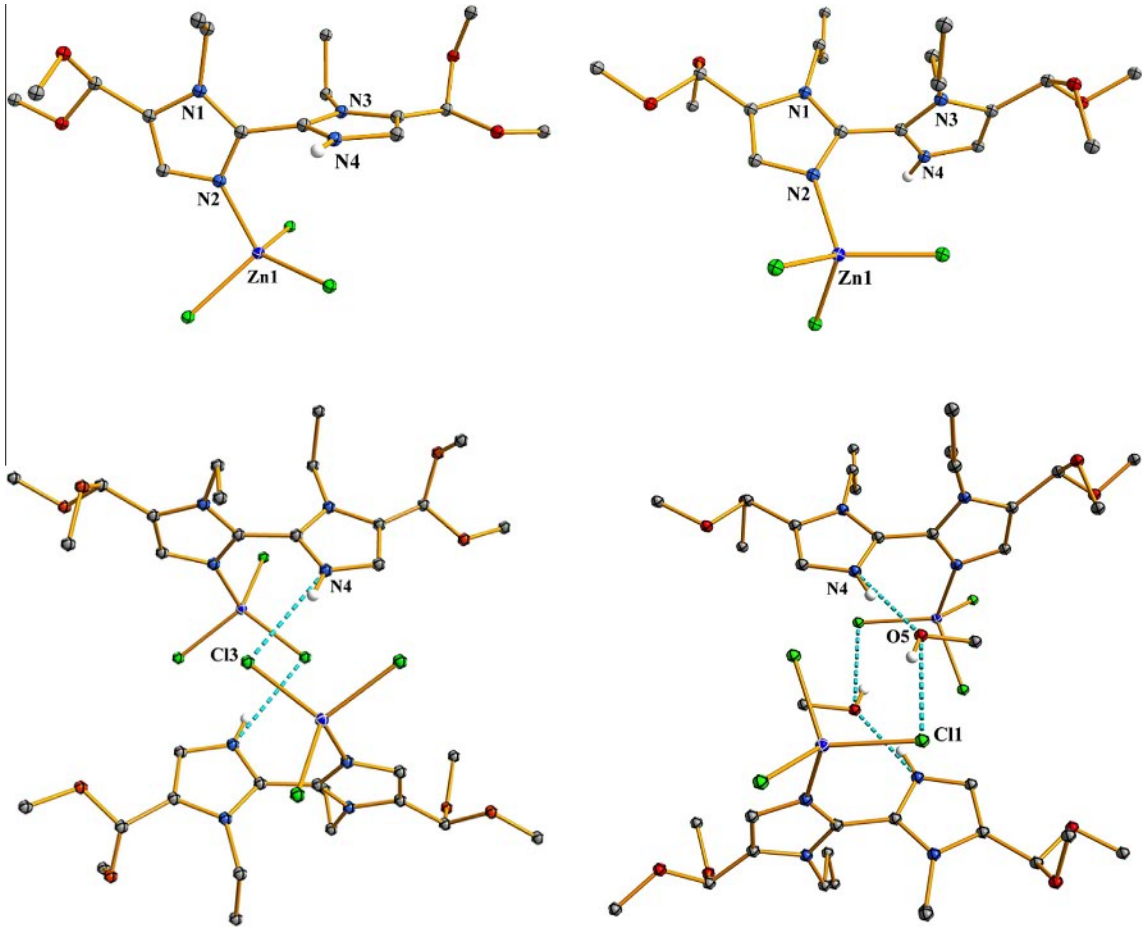

Fig. 5. Molecular structure and intermolecular H-bonding in structure **2a** (left) in $R_2^2(14)$ and **2b** (right) in $R_4^4(18)$ synthons. C–H hydrogens are omitted for clarity (50% probability ellipsoids).

H-bonds are observed between two Zwitterionic molecules with the distance of Cl3···N4^{i} = 3.144(2) Å (i = 1−X, 2−Y, 1−Z), and the angle of N–H···Cl = 154.5° in $R_2^2(14)$ synthon. The N···Cl distance falls in the range of typical N–H···Cl hydrogen bonds (2.91–3.62 Å) [9a,26a,27].

3.2.4. *[$ZnCl_3(C_{18}H_{31}N_4O_4)$] (**2b**)*

The coordination sphere of Zn consists of three chlorido ligands and one nitrogen atom from the biimidazole ligand $[C_{18}H_{31}N_4O_4]^+$ as in **2a**. The structure contains methanol of crystallization, which is hydrogen bonded to the protonated nitrogen of the imidazole ligand (N···O distance: 2.682 Å. The angle between the planes of imidazole rings is somewhat smaller (78.6°) than in **2a**, but the imidazole rings are again clearly not co-planar. During crystallization process, methanol of crystallization was trapped into the crystal voids by H-bonds. The N–H and Cl groups of the neighboring compounds were involved in intermolecular H-bonding with methanol [N···O = 2.682(2) and O···Cl = 3.229(2) Å] and the angles of N–H···O and O–H···Cl are 164.9° and 157.9° respectively. Methanol solvent was acting as H-bonding acceptor in D_1^1 (2)a, donor in D_1^1 (2)b and as both acceptor and donor in $R_4^4(18)$ synthons.

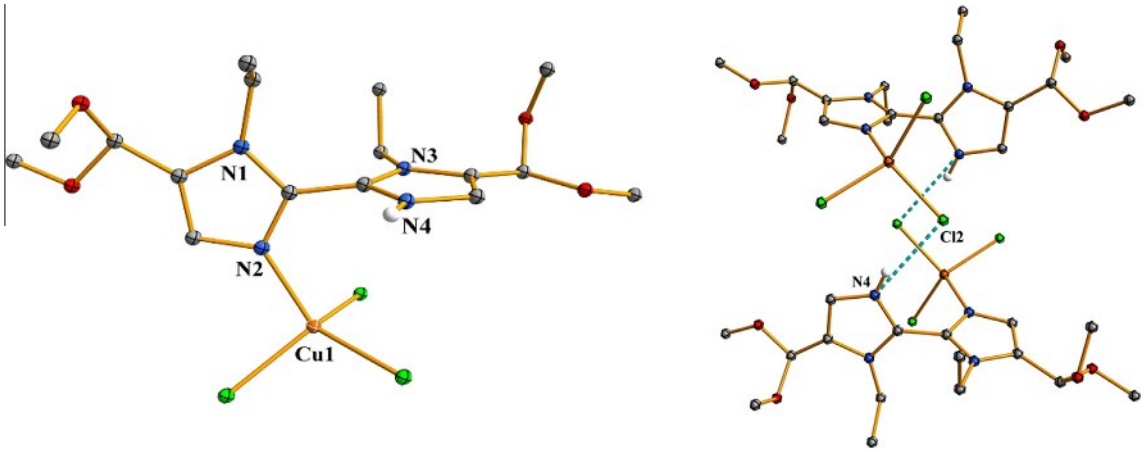

Fig. 6. Molecular structure and intermolecular H-bonding in structure **2c** in $R_2^2(14)$ synthon. C–H hydrogens are omitted for clarity (50% probability ellipsoids).

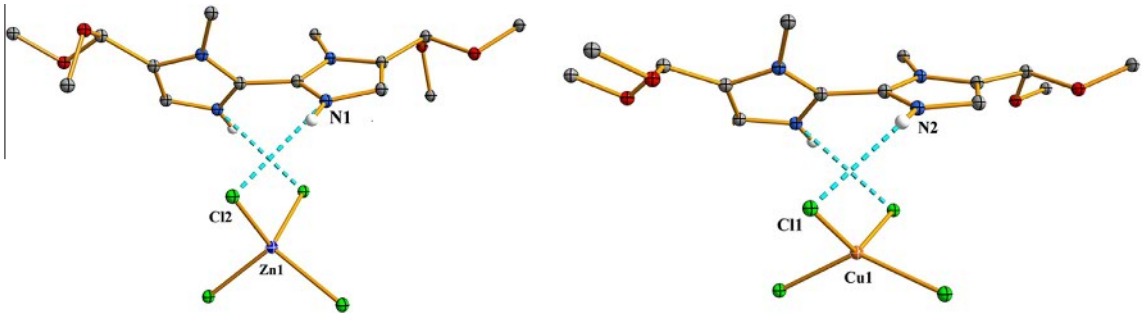

Fig. 7. Molecular structure and H-bonding of **3a** (Zn, right) and **3b** (Cu, left). C–H hydrogens are omitted for clarity. Thermal ellipsoids are drawn at the 50% probability level. The distance of Cl2···N1^{i} in **3a** is 3.172(2) Å (i = 1 − X, +Y, 3/2 − Z) and in **3b** is 3.218(3) Å (Cl1···N2^{i}; i = −X, +Y, 3/2 − Z).

*3.2.5. $[CuCl_3(C_{16}H_{27}N_4O_4)]$ (**2c**)*

The copper atom in this distorted tetrahedral molecule is surrounded by three chlorido ligands and one nitrogen from the imidazole ligand, $[C_{16}H_{27}N_4O_4]^+$. The Cu–N2 distance (2.002(4) Å) is shorter than the corresponding Zn–N2 bond length, which is in the range of typical Cu-N distances (1.94–2.002 Å). The angle between the planes of the two imidazole rings is about 79.2°. Similarly to **2a**, intermolecular H-bonds in **2c**, are observed between two Zwitterionic molecules with the distance of Cl2···N4^{i} = 3.141 (6) Å (i = 2 − X, 1 − Y, −Z), and the angle of N–H···Cl = 158.9° in $R_2^2(14)$ synthon.

No X-ray quality crystals could be obtained from ($[CuCl_3(C_{18}H_{31}N_4O_4)]$) **2d**.

*3.2.6. $[MCl_4][C_{14}H_{24}N_4O_4]$ (M = Zn, **3a**; M = Cu, **3b**)*

The ion pairs of **3a** and **3b** consist of anionic metal compounds ($[CuCl_4]^{2-}$ and $[ZnCl_4]^{2-}$) and fully protonated cationic $[C_{14}H_{24}N_4O_4]^{2+}$. In **3a** and **3b**, intermolecular H-bonding was seen between cation and anionic part of the compound ($R_2^2(9)$ synthon). The distance between Cl2–N1^{i} in **3a** is 3.172(2) Å (i = 1 − X, +Y, 3/2 − Z) and the corresponding distance Cl1–N2^{ii} in **3b** 3.218(3) Å (ii = −X, +Y, 3/2 − Z). In both structures, the imidazole rings of the cations are again not coplanar. The angles between the planes of imidazole rings are 69.3° and 56.9° for **3a** and **3b** respectively.

4. Conclusions

A series of ring-substituted biimidazoles (Df-R_2biim; R = Me, Et or Pr) were used for the synthesis of binuclear Zn(II) and mononuclear Cu(II) compounds. Compound formation was found to depend strongly on the pH of the reaction medium. In neutral reaction conditions the biimidazole ligands were bidentate and acting as bridging ligands in binuclear Zn(II) compounds or chelating ligands in mononuclear Cu(II) compound. Lowering the pH to 3–4 led to partial or full protonation of the two N sites of the ligand. With fully protonated ligands only ion pairs (**3a,b**) were obtained while reactions with partially protonated biimidazoles gave Zwitterionic compounds (**2a**–**d**). In addition to pH, the formation of the Zwitterionic products was found to be dependent on the ring and *N*-substituents of the biimidazoles. Both of these substituents were needed for Zwitterion formation. In acidic media, the aldehyde substituent on the ring was involved in acetal formation and this process was a crucial step in obtaining Zwitterions. Longer alkyl *N*-substituents (ethyl or propyl) were also required for Zwitterion formation while methyl substituent favored ion pairs regardless of aldehyde substituent. In alcoholic solution the Zwitterionic compounds were decomposed to form free neutral ligand and $HZnCl_3$ salt.

Appendix A. Supplementary data

Supplementary data associated with this article can be found, in the online version, at http://dx.doi.org/10.1016/j.ica.2016.08.015.

References

[1] (a) J.Z. Vlahakis, R.T. Kinobe, R.J. Bowers, J.F. Brien, K. Nakatsu, W.A. Szarek, J. Med. Chem. 49 (2006) 4473;
(b) F. Yang, N.G. Nickols, B.C. Li, G.K. Marinov, J.W. Said, P.B. Dervan, PNAS 110 (2013) 1863;
(c) D. Wang, J.T. Groves, PNAS 110 (2013) 15579;
(d) L. Schlechte, V. Bon, R. Grunker, N. Klein, I. Senkovska, S. Kaskel, Polyhedron 44 (2012) 179.

[2] (a) S. Karmakar, M. Nandi, S. Mukherjee, S. Baitalik, Inorg. Chim. Acta (2016) (in press);
(b) C. Tan, S. Hu, J. Liu, L. Ji, Eur. J. Med. Chem. 46 (2011) 1555;
(c) M. Akkawi, A. Aljazzar, M.A. Haj, Q. Abu-Remeleh, Br. J. Pharmacol. Taxicol. 3 (2012) 65;
(d) P. Melloni, E. Dradi, W. Logemann, J. Med. Chem. 15 (1972) 926;
(e) P. Gupta, S. Hameed, R. Jain, Eur. J. Med. Chem. 39 (2004) 805;
(f) Y. Li, Y. Wu, J. Zhao, P. Yang, J. Inorg. Biochem. 101 (2007) 283;
(g) D.P. Matthew, J.R. McCarthy, J.P. Whitten, P.R. Kastner, C.L. Barney, F.N. Marshall, M.A. Ertel, T. Burkhard, P.J. Shea, T. Kariya, J. Med. Chem. 33 (1990) 317.
[3] (a) A. Hoang, L. Mario, J. Am. Chem. Soc. 125 (2003) 4412;
(b) Y. Cui, H.-J. Mo, J.-C. Chen, Y.-L. Niu, Y.-R. Zhong, K.-C. Zheng, B.-H. Ye, Inorg. Chem. 46 (2007) 6427;
(c) Q. Zeng, P. Cai, Z. Li, J. Qin, B.Z. Tang, Chem. Commun. (2008) 1094;
(d) Q. Zeng, C.K.W. Jim, J.W.Y. Lam, Y. Dong, Z. Li, J. Qin, B.Z. Tang, Macromol. Rapid. Commun. 30 (2009) 170;
(e) A. Salinas-Castillo, M. Camprubi-Robles, R. Mallavia, Chem. Commun. 46 (2010) 1263.
[4] (a) S. Fortin, A.L. Beauchamp, Inorg. Chem. 39 (2000) 4886;
(b) A.K. Ghosh, A.D. Jana, D. Ghoshal, G. Mostafa, N. Ray Chaudhuri, Cryst. Growth Des. 6 (2006) 701.
[5] (a) R.-L. Sang, L. Xu, Eur. J. Inorg. Chem. (2006) 1260;
(b) J. Ying, X.-L. Lin, Y.-J. Liu, R. Xiao, X.-L. Wang, A.-X. Tian, Z. Anorg, Allg. Chem. 638 (2012) 135.
[6] (a) R.-L. Sang, L. Xu, Inorg. Chim. Acta 359 (2006) 2337;
(b) S. Sabiah, C.-S. Lee, W.-S. Hwang, Ivan J.B. Lin, Organometallics 29 (2010) 290;
(c) J.L. Ferguson, C.M. Fitchett, Cryst. Growth Des. 25 (2015) 1280.
[7] (a) L.-N. Yang, Y.-X. Zhi, J.-H. Hei, J. Li, F.-X. Zhang, S.-Y. Gao, J. Coord. Chem. 64 (2011) 2912;
(b) Y. Bao, H. Wang, Q. Li, B. Liu, Q. Li, W. Bai, B. Jin, R. Bai, Macromolecules 45 (2012) 3394;
(c) E. Laurila, L. Oresmaa, E. Kalenius, P. Hirva, M. Haukka, Polyhedron 52 (2013) 1231;
(d) Z.-Y. Shi, J. Peng, Y.-G. Li, Z-Y. Zhang, X. Yu, K. Alimaje, X. Wang, CrystEngComm 15 (2013) 7583.
[8] (a) J.S. Casas, A. Castineiras, Y. Parajo, J. Sordo, J.M. Varela, Acta Cryst. C54 (1998) 1777;
(b) J.S. Casas, A. Castineiras, Y. Parajo, A. Sanchez, A. Sanchez-Gonzalez, J. Sordo, Polyhedron 24 (2005) 1196;
(c) G.-G. Shan, H.-B. Li, Z.-C. Mu, D.-X. Zhu, Z.-M. Su, Y. Liao, J. Organomet. Chem. 702 (2012) 27.
[9] (a) R.-L. Sang, L. Xu, Polyhedron 25 (2006) 2167;
(b) R.-L. Sang, L. Xu, Inorg. Chim. Acta. 359 (2006) 525;
(c) L.M. Gruia, F.D. Rochon, A.L. Beauchamp, Inorg. Chim. Acta. 260 (2007) 1825;
(d) Y.-R. Zhong, M.-L. Cao, H.-J. Mo, B.-H. Ye, Cryst. Growth. Des. 8 (2008) 2282.
[10] (a) Z.-M. Hao, S.-L. Li, X.-M. Zhang, Inorg. Chem. Commun. 13 (2010) 1100;
(b) A.-X. Tian, X.-L. Lin, G.-Y. Liu, R. Xiao, J. Ying, X.-L. Wang, J. Coord. Chem. 66 (2013) 1340.
[11] (a) A. Maiboroda, G. Rheinwald, H. Lang, Inorg. Chem. Commun. 4 (2001) 381;
(b) Y.-H. Tan, J.-S. Wu, C.-S. Yang, Q.-R. Liu, Y.-Z. Tang, Y.-R. Zhong, B.-H. Ye, Inorg. Chim. Acta 399 (2013) 45;
(c) S. Mardanya, S. Karmakar, D. Mondal, S. Baitalik, Inorg. Chem. 55 (2016) 3475.
[12] (a) Y.-P. Li, Y. Pin, Chin. J. Chem. 28 (2010) 759;
(b) Y.-P. Li, Y. Pin, Inorg. Chem. Commun. 14 (2011) 545;
(c) H.-J. Jia, Z. Shi, Q.-F. Yang, J.-H. Yu, J.-Q. Xu, Dalton. Trans. 43 (2014) 5806.
[13] (a) J. Martinez-Lillo, D. Armentano, G. De Munno, N. Marino, F. Lloret, M. Julve, J. Faus, CrystEngComm 10 (2008) 1284;
(b) J. Martinez-Lillo, A.H. Pedersen, J. Faus, M. Julve, E.K. Brechin, Cryst. Growth Des. 15 (2015) 2598.
[14] (a) P.G. Apen, P.G. Rasmussen, J. Am. Chem. Soc. 113 (1991) 6178;
(b) C.P. Causey, W.E. Allen, J. Org. Chem. 67 (2002) 5963.
[15] (a) P.G. Rasmussen, O.H. Bailey, J.C. Bayon, Inorg. Chem. 23 (1984) 338;
(b) P.G. Rasmussen, O.H. Bailey, J.C. Bayon, W.M. Butler, Inorg. Chem. 23 (1984) 343;
(c) J.G. Malecki, Polyhedron 29 (2010) 2489.
[16] E. Laurilla, R. Tatikonda, L. Oresma, P. Hirva, M. Haukka, CrystEngComm 14 (2012) 8401.
[17] J.P. Whitten, D.P. Mathews, J.R. McCarthy, J. Org. Chem. 51 (1986) 1891.
[18] Agilent, CrysAlisPro, Agilent Technologies Inc, Yarnton, Oxfordshire, England, 2013.
[19] Z. Otwinowski, W. Minor, Processing of X-ray diffraction data collected in oscillation mode, in: C.W. Carter, J. Sweet (Eds.), Methods in Enzymology, Volume 276, Macromolecular Crystallography, Part A, Academic Press, New York, USA, 1997, pp. 307–326.
[20] L. Palatinus, G. Chapuis, J. Appl. Cryst. 40 (2007) 786.
[21] G.M. Sheldrick, Acta Cryst. A64 (2008) 112.
[22] G.M. Sheldrick, SADABS – Bruker AXS Scaling and Absorption Correction, Bruker AXS Inc, Madison, Wisconsin, USA, 2012.
[23] Graphsets were analysed by using Mercury.
[24] R. Sang, L. Xu, Inorg. Chem. 44 (2005) 3731.
[25] W.J. Geary, Coord. Chem. Rev. 7 (1971) 81.
[26] (a) R. Atencio, K. Ramirez, J.A. Reyes, T. Gonzalez, P. Silva, Inorg. Chim. Acta 358 (2005) 520;
(b) Q.-H. Jin, L.-L. Zhou, L.-J. Xu, Y.-Y. Zhang, C.-L. Zhang, X.-M. Lu, Polyhedron 29 (2010) 317.
[27] (a) M. Felloni, P. Hubberstey, C. Wilson, M. Schroder, CrystEngComm 6 (2004) 87;
(b) E. Laurilla, L. Oresmaa, M. Niskanen, P. Hirva, M. Haukka, Cryst. Growth Des. 10 (2010) 3775.

II

CONSTRUCTION OF COORDINATION POLYMERS FROM SEMI-RIGID DITOPIC 2,2´-BIIMIDAZOLE DERIVATIVES: SYNTHESIS, CRYSTAL STRUCTURES, AND CHARACTERIZATION

by

Rajendhraprasad Tatikonda, Evgeny Bulatov, Elina Kalenius, & Matti Haukka

Cryst. Growth Des., **2017**, *17*, 5918−5926

CRYSTAL GROWTH & DESIGN

Article

Cite This: Cryst. Growth Des. 2017, 17, 5918-5926

pubs.acs.org/crystal

Construction of Coordination Polymers from Semirigid Ditopic 2,2′-Biimidazole Derivatives: Synthesis, Crystal Structures, and Characterization

Rajendhraprasad Tatikonda, Evgeny Bulatov, Elina Kalenius, and Matti Haukka*

Department of Chemistry, University of Jyväskylä, P.O. Box 35, FI-40014 Jyväskylä, Finland

Supporting Information

ABSTRACT: Eight coordination polymers (CPs), $\{[Ag(\mathbf{L1})]ClO_4\}_n$ (**1**), $\{[Ag(\mathbf{L2})_{1.5}]ClO_4{\cdot}C_2H_3N\}_n$ (**2a**), $\{[Ag(\mathbf{L2})]ClO_4\}_n$ (**2b**), $[Zn(\mathbf{L1})Cl_2]_n$ (**3**), $\{[Zn(\mathbf{L2})Cl_2]{\cdot}CHCl_3\}_n$ (**4**), $\{[Cu(\mathbf{L1})_2Cl]Cl{\cdot}H_2O\}_n$ (**5**), $[Cu_2(\mathbf{L2})(\mu\text{-}Cl)_2]_n$ (**6**), and $[Cu_4(\mathbf{L2})(\mu\text{-}Cl)_4]_n$ (**7**) were synthesized via self-assembly of corresponding metal ions and biimidazole based ditopic ligands, 1,1′-bis(pyridin-3-ylmethyl)-2,2′-biimidazole **L1** and 1,1′-bis(pyridin-4-ylmethyl)-2,2′-biimidazole **L2**. These ligands possess conformational flexibility and two pairs of coordination sites: pyridine nitrogen (N_{Py}) atoms and imidazole nitrogen (N_{Im}) atoms. Depending on the metal center in CPs, the biimidazole compounds act as tetra- (**1**, **7**), tri- (**2a**), or bidentate (**2a**, **2b**, **3**–**6**) ligands binding to the metal either via N_{Py} or N_{Im}, or both. All these CPs were structurally fully characterized with single crystal X-ray structure, mass spectrometry, and NMR spectroscopy. The solid state photophysical properties and thermal stabilities of the CPs were also briefly studied in the solid state.

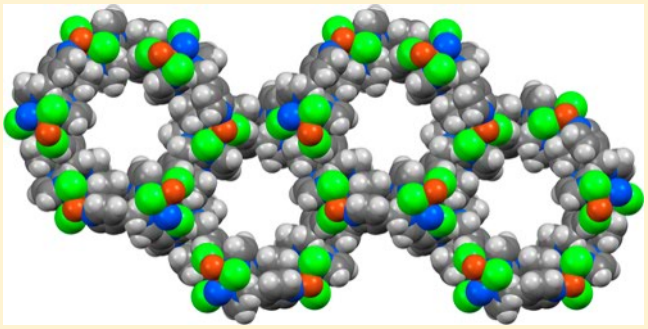

INTRODUCTION

The syntheses of self-assembled coordination polymers (CPs) are receiving growing attention in chemistry as well as in material sciences. Often, CPs are simply obtained by mixing bridging organic ligands and metal ions together. CPs can be tailored to display potential applications in various fields including gas storage,[1−3] nonlinear optics,[4,5] sensing,[6] magnetism,[7,8] catalysis,[9] photocatalysis,[10] and conductivity.[11] Design and production of phosphorescent light emitting devices can also benefit from incorporation of heavy elements into a polymeric chain in coordination polymers.[12] The final structure of CP is dependent on the selection of metal ions, the structure of the connecting ligands, possible counterions, the stoichiometric ratio of the reacting partners, reaction conditions, and the solvents used.[13,14] Recently, there has been increasing attention on flexible or semirigid ligands, particularly a ligand with multiple flexible arms containing several coordination sites.[15−17] Use of semirigid ligands in CPs allows the formation of more diverse structures compared to rigid linking ligands. However, it is still possible to design and obtain desired structures with semirigid ligands as well.[18,19] In this case, the control of the final structure is often more subtle involving adjustments in reaction conditions. The advance of ligand flexibility is that it can generate completely new properties on CPs. For example, the flexibility of the ligands can be used to produce adaptable cavities within CP structures and enhance properties such as molecular sensing and catalytic activity and selectivity.[20,21]

Over the past few decades, 2,2′-biimidazole (biim) and its derivatives have received much attention due to their versatile chemistry.[22−25] However, construction of novel CPs from imidazole and biim derivatives is less thoroughly studied.[26,27] With the aim of construction of new CPs, we have chosen two biim derivatives: 1,1′-bis(pyridin-3-ylmethyl)-2,2′-biimidazole (**L1**) and 1,1′-bis(pyridin-4-ylmethyl)-2,2′-biimidazole (**L2**) as the semirigid ditopic ligands (Figure 1). The presence of a freely rotatable methylene (CH_2) spacer between biim and pyridyl units provides the required flexibility to the ligand. This

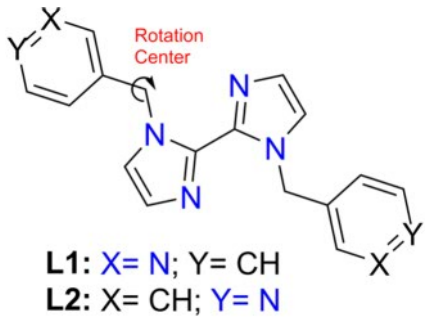

Figure 1. Schematic structure of semirigid ligands (**L1** and **L2**) used for the synthesis of CPs.

Received: July 25, 2017
Revised: October 1, 2017
Published: October 3, 2017

DOI: 10.1021/acs.cgd.7b01034
Cryst. Growth Des. 2017, 17, 5918−5926

type of ligand can provide four binding sites: two imidazole nitrogen (N_{Im}) atoms from the biim moiety and another two from pyridine nitrogen (N_{Py}) atoms.[28] The coordination ability of N_{Im} and N_{Py} donors is entirely different, which opens up possibilities to control the number of N donors involved in the actual coordination simply by choosing a suitable metal ion.

The ligands (**L1** and **L2**) have been studied as halogen and hydrogen bond acceptors by Aakeröy and co-workers.[29−31] They suggested that the negative electrostatic potentials (NEPs) associated with the pyridine nitrogen atoms (N_{Py}; **L1** = −182 kJ/mol and **L2** = −187 kJ/mol) of both the ligands were proven to be nearly the same but higher than the corresponding values of the imidazole nitrogen atoms (N_{Im}; **L1** = −128 kJ/mol and **L2** = −132 kJ/mol) atoms. The higher NEPs of N_{Py} makes them more prone to halogen/hydrogen bonding as well as to metal coordination. However, there are a few reports where N_{Im} coordination was seen along with N_{Py} coordination in the case of **L1**.[32] In acidic reaction conditions, the protonation of N_{Py} atoms directs the ligand toward coordination through N_{Im} atoms.[33]

Choice of the metal ion plays a crucial role in designing CPs due to various electronic structures affecting preferred coordination geometries. In this study, Zn^{2+} was chosen as a metal favoring tetrahedral coordination geometry. Copper and silver were selected to provide more flexible coordination geometries. The common geometries of silver(I) complexes are linear, trigonal, and tetrahedral.[34−37] Typical coordination geometries of copper(I or II) complexes include tetrahedral, square planar, and square pyramidal structures.[38−40]

In this study, we report the synthesis, crystal structures, and characterization of several transition metal (Cu^+, Cu^{2+}, Zn^{2+}, and Ag^+) coordination polymers with two biim based semirigid ligands (**L1** and **L2**), where they act as bi-, tri-, or tetradentate ligands.

EXPERIMENTAL SECTION

All the chemicals were purchased from commercial sources and used without purification. *Caution!!!* Although no problems were encountered in this work, silver perchlorate is potentially explosive. Only a small amount of the material was used and was handled with great care. The ligands (**L1** and **L2**) were synthesized by adopting a literature procedure.[29] NMR spectra (1D and 2D) of the ligands and their CPs were recorded on a Bruker Avance DRX 400, and 500 NMR spectrometers and chemical shifts are expressed in ppm. Elemental analyses were performed on a Vario EL elemental analyzer. Mass spectra were measured with an ABSciex QSTAR Elite ESI-Q-TOF mass spectrometer. Thermogravimetric (TG) analyses were performed under nitrogen with a PerkinElmer STA 6000 analyzer. Powder X-ray diffraction (PXRD) measurements were performed on a Panalytical ÝPert Pro MPD diffractometer operating at Cu Kα wavelength (1.54184 Å), and scans were performed at room temperature in the 2θ range 5−50°. Photoluminescence spectra were measured using Varian Cary Eclipse fluorescence spectrophotometer. Solid samples were ground to powder and pressed into a thin layer between quartz glass plates.

Synthesis of {[Ag(L1)]ClO_4}$_n$ (1). A clear solution of $AgClO_4$ (41.5 mg, 0.2 mmol) in acetonitrile (2 mL) was carefully layered on the top of the ligand solution (**L1**; 63.3 mg, 0.2 mmol) in acetonitrile (3 mL). By the next day, only a few crystals (2D-CP **1**) were obtained along with a white precipitate. Recrystallization of the white precipitate from a mixture of water and MeCN (2:8 v/v) gave colorless crystals of 2D-CP **1**.

*{[Ag(**L1**)]ClO_4}$_n$ (**1**).* Yield: 74.5 mg (~71%): ^{1}H NMR (400 MHz, DMSO-d_6) δ 8.43 (d, 2H), 8.27 (s, 2H), 7.52 (d, 2H), 7.47 (s, 2H), 7.31 (ddd, 2H), 7.11 (s, 2H), 5.75 (s, 4H). ^{13}C NMR (100 MHz, DMSO-d_6) δ 149.06, 148.59, 137.19, 135.43, 133.78, 128.35, 123.86, 122.74, 47.55. ^{1}H−^{15}N COSY NMR (DMSO-d_6 at 30 °C) δ= −207.39 (N1; imidazole), − 118.71 (N2; imidazole) and −70.47 (N3; pyridine). ESI-Q-TOF-MS Calcd for [Ag(**L1**)]$^+$ ($C_{18}H_{16}N_6Ag$)$^+$: 423.0482; found: 423.0475. Anal. calcd. for $C_{18}H_{16}N_6$ ClO_4Ag: C, 41.28: H, 3.08; N, 16.5. Found: C, 41.33; H, 3.17; N, 16.46.

Synthesis of {[Ag(L2)$_{1.5}$]ClO_4·C_2H_3N}$_n$ (2a) and {[Ag(L2)]ClO_4}$_n$ (2b). A clear solution of $AgClO_4$ (41.5 mg, 0.2 mmol) in acetonitrile (2 mL) was carefully layered on the top of ligand solution (**L2**; 63.3 mg, 0.2 mmol) in acetonitrile (3 mL). By next day, a single crystal of 2D-CP **2a** was found in a test tube along with white precipitate. When the product was redissolved in a mixture of water and MeCN (2:8 v/v), colorless crystals of 1D-CP **2b** were formed.

Or a clear solution of $AgClO_4$ (20.7 mg, 0.1 mmol) in water (0.4 mL) was added to the ligand solution (**L2**; 32 mg, 0.1 mmol) in acetonitrile (1.6 mL). In a week, colorless crystals of **2b** were obtained in a solution.

*{[Ag(L2)]ClO_4}$_n$ (**2b**).* Yield: 38.5 mg (~74%): ^{1}H NMR (400 MHz, DMSO-d_6) δ 8.43 (d, 4H), 7.42 (d, 2H), 7.10 (d, 2H), 6.95 (d, 4H), 5.82 (s, 4H). ^{13}C NMR (100 MHz, DMSO-d_6) δ 149.93, 147.37, 137.38, 128.26, 123.00, 121.74, 49.00. ^{1}H−^{15}N COSY NMR (DMSO-d_6 at 30 °C) δ − 212.88 (N1; imidazole), − 119.39 (N2; imidazole) and −73.54 (N3; pyridine). ESI-Q-TOF-MS Calcd for [Ag(L2)]$^+$ ($C_{18}H_{16}N_6Ag$)$^+$: 423.0482; found: 423.049. Anal. Calcd for $C_{18}H_{16}N_6$ ClO_4Ag: C, 41.28: H, 3.08; N, 16.5. Found: C, 41.32; H, 3.24; N,16.39.

Synthetic Procedure for Zinc CPs (3 and 4). A clear solution of $ZnCl_2$ (27.3 mg, 0.2 mmol) in methanol (3 mL) was carefully layered on the top of ligand solution (63.3 mg, 0.2 mmol) in chloroform (2 mL). By next day, only a few colorless crystals were obtained in test tube for CP **4** along with white precipitate, and only precipitate was obtained for CP **3**. Single crystals of CPs **3** and **4** were also obtained by dissolving the precipitate into the mixture of water and DMSO (1:9 v/v).

*[Zn(**L1**)Cl_2]$_n$ (**3**).* Yield: 81 mg (89.4%): ^{1}H NMR (400 MHz, DMSO-d_6) δ 8.43 (dd, 2H), 8.40 (d, 2H), 7.48 (dt, 2H), 7.44 (d, 2H), 7.27 (ddd, 2H), 7.10 (d, 2H), 5.77 (s, 4H). ^{13}C NMR (100 MHz, DMSO-d_6) δ 148.58, 148.50, 137.27, 135.18, 133.74, 128.19, 123.73, 122.60, 47.46. ^{1}H−^{15}N COSY NMR (DMSO-d_6 at 30 °C) δ −207.60 (N1; imidazole), −118.42 (N2; imidazole) and −62.15 (N3; pyridine). ESI-Q-TOF-MS calcd. for [Zn(**L1**)Cl]$^+$ ($C_{18}H_{16}N_6ZnCl$)$^+$: 415.0411; found: 415.0473. Anal. calcd. for $C_{18}H_{16}N_6Cl_2Zn$: C, 47.76: H, 3.56; N, 18.57. Found: C, 47.61; H, 3.73; N, 18.49.

*{[Zn(**L2**)Cl_2]·$CHCl_3$}$_n$ (**4**).* Yield: 82.6 mg (91.2%): ^{1}H NMR (400 MHz, DMSO-d_6) δ 8.43 (dd, 4H), 7.40 (d, 2H), 7.07 (d, 2H), 6.98 (d, 4H), 5.84 (s, 4H). ^{13}C NMR (100 MHz, DMSO-d_6) δ 149.52, 147.70, 137.41, 128.20, 122.95, 121.81, 49.04. ESI-Q-TOF-MS Calcd for [Zn(**L2**)Cl]$^+$ ($C_{18}H_{16}N_6ZnCl$)$^+$: 415.0411; found: 415.0392. Anal. calcd. for $C_{18}H_{16}N_6Cl_2Zn$: C, 47.76: H, 3.56; N, 18.57. Found: C, 47.70; H, 3.68; N, 18.52.

Synthesis of {[Cu(L1)$_2$Cl]Cl·H_2O}$_n$ (5). A solution of $CuCl_2$·$2H_2O$ (34.1 mg, 0.2 mmol) in methanol (2 mL) was carefully layered on top of ligand solution (**L1**; 126.6 mg, 0.4 mmol) in methanol (3 mL). The reaction only leads us to a blue-colored precipitate. The mixture was stirred for ca. 30 min at room temperature to ensure the completion of the reaction. The precipitate was filtered and washed with methanol and dried under vacuum. Single crystals of **5** were obtained from DMSO at room temperature.

Yield: 120 mg (78.2%): ESI-Q-TOF-MS calcd. for [Cu(**L1**)$_2$Cl]$^+$ ($C_{36}H_{32}N_{12}CuCl$)$^+$: 730.1852; found: 730.1845. Anal. calcd. for $C_{36}H_{32}N_{12}Cl_2Cu.H_2O$: C, 55.07: H, 4.36; N, 21.41. Found: C, 54.91; H, 4.42; N, 21.38.

Synthesis of [Cu_2(L2)$_2$(μ-Cl)$_2$]$_n$ (6). A water solution (0.2 mL) of $CuCl_2$·$2H_2O$ (34.1 mg, 0.2 mmol) was added to the DMSO solution (0.8 mL) of **L2** (63.3 mg, 0.2 mmol), and the resulting mixture was gently heated to obtain a clear solution. During heating, the color of the solution turned from green to yellow. When the solution was cooled down to the room temperature, the pale yellow crystalline product was obtained. The product was washed several times with water and dried under vacuum. Yield: 43.5 mg (52.3%): Anal. calcd. for $C_{18}H_{16}N_6ClCu$: C, 52.05: H, 3.88; N, 20.23. Found: C, 51.88; H,

DOI: 10.1021/acs.cgd.7b01034
Cryst. Growth Des. 2017, 17, 5918−5926

Table 1. Crystallographic Data for CPs 1−7

	1	2a	2b	3	4	5	6	7
formula	$C_{18}H_{16}N_6Ag$, ClO_4	$C_{27}H_{24}N_9Ag$, ClO_4, C_2H_3N	$2(C_{18}H_{16}N_6Ag)$, $2(ClO_4)$	$C_{18}H_{16}N_6Cl_2Zn$	$C_{18}H_{16}N_6Cl_2Zn$, $CHCl_3$	$C_{36}H_{32}N_{12}ClCu$, H_2O	$C_{18}H_{16}N_6Cl$ Cu	$C_9H_8N_3ClCu$
fw	523.69	722.92	1047.37	452.64	572.01	785.19	415.36	257.17
temp (K)	120	120	120	120	120	120	123	123
cryst syst	triclinic	triclinic	orthorhombic	monoclinic	monoclinic	tetragonal	monoclinic	trigonal
space group	$P\bar{1}$	$P\bar{1}$	$P2_12_12$	$P2_1/c$	$P2_1/c$	$P4/ncc$	$P2_1/c$	$R\bar{3}c$
a (Å)	9.574(2)	9.714(7)	23.020(2)	8.982(4)	12.291(3)	16.499(6)	6.808(2)	27.849(2)
b (Å)	9.657 (1)	10.624(1)	22.779(2)	10.061(3)	13.905(3)	16.499(6)	9.658(2)	27.849(2)
c (Å)	10.870(2)	16.101(1)	7.0740(6)	24.625(1)	14.808(4)	12.266(9)	27.070(9)	22.093(8)
α (deg)	91.746(1)	71.458(9)	90.00	90	90	90	90	90
β (deg)	105.911(1)	76.979(7)	90.00	122.878(7)	110.538(3)	90	105.397(3)	90
γ (deg)	102.003(1)	75.869(8)	90.00	90	90	90	90	120
V (Å^3)	941.3(2)	1508.0(3)	3709.31(5)	1868.87(2)	2369.93(1)	3339.0(3)	1716.07(9)	14839.0(2)
d_{calc} (g/cm^3)	1.848	1.592	1.876	1.609	1.603	1.562	1.608	1.036
Z	2	2	4	4	4	4	4	36
μ (mm^{-1})	1.254	0.811	10.422	1.616	1.620	2.826	3.351	1.036
ref. collected	5616	9875	23418	29060	15572	8434	12080	9855
ind. ref.	3397	5267	7669	4291	4654	1728	3522	3150
R_{int}	0.0592	0.0696	0.0281	0.0455	0.0276	0.0277	0.0497	0.0461
F(000)	524	734	2096	920	1152	1620	848	4644
GOF	1.162	1.045	1.021	1.060	1.034	1.081	1.168	4644
R_1[a] ($I \geq 2\sigma$)	0.0728	0.0809	0.0267	0.0302	0.0378	0.0388	0.0616	0.0614
wR_2[b] ($I \geq 2\sigma$)	0.1280	0.3004	0.0681	0.0695	0.0977	0.1122	0.1640	0.1820

[a] $R_1 = ||F_o| - |F_c||/|F_o|$. [b] $wR_2 = [[w(F_o^2 - F_c^2)^2]/[w(F_o^2)^2]]^{1/2}$.

4.08; N, 20.12. ESI-Q-TOF-MS Calcd for $[Cu(\mathbf{L2})]^+$ $(C_{18}H_{16}N_6Cu)^+$: 379.0732; found: 379.0727.

Formation of $[Cu_4(L2)_2(\mu\text{-}Cl)_4]_n$ (7). Only a few single crystal of **7** was found along with **6** as a byproduct in the synthesis of **6** described above. To improve the yield of **7**, the molar ratio of metal to ligand (**L2**) was changed from 1:1 to 2:1. However, even in these reaction conditions the compound **6** was the dominating product, and the compound **7** remained as a minor side product.

X-ray Data Collection. The single crystals of ligands (**L1** and **L2**) and their CPs were immersed in cryo-oil, mounted in a MiTeGen loop and measured at 120−123 K. The X-ray diffraction data were collected on Agilent Technologies Supernova diffractometer using Mo Kα (λ = 0.71073 Å) or Cu Kα (λ = 1.54184 Å) radiation. The *CrysAlisPro*[41] program packages were used for cell refinements and data reductions. Structures were solved by either charge-flipping method using a *SUPERFLIP*[42] program or by direct methods using *SHELXS−2008*[43] or *SHELXT−2015*[43] programs. Gaussian or Multiscan absorption correction was applied to all data, and structural refinements were carried out using *SHELXL−2015*[43] software. Details of data collections and structure refinements for CPs **1**−**7** are given in Table 1, while those of ligands (**L1** and **L2**) and **4a** are given in Table S2. In CP **7**, solvent molecules could not be unambiguously determined, and therefore the contribution of the missing solvent to the calculated structure factor was taken into account by using the SQUEEZE routine of PLATON.

RESULTS AND DISCUSSION

All the CPs of Cu(I), Cu(II), Zn(II), and Ag(I) with ligands **L1** and **L2** were synthesized via self-assembly.[44] The structures of coordination polymers in the solid state were determined by using single crystal X-ray diffraction, and their photoluminescence properties were screened using solid-state photoluminescence spectroscopy. Bulk phase purity of all the CPs (**1**, **2b**−**6**) were confirmed by powder X-ray diffraction. The diffractograms are given in the Supporting Information (Figures S19−S21). In all cases, the experimental patterns matched well with the simulated patterns based on the single-crystal X-ray diffraction results. The *N*-coordination of the ligand in Ag and Zn based CPs was also investigated in solution (DMSO-d_6) by 1D (^{1}H and ^{13}C) and 2D (^{1}H−^{15}N) NMR spectroscopy. Structures in the gas phase were analyzed by mass spectrometry (ESI-MS).

Silver(I) CPs from L1 (1; $\{[Ag(L1)]ClO_4\}_n$) and L2 (2a; $\{[Ag(L2)_{1.5}]ClO_4{\cdot}C_2H_3N\}_n$ and 2b; $\{[Ag(L2)]ClO_4\}_n$). The reaction of $AgClO_4$ with **L1** and **L2** at 1:1 molar amounts gave two-dimensional coordination polymers (2D-CPs; **1** and **2a**) and a one-dimensional coordination polymer (1D-CP; **2b**) respectively. Single crystals of 2D-CPs with the ligand **L1** (**1**) and **L2** (**2a**) were obtained from slow diffusion of metal solution into the ligand solution in acetonitrile. The product **2b** was obtained as an inseparable mixture with **2a**. However, when the synthesis was carried out in a mixture of water and MeCN (2:8 v/v), **2b** could be obtained as a pure product with no **2a**. The 2D-CPs were crystallized in triclinic space group $P\bar{1}$, while the 1D-CP was crystallized in orthorhombic space group $P2_12_12$.

In **1** (Figure 2), all the nitrogen atoms ($2N_{Im}$ and $2N_{Py}$) from **L1** were involved in coordination with four different silver atoms. The asymmetric unit contains one full ligand molecule and a silver atom along with the perchlorate anion. The coordination geometry around the silver is distorted tetrahedron with the N4Ag binding set.[45,46] The imidazole rings of biim are twisted out of plane (68.72°) due to bridging coordination of biim. Each silver atom is coordinated by two pyridine nitrogen atoms [Ag−N_{Py} = 2.268(6) Å and 2.372(6) Å] and two imidazole nitrogen atoms [Ag−N_{Im} = 2.293(6) Å and 2.385(6) Å] from four different ligand molecules to generate 2D layered structure (Figure S3). These 2D layers are

DOI: 10.1021/acs.cgd.7b01034
Cryst. Growth Des. 2017, 17, 5918−5926

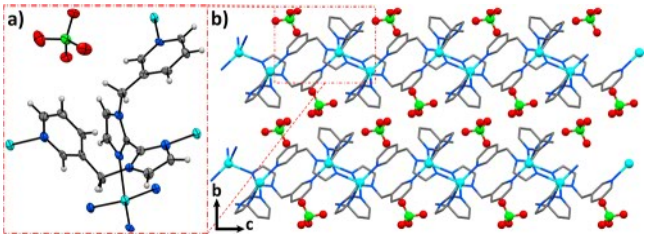

Figure 2. ORTEP plot (50% probability level) of **L1** coordination environment in silver CP **1** (a) and of the crystal packing of **1** viewed along the crystallographic *a*-axis (b).

packed as parallel layers, which interact with each other via several weak C═C−H_{Py}···O and CH_2···O hydrogen bonds through the perchlorate anion (Table S1). The Ag−N_{Py} and Ag−N_{Im} bond distances are in good agreement with those reported for silver complexes with imidazole and pyridine derivatives.[45−48]

In solution, the ^{1}H NMR spectrum of **1** showed a minimal downfield shift for imidazole proton (H2, 0.07 ppm) as well as a upfield shift for pyridine hydrogen (H5, 0.17 ppm) atom compared to that of free ligand **L1**. In addition to ^{1}H NMR, we also recorded ^{1}H−^{15}N COSY spectra for **L1** and CP **1** (Figure S12b). A significant upfield shift was observed for N_{Py} (8.46 ppm) and N_{Im} atoms (2.15 ppm) compared to the free ligand, which is an indication of pyridine and biimidazole coordination. These changes in the chemical shifts support the observed solid-state structure where silver ions are coordinated by the N_{Im} and N_{Py} atoms from the ligand.

The asymmetric unit of **2a** contains one complete ligand molecule, half a ligand molecule and a silver atom (2:3 of Ag to **L2**) along with perchlorate anion and acetonitrile solvent molecule. In **2a**, ligand **L2** exhibits two kinds of coordination modes: one is a μ_3-bridging mode with two N_{Im} and one N_{Py} atoms (uncoordinated pyridine ring shown in the red circle in Figure 3), and the other is a μ_2-bridging mode only with two

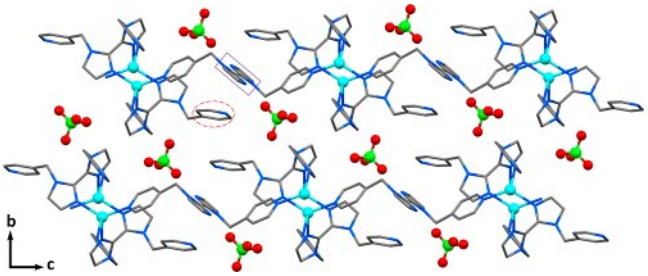

Figure 3. Crystal packing of **2a** viewed along the crystallographic *a*-axis. The uncoordinated pyridine ring is highlighted with a dotted circle and uncoordinate bridging biim with a solid box. Hydrogen atoms and solvent molecules (MeCN) are omitted for clarity.

N_{Py} atoms (uncoordinated biim ring shown in the purple box in Figure 3). The coordination geometry around the silver atom is again distorted tetrahedron with a N4Ag binding set. Similar to **1**, each silver atom is coordinated by two pyridine nitrogen atoms [Ag−N_{Py} = 2.316(7) Å and 2.512(8) Å] and two imidazole nitrogen atoms [Ag−N_{Im} = 2.267(7) Å and 2.277(8) Å] from four separate ligand molecules. In **1**, the crystal packing does not favor direct Ag···Ag contacts, but in **2a** the shortest Ag···Ag distance (3.0898(1) Å) was found which might be an indication of the presence of argentophilic interactions and comparable with those observed in Ag(I) biim compounds.[47,48]

The asymmetric unit of **2b** (Figure 4) contains two independent 1D polymeric chains where two ligand molecules

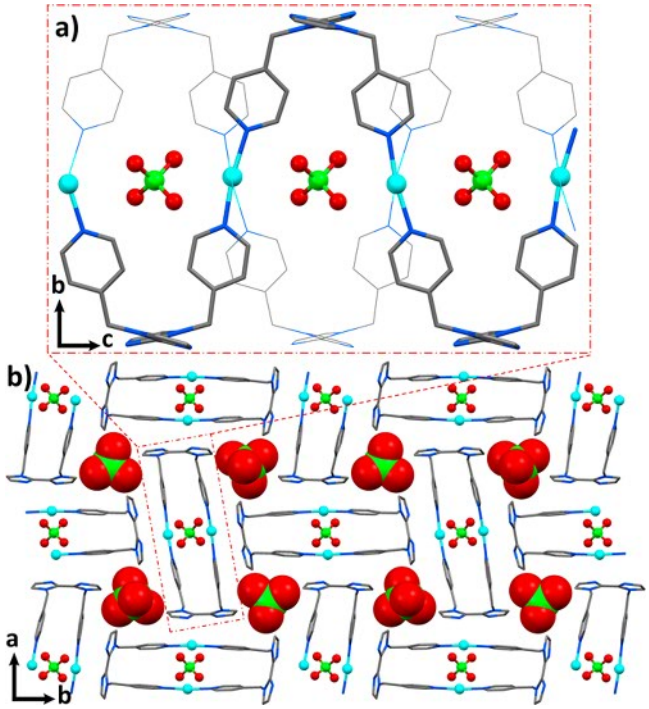

Figure 4. (a) One-dimensional chains of **2b** viewed along the crystallographic *a*-axis. (b) Packing of the chains of **2b** viewed along the crystallographic *c*-axis. Hydrogen atoms are omitted for clarity.

are coordinated to two separate silver atoms (1:1 of Ag to **L2**), one full and two halves of perchlorate anions. In this case, the coordination geometry around the silver is almost linear[49] (N−Ag−N = 170.12(2)° and 171.18(2)°) and bridging coordination was observed from the ligand molecule only through its pyridine nitrogen atoms [Ag−N_{Py} = 2.154(3) Å and 2.157(3) Å]. The two imidazole nitrogen atoms are not coordinated, and the two imidazole rings are somewhat twisted out of the plane (the angle between the mean planes of the two imidazole rings is 28.89°). The shortest Ag···Ag distance between Ag atoms in adjacent chains is 3.690(4) Å and 3.725(6) Å. This value is longer than the sum of the van der Waals radii of two Ag atoms (3.44 Å), indicating that absence of argentophilic interactions. These 1D zigzag polymeric chains interact further with each other through perchlorate anions via several weak C═C−H_{Py}···O, C═C−H_{Im}···O, and CH_2···O hydrogen bonds (Table S1). In solution, the 1D-NMR (^{1}H and ^{13}C) spectral results give no clear evidence on metal coordination, but in ^{1}H−^{15}N COSY spectra, only N_{Py} coordination was seen (5.51 ppm upfield shift for N_{Py}; Figure S13), which can be seen as evidence of CP **2b**.

Structures of Zinc(II) CPs from L1 $[Zn(L1)Cl_2]_n$ (3) and L2 $\{[Zn(L2)Cl_2]\cdot CHCl_3\}_n$ (4). Two 1D-CPs (**3** and **4**) were obtained from the reaction of $ZnCl_2$ with **L1** or **L2** respectively. The single crystals of **3** (Figure 5a,b) were obtained from a mixture of water and DMSO (2:8 v/v) and **4** either from careful diffusion of metal solution (MeOH) into the ligand solution in chloroform (Figure 5c,d) or simply by dissolving obtained CP into the mixture of water and DMSO (2:8 v/v; Figure S5; **4a**).

DOI: 10.1021/acs.cgd.7b01034
Cryst. Growth Des. 2017, 17, 5918−5926

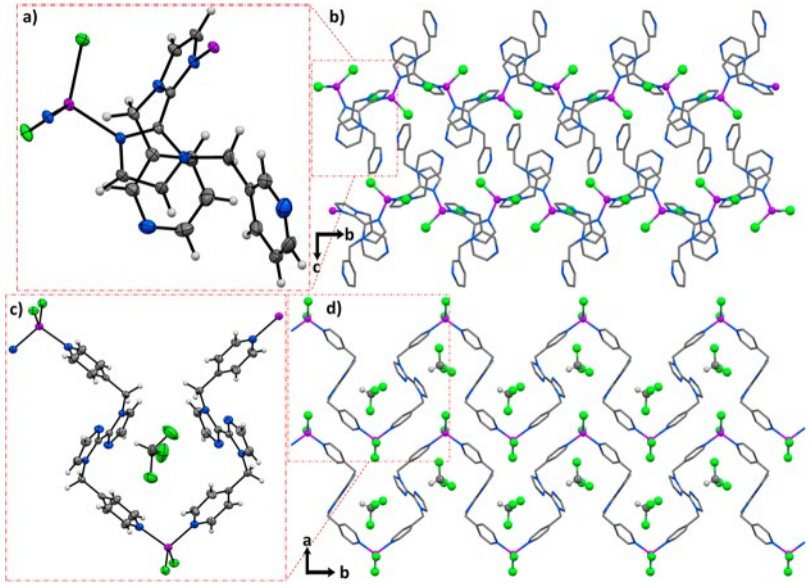

Figure 5. ORTEP plot (50% probability level) of ligand coordination environment in zinc CPs with **L1** (**3**, a) and **L2** (**4**, c). Crystal packing of **3** (b) and **4** (d) along the crystallographic *a*-axis and *c*-axis, respectively. Hydrogen atoms are omitted for clarity.

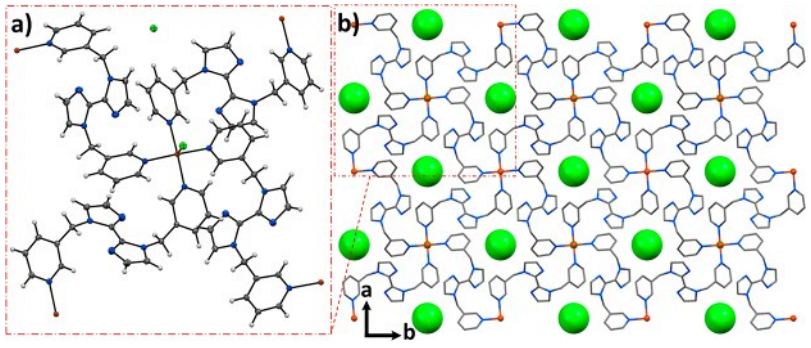

Figure 6. (a) ORTEP plot (50% probability level) of the coordination environment of Cu^{2+} in CP **5** with **L1**. (b) View of the 2D layered structure of **5** along the crystallographic *c*-axis. Solvent molecules (H_2O) and hydrogen atoms are omitted for clarity.

Both CPs, **3** and **4** were crystallized in the monoclinic $P2_1/c$ space group. Solid state structures of **3** and **4** revealed that the coordination geometry around the metal was in both cases slightly distorted tetrahedron. Furthermore, both the ligands **L1** and **L2** acted as bidentate bridging ligands. In **3**, only imidazole nitrogen atoms [Zn−N_{Im} = 2.031(2) Å and 2.032(2) Å] are involved in coordination, and the Zn−N_{Im} distances are close to those found in molecules such as $[Zn(Me_2biim)Cl_2]_n$.[27] In **4** only pyridine nitrogen atoms are involved in coordination, while imidazole rings remained free of coordination. The Zn−N_{Py} (2.044(2) Å and 2.047(2) Å) distances in **4** are in very good agreement with those found in molecular structures such as $[Zn(4,4'\text{-bipy})Cl_2]_n$.[50] The coordination spheres in **3** and **4** are completed with two chlorido ligands [Zn−Cl1 = 2.223(5) Å, Zn−Cl2 = 2.244(5) Å in **3**; Zn−Cl1 = 2.217(7) Å, Zn−Cl2 = 2.239(7) Å in **4**] leading to 1D-zigzag infinite chains. Because of imidazole coordination in **3**, two imidazole rings are twisted out of plane (the angle between the mean planes of the two imidazole rings is 64.38°). However, in **4** the imidazole rings are completely coplanar. In **4**, the solvent molecule ($CHCl_3$) was trapped in the crystal packing by forming weak Cl_3C−H···N_{Im} hydrogen bonding (Table S1). In crystal packing of **4**, the adjacent 1D chains interact with each other via several weak C═C−H_{Im}···Cl and CH_2···Cl hydrogen bonds to the chlorido ligand (Cl^-). In **3**, several weak intra- and intermolecular hydrogen bonds were observed between the chlorido ligand and aromatic or aliphatic hydrogen atoms and also C═C−H_{Py}···N_{Py}.

In solution, both 1D and 2D NMR (Figure S12c) spectra indicate N_{Im} coordination to the zinc atom in CP **3**. A minimum downfield shift for imidazole proton (H2, 0.03 ppm) was seen in ^{1}H NMR spectrum, and it is also supported with ^{1}H−^{15}N COSY spectra (N_{Im}, 1.18 ppm upfield shift). The ^{1}H NMR spectra of CP **4** indicate N_{Py} coordination (0.04 ppm downfield from H4) to the zinc atom.

Structures of $\{[Cu(L1)_2Cl]Cl\cdot H_2O\}_n$ (5) from L1. The reaction of $CuCl_2\cdot 2H_2O$ with ligand **L1** in a 1:1 ratio gave unexpectedly crystals of the two-dimensional CP **5**, where **L1** was acting as a bidentate bridging ligand and was coordinated only through its N_{Py} atoms (Figure 6). The yield of CP **5** was improved by changing the molar ratio of metal to ligand from 1:1 to 1:2. Single crystals of **5**, crystallized in tetragonal space group *P*4/*ncc*, were obtained from DMSO. The asymmetric unit contains half a ligand molecule, Cu^{2+} ion, chlorido ligand, and a chloride anion along with a disordered water molecule. The coordination geometry around the copper atom is square pyramidal with a N4ClCu binding set.[51,52] Each copper atom is coordinated by four pyridine nitrogen [Cu−N_{Py} = 2.041(2) Å,

DOI: 10.1021/acs.cgd.7b01034
Cryst. Growth Des. 2017, 17, 5918−5926

Cu−Cl = 2.539(1) Å] atoms from four individual ligand molecules, and imidazole nitrogens are free of coordination.

Structure of $[Cu_2(L2)(\mu\text{-}Cl)_2]_n$ (6) from L2. The reaction of $CuCl_2{\cdot}2H_2O$ with **L2** from a mixture of water and DMSO (2:8 v/v) at equimolar amounts gave 1D-CP **6** (Figure 7). In these reaction conditions, the copper was reduced from Cu^{2+} to Cu^+ and crystallized in monoclinic with $P2_1/c$ space group. Reduction of Cu(II) to Cu(I) in DMSO/Water solution is unusual, but under similar conditions reduction of silver and gold has been reported.[53,54] The reduction of copper is also evident based on ESI-MS spectra, in which the ion $[Cu(\mathbf{L2})]^+$ was observed. The asymmetric unit contains one full ligand molecule, Cu^+ ion, and one chlorido ligand (Cl adopts in μ_2-bridging mode). The coordination geometry around copper atom is distorted tetrahedron with two N_{Py} atoms [Cu−N_{Py} = 1.984(4) Å and 1.988(4) Å] from two different ligand molecules and two bridging chlorido ligands [Cu−Cl1 = 2.511(7) Å, Cu−Cl1$^{\#1}$ = 2.502(5) Å ($^{\#1}$ = −*X*, 2 − *Y*, 1 − *Z*)],

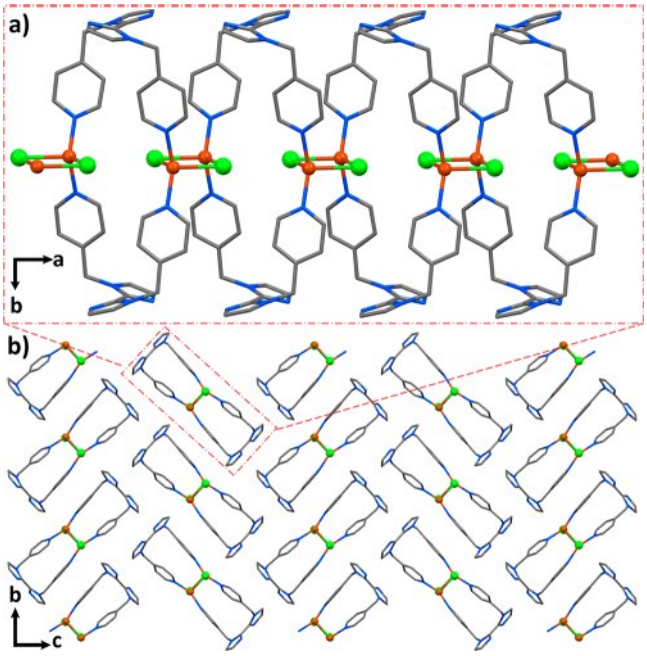

Figure 7. (a) One-dimensional chains of **6** viewed along the crystallographic *c*-axis. (b) Packing of the chains of **6** viewed along the crystallographic *a*-axis.

and the Cu···Cu distance is 2.849(1) Å. The distortion from ideal tetrahedral geometry arises from the angle of N−Cu−N (149.74°). The two N_{Im} atoms are not coordinated, and the two imidazole rings are twisted out of plane (the angle between the mean planes of the two imidazole rings is 31.56°). The copper atoms and bridging chlorido ligands are positioned on the same plane, with no deviation from planarity, which is caused by a symmetry operation, resulting in a Cl−Cl separation of 4.126(2) Å. These 1D chains interact with each other via weak C═C−H_{Im}···N_{Im} and CH_2···N_{Im} hydrogen bonding interactions.

Crystal Structure of $[Cu_4(L2)(\mu\text{-}Cl)_4]_n$ (7) from L2. Upon X-ray diffraction, it was revealed that in **7** (Figure 8) the copper was reduced to Cu^+ as in CP **6**. Despite several attempts, no rational route to pure **7** without **6** could be developed. The CP **7** was crystallized in trigonal space group $R\,\bar{3}c$. The asymmetric unit contains half of the ligand molecule, Cu^+ ion, and chlorido ligand. The geometry around the copper atom is again distorted tetrahedron with one N_{Py} atom [Cu−N_{Py} = 2.025(4) Å] and one N_{Im} atom [Cu−N_{Im} = 1.981(4) Å] from two separate ligand molecules. The coordination sphere is completed by two bridging chlorido ligands [Cu−Cl = 2.421(2) Å, Cu−Cl$^{\#1}$ = 2.411(1) Å]. The Cu···Cu distance is 2.696(1) Å, which is shorter than the sum of van der Waals radii (2.8 Å) and an indication of the presence of cuprophilic interactions.[55]

Thermal Analysis. To evaluate the thermal stability of CPs **1**, **2b**−**6**, their thermal decomposition behaviors were studied by thermogravimetric analysis (TGA) (Figure 9). The

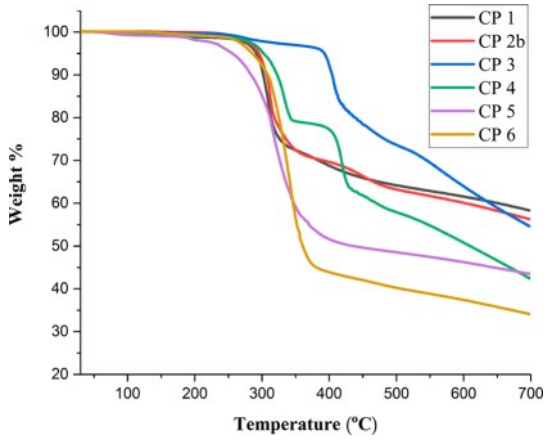

Figure 9. TGA curves of the CPs **1**, **2b**−**6** recorded at a heating rate of 10 °C min^{-1}.

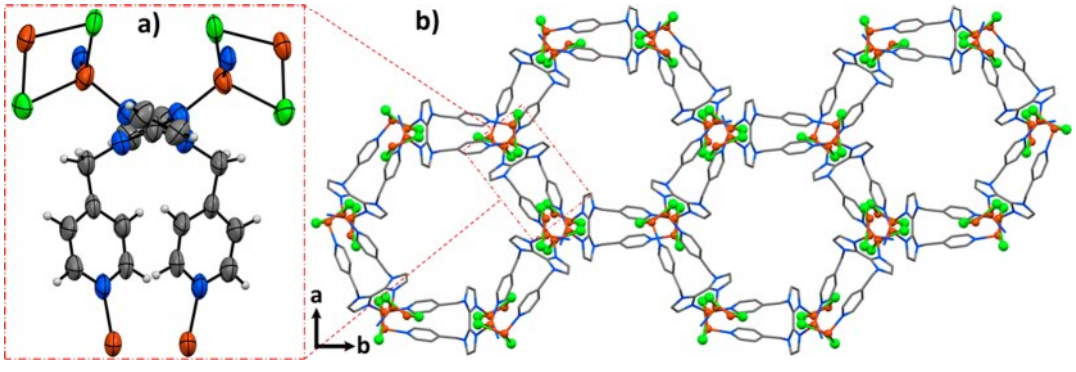

Figure 8. (a) ORTEP plot (50% probability level) of **L2** coordination environment in Cu^+ CP **7**. (b) Crystal packing of **7** viewed along the crystallographic *c*-axis.

DOI: 10.1021/acs.cgd.7b01034
Cryst. Growth Des. 2017, 17, 5918−5926

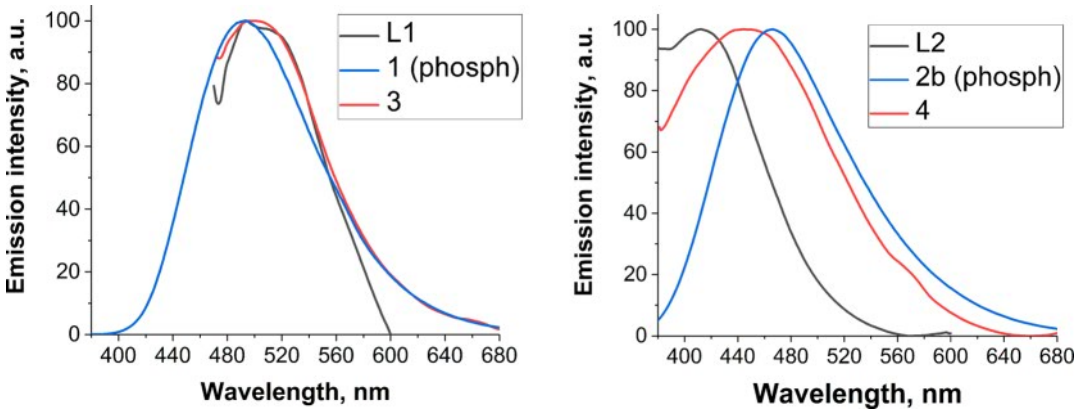

Figure 10. Normalized photoluminescence spectra of **L1** and its CPs **1** and **3** (left) and **L2** and its CPs **2b** and **4** (right).

experiments were performed under nitrogen atmosphere at a heating rate of 10 °C min^{-1} in the temperature range of 30−700 °C. The TGA curves of silver CPs (**1**, **2b**) showed that their networks were stable up to 288 and 283 °C, respectively. Beyond these temperatures, the networks began to decompose. The TGA curve of **3** showed that the network was stable up to 393 °C and then started to decompose on further heating. For CPs **4** and **5**, the first weight losses between 50−350 and 50−220 °C correspond to the loss of the solvent of crystallization, i.e., chloroform (expt. 20.97%; calcd. 20.87%) and water (expt. 1.93%; calcd. 2.01%) molecules, respectively. The CP network of **4** and **5** began to decompose beyond 405 and 247 °C, respectively. The CP network of **6** was found to be stable up to 260 °C and then started to decompose.

Photoluminescence in Solid State. Photoluminescence properties of the obtained CPs **1**, **2b**, **3**−**6** and free ligands **L1** and **L2** in the solid state were examined, and obtained spectra are presented in Figure 10.

The free ligands **L1** and **L2** display fluorescence with different emission maxima at 495 nm (excitation at 450 nm) for **L1** and 410 nm (excitation at 350 nm) for **L2**. It has to be pointed out that fluorescence emission of both **L1** and **L2** in the solid state depends on excitation wavelength and possesses additional emission peaks in the UV range (see Supporting Information for fluorescence excitation−emission matrices). Similar dual fluorescence can be seen in the literature for biim[56] and its dimethyl derivatives[57] in the solid state. A detailed study of the nature of such luminescent properties of **L1** and **L2** requires a comprehensive analysis that is beyond of the scope of this work.

Silver-based CPs, **1** and **2b** do not display any detectable fluorescence but exhibit intense phosphorescence with emission maxima at 490 nm (excitation at 280 nm) for **1**, and at 465 nm (excitation 250 nm) for **2b**. The absence of fluorescence can be attributed to the heavy atom effect of the metal center. The ability of the silver(I) cation to promote intersystem crossing to the triplet excited states within coordination polymers is well-known in the literature.[58]

Zinc-based CPs (**3** and **4**) both possess fluorescence emission with maxima at 495 nm (excitation at 450 nm) for **3** and 445 nm (excitation at 370 nm) for **4**. Apart from fluorescence, both compounds display weak phosphorescence emission at 520 nm.

Copper-based CPs (**5** and **6**) do not display any detectable fluorescence or phosphorescence. Quenching of luminescence is common in copper(II) (via electron or energy transfer)[59] and copper(I) (via excited state distortions)[60] containing compounds.

Unambiguous assignment of the observed photoluminescence band to a certain electronic transition without further spectroscopic and computational studies is challenging due to complicated fluorescence of **L1** and **L2** in the solid state. Nonetheless, some interesting observations can be pointed out based on obtained data. As can be seen in Figure 10, CPs **1** and **3** display nearly the same luminescence as the free ligand **L1**. As discussed above, in these CPs the metal atoms are coordinated to the biimidazole nitrogen atoms of **L1**, while pyridine nitrogen atoms remain free. On the other hand, only the pyridine atoms of **L2** ligand are coordinated in CPs **2b** and **4**, and therefore a significant shift of emission maximum compared to the free ligand can be observed. Therefore, luminescent properties of the obtained CPs are not only defined by the nature of metal ion (whether luminescence will be quenched or not) but are also influenced by the mode of coordination of the ligand. This provides a potential tool for fine-tuning of emission wavelength and intensity via design of the ligand. Since the emission is within the visible range, CPs containing **L1** and **L2** ligands may be useful for practical applications, such as the production of organic light emitting devices.

CONCLUSIONS

In summary, we have utilized two semirigid biimidazole based ligands (**L1** and **L2**) as organic linkers for the construction of several CPs from Ag, Zn, and Cu metal ions. These ligands display pyridine (N_{Py}) and imidazole (N_{Im}) coordination groups which differ in their coordination ability (N_{Py} coordination ability is higher than the N_{Im}).[28−30] According to the structures of these eight CPs, we have found that the final structure can be influenced by the structure of the ligand, nature of the metal ion, the molar ratio of reactants, and the reaction solvent used. The single crystal X-ray analyses of these eight CPs reveal versatile coordination modes of ligands, including bidentate (**2a**, **2b**, **3**−**6**), tridentate (**2a**), and tetradentate (**1**, **7**), which are responsible for different structural topologies. The influence of reaction solvent on coordination geometry of silver atom was observed in CPs **1** and **2**. A linear (**2b**) coordination was obtained in a mixture of water and MeCN and tetrahedral coordination (**1**, **2a**) in MeCN. An unusual reduction of Cu^{2+} to Cu^{+} in a mixture of water and DMSO was observed during the synthesis and formation of CPs **6** and **7**. The photophysical behavior of CPs **1**−**4** in the

DOI: 10.1021/acs.cgd.7b01034
Cryst. Growth Des. 2017, 17, 5918−5926

solid state was found to be dependent primarily on the nature of the metal center, but it was also influenced by the coordination mode of the ligand. The results show that the semirigid ligands such as **L1** and **L2** can be used to produce a range of coordination polymers with different structural and photophysical properties. Both the structures and the properties can be adjusted by the choice of the metal and by modifying the reaction conditions.

■ ASSOCIATED CONTENT

Supporting Information

The Supporting Information is available free of charge on the ACS Publications website at DOI: 10.1021/acs.cgd.7b01034.

Ligand synthesis (**L1** and **L2**) and single crystal X-ray data, selected bond lengths and angles for CPs **1**−**4**, solid state photoluminescence of ligands, 2D NMR spectra of ligands and CPs **1**−**4**. Accurate mass spectral results for all the CPs (**1**, **2b**−**6**), EPR of CP **5**, and the experimental PXRD patterns of CPs **1**, **2b**−**6** compared with the simulated pattern (PDF)

Accession Codes

CCDC 1541300−1541301, 1545343−1545348, and 1545350−1545352 contain the supplementary crystallographic data for this paper. These data can be obtained free of charge via www.ccdc.cam.ac.uk/data_request/cif, or by emailing data_request@ccdc.cam.ac.uk, or by contacting The Cambridge Crystallographic Data Centre, 12 Union Road, Cambridge CB2 1EZ, UK; fax: +44 1223 336033.

■ AUTHOR INFORMATION

Corresponding Author

*E-mail: matti.o.haukka@jyu.fi.

ORCID

Rajendhraprasad Tatikonda: 0000-0003-1277-3492

Matti Haukka: 0000-0002-6744-7208

Notes

The authors declare no competing financial interest.

■ ACKNOWLEDGMENTS

R.T., M.H., and E.K. kindly acknowledge the financial support from the Academy of Finland (Project Nos. 295581, 284562, and 278743). EU COST action CM 1302 "Smart Inorganic Polymers" is also gratefully acknowledged.

■ REFERENCES

(1) Getman, R. B.; Bae, Y.-S.; Wilmer, C. E.; Snurr, R. Q. *Chem. Rev.* **2012**, *112*, 703−723.

(2) Lv, X.; Li, L.; Sun, X.; Zhang, H.; Cai, J.; Wang, C.; Tang, S.; Zhao, X. *Chem. - Asian J.* **2014**, *9*, 901−907.

(3) Noro, S.-I.; Mizutani, J.; Hijikata, Y.; Matsuda, R.; Sato, H.; Kitagawa, S.; Sugimoto, K.; Inubushi, Y.; Kubo, K.; Nakamura, T. *Nat. Commun.* **2015**, *6*, 5851.

(4) Zhao, M.; Tan, J.; Su, J.; Zhang, J.; Zhang, S.; Wu, J.; Tian, Y. *Dyes Pigm.* **2016**, *130*, 216−225.

(5) Melnic, E.; Coropceanu, E. B.; Forni, A.; Cariati, E.; Kulikova, O. V.; Siminel, A. V.; Kravtsov, V. C.; Fonari, M. S. *Cryst. Growth Des.* **2016**, *16*, 6275−6285.

(6) Wen, T.; Zhang, D.-X.; Ding, Q.-R.; Zhang, H.-B.; Zhang, J. *Inorg. Chem. Front.* **2014**, *1*, 389−392.

(7) Zhang, W.; Xiong, R.-G. *Chem. Rev.* **2012**, *112*, 1163−1195.

(8) Jiang, X.; Liu, C.-M.; Kou, H.-Z. *Inorg. Chem.* **2016**, *55*, 5880−5885.

(9) Sun, R. W.-Y.; Zhou, X.-P.; Wang, J.-H.; Li, D.; Hou, Y.-L. *Chem. Commun.* **2014**, *50*, 2295−2297.

(10) Wen, T.; Zhang, D.-X.; Zhang, J. *Inorg. Chem.* **2013**, *52*, 12−14.

(11) Givaja, G.; Amo-Ochoa, P.; Gomez-Garcia, C. J.; Zamora, F. *Chem. Soc. Rev.* **2012**, *41*, 115−147.

(12) Minaev, B.; Baryshnikov, G.; Agren, H. *Phys. Chem. Chem. Phys.* **2014**, *16*, 1719−1758.

(13) Uemura, K. *Inorg. Chem. Commun.* **2008**, *11*, 741−744.

(14) Nath, K.; Husain, A.; Dastidar, P. *Cryst. Growth Des.* **2015**, *15*, 4635−4645.

(15) Dong, Y.-B.; Jiang, Y.-Y.; Li, J.; Ma, J.-P.; Liu, F.-L.; Tang, B.; Huang, R. Q.; Batten, S. R. *J. Am. Chem. Soc.* **2007**, *129*, 4520−4521.

(16) Wang, X.-M.; Chen, S.; Fan, R.-Q.; Zhang, F.-Q.; Yang, Y.-L. *Dalton Trans.* **2015**, *44*, 8107−8125.

(17) Cui, J.-W.; An, W.-J.; Van Hecke, K.; Cui, G.-H. *Dalton Trans.* **2016**, *45*, 17474−17484.

(18) Zheng, S.-R.; Yang, Q.-Y.; Yang, R.; Pan, M.; Cao, R.; Su, C.-Y. *Cryst. Growth Des.* **2009**, *9*, 2341−2353.

(19) Guo, X.; Guo, H.; Zou, H.; Qi, Y.; Chen, R. *CrystEngComm* **2013**, *15*, 9112−9120.

(20) Bu, X.-H.; Chen, W.; Lu, S.-L.; Zhang, R.-H.; Liao, D.-Z.; Bu, W.-M.; Shionoya, M.; Brisse, F.; Ribas, J. *Angew. Chem., Int. Ed.* **2001**, *40*, 3201−3203.

(21) Chen, C.-L.; Zhang, J.-Y.; Su, C.-Y. *Eur. J. Inorg. Chem.* **2007**, *2007*, 2997−3010.

(22) Xiao, J.-C.; Twamley, B.; Shreeve, J. M. *Org. Lett.* **2004**, *6*, 3845−3847.

(23) Laurila, E.; Tatikonda, R.; Oresmaa, L.; Hirva, P.; Haukka, M. *CrystEngComm* **2012**, *14*, 8401−8408.

(24) Mardanya, S.; Karmakar, S.; Mondal, D.; Baitalik, S. *Inorg. Chem.* **2016**, *55*, 3475−3489.

(25) Sorsche, D.; Fleischmann, M.; Rau, S.; Rommel, S. A. *Chem. - Eur. J.* **2017**, DOI: 10.1002/chem.201605782.

(26) Zhu, H.-F.; Fan, J.; Okamura, T.-A.; Sun, W.-Y.; Ueyama, N. *Cryst. Growth Des.* **2005**, *5*, 289−294.

(27) Yang, L.-N.; Zhi, Y.-X.; Hei, J.-H.; Li, J.; Zhang, F.-X.; Gao, S.-Y. *J. Coord. Chem.* **2011**, *64*, 2912−2922.

(28) CCDC 1541300 and 1541301 contain the supplementary crystallographic data for ligands **L1** and **L2** respectively.

(29) Aakeröy, C. B.; Wijethunga, T. K.; Desper, J. *J. Mol. Struct.* **2014**, *1072*, 20−27.

(30) Aakeröy, C. B.; Wijethunga, T. K.; Desper, J.; Moore, C. *J. Chem. Crystallogr.* **2015**, *45*, 267−276.

(31) Aakeröy, C. B.; Wijethunga, T. K.; Desper, J. *New J. Chem.* **2015**, *39*, 822−828.

(32) Fu, Y.-M.; Zhao, Y.-H.; Lan, Y.-Q.; Shao, K.-Z.; Qiu, Y.-Q.; Hao, X.-R.; Su, Z.-M. *J. Solid State Chem.* **2008**, *181*, 2378−2385.

(33) Zang, H.-Y.; Tan, K.; Guan, W.; Li, S.-L.; Yang, G.-S.; Shao, K.-Z.; Yan, L.-K.; Su, Z.-M. *CrystEngComm* **2010**, *12*, 3684−3690.

(34) Khlobystov, A. N.; Blake, A. J.; Champness, N. R.; Lemenovskii, D. A.; Majouga, A. G.; Zyk, N. V.; Schröder, M. *Coord. Chem. Rev.* **2001**, *222*, 155−192.

(35) Chen, C.-J.; Liu, F.-N.; Zhang, A.-J.; Zhang, L.-W.; Liu, X. *Acta Crystallogr., Sect. E: Struct. Rep. Online* **2009**, *65*, m1674−m1675.

(36) Kandaiah, S.; Huebner, R.; Jansen, M. *Polyhedron* **2012**, *48*, 68−71.

(37) Tzeng, B.-C.; Banik, M.; Selvam, T.; Lee, G.-H. *Cryst. Growth Des.* **2013**, *13*, 4245−4251.

(38) Pedireddi, V. R.; Shimpi, M. R.; Yakhmi, J. V. *Macromol. Symp.* **2006**, *241*, 83−87.

(39) Jayamani, A.; Sengottuvelan, N.; Kang, S. K.; Kim, Y. I. *Polyhedron* **2015**, *98*, 203−216.

(40) Tatikonda, R.; Kalenius, E.; Haukka, M. *Inorg. Chim. Acta* **2016**, *453*, 298−304.

(41) *CrysAlisPro*; Agilent Technologies: Yarnton, England, 2013.

(42) Palatinus, L.; Chapuis, G. *J. Appl. Crystallogr.* **2007**, *40*, 786−790.

(43) Sheldrick, G. M. *Acta Crystallogr., Sect. A: Found. Crystallogr.* **2008**, *64*, 112−122; *Acta Crystallogr., Sect. A: Found. Adv.* **2015**, *71*, 3−8; *Acta Crystallogr. Sect. C* **2015**, *71*, 3−8.
(44) Robin, A. Y.; Fromm, K. M. *Coord. Chem. Rev.* **2006**, *250*, 2127−2157.
(45) Jiang, J.-J.; Li, X.-P.; Zhang, X.-L.; Kang, B.-S.; Su, C.-Y. *CrystEngComm* **2005**, *7*, 603−607.
(46) Noh, T. H.; Choi, Y. J.; Ryu, Y. K.; Lee, Y.-A.; Jung, O.-S. *CrystEngComm* **2009**, *11*, 2371−2374.
(47) Sang, R.-L.; Xu, L. *Eur. J. Inorg. Chem.* **2006**, *2006*, 1260−1267.
(48) Laurila, E.; Oresmaa, L.; Kalenius, E.; Hirva, P.; Haukka, M. *Polyhedron* **2013**, *52*, 1231−1238.
(49) Wang, L.-S.; Zhang, J.-F.; Yang, S.-P. *Acta Crystallogr., Sect. E: Struct. Rep. Online* **2004**, *60*, m1484−m1486.
(50) Hu, C.; Englert, U. *Angew. Chem., Int. Ed.* **2005**, *44*, 2281−2283.
(51) Linfoot, C. L.; Richardson, P.; Hewat, T. E.; Moudam, O.; Forde, M. M.; Collins, A.; White, F.; Robertson, N. *Dalton Trans.* **2010**, *39*, 8945−8956.
(52) Petrovic, K.; Potocnak, I.; Raczova, K.; Cizmar, E.; Petrovic, M. *Transition Met. Chem.* **2015**, *40*, 541−553.
(53) Tatikonda, R.; Bertula, K.; Nonappa, N.; Hietala, S.; Rissanen, K.; Haukka, M. *Dalton Trans.* **2017**, *46*, 2793−2802.
(54) Nitsch, J.; Lacemon, F.; Lorbach, A.; Eichhorn, A.; Cisnetti, F.; Steffen, A. *Chem. Commun.* **2016**, *52*, 2932−2935.
(55) Nitsch, J.; Lacemon, F.; Lorbach, A.; Eichhorn, A.; Cisnetti, F.; Steffen, A. *Chem. Commun.* **2016**, *52*, 2932−2935.
(56) Shi, Z.; Peng, J.; Zhang, Z.; Yu, X.; Alimaje, K.; Wang, X. *Inorg. Chem. Commun.* **2013**, *33*, 105−108.
(57) Sang, R.; Xu, L. *Inorg. Chem.* **2005**, *44*, 3731−3737.
(58) Xiao, Y.-H.; Huang, J.; Deng, Z.-P.; Huo, L.-H.; Gao, G. *J. Solid State Chem.* **2017**, *251*, 255−265.
(59) Chen, H.-F.; Yang, W.-B.; Lin, L.; Guo, X.-G.; Dui, X.-J.; Wu, X.-Y.; Lu, C.-Z.; Zhang, C.-J. *J. Solid State Chem.* **2013**, *201*, 215−221.
(60) Eggleston, M. K.; Koenig, K. S.; Pallenberg, A. J.; McMillin, D. R. *Inorg. Chem.* **1997**, *36*, 172−176.

DOI: 10.1021/acs.cgd.7b01034
Cryst. Growth Des. 2017, 17, 5918−5926

III

BIPYRIDINE BASED METALLOGELS: AN UNPRECEDENTED DIFFERENCE IN PHOTOCHEMICAL AND CHEMICAL REDUCTION IN THE *IN SITU* NANOPARTICLE FORMATION

by

Rajendhraprasad Tatikonda, Kia Bertula, Nonappa, Sami Hietala, Kari Rissanen, & Matti Haukka

Dalton Trans., **2017**, *46*, 2793−2802

Dalton Transactions

PAPER

View Article Online
View Journal | View Issue

Cite this: *Dalton Trans.*, 2017, **46**, 2793

Bipyridine based metallogels: an unprecedented difference in photochemical and chemical reduction in the *in situ* nanoparticle formation†

Rajendhraprasad Tatikonda,[a] Kia Bertula,[b] Nonappa,[b] Sami Hietala,[c] Kari Rissanen*[a] and Matti Haukka*[a]

Received 8th November 2016,
Accepted 2nd February 2017

DOI: 10.1039/c6dt04253h

rsc.li/dalton

Metal co-ordination induced supramolecular gelation of low molecular weight organic ligands is a rapidly expanding area of research due to the potential in creating hierarchically self-assembled multi-stimuli responsive materials. In this context, structurally simple *O*-methylpyridine derivatives of 4,4′-dihydroxy-2,2′-bipyridine ligands are reported. Upon complexation with Ag(I) ions in aqueous dimethyl sulfoxide (DMSO) solutions the ligands spontaneously form metallosupramolecular gels at concentrations as low as 0.6 w/v%. The metal ions induce the self-assembly of three dimensional (3D) fibrillar networks followed by the spontaneous *in situ* reduction of the Ag-centers to silver nanoparticles (AgNPs) when exposed to daylight. Significant size and morphological differences of the AgNP's was observed between the standard chemical and photochemical reduction of the metallogels. The gelation ability, the nanoparticle formation and rheological properties were found to be depend on the ligand structure, while the strength of the gels is affected by the water content of the gels.

Introduction

Metallosupramolecular chemistry offers control over self-assembly from molecular, nanoscale to mesoscale superstructures with multiple stimuli and functionalities.[1] Among supramolecular self-assembled systems, the hierarchical assembly of low molecular weight building blocks ranging from morphologically diverse nano- and micrometer structures to hydro- and organogelation is a topical and highly attractive area of research.[2] The ability of structurally simple building blocks to generate highly entangled three dimensional (3D) fibrillar networks and encapsulation of solvents provides potential applications in the field of tissue engineering,[3] separations,[4] biomedicine,[5] optoelectronics,[6] catalysis,[7] chiral plasmonics,[8] *in situ* nanoparticle formation,[9] and templating of porous/hollow inorganic nanotubes.[10] Molecular building blocks used, *viz.* low molecular weight gelators (LMWG), range from simple heteroatom containing hydrocarbons[11] to peptides,[12] steroids,[13] nucleobases,[14] carbohydrates,[15] polyaromatics[16] and alkaloids,[17] all of which have been extensively studied as gel forming agents. The gelator molecules are able to utilize one or several supramolecular interactions such as H-bonding, electrostatic interactions, π-stacking, van der Waals interaction, charge transfer complexation, halogen bonding, fluorine–fluorine interactions and dynamic covalent bonds in the gel formation.[18] Metal complexation has been extensively studied in the field of supramolecular self-assembly to generate molecular, supramolecular and nanoscopic structures.[19] Recently, the metal chelation induced aggregation of low molecular weight organic ligands has been extended to hydro- and organogelation, now known as metallogels or metallosupramolecular gels.[18d,20] In order to obtain metallogels, at least one of the above mentioned supramolecular interactions is needed in addition to metal coordination. Therefore, gelators containing metal binding sites (ligands) such as pyridine, bipyridine, terpyrdines and carboxylates, have been utilized as the core of the metallogelator.[21] Examples include cholesterol derivatives, dendrimers, oligopeptides and oligoethylene glycol derivatives.[22] Recently, subcomponent self-assembly,[22] has been used as a facile route for metallogels.[23] The bipyridine derivatives have been studied for their ability to form supramolecular gels upon complexation with metal ions such as Fe(II), Co(II), Ni(II), Cu(II), Zn(II) and

[a]*Department of Chemistry, Nanoscience Center, University of Jyväskylä, P. O. Box 35, FI-40014 Jyväskylä, Finland. E-mail: matti.o.haukka@jyu.fi, kari.t.rissanen@jyu.fi*
[b]*Department of Applied Physics, Molecular Materials Group, Aalto University School of Science, Puumiehenkuja 2, FI-02150 Espoo, Finland*
[c]*Department of Chemistry, University of Helsinki, P. O. Box 55, FI-00014 Helsinki, Finland*

†Electronic supplementary information (ESI) available: General methods and materials, single crystal X-ray data, ^{1}H, ^{13}C and 2D NMR spectra of ligands 2–4 and its complexes, additional SEM and TEM micrographs. CCDC 1500637–1500639. For ESI and crystallographic data in CIF or other electronic format see DOI: 10.1039/c6dt04253h

Ag(I).[24] The formed metal complex can induce or disrupt the gelation and even act as precursor for *in situ* nanoparticle formation.[25,26] Because of their antibacterial properties the polymeric as well as low molecular weight hybrid gels containing silver nanoparticles (AgNP) have gained considerable interest.[27] Typically this type of gels are synthesized by using sodium borohydride mediated chemical reduction,[28] photochemical reduction,[29] microwave irradiation,[30] sonochemical reduction,[31] or by using ascorbic acid and glucose as reducing agents.[32] It has been demonstrated that the size of AgNPs are dependent on the ratio of metal ion to the capping agent and the strength of the reducing agent.[31] Silver nanoparticles are sensitive to light and atmospheric oxygen, therefore proper capping agents and stabilizers are needed to prevent the aggregation. Furthermore, it has been shown that photo-irradiation using appropriate source of light in the presence of photochemical reducing agents AgNPs can be obtained without using additional stabilizers.[33] *In situ* AgNP formation upon standing the pyridyl containing bis(urea) based hybrid gels have been reported, where in the formation of AgNPs was accelerated using UV irradiation.[34] Similarly, oligo(*p*-phenylvinylene) based metallogels have been reported to act as templates for AgNP formation.[35] The photochemical deposition of AgNPs on helical fibers based on unsymmetrical triphenylene derivatives containing imidazole moieties have been carried out by using UV irradiation. It has been shown that in this case the nanoparticle formation is dependent on the structural isomers of imidazole moieties.[36] In majority of hybrid gels the nanoparticles were stabilized by the gelator/gel fibers and no external capping agents were necessary.[37] Even though, extensive research on *in situ* chemical reduction as well as photo-irradiation mediated reduction of nanoparticles in supramolecular gels have been reported, a comparison of simple daylight mediated AgNP formation with chemical reduction in the same gel has not been pursued extensively. In this context, we report Ag(I) induced self-assembly of synthetically simple 4,4′-bis(pyridinylmethoxy)-2,2′-bipyridine derivatives in aqueous dimethyl sulfoxide to supramolecular gels. We demonstrate that the metal complexation not only furnishes self-assembled fibrillar networks (SAFINs), but also acts as a precursor for the *in situ* silver nanoparticle formation within the gel matrix *via* photochemical reduction upon exposure to daylight. A remarkable size and morphological differences between standard chemical reduction and the photochemical daylight reduction was observed. While the gelation itself and the nanoparticle formation upon reduction of the gel depends on the structure of the gelator, the rheological properties are affected by the water content of the gel as well as the counter anions. More importantly, unlike many metallogelators, the gelators presented in this work lack the conventional hydrogen bonding moieties. The structures of the ligands, complexes, gels and xerogels are characterized using NMR spectroscopy (1D and 2D), single crystal X-ray diffraction, electron microscopy and rheological measurements.

Results and discussion

The bipyridyl ligands were prepared upon reacting 4,4′-dihydroxy-2,2′-bipyridine **1**, with 2-, 3-, or 4-chloromethyl pyridine hydrochloride in the presence of potassium carbonate (K_2CO_3) resulting in ligands **2**, **3** or **4** (Scheme 1), respectively. The solid materials obtained after purification were used for further studies. Ligands **2**, **3** and **4** resulted in single crystals upon recrystallization from chloroform (ESI†).[38] Fig. 1a–c

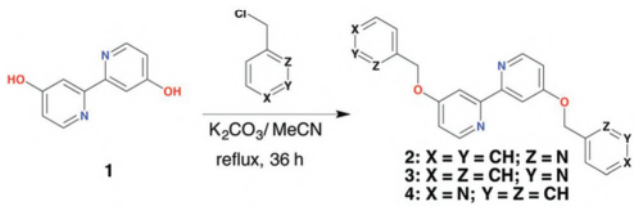

Scheme 1 Synthesis and chemical structures of ligands **2**–**4**.

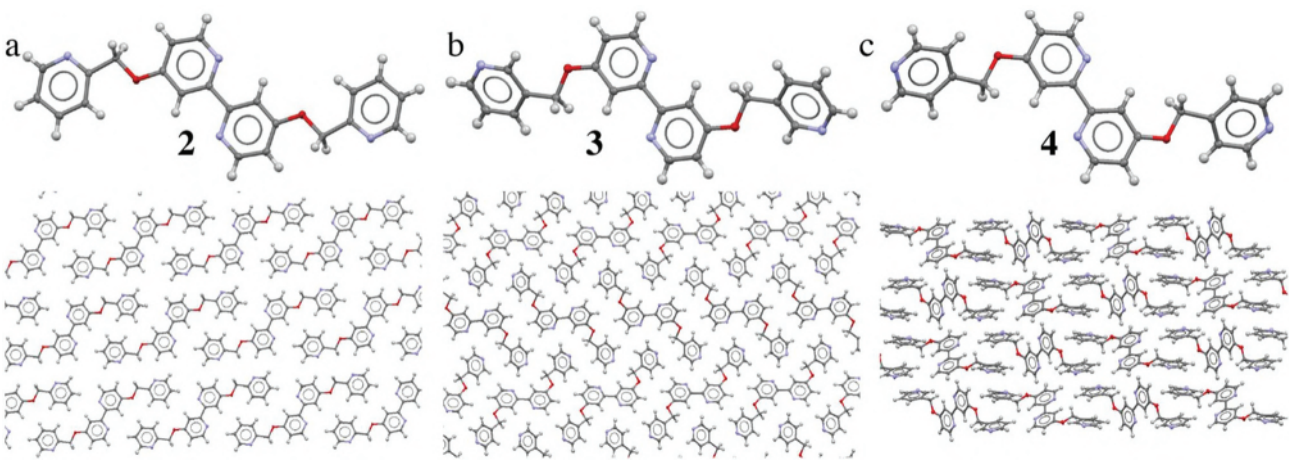

Fig. 1 Single crystal X-ray studies. Single crystal X-ray structures and packing patterns of ligands (a) **2**, (b) **3** and (c) **4**.

shows the single crystal X-ray structures as well as unit cell packing of ligands **2**, **3** and **4**, respectively.

The ligands **2** and **3** crystallized in triclinic space group $P\bar{1}$ and ligand **4** in monoclinic space group $P2_1/c$ (see ESI, Table S1 and Fig. S1–S3†). A systematic analysis of the crystal packing of ligand **2**, **3** and **4** reveals that **2** has weak C═C–H···N and CH_2···N hydrogen bonding to the pyridine nitrogens, while **4** shows only C═C–H···N to pyridine nitrogens. Contrary to **2** and **4**, the ligand **3** exhibits weak C═C–H···N and CH_2···N hydrogen bonding to both bipyridine and pyridine nitrogens. In addition to these weak hydrogen bonds, the packing commences through off-set π···π interactions for **2** and **4** (3.5 Å in both structures), while the ligand **3** shows the face-to-face π···π interactions at slightly longer distance (3.6 Å) (Fig. 1a–c).

The ligands were then studied for metal complexation by dissolving them in DMSO by heating, followed by addition of equimolar $AgNO_3$ as water solution, creating a dimethyl sulfoxide : water (DMSO : H_2O) solvent system. Ligand **2** upon complexation with $AgNO_3$ forms [**2·AgNO$_3$**] which precipitates out of the solution as a powder. Whereas the addition of aqueous $AgNO_3$ to a solution of ligands **3** and **4** resulted in an instantaneous gelation (Fig. 2 and 3) and stable gels were obtained after heating the mixture to obtain a clear solution followed by allowing the sol to attain room temperature. However, when the similar tests were performed for ligands without any metal ions, ligand **3** resulted in an unstable gel, which collapsed upon standing at room temperature for several hours. Ligand **4** produced only precipitate (see ESI Fig. S4†) due to the formation of microcrystalline aggregates as revealed by scanning electron microscopy (SEM) imaging (Fig. 2a and b). To confirm the role of the metal we performed further studies on metallogels. Gelation tests with $CuCl_2$, $ZnCl_2$, $CdCl_2$, $HgCl_2$ and $HAuCl_4$ produced only precipitates and no metallogels were obtained (ESI, Table S2†). This suggests that the gelation is cation specific.

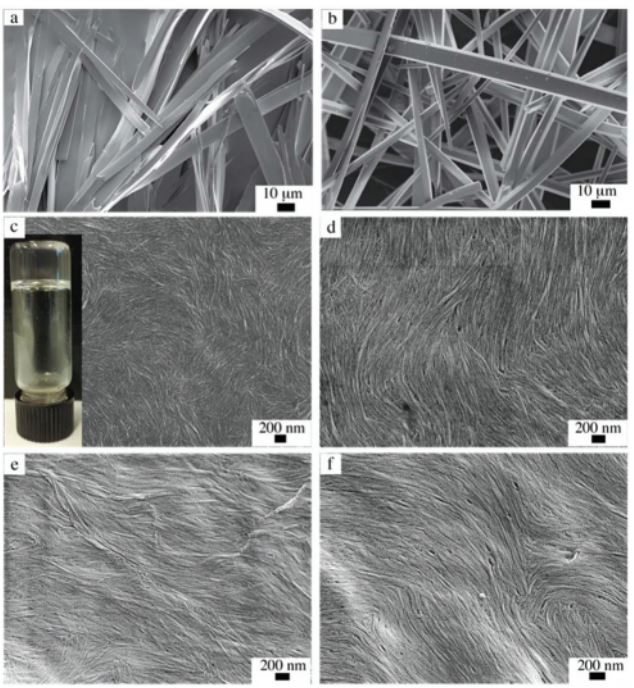

Fig. 2 SEM micrographs of xerogels derived from 0.6 w/v% of (a) ligand **3**; (b) ligand **4**, [**3·AgNO$_3$**] at different v/v DMSO/H_2O ratio (c) 8 : 2; (d) 7 : 3; (e) 6 : 4 and (f) 1 : 1.

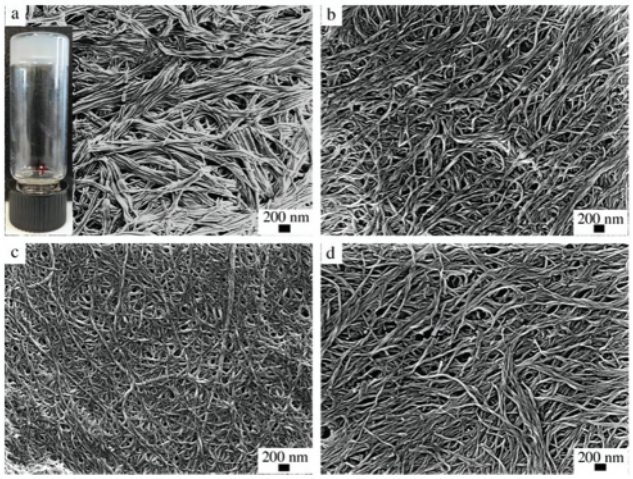

Fig. 3 SEM micrographs of xerogels derived from 0.6 w/v% [**4·AgNO$_3$**] at different v/v DMSO/H_2O ratio. (a) 8 : 2; (b) 7 : 3; (c) 6 : 4 and (d) 1 : 1.

The gelation was observed at various DMSO : H_2O (v/v) ratios and in this study four different ratios were used, *viz*. 8 : 2, 7 : 3, 6 : 4 and 1 : 1. The gels obtained are either transparent or translucent depending on the ratio of DMSO : H_2O used for gelation. As there is no gelation with the ligand **2** upon Ag(I) complexation but a precipitate formation, the importance of nitrogen atom position in the pyridine ring becomes crucial for the gelation. The structural information and the morphological features of the self-assembled fibrillar metallogel networks in the DMSO : H_2O gels [**3·AgNO$_3$**] and [**4·AgNO$_3$**] were studied using scanning electron microscopy, SEM (see ESI† for details). Fig. 2 shows the SEM micrographs of the dried gels (xerogels) of [**3·AgNO$_3$**] upon drying under ambient conditions at different v/v ratio of DMSO : H_2O.

The presence of the very fine/thin nanofibrillar networks formed upon gelation is evident from SEM micrographs and the nature of the fibers does not display any significant changes upon changing the ratio of solvents. However, increasing the water content resulted in more translucent gels. The [**4·AgNO$_3$**] gels showed more robust/thick highly entangled nanofibers under SEM analysis (Fig. 3). The morphological features remained similar in different solvent ratio. The metallogelation was also observed in DMF : H_2O system. However, dissolving the precipitate formed upon complexation by heating resulted in an immediate dark brown coloured gel. It is attributed to the rapid reduction of silver ions (see ESI†) by DMF, which is well documented in the literature. Importantly, the morphological features of the xerogels were found to be similar to that of DMSO : H_2O gels.

The mechanical properties of the [**3**·$AgNO_3$] and [**4**·$AgNO_3$] gels were studied using rheological measurements (Fig. 4). Accordingly, time sweep and frequency sweep experiments using freshly prepared gels were performed. The gels showed characteristic features of viscoelastic solids as the storage moduli G′ was higher than the loss moduli G″ for gels derived from both the ligands. Interestingly, the [**4**·$AgNO_3$] gels are somewhat stronger than that of [**3**·$AgNO_3$] (Fig. 4). Fig. 4a and b shows the storage (G′) and loss moduli G″ of [**3**·$AgNO_3$] and [**4**·$AgNO_3$]. The [**3**·$AgNO_3$] gels with elastic modulus G′ of 100 Pa, showed no significant change upon changing the DMSO/H_2O ratio. However, [**4**·$AgNO_3$] gels showed higher G′ values (800–1000 Pa) compared to that of [**3**·$AgNO_3$] gels at 8 : 2 DMSO : H_2O ratio. Unlike [**3**·$AgNO_3$] gels, a significant change in the gel strength was observed upon changing the DMSO : H_2O ratio. The gels at 8 : 2 and 7 : 2 ratio display similar G′ values (800–1000 Pa). However, G′ values for 6 : 4 and 1 : 1 gels dropped by almost four times compared to that of 8 : 2 and 7 : 3 gels. The difference observed in the gel strength between [**3**·$AgNO_3$] and [**4**·$AgNO_3$] gels can be attributed to the difference in morphological features of two gels. The scanning electron micrograph of gels also shows a clear difference in the fibrillar networks formed during gelation. The [**3**·$AgNO_3$] gels have the tendency to form fine, more film-like, structures upon casting over substrate (Fig. 2), while those of [**4**·$AgNO_3$] clearly show thicker nanofibrillar networks (Fig. 3).

Gelation was also observed when the complexation of ligand **3** and **4** was performed with other counter anions of silver(I) such as PF_6, BF_4, ClO_4, OAc, CF_3SO_3. Stable metallogels were obtained with all counter anions of silver(I) when ligand **3** was used (see ESI, Table S3 and Fig. S7†). However, gels obtained with ligand **4** were less stable and most of them collapsed after a few hours at room temperature. SEM micrographs revealed the formation of entangled fibrillar networks

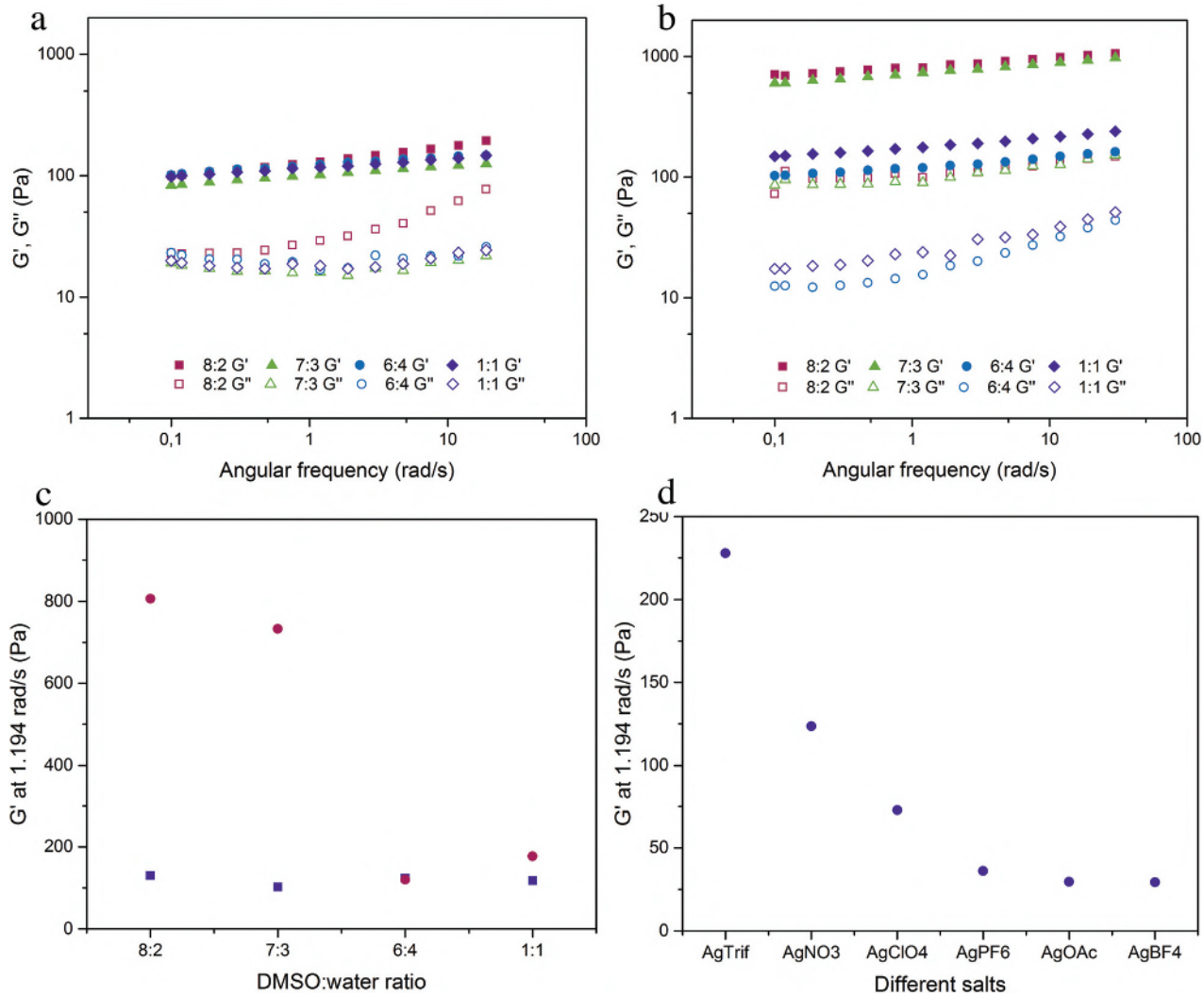

Fig. 4 Rheological properties. (a) Frequency sweep experiments for 0.6 w/v% DMSO/H_2O gels of [**3**·$AgNO_3$]; (b) frequency sweep experiments for DMSO/H_2O gels of [**4**·$AgNO_3$]; (c) storage modulus G′ as a function of DMSO/H_2O ratio of [**3**·$AgNO_3$]; (purple square) and [**4**·$AgNO_3$]; (red circle) and (d) shows the effect of counter anions on the mechanical properties of metallogels derived from ligand **3**.

similar to those obtained using $AgNO_3$ metallogels (see ESI Fig. S8 and S9†). The anions have a significant effect on the mechanical property of the gels as revealed by rheological measurements (see ESI Fig. S10†). The strength of the gel varies in the order $CF_3SO_3 > NO_3 > ClO_4 > PF_6 > BF_4 \cong OAc$ (Fig. 4d).

NMR spectroscopic studies of the conventional and metallogels have been done both in solution and in the solid state to gain more detailed information about the mode of intermolecular interactions, for determination the gel melting temperatures, gelation kinetics and packing modes of the gel states.[39] In this work, one dimensional (1D) ^1H, $^{13}C\{^1H\}$ NMR spectroscopy as well as two dimensional (2D) ^1H–^1H correlation spectroscopy (COSY), ^1H–^{13}C heteronuclear multiple quantum coherence (HMQC) and ^1H–^{15}N COSY were performed for **2**, **3** and **4** and their Ag-complexes (see ESI Fig. S11–S20†). The assignment of resonance peaks arising from ^1H and ^{13}C and their correlation allows monitoring the changes that occur during metal coordination. The ligands **2–4** used in this study, unlike many gelator molecules reported in the literature lack the hydrogen bonding ability. Therefore, the weak supramolecular interactions very likely enhanced by the nitrate anions between metallopolymer chains lead to the formation of the nanofibrillar networks (see below) and are thus the major driving forces for the gel formation. The Ag-cation coordinates to the nitrogen atoms of the ligands and thus affects the α-protons to the coordination site allowing the comparison of metal complexes. Fig. 5a shows the ^1H NMR spectra of ligand **3** and its 1 : 1 metal complex, [**3·AgNO$_3$**], in pure DMSO-d_6 (see ESI Fig. S18 and S19† for ligands **2** and **4** as well as their Ag(I) complexes).

Upon metal complexation, a significant change in the chemical shifts for all the protons was observed. A systematic analysis of ^1H NMR spectrum of [**3·AgNO$_3$**] showed that the protons adjacent to the nitrogen atoms (H1, H5 and H6) are 0.07–0.04 ppm downfield shifted compare to that of the free ligand. Similarly, the protons H7 and H8 showed a similar downfield shift (0.07 ppm) upon complexation. However, relatively large and significant changes in the chemical shift values were observed for protons H3 and H2 (0.13 and 0.2 ppm respectively). The proton signals of the ligands move downfield due to the deshielding effect of the metal coordination. A similar behaviour was also observed for the ^{13}C signals (see ESI, Fig. S20†). The Ag-complexation clearly affects all the protons of the ligand and indicates that all the four nitrogens, both in the bipyridine and pyridine moieties are involved in metal complexation. To probe it further 2D ^1H–^{15}N correlation spectroscopy in DMSO-d_6 for free ligand and its complexes was done. Fig. 5b and c show the ^1H–^{15}N 2D correlation spectra of the free ligand **3** and the 1 : 1 metal complex [**3·AgNO$_3$**], respectively.

Upon complexation, clear changes in the chemical shift value of nitrogen atoms was observed. The nitrogen atoms of the bipyridine moiety (N1) showed an upfield shift of 24.91 ppm, while the pyridine nitrogens (N2) were shifted by 5.65 ppm (Fig. 5b). This supports the ^1H NMR observation that

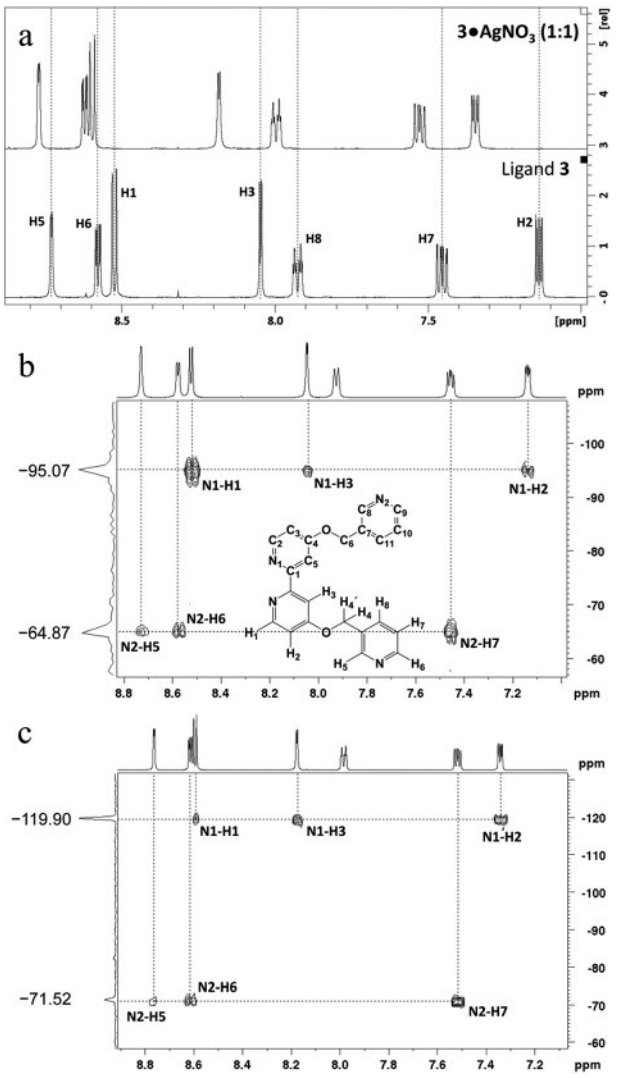

Fig. 5 The ^1H NMR spectra of ligand **3** and [**3·AgNO$_3$**] (a), ^1H–^{15}N 2D correlation spectrum of ligand **3** (b) and ^1H–^{15}N 2D correlation spectrum of ligand [**3·AgNO$_3$**] (c) in DMSO-d_6 at 30 °C.

all nitrogen atoms of the ligand are involved in the metal coordination. The most common Ag^+ coordination geometry is tetrahedral, especially with bipyridine and pyridine ligands.[40]

Based on the 1 : 1 ratio of the ligand and the $AgNO_3$, and the NMR spectral analysis (Fig. 5) and MM-level Spartan® molecular modelling (see ESI, Fig. S22–S24†), the structure of the $AgNO_3$ complex is a metallopolymer, where the silver cation is tetrahedrally coordinated one bipyridine unit and to a pyridine nitrogen of two adjacent ligands (Fig. 6). To support this, gelation studies performed using 1 : 2 ligand to metal ratio resulted in crystallization of the excess silver nitrate, indicating that all the four nitrogen atoms of ligand are involved in coordination in the 1 : 1 ratio complex.

Thermal behaviour of the [**3·AgNO$_3$**] gel in DMSO-d_6/D_2O was probed by variable temperature (VT) ^1H NMR experiments from 30 °C–90 °C with 10 °C increments (see ESI Fig. S21†). The gels showed characteristic broad signals at room tempera-

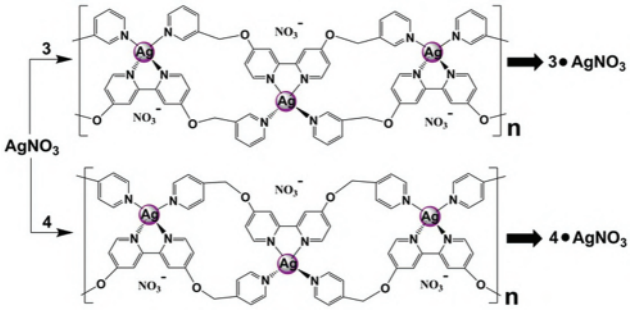

Fig. 6 The proposed structure of the metallosupramolecular polymer [3·$AgNO_3$] and [4·$AgNO_3$]. The MM-level molecular modeling of [3·$AgNO_3$] and [4·$AgNO_3$], see ESI.†

ture and line sharpening was observed upon increasing the temperature. However, due to high thermal stability of the gels the complete gel–sol transition was not reached as the gels remained stable even at high temperatures. Therefore, both gel melting and extensive VT NMR experiments were not performed. Investigations using FT-IR spectroscopic experiments showed a significant shift in the C=C, C=N stretching frequencies between the ligands and the complexes (see ESI Fig. S25 and S26†). In detail, FT-IR spectra of pure ligands, ligand xerogels and the xerogels obtained from the metallogels were compared. The peaks at 1558 and 1565 cm^{-1} of the ligand **3** shifted to 1565 and 1600 cm^{-1} for [**3**·$AgNO_3$]. Similarly, for ligand **4**, the stretching frequencies 1561 and 1568 cm^{-1} shifted to 1562 cm^{-1} and 1601 cm^{-1} respectively for [**4**·$AgNO_3$].

Unprecedentedly upon exposing the [**3**·$AgNO_3$] gels to daylight, a gradual color change from colorless transparent gel to pale brown was observed. Fig. 7 shows the visual color change in [**3**·$AgNO_3$] gel after 14 days of daylight exposure. However, the [**4**·$AgNO_3$] gels this colour change was very weak. The [**3**·$AgNO_3$] gel network remained stable for months after the daylight reduction, this might be due to the gelation ability of ligand **3** without silver in similar conditions. It may also indicate that only part of silver(I) ions reduced forming nanoparticles. The color change turned out to be result from the daylight induced reduction of the silver ions into silver nanoparticles. Nanoparticle formation was confirmed by using UV-Vis spectroscopy with characteristic surface plasmon resonance around 430 nm (Fig. 7b, see ESI Fig. S27†).[41]

Detailed morphological analysis was done using transmission electron microscopy (TEM). The TEM micrographs revealed highly entangled fibrillar networks in both [**3**·$AgNO_3$] and [**4**·$AgNO_3$] gels (ESI†). Fig. 8a and b show the TEM images of the *in situ* formed AgNP's over gel network under daylight reduction for [**3**·$AgNO_3$] gel. Highly monodisperse AgNP's with a diameter of 3–4 nm arrays were formed on the gel network fibres under daylight reduction (See Fig. S25–S28† for additional TEM micrographs). To compare these photochemically obtained *in situ* nanoparticles, we conducted a standard sodium borohydride reduction of the [**3**·$AgNO_3$] gel (see ESI†

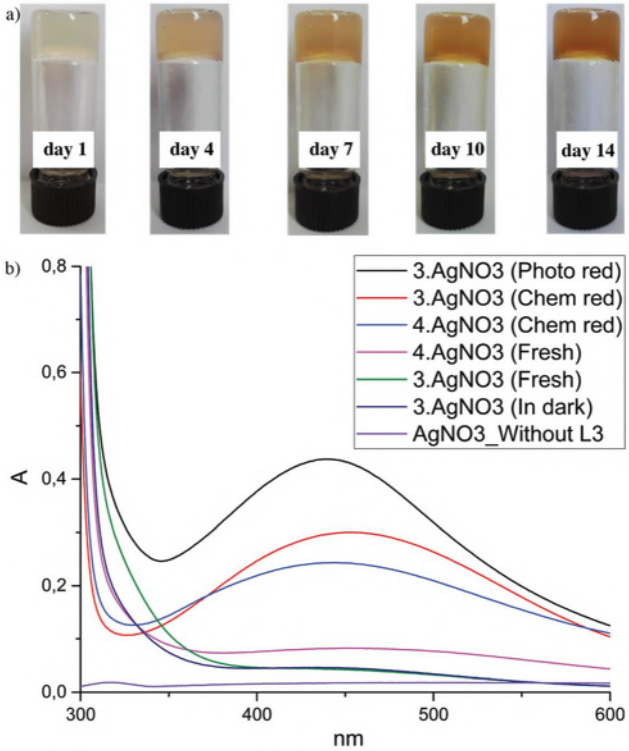

Fig. 7 (a) Photographs showing colour change of 0.6 w/v% DMSO/H_2O gel of [3·$AgNO_3$] upon exposure to daylight. (b) UV-vis spectra of freshly prepared, daylight reduced, chemically reduced metallogels in DMSO and control samples.

for experimental details). To our surprise the chemical reduction resulted in quite polydisperse and much larger AgNP's (*ca.* 20–25 nm in diameter, Fig. 8c and d) scattered quite uniformly across the gel matrix, not situated on the network fibres. The results are in agreement with the UV-Vis spectroscopy, which shows a broad surface plasmon resonance peak around 450 nm (Fig. 7b).

To probe what happen with the photochemically inactive [**4**·$AgNO_3$] gels a similar sodium borohydride reduction was done (see ESI† for experimental details). The TEM micrographs from the AgNP's from the [**4**·$AgNO_3$] were very symmetrical, either cuboctahedron or prismatic in shape, and much larger (>50 nm) (Fig. 8e and f). The above results suggest that the molecular structure of the ligands not only affect the strength and morphological features of the gel network but also on the *in situ* nanoparticle formation. The TEM micrographs obtained from freshly prepared gels in DMF : H_2O showed the random aggregates of silver nanoparticles (see ESI Fig. S35†). A control experiment using a solution of $AgNO_3$ in DMSO : H_2O upon exposing for daylight for one week remained unchanged without any color change. Similarly, freshly prepared [**3**·$AgNO_3$] gel upon storing under dark remained colorless for one week and no plasmon resonance was observed in UV-Vis spectra (Fig. 7b). The above results further supporting the importance of daylight mediated *in situ* nanoparticle formation.

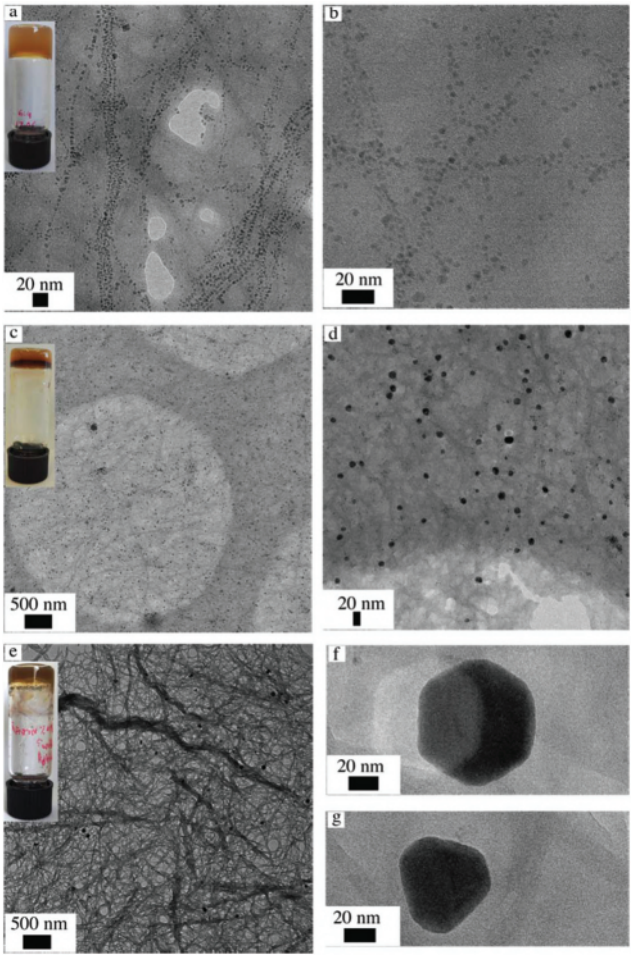

Fig. 8 *In situ* nanoparticle formation. TEM micrographs of (a & b) photochemically reduced [**3·AgNO$_3$**] gel upon exposure to daylight; (c & d) $NaBH_4$ mediated chemically reduced [**3·AgNO$_3$**] gel; (e) chemically reduced [**4·AgNO$_3$**] gel and (f & g) shows cuboctohedron and prismatic nanoparticles respectively from [**4·AgNO$_3$**] gel.

Conclusions

We have shown that simple bipyridyl based ligands are able to act as supergelators upon complexation with silver ions. The gels are formed at a concentration as low as 0.6 w/v% in aqueous dimethyl sulfoxide. The gelation ability, morphological features and mechanical properties strongly depends on the ligand molecular structure. More importantly, the metal coordination not only induces gel formation but also act as a precursor for *in situ* silver nanoparticle formation. The significant differences between chemical and daylight induced *in situ* nanoparticle formation for the [**3·AgNO$_3$**] gel result in from the morphology of the nanofibrillar networks of the gels and also the structure of the metallopolymer responsible for the gelation. In addition the differences in the size and morphology of the AgNP's from the chemical reduction of [**3·AgNO$_3$**] and [**4·AgNO$_3$**] gel highlights the importance of accessibility of the reducing agent to the metal center of the metallopolymers. This, in turn, is greatly affected by structure of the metallopolymer. The discovery that in the [**3·AgNO$_3$**] gel the photochemical reduction of the Ag-centers produced AgNP's embedded in the fibres of the gel matrix with narrow size distribution was a totally unexpected result. Recently, there is a growing interesting in developing methods to control nanoparticles with well-defined size and shape, as they possess unique self-assembling abilities as well as material properties. Therefore, our findings become relevant both in molecular gels and nanoparticle synthesis. Such a finding can pave a way to new soft photoactive materials, which are responsive to daylight.

Experimental section

General procedure for the synthesis of ligands 2, 3 and 4

A mixture of 4,4′-dihydroxy-2,2′-bipyridine (188.2 mg, 1 mmol), potassium carbonate, K_2CO_3 (276.5 mg, 2 mmol) in 30 mL of acetonitrile was stirred at room temperature for 2 h. 2- or 3- or 4-(chloromethyl) pyridine hydrochloride (328.1 mg, 2 mmol) was added to the above mixture and heated to reflux for 36 h. After the reaction time, the filtrate was collected by filtration and evaporated to dryness. The product was recrystallized from MeOH and dried under vacuum.

4,4′-Bis(pyridin-2-ylmethoxy)-2,2′-bipyridine (2). ^{1}H NMR (400 MHz, $CDCl_3$) δ 8.63 (dq, 1H), 8.51 (d, 1H), 8.50 (d, 1H), 8.10 (d, 1H), 7.73 (td, 1H), 7.52 (dt, 1H), 7.25 (m, 1H), 6.93 (dd, 1H), 5.35 (s, 2H). ^{13}C NMR (100 MHz, $CDCl_3$) δ = 165.77, 157.98, 156.23, 150.64, 149.66, 137.15, 123.16, 121.64, 111.21, 107.96, 70.71.

^{1}H NMR (500 MHz, DMSO-d_6 at 70 °C) δ 8.59 (dq, 1H), 8.50 (d, 1H), 8.01 (d, 1H), 7.84 (dt, 1H), 7.55 (d, 1H), 7.35 (qd, 1H), 7.11 (dd, 1H), 5.36 (s, 2H). ^{1}H–^{15}N COSY NMR (DMSO-d_6 at 70 °C) δ = −68.12 (pyridine) and −94.41 (bipy).

4,4′-Bis(pyridin-3-ylmethoxy)-2,2′-bipyridine (3). ^{1}H NMR (400 MHz, $CDCl_3$) δ = 8.71 (d, 1H), 8.61 (dd, 1H), 8.50 (d, 1H), 8.10 (d, 1H), 7.79 (dt, 1H), 7.34 (dd, 1H), 6.91 (dd, 1H), 5.24 (s, 2H). ^{13}C NMR (100 MHz, $CDCl_3$) δ 165.66, 157.99, 150.54, 150.00, 149.25, 135.56, 131.61, 123.79, 111.81, 107.01, 67.62.

^{1}H NMR (500 MHz, DMSO-d_6) δ 8.73 (d, 1H), 8.58 (dd, 1H), 8.52 (d, 1H), 8.05 (d, 1H), 7.92 (dt, 1H), 7.45 (qd, 1H), 7.14 (dd, 1H), 5.35 (s, 2H). ^{13}C NMR (100 MHz, DMSO-d_6) δ 165.15, 150.62, 149.41, 149.17, 135.84, 131.79, 123.67, 111.42, 106.74, 67.07. ^{1}H–^{15}N COSY NMR (DMSO-d_6 at 30 °C) δ = −64.87 (pyridine) and −95.07 (bipy).

4,4′-Bis(pyridin-4-ylmethoxy)-2,2′-bipyridine (4). ^{1}H NMR (400 MHz, $CDCl_3$) δ 8.65 (dd, 2H), 8.51 (d, 1H), 8.08 (d, 1H), 7.38 (d, 2H), 6.93 (dd, 1H), 5.26 (s, 2H). ^{13}C NMR (100 MHz, $CDCl_3$) δ 165.61, 157.79, 150.52, 150.34, 145.09, 121.69, 111.83, 107.25, 68.20.

^{1}H NMR (500 MHz, DMSO-d_6 at 70 °C) δ 8.60 (dd, 2H), 8.51 (d, 1H), 8.02 (d, 1H), 7.47(d, 2H), 7.11 (dd, 1H), 5.37 (s, 2H). ^{1}H–^{15}N COSY NMR (DMSO-d_6 at 70 °C) δ = −65.35 (pyridine) and −94.18 (bipy).

Metal complexes

[**2·AgNO$_3$**]: ^{1}H NMR (500 MHz, DMSO-d_6) δ 8.62 (dq, 1H), 8.54 (d, 1H), 8.05 (d, 1H), 7.88 (dt, 1H), 7.59 (d, 1H), 7.39 (qd,

1H), 7.22 (dd, 1H), 5.42 (s, 2H). ^{1}H–^{15}N COSY NMR (DMSO-d_6 at 70 °C) δ = −71.01 (pyridine) and −112.41 (bipy).

[**3·AgNO$_3$**]: ^{1}H NMR (500 MHz, DMSO-d_6) δ 8.77 (d, 1H), 8.62 (dd, 1H), 8.59 (d, 1H), 8.18 (d, 1H), 7.99 (dt, 1H), 7.52 (qd, 1H), 7.34 (dd, 1H), 5.44 (s, 2H). ^{13}C NMR (100 MHz, DMSO-d_6) δ 166.10, 153.85, 151.92, 149.95, 149.63, 136.49, 131.66, 123.98, 112.03, 109.60, 67.67. ^{1}H–^{15}N COSY NMR (DMSO-d_6 at 30 °C) δ = −71.52 (pyridine) and −119.98 (bipy).

[**4·AgNO$_3$**]: ^{1}H NMR (500 MHz, DMSO-d_6) δ 8.63 (dd, 2H), 8.57 (d, 1H), 8.09 (d, 1H), 7.51 (d, 2H), 7.25 (dd, 1H), 5.44 (s, 2H). ^{1}H–^{15}N COSY NMR (DMSO-d_6 at 70 °C) δ = −69.32 (pyridine) and −107.53 (bipy).

General procedure for metallogelation

In a typical gelation experiment, the appropriate amounts of solid ligand (**3** or **4**) is placed in a test tube (45 × 15 mm) and dissolved in DMSO upon heating, whereupon equimolar amount of $AgNO_3$ solution in water is added to reach the final volume of 1.0 mL. The mixture is then heated to obtain a clear solution which, as it cooled down to room temperature, would afford a translucent gel. The gelation was observed at various ratios of DMSO/H_2O (v/v) and in this study four different ratios were used, *viz.* 8 : 2, 7 : 3, 6 : 4 and 1 : 1. No gels were obtained by using DMSO only.

Only ligand **3** forms unstable gel in an aqueous DMSO solvent at 1 wt%. No gelation was observed for ligand **4**.

Chemical reduction

In chemical reduction, the gel (**3·AgNO$_3$** or **4·AgNO$_3$**) was reduced from aqueous solution of $NaBH_4$. 1.0 mL of $NaBH_4$ solution which is 20 wt% to the silver molar amount in the gel was placed on the top of the gel and allowed it for slow diffusion at room temperature. During this time, $NaBH_4$ was diffused into the gel and reduces Ag^+ to Ag^0. In [**3·AgNO$_3$**] gel, the complete reduction was observed in a week period and in [**4·AgNO$_3$**] gel the reduction was slower and takes about 3 weeks. At high wt% of $NaBH_4$ (more than 40 wt% of $NaBH_4$) the reduction was faster and gel network was collapsed.

X-ray crystallography

Single crystal X-ray structure determination: the single crystals of ligands **2–4** were obtained by slow evaporation of chloroform solution. The X-ray diffraction data were collected on an Agilent Technologies Supernova diffractometer using Mo Kα or Cu Kα radiation. The CrysAlisPro program packages were used for cell refinements and data reductions. Structures were solved by charge flipping method using SUPERFLIP program or by direct methods using SHELXS-2008 program. Gaussian absorption correction was applied to all data and structural refinements were carried out using SHELXL-2015 software.

Scanning electron microscopy (SEM)

The sample preparation for SEM was performed by dissolving 6 mg of ligand (**3** or **4**) in 800 μL of DMSO with heating, to this clear solution equimolar amount of $AgNO_3$ in 200 μL of water was added. The resulting precipitate was solubilized by heating and let it cool down to room temperature to get a gel. The gel was then heated until it turned into a clear solution and drop casted over a carbon tape placed over aluminium stub. The sample was then allowed to dry under ambient conditions subjected for 6 nm sputter coating with Pt under vacuum conditions at 20 mA for 1 min. The samples were then subjected for imaging with Sigma Zeiss scanning electron microscope.

Rheological measurements

TA AR2000 stress controlled rheometer equipped with 20 mm steel plate and a Peltier heated plate was used for rheological characterization. The measuring setup was covered with a sealing lid in order to prevent evaporation during the measurements. Measurements were performed using 1.0% strain and oscillation frequency of 1.0 rad s^{-1} at 20 °C unless otherwise noted.

Transmission electron microscopy (TEM)

The transmission electron microscopy (TEM) images were collected using FEI Tecnai G2 operated at 120 kV and JEM 3200FSC field emission microscope (JEOL) operated at 300 kV in bright field mode with Omega-type Zero-loss energy filter. The images were acquired with GATAN DIGITAL MICROGRAPH software while the specimen temperature was maintained at −187 °C. The TEM samples were prepared by placing 3–5 μL of the pre-made gel on to a 300 mesh copper grid with holey carbon support film. The samples were dried under ambient condition prior to imaging.

Acknowledgements

T. R. and M. H. kindly acknowledge the financial support from the Academy of Finland (M. H. Proj. no. 295581, K. R. Proj. no. 263256, 265328, and 292746). Academy Professor Olli Ikkala, Aalto University, Finland is kindly acknowledged for financial support through the Academy of Finland, Centre of Excellence in Molecular Engineering of Biosynthetic Hybrid Materials (HYBER, 2014–2019) and ERC advanced grant (ERC-2011-AdG-291364) MIMEFUN (postdoc grant to Nonappa). The Aalto University Nanomicroscopy Center (Aalto-NMC) is kindly acknowledged for the use of its facilities. EU COST action CM 1302 "Smart Inorganic Polymers" is also gratefully acknowledged.

References

1 (*a*) S. J. Dalgarno, N. P. Power and J. L. Atwood, *Coord. Chem. Rev.*, 2008, **252**, 825–841; (*b*) B. H. Northrop, Y.-R. Zheng, K.-W. Chi and P. J. Stang, *Acc. Chem. Res.*, 2009, **42**, 1554–1563.

2 (*a*) R. G. Weiss and P. Terech, *Molecular Gels: Materials with self-assembled fibrillar, networks*, Springer, Dordrecht, The Netherlands, 2006; (*b*) A. R. Hirst, B. Escuder, J. F. Miravet

and D. K. Smith, *Angew. Chem., Int. Ed.*, 2008, **47**, 8002–8018.

3 J. Yan, B. S. Wong and L. Kang, Molecular Gels for Tissue Engineering, in *Soft fibrillar materials: Fabrication and applications*, ed. X. Y. Liu and J.-L. Li, Wiley-VCH Verlag GmbH & Co. KGaA, Weinheim, Germany, 2013, pp. 129–162.

4 C. K. Karan and M. Bhattacharjee, *Appl. Mater. Interfaces*, 2016, **8**, 5526–5535.

5 (*a*) P. K. Vemula, J. Li and G. John, *J. Am. Chem. Soc.*, 2006, **128**, 8932–8938; (*b*) E. Busseron, Y. Ruff, E. Moulin and N. Giuseppone, *Nanoscale*, 2013, **5**, 7098–7140; (*c*) R. Dong, Y. Pang, Y. Su and X. Zhu, *Biomater. Sci.*, 2015, **3**, 937–954.

6 (*a*) L. Korala, Z. Wang, Y. Liu, S. Maldonado and S. L. Brock, *ACS Nano*, 2013, **7**, 1215–1223; (*b*) S. Nardecchia, D. Carriazo, M. L. Ferrer, M. C. Gutierrez and F. del Monte, *Chem. Soc. Rev.*, 2013, **42**, 794–830; (*c*) J. D. Tovar, *Acc. Chem. Res.*, 2013, **46**, 1527–1537.

7 (*a*) J. F. Miravet and B. Escuder, *Chem. Commun.*, 2005, 5796–5798; (*b*) J. Potier, S. Menuel, M.-H. Chambrier, L. Burylo, J.-F. Blach, P. Woisel, E. Monflier and F. Hapiot, *Catal.*, 2013, **3**, 1618–1621.

8 (*a*) S. H. Jung, J. Jeon, H. Kim, J. Jaworski and J. H. Jung, *J. Am. Chem. Soc.*, 2014, **136**, 6446–6452; (*b*) X. Lan and Q. Wang, *Adv. Mater.*, 2016, **28**, 10499–10507.

9 (*a*) S. Ray, A. K. Das and A. Banerjee, *Chem. Commun.*, 2006, 2816–2818; (*b*) Z. X. Liu, Y. Feng, Z. Y. Zhao, Z. C. Yan, Y. M. He, X. J. Luo, C. Y. Liu and Q. H. Fan, *Chem. – Eur. J.*, 2014, **20**, 533–541; (*c*) B. O. Okesola, S. K. Suravaram, A. Parkin and D. K. Smith, *Angew. Chem., Int. Ed.*, 2016, **128**, 191–195.

10 J. H. Jung and S. Shinkai, *Top. Curr. Chem.*, 2004, **248**, 223–260.

11 D. J. Abdallah, L. Lu and R. G. Weiss, *Chem. Mater.*, 1999, **11**, 2907.

12 (*a*) C. Tomasini and N. Castellucci, *Chem. Soc. Rev.*, 2013, **42**, 156–172; (*b*) S. Federico, U. Nöchel, C. Löwenberg, A. Lendlein and A. T. Neffe, *Acta Biomater.*, 2016, **38**, 1–10; (*c*) F. Xie, L. Qin and M. Liu, *Chem. Commun.*, 2016, **52**, 930–933; (*d*) M. Tena-Solsona, J. Nanda, S. Diaz-Oltra, A. Chotera, G. Ashkenasy and B. Escuder, *Chem. – Eur. J.*, 2016, **22**, 6687–6694.

13 (*a*) Nonappa and U. Maitra, *Org. Biomol. Chem.*, 2008, **6**, 657–669; (*b*) S. Banerjee, V. M. Vidya, A. J. Savyasachi and U. Maitra, *J. Mater. Chem.*, 2011, **21**, 14693–14705; (*c*) H. Svobodova, Nonappa, Z. Wimmer and E. Kolehmainen, *J. Colloid Interface Sci.*, 2011, **361**, 587–593; (*d*) S. Ikonen, Nonappa and E. Kolehmainen, *CrystEngComm*, 2010, **12**, 4304–4311; (*e*) S. Ikonen, Nonappa, A. Valkonen, R. Juvonen, H. Salo and E. Kolehmainen, *Org. Biomol. Chem.*, 2010, **8**, 2784–2794; (*f*) Nonappa and U. Maitra, *Soft Matter*, 2007, **3**, 1428–1433; (*g*) T. T. T. Myllymäki, Nonappa, H. Yang, V. Liljeström, M. A. Kostiainen, J.-M. Malho, X. X. Zhu and O. Ikkala, *Soft Matter*, 2016, **12**, 7159–7165.

14 (*a*) I. Yoshikawa, S. Yanagi, Y. Yamaji and K. Araki, *Tetrahedron*, 2007, **63**, 7474–7481; (*b*) Z. Yang, P.-L. Ho, G. Liang, K. H. Chow, Q. Wang, Y. Cao, Z. Guo and B. Xu, *J. Am. Chem. Soc.*, 2007, **129**, 266–267; (*c*) G. Godeau and P. Barthelemy, *Langmuir*, 2009, **25**, 8447–8450; (*d*) G. M. Peters and J. T. Davis, *Chem. Soc. Rev.*, 2016, **45**, 3188–3206.

15 (*a*) R. J. H. Hafkamp, M. C. Feiters and R. J. M. Nolte, *J. Org. Chem.*, 1999, **64**, 412–426; (*b*) N. Yan, G. He, H. Zhang, L. Ding and Y. Fang, *Langmuir*, 2010, **26**, 5909–5917; (*c*) Y. Ogawa, C. Yoshiyama and T. Kitaoka, *Langmuir*, 2012, **28**, 4404–4412.

16 (*a*) D. Rizkov, J. Gun, O. Lev, R. Sicsic and A. Melman, *Langmuir*, 2005, **21**, 12130–12138; (*b*) P. Mukhopadhyay, Y. Iwashita, M. Shirakawa, S. Kawano, N. Fujita and S. Shinkai, *Angew. Chem., Int. Ed.*, 2006, **45**, 1592–1595; (*c*) D. Singh and J. B. Baruah, *Tetrahedron Lett.*, 2008, **49**, 4374–4377.

17 Nonappa and E. Kolehmainen, *Gels*, 2016, **2**, 9.

18 (*a*) M. Suzuki, Y. Nakajima, M. Yumoto, M. Kimura, H. Shirai and K. Hanabusa, *Langmuir*, 2003, **19**, 8622–8624; (*b*) J. Seo, J. W. Chung, E.-H. Jo and Y. Park, *Chem. Commun.*, 2008, 2794–2796; (*c*) S. Bhowmik, B. N. Ghosh and K. Rissanen, *Org. Biomol. Chem.*, 2014, **12**, 8836–8839; (*d*) R. Tatikonda, S. Bhowmik, K. Rissanen, M. Haukka and M. Cametti, *Dalton Trans.*, 2016, **45**, 12756–12762.

19 G. R. Whittell, M. D. Hager, U. S. Schubert and I. Manners, *Nat. Mater.*, 2011, **10**, 176–188.

20 (*a*) Q. Liu, Y. Wang, W. Li and L. Wu, *Langmuir*, 2007, **23**, 8217–8223; (*b*) B. N. Ghosh, S. Bhowmik, P. Mal and K. Rissanen, *Chem. Commun.*, 2014, **50**, 734–736; (*c*) M. Xue, Y. Lu, Q. Sun, K. Liu, Z. Liu and P. Sun, *Cryst. Growth Des.*, 2015, **15**, 5360–5367; (*d*) M. Paul, K. Sarkar and P. Dastidar, *Chem. – Eur. J.*, 2015, **21**, 255–268.

21 (*a*) N. N. Adarsh and P. Dastidar, *Cryst. Growth Des.*, 2011, **11**, 328–336; (*b*) L. Sambri, F. Cucinotta, G. D. Paoli, S. Stagni and L. D. Cola, *New J. Chem.*, 2010, **34**, 2093–2096; (*c*) S. Song, A. Song, L. Feng, G. Wei, S. Dong and J. Hao, *Appl. Mater. Interfaces*, 2014, **6**, 18319–18328.

22 (*a*) J. R. Nitschke, *Acc. Chem. Res.*, 2007, **40**, 103–112; (*b*) P. Mal, D. Schultz, K. Beyeh, K. Rissanen and J. R. Nitschke, *Angew. Chem., Int. Ed.*, 2008, **47**, 8297–8301; (*c*) P. Mal, B. Breiner, K. Rissanen and J. R. Nitschke, *Science*, 2009, **324**, 1697–1698; (*d*) W. Meng, B. Breiner, K. Rissanen, J. D. Thoburn, J. K. Clegg and J. R. Nitschke, *Angew. Chem., Int. Ed.*, 2011, **50**, 3479–3483; (*e*) T. K. Ronson, C. Giri, N. K. Beyeh, A. Minkkinen, F. Topić, J. J. Holstein, K. Rissanen and J. R. Nitschke, *Chem. – Eur. J.*, 2013, **19**, 3374–3382; (*f*) C. Giri, F. Topić, P. Mal and K. Rissanen, *Dalton Trans.*, 2014, **43**, 17889–17892; (*g*) A. M. Castilla, W. J. Ramsay and J. R. Nitschke, *Acc. Chem. Res.*, 2014, **47**, 2063–2073; (*h*) J. Roukala, J. Zhu, C. Giri, K. Rissanen, P. Lantto and V.-V. Telkki, *J. Am. Chem. Soc.*, 2015, **137**, 2464–2467; (*i*) C. Giri, F. Topić, M. Cametti and K. Rissanen, *Chem. Sci.*, 2015, **6**, 5712–5718.

23 (*a*) A. Y.-Y. Tam and V. W.-W. Yam, *Chem. Soc. Rev.*, 2013, **42**, 1540; (*b*) W. Fang, X. Liu, Z. Lu and T. Tu, *Chem. Commun.*, 2014, **50**, 3313; (*c*) K. Hong, Y. K. Kwon, J. Ryu, J. Y. Lee, S. H. Kim and K. H. Lee, *Sci. Rep.*, 2016, **6**, 29805; (*d*) Z.-X. Liu, Y. Feng, Z.-Y. Zhao, Z.-C. Yan, Y.-M. He, X.-J. Luo, C.-Y. Liu and Q.-H. Fan, *Chem. – Eur. J.*, 2014, **20**, 533–541.

24 K. Nath, A. Husain and P. Dastidar, *Cryst. Growth Des.*, 2015, **15**, 4635–4645.

25 (*a*) Y. He, Z. Bian, C. Kang, Y. Cheng and L. Gao, *Chem. Commun.*, 2010, **46**, 3532–3534; (*b*) Y. Zhang, B. Zhang, Y. Kuang, Y. Gao, J. Shi, X. X. Zhang and B. Xu, *J. Am. Chem. Soc.*, 2013, **135**, 5008–5011.

26 (*a*) R. Aoyama, H. Sako, M. Amakatsu and M. Yamanaka, *Polym. J.*, 2015, **47**, 136–140; (*b*) P. Wei, X. Yan and F. Huang, *Chem. Soc. Rev.*, 2015, **44**, 815–832.

27 (*a*) S. Butun and N. A. Sahiner, *Polymer*, 2011, **52**, 4834–4840; (*b*) Y. Lu, P. Spyra, Y. Mei, M. Ballauff and A. Pich, *Macromol. Chem. Phys.*, 2007, **208**, 254–261; (*c*) V. Thomas, M. M- Yallapu, B. Sreedhar and S. K. Bajpai, *J. Colloid Interface Sci.*, 2007, **315**, 389–395; (*d*) B. Xia, Q. Cui, F. He and L. Li, *Langmuir*, 2012, **28**, 11188–11194; (*e*) P. Rajamalli, P. Malakar, S. Atta and E. Prasad, *Chem. Commun.*, 2014, **50**, 11023–11025.

28 (*a*) J. Wu, S. Hou, D. Ren and P. T. Mather, *Biomacromolecules*, 2009, **10**, 2686–2693; (*b*) J. Nanda, B. Adhikari, S. Basak and A. Banerjee, *J. Phys. Chem. B*, 2012, **116**, 12235–12244.

29 (*a*) B. Adhikari and A. Banerjee, *Chem. – Eur. J.*, 2010, **16**, 13698–13705; (*b*) M. Eid, *J. Inorg. Organomet. Polym.*, 2011, **21**, 297–301.

30 B. Hu, S. Wang, K. Wang, M. Zhang and S. Yu, *J. Phys. Chem. C*, 2008, **112**, 11169–11174.

31 I. A. Wani, A. Ganguly, J. Ahmed and T. Ahmad, *Mater. Lett.*, 2011, **65**, 520–522.

32 X. Gao, L. Wei, H. Yan and B. Xu, *Mater. Lett.*, 2011, **65**, 2963–2965.

33 (*a*) H. Jia, J. Zeng, W. Song, J. An and B. Zhao, *Thin Solid Films*, 2006, **2**, 281–287; (*b*) P. Kshirsagar, S. S. Sangaru, M. A. Malvindi, L. Martiradonna, R. Cingolani and P. P. Pomp, *Colloids Surf., A*, 2011, **392**, 264–270.

34 M.-O. M. Piepenbrock, N. Clarke and J. W. Steed, *Soft Matter*, 2011, **7**, 2412.

35 S. Bhattacharjee, S. K. Samanta, P. Moitra, K. Pramoda, R. Kumar, S. Bhattacharya and C. N. R. Rao, *Chem. – Eur. J.*, 2015, **21**, 5467–5476.

36 M. Kimura, T. Htanaka, H. Nomoto, J. Takizawa, T. Fukawa, Y. Tatewaki and H. Shirai, *Chem. Mater.*, 2010, **22**, 5732–5738.

37 M. Cametti and Z. Dzolic, *Chem. Commun.*, 2014, **50**, 8273–8286.

38 CCDC 1500637–1500639 contain the supplementary crystallographic data for this paper.

39 (*a*) B. Escuder, M. LLusar and J. F. Miravet, *J. Org. Chem.*, 2006, **71**, 7747–7752; (*b*) Nonappa and E. Kolehmainen, *Soft Matter*, 2016, **12**, 6015–6026; (*c*) Nonappa, M. Lahtinen, B. Behera, E. Kolehmainen and U. Maitra, *Soft Matter*, 2010, **6**, 1748–1757; (*d*) V. Noponen, Nonappa, M. Lahtinen, A. Valkonen, H. Salo, E. Kolehmainen and E. Sievänen, *Soft Matter*, 2010, **6**, 3789–3796; (*e*) Nonappa, D. Saman and E. Kolehmainen, *Magn. Reson. Chem.*, 2015, **53**, 256–260.

40 (*a*) O. V. Dolomanov, A. J. Blake, N. R. Champness, M. Schröder and C. Wilson, *Chem. Commun.*, 2003, 682–683; (*b*) A. R. Biju and M. V. Rajasekharan, *Polyhedron*, 2008, **27**, 2065–2068; (*c*) L.-M. Wang, Y. Wang, Y. Fan, L.-N. Xiao, Y.-Y. Hu, Z.-M. Gao, D.-F. Zheng, X.-B. Cui and J.-Q. Xu, *CrystEngComm*, 2014, **16**, 430–440.

41 H. Svobodová, Nonappa, M. Lahtinen, Z. Wimmer and E. Kolehmainen, *Soft Matter*, 2012, **8**, 7840–7847.

IV

SELF-ASSEMBLY INDUCED PHOTOLUMINESCENCE AND *IN-SITU* ULTRASMALL NANOPARTICLE FORMATION IN COORDINATION POLYMER BASED METALLOGELS

by

Rajendhraprasad Tatikonda, Evgeny Bulatov, Nonappa, & Matti Haukka

manuscript

Self-assembly induced photoluminescence and *in-situ* ultrasmall nanoparticle formation in coordination polymer based metallogels

Rajendhraprasad Tatikonda,[a] Evgeny Bulatov,[a] Nonappa,*[b,c] and Matti Haukka*[a]

Abstract: Herein we report silver(I) coordination induced self-assembly of ligands derived from 3-aminopyridine and 4-aminopyridine conjugates of either pyridine or 2,2´-bipyridine cores in aqueous dimethyl sulfoxide leading to metallosupramolecular gels. The ligands display aggregation induced photoluminescence upon metallogel formation. The resulting metallogels show spontaneous, *in-situ* ultrasmall (< 2-3 nm) nanoparticle formation without any additional reducing agent. The cation specific gelation was found to be independent of counter anion, leading to highly entangled fibrillar network containing nanoparticles embedded in it. The gels derived from bipyridyl based ligands revealed the thermoirreversible nature as suggested by variable temperature NMR. Further, using single crystal X-ray crystallography and ^{1}H-^{15}N two-dimensional (2D) NMR spectroscopy, we show that the tetrahedral coordination of silver ions allows simultaneous coordination polymerization and supramolecular cross-linking leading to gelation. The fibrillar network formation and *in-situ* nanoparticle formation were followed using spectroscopic studies and transmission electron microscopy imaging.

Introduction

Metal-ligand (M-L) interaction induced assembly of small organic molecules (i.e. metallosupramolecular chemistry) evolved as one of the versatile ways to build topologically diverse metallosupramolecular structures.[1] The ability to tune the interaction strength, number of metal binding sites with synthetically simple organic ligands offer rapid access to one, two, or three-dimensional metallosupramolecular polymeric structures.[2] In certain cases, the resulting superstructures undergo hierarchical assembly to highly entangled fibrillar networks and immobilize the solvents leading to gelation. The resulting gels are known as metallosupramolecular gels or simply metallogels.[3] Metallogels are either produced from discrete coordination compounds,[4] infinite coordination polymers (CPs),[5] or cross-linked CPs[6]. The presence of metal ions provides some of the unique responsiveness to temperature,[7] mechanical perturbance,[8] light,[9] oxidation-reduction,[10] electric- and magnetic fields[11]. The structure and coordination ability of organic ligand has an impact on topologies and functional properties of metal complexes. Therefore, selection of organic ligand is vital in preparing functional metallogels. Ligands containing different metal binding sites have been studied in metallogelation, for example, polypyridyl compounds, porphyrin derivatives, amines, thiols, azoles and carboxylates.[12-16] In order to obtain a metallogel, ligand should able to participate in one or more than one noncovalent intermolecular interactions (such as H-bonding, π-stacking, van der Waals in interaction, electrostatic interactions, London dispersion forces) in addition to metal coordination.[17] Various approaches have been reported in the literature on the preparation of metallogels, including subcomponent self-assembly.[18] Potential applications of metallogels in cosmetics, lubrication, magnetic materials, and sensors for dye molecules have been demonstrated in the literature.[19-21] Further, properties such as the self-assembly induced luminescence provides promising applications in optoelectronics[22] and in developing vapochromic sensors[23]. Recently, terpyridine ligands containing perfluoroalkyl chains have been reported to exhibit anion selective gelation and rapid self-healing properties.[24] The transition metal containing gels such as palladium have also been shown to improve the catalytic activities.[25]

Metallogels containing Ag(I) as metal ions and pyridine derivatives as ligands, represents one of the extensively studied systems. This attributed to their antimicrobial and photophysical properties.[26] In addition to its role as coordinating agent, Ag(I) also serves as a precursor for *in-situ* nanoparticle formation without any additional stabilizing agents.[27] *In-situ* silver nanoparticle (AgNP) formation in metallogels involving pyridine and bipyridyl molecules have been reported either under ambient conditions, UV irradiation or sodium borohydride reduction.[28,29] However, in a majority of the reports, the resulted AgNPs were relatively large (>5 nm). We have recently reported synthetically simple bipyridyl based gelators displaying a remarkable difference in their ability to size and shape selective AgNP formation depending on the source of reducing agent and gelator chemical structure.[30] Further, the binding of Ag(I) to form polymeric structures *via* tetra coordination of Ag(I) has been proposed based on 2D NMR spectroscopic studies. However, the unambiguous proof on the nature of metal-ligand coordination leading to gelation remains elusive. Understanding the exact metal-ligand interaction in hierarchical structure formation is important not only to gain insights on the gelation mechanism, but also in rational design of materials with desired properties.

Here in, we report the synthesis, metal chelation directed gelation, self-assembly induced luminescence and *in-situ* ultrasmall (≤ 3 nm) AgNP formation of pyridyl and bipyridyl amides (**1-4**) in aqueous dimethyl sulfoxide (Fig. 1). Further, using a combined single crystal X-ray diffraction and ^{1}H-^{15}N 2D

[a] M.Sc. R. Tatikonda, M. Sc. E, Bulatov, Prof. M. Haukka
Department of Chemistry, University of Jyväskylä, P. O. Box 35, FI-40014 Jyväskylä, Finland.
E-mail: matti.o.haukka@jyu.fi
[b] Dr. Nonappa
Department of Applied Physics, Aalto University School of Science, Puumiehenkuja 2, FI-02150 Espo, Finland.
[c] Department of Bioproducts and Biosystems, Aalto University School of Chemical Engineering, Kemistintie 1, FI-02150 Espo, Finland.

Supporting information for this article is given via a link at the end of the document.((Please delete this text if not appropriate))

NMR spectroscopy, we show that, tetra coordinated silver is responsible for metallosupramolecular polymerization. Importantly, silver(I) directs, coordination polymerization (CP), supramolecular cross linking between the polymeric chains thereby leading to highly entangled fibrillar network formation and also acts as a source for ultrasmall AgNPs. The gelation is cation specific and their stability depends on the counter anion.

Results and Discussion

The pyridyl amide ligands (**1** and **2**) were synthesized according to the reported literature procedure.[31] The synthesis of bipyridyl amide ligands (**3** and **4**) were achieved by the reaction of 4,4´-dicarboxy-2,2´-bipyridine with 3-, or 4-aminopyridines in the presence of *N*-ethyl-*N*'-(3-dimethylaminopropyl carbodiimide (EDC) in *N*, *N*-dimethyl formamide (DMF) solvent (see ESI).

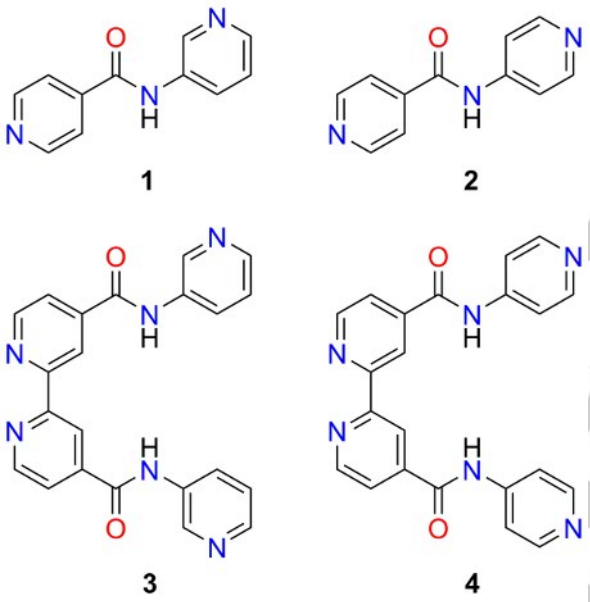

Figure 1. Chemical structures of ligands used in this study.

First, we discuss the structural properties of ligands **1-4** (Fig. 1). The solid state structural details of ligands **1-2** are already documented in literature.[32] Therefore, no attempts were made to obtain single crystals. Instead, efforts were made to grow single crystal X-ray structures of ligands **3** and **4**. However, only ligand **4** was resulted in quality single crystal either from acetonitrile, dimethyl sulfoxide (DMSO) or *N, N*- dimethyl formamide (DMF) (Fig. 2).[33] Ligand **3** either remained in solution or resulted in a precipitate. The solid-state structure of **4** obtained from acetonitrile (Fig. 2c) shows well organized intermolecular H-bonding (N–H···O = 2.18 Å) between the adjacent molecules through amide groups. The crystal packing also reveals that the presence of weak intermolecular C=C–H···N and C=C–H···O H-bonding. In addition to these weak H-bonds, the packing commences through off-set π···π interactions (3.3 Å). When ligand **4** was crystallized from DMSO (Fig. 2a) or DMF (Fig. 2b), solvates were obtained, and the ligand molecule participated in H-bonding with the oxygen atom of solvent molecules.

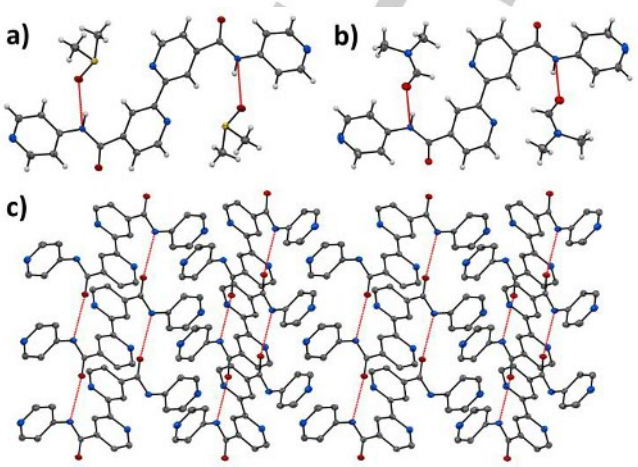

Figure 2. X-ray single crystal structure: Molecular unit of **4** obtained from DMSO (a), DMF (b) and crystal packing of well-organized H-bonding in **4** obtained from acetonitrile (c). Thermal ellipsoids are drawn at 50% probability.

Ligands **1** and **2** have been previously studied for their hydrogelation ability without addition of metal ions by Das *et al*., and their experimental results have shown that only **2** was able to form a hydrogel (*note*: no metallogelation was reported).[32] In this study, ligands **1** and **2** along with their dimeric forms (**3** and **4**) are screened for metallogelation in a solvent mixture of water and DMSO. Six different counter anions *viz*. nitrate ($-NO_3^-$), triflate ($-OTf^-$), perchlorate ($-ClO_4^-$), acetate ($-OAc^-$), tetrafluoroborate ($-BF_4^-$) and hexafluorophosphate ($-PF_6^-$) were used. In a typical gelation experiment, an appropriate amount of solid ligand (**1-4**) was placed in a test tube (*l*=45 mm, *d*=15 mm) and dissolved in DMSO upon heating, whereupon an aqueous solution of the corresponding silver salt (AgX) was added to reach a final volume of 1.0 mL. The mixture was then cooled down to room temperature, which furnished a translucent/transparent gel or precipitate depending on the ligand and silver salt (Table 1 and Fig. 3).

Table 1. Gelation studies of ligands **1-4** with various silver salts in a mixture of water and DMSO. (Note: **G**= gel, **G***= gels are unstable and collapsed upon standing at room temperature for an hour, **P**= precipitate)

	L	NO_3^-	ClO_4^-	OTf^-	PF_6^-	BF_4^-	OAc^-
3:7 (v/v)	**1**	**G**	**G***	**G***	**G**	**G**	**G**
(DMSO:H_2O)	**2**	**P**	**P**	**G**	**G**	**P**	**G**
7:3 (v/v)	**3**	**G**	**G**	**G**	**G**	**G**	**G**
(DMSO:H_2O)	**4**	**G***	**G***	**G***	**G**	**G***	**G**

Figure 3. Photographs of gels prepared from ligands **1-4** with various silver salts in aqueous DMSO.

The molar ratio of ligands **1** or **2** with the corresponding silver salt is respectively 2:1 (ligand:metal) and the gelation was observed at different ratios of DMSO/H_2O (v/v) as 2:8, 3:7 (Fig. 3) and 4:6. The gel obtained from 1:1 of ligand to silver was found to be unstable and collapsed at room temperature within *ca.* 10 minutes. It should be stated that the solvent mixture has an impact on metallogelation and no gelation was observed in pure DMSO or when the volume of DMSO was higher than the water in a mixture. The minimum gelation concentration (mgc) was found fond to be 0.8 wt% for both the tested ligands in 3:7 (v/v) of DMSO/H_2O. In the case of ligands **3** and **4**, the molar ratio of ligand to the silver is 1:1 and the gelation was observed at different ratios of DMSO/H_2O (v/v) as 8:2, 7:3 (Fig. 3) and 6:4. The mgc is 0.4 wt% for both the tested ligands in 6:4 (v/v) of DMSO/H_2O. The gelation experiments of **1** and **3** with all the tested silver salts resulted in metallogels. Gels obtained from **1** with $ClO4^-$, OTf^- counter anions were found to be unstable and collapsed to precipitate. Surprisingly, **2** gave metallogels only with the larger counter anions (OTf^-, PF_6^- and OAc^-). Ligand **4** also able to form gels with all the tested salts but most of them are unstable except with PF_6^- and OAc^- anions. These metallogels were found to be robust and most importantly, thermoirreversible due to the poor solubility of the ligand to silver aggregates. In order to further support the thermoirreversible nature of the metallogels, NMR spectroscopy experiments were performed. NMR spectroscopy is useful both in understanding the interactions involved in self-assembly as well as determining the gel-sol transition.[34] The thermoirreversibility of **[3•AgNO$_3$]** gel (8:2 of DMSO-d_6/D_2O) was proven by performing variable temperature (VT) ^{1}H NMR experiments from 30 °C-90 °C (Fig. S9). The VT NMR spectra showed characteristic broad signals at room temperature, and no changes were noted even at higher temperatures. This suggests that the gel is stable at higher temperatures, and no gel-sol transition is occurring at the experimental conditions.

To gain further insights, 1D (^{1}H and ^{13}C) and 2D (^{1}H-^{1}H correlation NMR spectroscopy (COSY), ^{1}H-^{13}C heteronuclear multiple bond correlation (HMBC) and ^{1}H-^{15}N COSY NMR spectroscopic measurements were performed for ligands **1-4** and their Ag-complexes. Upon metal complexation, a significant change in the chemical shifts for the protons was observed (see ESI for ^{1}H NMR spectral comparison). To probe the effect of metal coordination, 2D ^{1}H-^{15}N correlation spectroscopy for free ligand and its Ag-complexes were performed in DMSO-d_6.[30] Fig. 4a shows ^{1}H-^{15}N 2D-COSY of the free ligand **1** and fig. 4b of its 2:1 metal complex **[1$_2$•AgNO$_3$]**. ^{1}H-^{15}N 2D COSY spectrum of ligands and its Ag-complexes were measured to know metal coordination. Upon complexation, an obvious change in the chemical shift values of nitrogen atoms was observed. The nitrogen atoms (N1 and N3) of ligand **1** showed an upfield shift of 6.84 and 10.62 ppm respectively, which is a clear indication of coordination of both the nitrogen atoms from the ligand. These NMR spectroscopic results further supported by observed solid state structures. The 2D ^{1}H-^{15}N correlation spectra of ligand **3** and its complex **[3•AgNO$_3$]** (Fig. S7) was measured 70 °C due to its solubility issue. Even at this high temperature a significant upfield shift from the nitrogen atoms of bipyridine (N1) and pyridine (N3) moieties were observed and the shift is 4.35 and 4.57 ppm respectively.

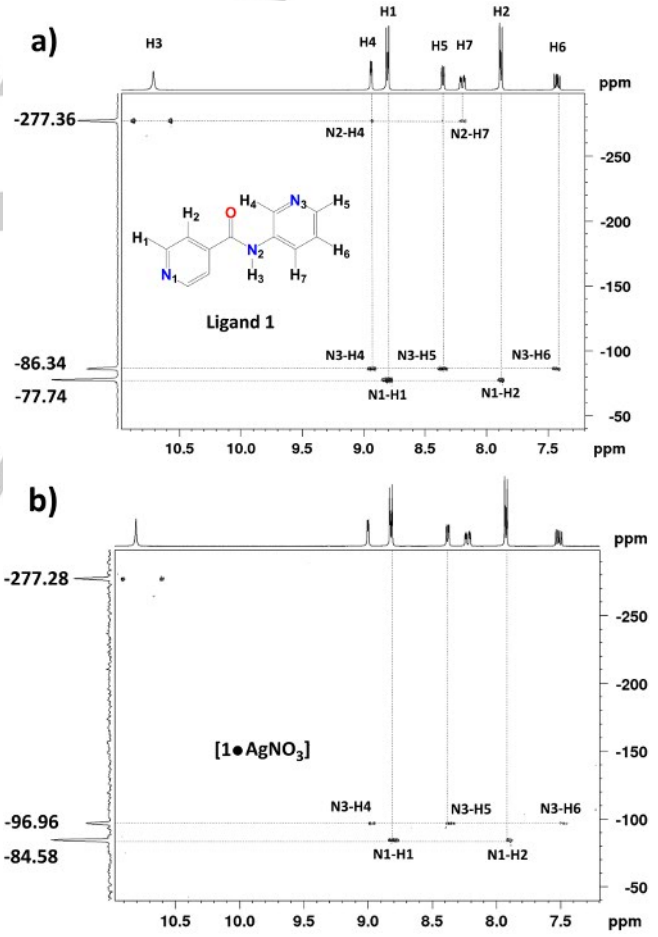

Figure 4. ^{1}H-^{15}N 2D correlated spectrum of ligand **1** and **[1$_2$•AgNO$_3$]** in DMSO-d_6 at 30 °C.

The position of the counter anion in Ag-complex was predicted based on ^{1}H NMR spectral results. The NH signals of **1** (Fig. S1) and **3** (Fig. S4) showed a downfield shift 0.07 and 0.04 ppm respectively, in their Ag-complexes. This suggests that the presence of intermolecular H-bonding between the hydrogen atoms from amide group and counter anions, which can be seen in the solid-state structure of silver CPs with the ligand **1**. Based on the molar ratio of bipyridine ligands (**3** or **4**) to **AgX** (1:1) and the NMR spectral analysis, the complex was assigned as CP where the silver cation is tetrahedrally coordinated by one chelating bipyridine unit and two bridging pyridine rings from adjacent ligands (Fig. 5 and S11).

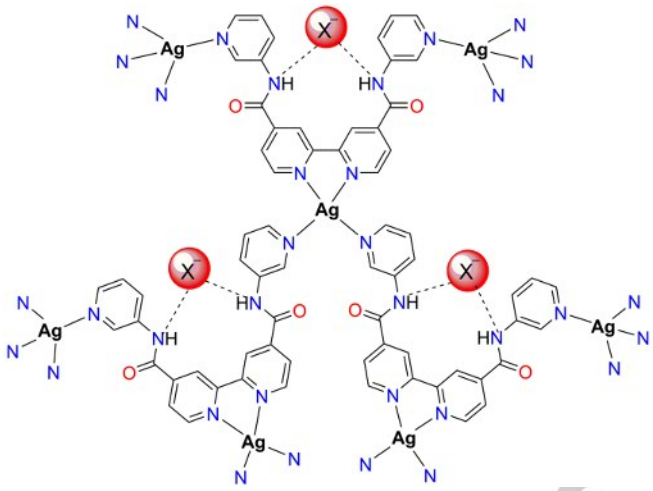

Figure 5. The proposed structure of the coordination polymer **[3●AgX]$_n$** (X= NO_3^-, ClO_4^-, OTf^-, PF_6^- and BF_4^-).

In order to understand detailed packing and interactions involved in coordination polymerization, we investigated the X-ray crystal structure of CPs. The gelation experiments of **1** with silver(I) in 7:3 or 8:2 (v/v) of DMSO and water (non-gelling conditions) leads to the formation of single crystals or precipitate. The reaction of **1** with AgX (X= ClO_4^-, OTf^- and PF_6^-) at 2:1 molar amounts gave two-dimensional coordination polymers (2D-CPs) where the silver was tetra coordinated by four individual ligand molecules.[33] The **[1$_2$●AgClO$_4$]** (Fig. 6a)**, [1$_2$●AgOTf]** (Fig. 6b)**,** and **[1$_2$●AgPF$_6$]**[35] (Fig. S15) were crystallized in monoclinic space group $P2_1/n$. These 2D layers interact further with each other through counter anions *via* classical N–H···O and several weak C=C–H_{Py}···O, and C=C–H_{Py}···F hydrogen bonds (Table S3) to immobilize the solvent molecules. One-dimensional ladder type coordination polymer was obtained from the reaction of **1** with AgOAc. The **[1$_2$●AgOAc]** (Fig. 6c) was crystallized in triclinic space group $P\bar{1}$. Similarly, each silver atom is tetra coordinated by two ligand molecules and two bridging acetate molecules to form infinite ladder type architecture. These ladders are further self-assembled to generate 2D layered structure *via* N–H···O hydrogen bonding involving amide N and acetate O atoms of the adjacent chains (N···O= 2.760(2) Å).

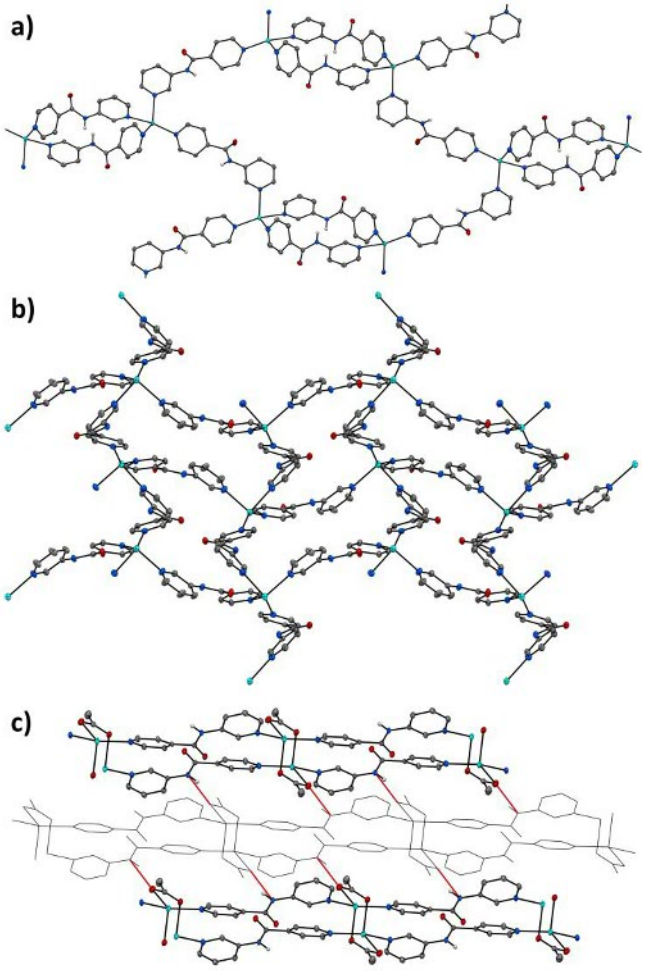

Figure 6. Crystal packing of 2D-CPs of **[1$_2$●AgClO$_4$] (a)**, **[1$_2$●AgOTf] (b)** and 1D-CP of **[1●AgOAc] (c)**. Thermal ellipsoids are drawn at 50 % probability level and counter anions (ClO_4^- and $CF_3SO_3^-$) are omitted for clarity.

Morphology and *in-situ* nanoparticle formation

The morphological features of gels were investigated using electron microscopy for all the gels studied in this work. The transmission electron microscopy (TEM) suggested that the metallogels derived from **[1$_2$●AgX] and [2$_2$●AgX]** forms either film-like or rod-like networks depending on the counter anions. Whereas, the metallogels derived from **[3●AgX]** and **[4●AgX]** showed highly entangled fibrillar networks except with BF_4. The most interesting finding from this work is the *in-situ* formation of ultrasmall nanoparticle. Figure 7 shows representative TEM micrographs from **[1$_2$●AgX]** and **[3●AgX]** with various silver salts. While most of the gels showed the formation of fibers with uniformly distributed ultrasmall silver nanoparticles, the perchlorate and acetate furnished film-like structures with uniformly distributed nanoparticles. Larger particles >2 nm was also observed in the case **[1$_2$●AgOAc]** gels. Whereas, the gels

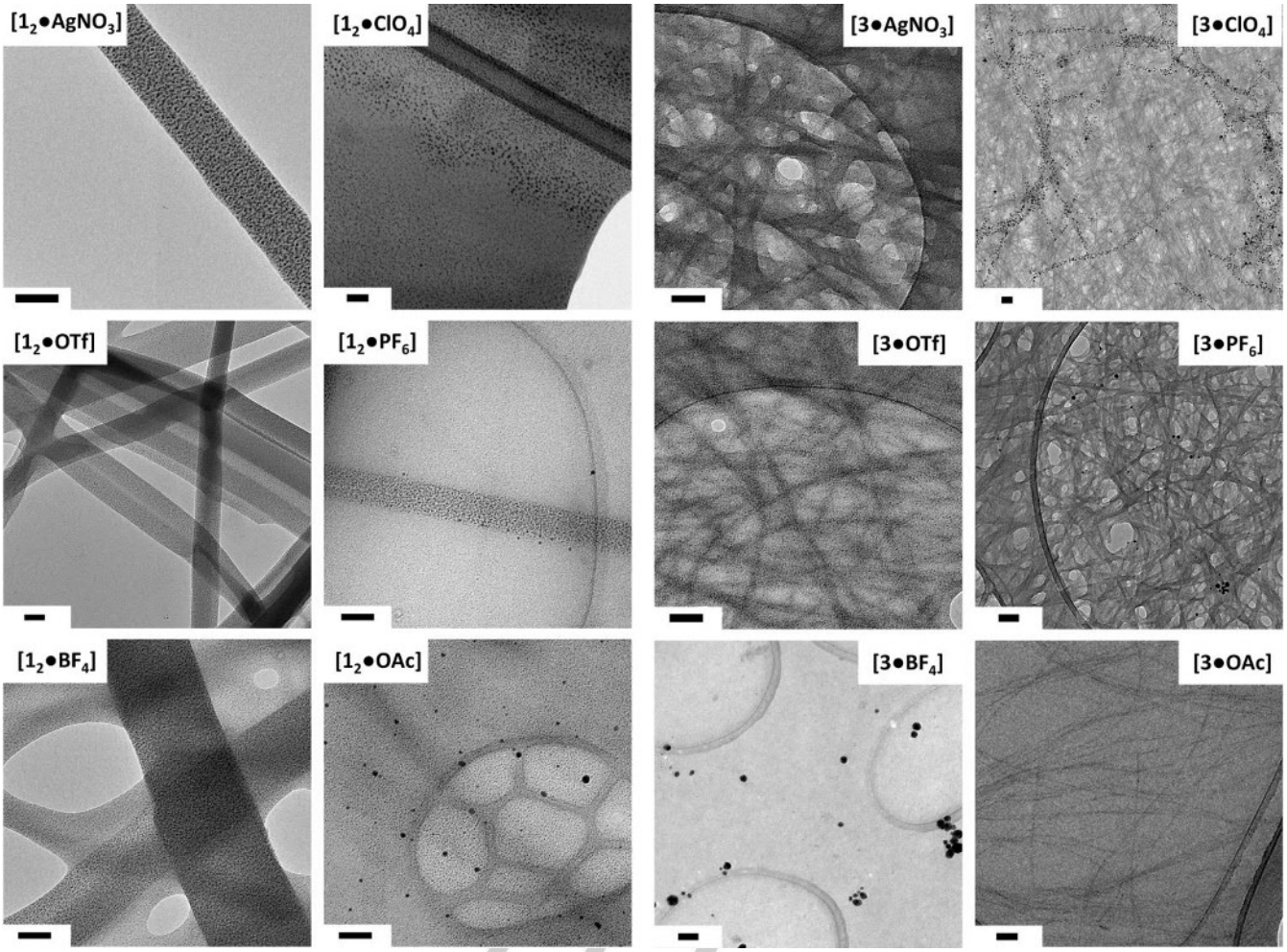

Figure 7. TEM micrographs of *in-situ* formed nanoparticles. 50 nm bar scale.

derived from **[3●AgX]** and **[4●AgX]** (see ESI) showed both ultrasmall and relatively larger nanoparticles. This is also evident from the surface plasmon resonance (SPR) spectra of the gels (Fig. S18). As in the case of gels derived from **[1_2●AgX]** and **[2_2●AgX],** they show the formation of ultrasmall AgNPs uniformly distributed along the fibers and film-like materials. However, in addition to ultrasmall nanoparticles, the gels derived from **[3●$AgPF_6$]**, **[3●$AgClO_4$]** and **[3●$AgBF_4$]** also showed the formation of larger nanoparticles.

Photoluminescence

Another interesting finding in our study is the self-assembly induced photoluminescence displayed by all the metallogels studied in this work. Accordingly, the photoluminescence properties of metallogels prepared from ligands **1-4** with **AgX** in a mixture of DMSO and water were investigated. We used the $AgPF_6$ since it resulted in stable gels upon complexation with all the ligands (Table 1). All the gels displayed a weak emission in the visible range upon photoexcitation at 300 nm (see Fig. S16a). Emission measurements at different temperatures revealed that the luminescence intensity decreases upon heating (Fig. 8, Fig. S16b,c).

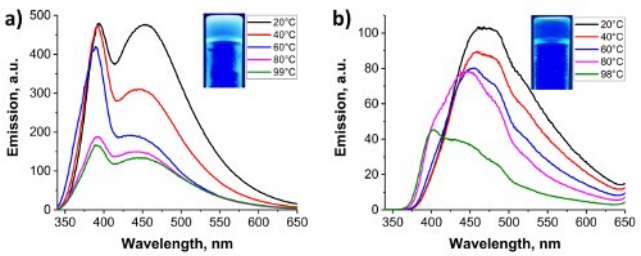

Figure 8. The proposed structure of the coordination polymer **[3●AgX]$_n$** (X= NO_3^-, ClO_4^-, OTf^-, PF_6^- and BF_4^-).

Taking into account low emission intensity and slight dependence of emission on orientation of the gel sample, no significant influence of the anion on luminescence was observed within PF_6 and NO_3 series (Fig. S16e,f). All emission spectra of the gels displayed emission band with maxima at 362 and 393 nm, which is attributed to solvent admixture and its intensity depends on the sample transparency. Comparison of the emission spectra of hydrogel of **2** and metallogel **[2_2●$AgPF_6$]** (Fig. S16d) reveals essentially the same emission wavelength, even though the emission intensity of the metallogel is several orders of magnitude lower. This allows for preliminary assignment of the luminescence of the metallogels under study to intraligand π*-π or π*-n transitions. Low emission intensity of the metallogels probably results from interplay of the two counteracting factors: facilitated by silver(I) singlet-triplet transitions (reducing luminescence intensity)[36] on one hand and suppressed vibrational relaxation due to increased rigidity of the polymer on the other hand.

This suggestion is also supported by similarity between emission spectra of solid **1** and **2** (Fig. S17) and their silver metallogels, which has also been observed for other **1**-based coordination polymers.[37] At the same time, **3** and **4** based metallogels display red-shifted emission compared to pure solid ligands. This observation can be attributed to chelation of silver atoms by bipyridyl moieties, resulting in the shift of luminescence emission. Further, variable temperature studies revealed that the upon gel-sol transition, there is a significant decrease in the luminescence and is reversible.

Conclusions

Metallogels are continuously evolving area in metallosupramolecular chemistry. Silver(I) coordinated metallogels offers many additional properties such as spontaneous *in-situ* silver nanoparticle formation, optical and mechanical properties. They are also model systems to understand the structural details, interactions involved in the self-assembly as well as gelation. This work demonstrates that strategically simple pyridyl and bipyridyl amides lead to an unprecedented self-assembly induced gelation, photoluminescence as well as rapid access to ultrasmall nanoparticles. The noble metal ultrasmall nanoparticles are gaining considerable attention in recent years because of their unique size and shape dependent optical properties and possibilities to construct hierarchical colloidal superstructures.[38] The structural details obtained by X-ray crystallography studies are useful in rational design of new gelators. The assembly induced luminescence properties are applicable in designing sensors. The *in-situ* nanoparticle formation provides rapid access to hybrid plasmonic nanomaterial.

Experimental Section

General synthetic procedure for N-(Pyridin-3-yl)isonicotinamide (1) and N-(Pyridin-4-yl)isonicotinamide (2)

The synthesis of ligands **1** and **2** are carried out by following the literature procedure. A mixture of Isonicotinoyl chloride Hydrochloride (0.712 g, 4 mmol) and corresponding aromatic amine (0.377 g, 4 mmol) in pyridine solution (6 mL) was heated to reflux for 2h. After the reaction time, the reaction mixture was cooled to room temperature and poured into the ice-cold water (20 mL) with constant stirring. During stirring, the off-white precipitate was formed which is filtered and washed with excess of water and dried under vacuum.

(1). ^{1}H NMR (300 MHz, DMSO-d_6) δ 10.71 (s, 1H), 8.93 (d, 1H), 8.80 (dd, 2H), 8.35 (dd, 1H), 8.19 (dq, 1H), 7.87 (dd, 2H), 7.43 (q, 1H). ^{13}C NMR (75 MHz, DMSO-d_6) δ 164.44, 150.32, 144.99, 141.97, 141.37, 135.32, 127.67, 123.65, 121.57. ^{1}H-^{15}N COSY NMR (DMSO-d_6 at 30 °C) δ -77.74 (Carbonyl pyridine N^C), -86.34 (amino pyridine N^N) and -277.36 (amide nitrogen N^A). FTIR: 1677.32 cm-1 (CO), 3299.36 cm-1 (NH). Anal. Calcd for $C_{11}H_9N_3O$: C, 66.32: H, 4.55; N, 21.09. Found: C, 66.45; H, 4.92; N, 20.86.

(2). ^{1}H NMR (300 MHz, DMSO-d_6) δ 10.81 (s, 1H), 8.81 (dd, 2H), 8.51 (dd, 2H), 7.86 (dd, 2H), 7.77 (dd, 2H). ^{13}C NMR (75 MHz, DMSO-d_6) δ 165.03, 150.40, 150.34, 145.37, 141.24, 121.58, 114.11. FTIR: 1683.01 cm-1 (CO), 3481.04 cm-1 (NH). Anal. Calcd for $C_{11}H_9N_3O$: C, 66.32: H, 4.55; N, 21.09. Found: C, 66.58; H, 4.72; N, 20.93.

General synthetic procedure for 4,4′-Di(pyridin-3-yl)-[2,2′-bipyridine]-4,4′-dicarboxamide (3) and 4,4′-Di(pyridin-4-yl)-[2,2′-bipyridine]-4,4′-dicarboxamide (4)

A mixture of 4,4´-dicarboxy-2,2´-bipyridine (0.245 g, 1 mmol), corresponding aromatic amine (0.190 g, 2 mmol) and N-ethyl-N'-(3-dimethylaminopropyl)carbodiimide (0.770 g, 4 mmol) in DMF (5 mL) was stirred at room temperature overnight. After the reaction, the resulting off white solid was filtered and washed with excess of water followed by acetone and dried under vacuum.

(3). Yield (0.261 g, 71.7%); ^{1}H NMR (300 MHz, DMSO-d_6 at 30 °C) δ 10.90 (s, 1H), 8.99 (d, 2H), 8.95 (d, 1H), 8.37 (dd, 1H), 8.23 (dq, 1H), 8.01 (dd, 1H), 7.45 (q, 1H). ^{13}C NMR (75 MHz, DMSO-d_6) δ 164.22, 154.86, 150.50, 145.37, 143.07, 142.35, 135.36, 127.94, 123.79, 122.66, 118.99. FTIR: 1678.11 cm-1 (CO), 3233.30 cm-1 (NH). Anal. Calcd for $C_{22}H_{16}N_6O_2$: C, 66.66: H, 4.07; N, 21.20. Found: C, 66.45; H, 4.28; N, 21.00.

^{1}H NMR (500 MHz, DMSO-d_6 at 70 °C) δ 10.76 (s, 1H), 8.98 (d, 2H), 8.94 (d, 1H), 8.37 (dd, 1H), 8.22 (dq, 1H), 8.00 (dd, 1H), 7.43 (q, 1H). ^{13}C NMR (125 MHz, DMSO-d_6 at 30 °C) δ 164.31, 155.48, 150.26, 145.13, 142.87, 142.21, 135.29, 127.67, 123.60, 122.43, 118.55. ^{1}H-^{15}N COSY NMR (DMSO-d_6 at 70 °C) δ -60.00 (Bipy N^B), -62.66 (Py N^P) and -253.37 (Amide N^A).

(4). Yield (0.190 g, 52.2%); 1H NMR (300 MHz, DMSO-d_6) δ 11.03 (s, 1H), 8.99 (d, 1H), 8.91 (d, 1H), 8.53 (dd, 2H), 7.99 (dd, 1H), 7.82 (dd, 2H). FTIR: 1698.68 cm-1 (CO), 3480.43 cm-1 (NH). Anal. Calcd for $C_{22}H_{16}N_6O_2$: C, 66.66: H, 4.07; N, 21.20. Found: C, 66.39; H, 4.20; N, 20.94.

Metal Complexes

[1_2●$AgNO_3$]: ^{1}H NMR (300 MHz, DMSO-d_6) δ 10.78 (s, 1H), 8.99 (d, 1H), 8.82 (dd, 2H), 8.37 (dd, 1H), 8.22 (dq, 1H), 7.92 (dd, 2H), 7.50 (q, 1H). ^{13}C NMR (75 MHz, DMSO-d_6) δ 164.32, 150.70, 145.61, 14.42, 141.64, 135.65, 128.41, 124.17, 121.88. ^{1}H-^{15}N COSY NMR (DMSO-d_6 at 30 °C) δ -84.58 (Carbonyl pyridine N^C), -96.96 (amino pyridine N^N) and -277.29 (amide nitrogen N^A).

[2_2●$AgNO_3$]: ^{1}H NMR (300 MHz, DMSO-d_6) δ 10.95 (s, 1H), 8.83 (dd, 2H), 8.54 (dd, 2H), 7.89 (dd, 2H), 7.86 (dd, 2H).

[3●$AgNO_3$]: ^{1}H NMR (300 MHz, DMSO-d_6) δ 10.94 (s, 1H), 9.00 (d, 2H), 8.96 (d, 1H), 8.39 (dd, 1H), 8.24 (dq, 1H), 8.05 (dd, 1H), 7.48 (q, 1H). ^{13}C NMR (75 MHz, DMSO-d_6 at 80 °C) δ 163.94, 154.95, 149.89, 144.92, 142.79, 142.21, 134.94, 127.62, 123.12, 121.95, 118.56.

^{1}H NMR (500 MHz, DMSO-d_6 at 70 °C) δ 10.80 (s, 1H), 8.99 (d, 2H), 8.95 (d, 1H), 8.38 (dd, 1H), 8.22 (dq, 1H), 8.03 (dd, 1H), 7.46 (q, 1H). ^{1}H-^{15}N COSY NMR (DMSO-d_6 at 70 °C) δ -64.35 (Bipy N^B), -67.23 (Py N^P) and -253.16 (Amide N^A).

[4●$AgNO_3$]: No solubility was found.

X-ray crystallography

The single crystals of **4** and silver CPs from **1** were immersed in cryo-oil, mounted in a MiTeGen loop and measured at 120°C. The X-ray diffraction data were collected on an Agilent Technologies Supernova diffractometer using Mo Kα radiation. The *CrysAlisPro*[39] program packages were used for cell refinements and data reductions. Structures were solved by intrinsic phasing *SHELXT*[40] program. Analytical or multi-scan absorption correction was applied to all data and structural refinements were carried out using *SHELXL*[40] and Olex2 graphical user interface[41] software. The crystallographic details are given in the supplementary material.

Transmission electron microscopy (TEM)

The transmission electron microscopy (TEM) images were collected using FEI Tecnai G2 operated at 120 kV and JEM 3200FSC field emission microscope (JEOL) operated at 300 kV in bright field mode with Omega-type Zero-loss energy filter. The images were acquired with GATAN DIGITAL MICROGRAPH software. The TEM samples were prepared by placing 3.0 µL of the gel on to a 300 mesh copper grid with holey carbon support film. The TEM grids were plasma cleaned prior to use. The samples were dried under ambient condition prior to imaging.

Acknowledgements

TR and MH kindly acknowledge the financial support from the Academy of Finland (M.H. Proj. no. 295581). Academy of Finland, Centre of Excellence in Molecular Engineering of Biosynthetic Hybrid Materials (HYBER, 2014–2019) and the Aalto University Nanomicroscopy Center (Aalto-NMC) is kindly acknowledged for the use of its facilities. COST Action 1302 “Smart Inorganic Polymers” is also acknowledged as a valuable source of inspiration.

Keywords: metallogels • photoluminescence • *in-situ* nanoparticle • self-assembly • hybrid gels

[1] S. Leininger, B. Olenyuk, and P. J. Stang, *Chem. Rev*. **2000**, *100*, 853-908.

[2] S. Kitagawa, R. Kitaura, and S. Noro, *Angew. Chem. Int*. Ed. **2004**, *43*, 2334-2375.

[3] a) M.-O. M. Piepenbrock, G. O. Lloyd, N. Clarke, and J. W. Steed. *Chem. Rev*, **2010**, *110*, 1960-2004; b) Y. He, Z. Bian, C. Kang, and L. Gao, *Chem. Commun*. **2010**, *46*, 5695-5697; *Chem. Commun*. **2011**, *47*, 1589-1591; c) L.-J. Chen, Y.-Y. Ren, N.-W. Wu, B. Sun, J.-Q. Ma, L. Zhang, H. Tan, M. Liu, X. Li, H.-B. Yang, *J. Am. Chem. Soc*. **2015**, *137*, 11725-11735.

[4] a) J. Zhang, C.-Y. Su, *Coord. Chem. Rev*. **2013**, *257*, 1373-1408; b) S. Bhowmik, B. N. Ghosh, and K. Rissanen, *Org. Biomol. Chem*. **2014**, *12*, 8836-8839.

[5] a) K. Chen, L. Tang, Y. Xia, and Y. Wang, *Langmuir*. **2008**, *24*, 13838-13841; b) P. Sutar, and T. K. Maji, *Chem. Commun*. **2016**, *52*, 8055-8074.

[6] a) J. B. Beck and S. J. Rowan, *J. Am. Chem. Soc*. **2003**, *125*, 13922-13923; b) X. Yan, D. Xu, X. Chi, J. Chen, S. Dong, X. Ding, Y. Yu, and F. Huang, *Adv. Mater*. **2012**, *24*, 362-369.

[7] A. Y. -Y. Tam, K. M.-C. Wong, and V. W.-W. Yam, J. Am. Chem. Soc. **2009**, *131*, 6253-6260.

[8] a) X. Yu, L. Chen, M. Zhang, and T. Yi, *Chem. Soc. Rev*. **2014**, *43*, 5346-5371; b) A. V. Zhukhovitskiy, M. Zhong, E. G. Keeler, V. K. Michaelis, J. E. P. Sun, M. J. A. Hore, D. J. Pochan, R. G. Griffin, A. P. Willard, J. A. Johnson, *Nat. Chem*. **2016**, *8*, 33-41.

[9] a) M. Burnworth, L. Tang, J. R. Kumpfer, A. J. Duncan, F. L. Beyer, G. L. Fiore, S. J. Rowan, and C. Weder, *Nature*. **2011**, *472*, 334-337; b) G. E. Giammanco, C. T. Sosnofsky, and A. D. Ostrowski, *ACS Appl. Mater. Interfaces*. **2015**, *7*, 3068-3076; c) M. Mauro, S. Bellemin-Laponnaz, and C. Cebrian, *Chem. Eur. J*. **2017**, ***23***, 17626-17636.

[10] a) S.-I. Kawano, N. Fujita, and S. Shinkai, *J. Am. Chem. Soc*. **2004**, *126*, 8592-8593; b) S. Sarkar, S. Dutta, S. Chakrabarti, P. Bairi, and T. Pal, *ACS Appl. Mater. Interfaces*. **2014**, *6*, 6308-6316; c) Y. Zhang, B. Zhang, Y. Kuang, Y. Gao, J. Shi, X. X. Zhang, and B. Xu, J. Am. Chem. Soc. **2013**, *135*, 5008-5011; d) K.Mitsumoto, J. M. Cameron, R. -J. Wei, H. Nishikawa, T. Shiga, M. Nihei, G. N. Newton, H. Oshio, *Chem. Eur. J*. **2017**, *23*,1502-1506.

[11] C. Wang, D. Zhang, and D. Zhu *J. Am. Chem. Soc*. **2005**, *127*, 16372-16373.

[12] J. Zhang and C.-Y. Su, Coord. *Chem. Rev*. **2013**, *257*, 1373-1408.

[13] a) T. Kishida, N. Fujita, K. Sada, and S. Shinkai, *Langmuir*. **2005**, *21*, 9432-9439; b) Y. Cho, J. H. Lee, J. Jaworski, S. Park, S. S. Lee and J. H. Jung, *New. J. Chem*. **2012**, *36*, 32-35.

[14] a) J. H. Lee, S. Kang, J. Y. Lee and J. H. Jung, *Soft Matter*. **2012**, ***8***, 6557-6563; b) L. Yan, L. Shen, M. Lv, W. Yu, J. Chen, S. Wang, X. Fu and Z. Ye, *Chem. Commun*. **2015**, ***51***, 17627-17629; c) S. Ganta and D. K. Chand, *Dalton Trans*. **2015**, *44*, 15181-15188; d) S.-L. Yim, H.-F. Chow, M.-C. Chan, C.-M. Che, K.-H. Low, *Chem. Eur. J*. **2013**, *19*, 2478-2486

[15] P. Casuso, P. Carrasco, I. Loinaz, G. Cabanero, H. J. Grande and I. Odriozola, *Soft Matter*. **2011**, *7*, 3627-3633.

[16] a) J. J. Marrero-Tellado and D. D. Díaz, *CrystEngComm*. **2015**, *17*, 7978-7985; b) A. Husain, R. Parveen, and P. Dastidar, *Cryst. Growth Des*. **2015**, *15*, 5075-5085.

[17] a) K. K. Kartha, V. K. Praveen, S. S. Babu, S. Cherumukkil, and A. Ajayaghosh, *Chem. Asian. J*. **2015**, *10*, 2250-2256; b) R. Tatikonda, S. Bhowmik, K. Rissanen, M. Haukka, and M. Cametti, *Dalton Trans*. **2016**, *45*, 12756-12762.

[18] a) N. N. Adarsh, P. Sahoo, and P. Dastidar, *Cryst. Growth Des.* **2010**, *10*, 4976-4986; b) H. Bunzen, Nonappa, E. Kalenius, S. Hietala, and E. Kolehmainen, *Chem. Eur. J*. **2013**, *19*, 12978-12981.

[19] R. G. Weiss, *J. Am. Chem. Soc*. **2014**, *136*, 7519-7530.

[20] A. Y.-Y. Tam, and V. W.-W. Yam, *Chem. Soc. Rev*. **2013**, *42*, 1540-1567.

[21] a) S. Bhowmik, B. N. Ghosh, V. Marjomaki, and K. Rissanen, *J. Am. Chem. Soc*. **2014**, *136*, 5543-5546. (b) Q. Lin, T.-T. Lu, X. Zhu, B. Sun, Q.-P. Yang, T.-B. Wei and Y.-M. Zhang, *Chem. Commun*. **2015**, *51*, 1635-1638.

[22] a) P. Chen, Q. Li, S. Grindy, and N. Holten-Andersen, *J. Am. Chem. Soc*. **2015**, *137*, 11590-11593; b) P. Sutar, V. M. Suresh, and T. K. Maji, *Chem. Commun*. **2015**, *51*, 9876-9879; c) K. Hong, Y. K. Kwon, J. Ryu, J. Y. Lee, S. H. Kim, and K. H. Lee, *Sci. Rep*. **2016**, *6, 29805.* Doi:10.1038/srep29805; d) P. Sutar, and T: K. Maji, *Inorg. Chem*. **2017**, *56*, 9417-9425.

[23] M. J. Bryant, J. M. Skelton, L. E. Hatcher, C. Stubbs, E. Madrid, A. R. Pallipurath, L. H. Thomas, C. H. Woodall, J. Christensen, S. Fuertes, T. P. Robinson, C. M. Beavers, S. J. Teat, M. R. Warren, F. Pradaux-Cassiano, A. Walsh, F. Marken, D. R. Carbery, S. C. Parker, N. B. McKeown, R. Malpass-Evans, M. Carta, and P. R. Raithby, *Nat. Commun.* **2017**, *8,* 1800. Doi:10.1038/s41467-017-01941-2.

[24] L. Arnedo-Sanchez, Nonappa, S. Bhowmik, S. Hietala, R. Puttreddy, M. Lahtinen, L. DeCola, and K. Rissanen, *Dalton Trans*. **2017**, *46*, 7309-7316.

[25] a) B. Xing, M.-F. Choi and B. Xu, *Chem. Eur. J*. **2002**, *8*, 5028-5032; b) Y.-R. Liu, L. He, J. Zhang, X. Wang, and C.-Y. Su, *Chem. Mater*. **2009**, *21*, 557-563.

[26] L. Qin, P. Wang, Y. Guo, C. Chen, and M. Liu, *Adv. Sci*. **2015**, *2*, 1500134. DOI: 10.1002/advs.201500134.

[27] a) M.-O. M. Piepenbrock, N. Clarke, and J. W. Steed, *Soft Matter.* **2011**, *7*, 2412-2418; b) H. Svobodová, Nonappa, M. Lahtinen, Z. Wimmer, and E. Kolehmainen, *Soft Mattter.* **2012**, *8*, 7840-7847; c) M. Cametti, and Z. Džolić, *Chem. Commun*. **2014**, *50*, 8273-8286.

[28] P. Rajamalli, P. Malakar, S. Atta, and E. Prasad, *Chem. Commun*. **2014**, *50*, 11023-11025.

[29] a) M.-O. M. Piepenbrock, N. Clarke, J. W. Steed, *Soft Matter*. **2011**, *7*, 2412-2418; b) K. Nath, A. Husain, and P. Dastidar, *Cryst. Growth Des*. **2015**, *15*, 4635-4645; c) M. Paul, K. Sarkar and P. Dastidar, *Chem. Eur. J*. **2015**, *21*, 255-268.

[30] R. Tatikonda, K. Bertula, N. Nonappa, S. Hietala, K. Rissanen, and M. Haukka, *Dlaton Trans.* **2017**, *46*, 2793-2802.

[31] C. Zimmer, M. Hafner, M. Zender, D. Ammann, R. W. Hartmann, *Bioorganic Med. Chem. Lett*. **2011**, *21*, 186-190.

[32] D. K. Kumar, D. A. Jose, P. Dastidar, and A. Das, *Langmuir.* **2004**, *20*, 10413-10418.

[33] CCDC 1823427–1823433 contains the supplementary crystallographic data for this paper.

[34] a) Nonappa and E. Kolehmainen, *Soft Matter*. **2016**, *12*, 6015-6026; b) Nonappa, M. Lahtinen, B. Behera, E. Kolehmainen, and U. Maitra, *Soft Matter*. **2010**, *6*, 1748-1757; c) V. Noponen, Nonappa, M. Lahtinen, A. Valkonen, H. Salo, E. Kolehmainen, and E. Sievänen, *Soft Matter*. **2010**, *6*, 3789-3796; d) Nonappa and E. Kolehmainen, *Gels*. **2016**, *2*, 9; e) Nonappa, D. Saman, and E. Kolehmainen, *Magn. Reson. Chem*. **2015**, *53*, 256-260.

[35] K. Uemura, *Inorg. Chem. Commun*. **2008**, *11*, 741-744.

[36] R. Tatikonda, E. Bulatov, E. Kalenius, and M. Haukka, *Cryst. Growth Des.* **2017**, *17*, 5918-5926.

[37] a) J. A. Wilson, R. L. LaDuca, *Inorg. Chem. Acta*. **2013**, *403*, 136-141; b) T. A. Beard, J. A. Wilson, R. L. LaDuca, *Inorg. Chem. Acta*. **2017**, *466*, 30-38.

[38] a) Nonappa, T. Lahtinen, J. S. Haataja, T. -R. Tero, H. Häkkinen and O. Ikkala, *Angew. Chem. Int. Ed*. **2016**, *55*, 16035-16038; b) Nonappa, J. S. Haataja, J. V. I Timonen, S. Malola, P. Engelhardt, N. Houbenov, M. Lahtinen, H. Häkkinen and O. Ikkala, *Angew. Chem. Int. Ed.* **2017**, *56*, 6473-6477; c) Nonappa, O. Ikkala, *Adv. Funct. Mater*. **2017**, 1704328.

[39] Rigaku Oxford Diffraction, CrysAlisPro. **2013**, Yarnton, Oxfordshire, England.

[40] G. M. Sheldrick, *Acta Cryst*. **2015**, *C71*, 3-8; *Acta Cryst*. **2015**, *A71*, 3-8.

[41] O. V. Dolomanov, L. J. Bourhis, R. J. Gildea, A. J. K. Howard, and H. Puschmann, *J. Appl. Cryst*. **2009**, *42*, 339-341.

DEPARTMENT OF CHEMISTRY, UNIVERSITY OF JYVÄSKYLÄ
RESEARCH REPORT SERIES

1. Vuolle, Mikko: Electron paramagnetic resonance and molecular orbital study of radical ions generated from (2.2)metacyclophane, pyrene and its hydrogenated compounds by alkali metal reduction and by thallium(III)trifluoroacetate oxidation. (99 pp.) 1976
2. Pasanen, Kaija: Electron paramagnetic resonance study of cation radical generated from various chlorinated biphenyls. (66 pp.) 1977
3. Carbon-13 Workshop, September 6-8, 1977. (91 pp.) 1977
4. Laihia, Katri: On the structure determination of norbornane polyols by NMR spectroscopy. (111 pp.) 1979
5. Nyrönen, Timo: On the EPR, ENDOR and visible absorption spectra of some nitrogen containing heterocyclic compounds in liquid ammonia. (76 pp.) 1978
6. Talvitie, Antti: Structure determination of some sesquiterpenoids by shift reagent NMR. (54 pp.) 1979
7. Häkli, Harri: Structure analysis and molecular dynamics of cyclic compounds by shift reagent NMR. (48 pp.) 1979
8. Pitkänen, Ilkka: Thermodynamics of complexation of 1,2,4-triazole with divalent manganese, cobalt, nickel, copper, zinc, cadmium and lead ions in aqueous sodium perchlorate solutions. (89 pp.) 1980
9. Asunta, Tuula: Preparation and characterization of new organometallic compounds synthesized by using metal vapours. (91 pp.) 1980
10. Sattar, Mohammad Abdus: Analyses of MCPA and its metabolites in soil. (57 pp.) 1980
11. Bibliography 1980. (31 pp.) 1981
12. Knuuttila, Pekka: X-Ray structural studies on some divalent 3d metal compounds of picolinic and isonicotinic acid N-oxides. (77 pp.) 1981
13. Bibliography 1981. (33 pp.) 1982
14. 6th National NMR Symposium, September 9-10, 1982, Abstracts. (49 pp.) 1982
15. Bibliography 1982. (38 pp.) 1983
16. Knuuttila, Hilkka: X-Ray structural studies on some Cu(II), Co(II) and Ni(II) complexes with nicotinic and isonicotinic acid N-oxides. (54 pp.) 1983
17. Symposium on inorganic and analytical chemistry May 18, 1984, Program and Abstracts. (100 pp.) 1984
18. Knuutinen, Juha: On the synthesis, structure verification and gas chromatographic determination of chlorinated catechols and guaiacols occuring in spent bleach liquors of kraft pulp mill. (30 pp.) 1984
19. Bibliography 1983. (47 pp.) 1984
20. Pitkänen, Maija: Addition of BrCl, B_2 and Cl_2 to methyl esters of propenoic and 2-butenoic acid derivatives and ^{13}C NMR studies on methyl esters of saturated aliphatic mono- and dichlorocarboxylic acids. (56 pp.) 1985
21. Bibliography 1984. (39 pp.) 1985
22. Salo, Esa: EPR, ENDOR and TRIPLE spectroscopy of some nitrogen heteroaromatics in liquid ammonia. (111 pp.) 1985

23. Humppi, Tarmo: Synthesis, identification and analysis of dimeric impurities of chlorophenols. (39 pp.) 1985
24. Aho, Martti: The ion exchange and adsorption properties of sphagnum peat under acid conditions. (90 pp.) 1985
25. Bibliography 1985 (61 pp.) 1986
26. Bibliography 1986. (23 pp.) 1987
27. Bibliography 1987. (26 pp.) 1988
28. Paasivirta, Jaakko (Ed.): Structures of organic environmental chemicals. (67 pp.) 1988
29. Paasivirta, Jaakko (Ed.): Chemistry and ecology of organo-element compounds. (93 pp.) 1989
30. Sinkkonen, Seija: Determination of crude oil alkylated dibenzothiophenes in environment. (35 pp.) 1989
31. Kolehmainen, Erkki (Ed.): XII National NMR Symposium Program and Abstracts. (75 pp.) 1989
32. Kuokkanen, Tauno: Chlorocymenes and Chlorocymenenes: Persistent chlorocompounds in spent bleach liquors of kraft pulp mills. (40 pp.) 1989
33. Mäkelä, Reijo: ESR, ENDOR and TRIPLE resonance study on substituted 9,10-anthraquinone radicals in solution. (35 pp.) 1990
34. Veijanen, Anja: An integrated sensory and analytical method for identification of off-flavour compounds. (70 pp.) 1990
35. Kasa, Seppo: EPR, ENDOR and TRIPLE resonance and molecular orbital studies on a substitution reaction of anthracene induced by thallium(III) in two fluorinated carboxylic acids. (114 pp.) 1990
36. Herve, Sirpa: Mussel incubation method for monitoring organochlorine compounds in freshwater recipients of pulp and paper industry. (145 pp.) 1991
37. Pohjola, Pekka: The electron paramagnetic resonance method for characterization of Finnish peat types and iron (III) complexes in the process of peat decomposition. (77 pp.) 1991
38. Paasivirta, Jaakko (Ed.): Organochlorines from pulp mills and other sources. Research methodology studies 1988-91. (120 pp.) 1992
39. Veijanen, Anja (Ed.): VI National Symposium on Mass Spectrometry, May 13-15, 1992, Abstracts. (55 pp.) 1992
40. Rissanen, Kari (Ed.): The 7. National Symposium on Inorganic and Analytical Chemistry, May 22, 1992, Abstracts and Program. (153 pp.) 1992
41. Paasivirta, Jaakko (Ed.): CEOEC'92, Second Finnish-Russian Seminar: Chemistry and Ecology of Organo-Element Compounds. (93 pp.) 1992
42. Koistinen, Jaana: Persistent polychloroaromatic compounds in the environment: structure-specific analyses. (50 pp.) 1993
43. Virkki, Liisa: Structural characterization of chlorolignins by spectroscopic and liquid chromatographic methods and a comparison with humic substances. (62 pp.) 1993
44. Helenius, Vesa: Electronic and vibrational excitations in some

biologically relevant molecules. (30 pp.) 1993

45. Leppä-aho, Jaakko: Thermal behaviour, infrared spectra and x-ray structures of some new rare earth chromates(VI). (64 pp.) 1994
46. Kotila, Sirpa: Synthesis, structure and thermal behavior of solid copper(II) complexes of 2-amino-2- hydroxymethyl-1,3-propanediol. (111 pp.) 1994
47. Mikkonen, Anneli: Retention of molybdenum(VI), vanadium(V) and tungsten(VI) by kaolin and three Finnish mineral soils. (90 pp.) 1995
48. Suontamo, Reijo: Molecular orbital studies of small molecules containing sulfur and selenium. (42 pp.) 1995
49. Hämäläinen, Jouni: Effect of fuel composition on the conversion of fuel-N to nitrogen oxides in the combustion of small single particles. (50 pp.) 1995
50. Nevalainen, Tapio: Polychlorinated diphenyl ethers: synthesis, NMR spectroscopy, structural properties, and estimated toxicity. (76 pp.) 1995
51. Aittola, Jussi-Pekka: Organochloro compounds in the stack emission. (35 pp.) 1995
52. Harju, Timo: Ultrafast polar molecular photophysics of (dibenzylmethine)borondifluoride and 4-aminophthalimide in solution. (61 pp.) 1995
53. Maatela, Paula: Determination of organically bound chlorine in industrial and environmental samples. (83 pp.) 1995
54. Paasivirta, Jaakko (Ed.): CEOEC'95, Third Finnish-Russian Seminar: Chemistry and Ecology of Organo-Element Compounds. (109 pp.) 1995
55. Huuskonen, Juhani: Synthesis and structural studies of some supramolecular compounds. (54 pp.) 1995
56. Palm, Helena: Fate of chlorophenols and their derivatives in sawmill soil and pulp mill recipient environments. (52 pp.) 1995
57. Rantio, Tiina: Chlorohydrocarbons in pulp mill effluents and their fate in the environment. (89 pp.) 1997
58. Ratilainen, Jari: Covalent and non-covalent interactions in molecular recognition. (37 pp.) 1997
59. Kolehmainen, Erkki (Ed.): XIX National NMR Symposium, June 4-6, 1997, Abstracts. (89 pp.) 1997
60. Matilainen, Rose: Development of methods for fertilizer analysis by inductively coupled plasma atomic emission spectrometry. (41 pp.) 1997
61. Koistinen, Jari (Ed.): Spring Meeting on the Division of Synthetic Chemistry, May 15-16, 1997, Program and Abstracts. (36 pp.) 1997
62. Lappalainen, Kari: Monomeric and cyclic bile acid derivatives: syntheses, NMR spectroscopy and molecular recognition properties. (50 pp.) 1997
63. Laitinen, Eira: Molecular dynamics of cyanine dyes and phthalimides in solution: picosecond laser studies. (62 pp.) 1997
64. Eloranta, Jussi: Experimental and theoretical studies on some

quinone and quinol radicals. (40 pp.) 1997

65. Oksanen, Jari: Spectroscopic characterization of some monomeric and aggregated chlorophylls. (43 pp.) 1998
66. Häkkänen, Heikki: Development of a method based on laser-induced plasma spectrometry for rapid spatial analysis of material distributions in paper coatings. (60 pp.) 1998
67. Virtapohja, Janne: Fate of chelating agents used in the pulp and paper industries. (58 pp.) 1998
68. Airola, Karri: X-ray structural studies of supramolecular and organic compounds. (39 pp.) 1998
69. Hyötyläinen, Juha: Transport of lignin–type compounds in the receiving waters of pulp mills. (40 pp.) 1999
70. Ristolainen, Matti: Analysis of the organic material dissolved during totally chlorine-free bleaching. (40 pp.) 1999
71. Eklin, Tero: Development of analytical procedures with industrial samples for atomic emission and atomic absorption spectrometry. (43 pp.) 1999
72. Välisaari, Jouni: Hygiene properties of resol-type phenolic resin laminates. (129 pp.) 1999
73. Hu, Jiwei: Persistent polyhalogenated diphenyl ethers: model compounds syntheses, characterization and molecular orbital studies. (59 pp.) 1999
74. Malkavaara, Petteri: Chemometric adaptations in wood processing chemistry. (56 pp.) 2000
75. Kujala Elena, Laihia Katri, Nieminen Kari (Eds.): NBC 2000, Symposium on Nuclear, Biological and Chemical Threats in the 21st Century. (299 pp.) 2000
76. Rantalainen, Anna-Lea: Semipermeable membrane devices in monitoring persistent organic pollutants in the environment. (58 pp.) 2000
77. Lahtinen, Manu: *In situ* X-ray powder diffraction studies of Pt/C, CuCl/C and Cu_2O/C catalysts at elevated temperatures in various reaction conditions. (92 pp.) 2000
78. Tamminen, Jari: Syntheses, empirical and theoretical characterization, and metal cation complexation of bile acid-based monomers and open/closed dimers. (54 pp.) 2000
79. Vatanen, Virpi: Experimental studies by EPR and theoretical studies by DFT calculations of a-amino-9,10-anthraquinone radical anions and cations in solution. (37 pp.) 2000
80. Kotilainen, Risto: Chemical changes in wood during heating at 150-260 °C. (57 pp.) 2000
81. Nissinen, Maija: X-ray structural studies on weak, non-covalent interactions in supramolecular compounds. (69 pp.) 2001
82. Wegelius, Elina: X-ray structural studies on self-assembled hydrogen-bonded networks and metallosupramolecular complexes. (84 pp.) 2001
83. Paasivirta, Jaakko (Ed.): CEOEC'2001, Fifth Finnish-Russian Seminar: Chemistry and Ecology of Organo-Element Compounds. (163 pp.) 2001
84. Kiljunen, Toni: Theoretical studies on spectroscopy and

atomic dynamics in rare gas solids. (56 pp.) 2001

85. Du, Jin: Derivatives of dextran: synthesis and applications in oncology. (48 pp.) 2001
86. Koivisto, Jari: Structural analysis of selected polychlorinated persistent organic pollutants (POPs) and related compounds. (88 pp.) 2001
87. Feng, Zhinan: Alkaline pulping of non-wood feedstocks and characterization of black liquors. (54 pp.) 2001
88. Halonen, Markku: Lahon havupuun käyttö sulfaattiprosessin raaka-aineena sekä havupuun lahontorjunta. (90 pp.) 2002
89. Falábu, Dezsö: Synthesis, conformational analysis and complexation studies of resorcarene derivatives. (212 pp.) 2001
90. Lehtovuori, Pekka: EMR spectroscopic studies on radicals of ubiquinones Q-*n*, vitamin K_3 and vitamine E in liquid solution. (40 pp.) 2002
91. Perkkalainen, Paula: Polymorphism of sugar alcohols and effect of grinding on thermal behavior on binary sugar alcohol mixtures. (53 pp.) 2002
92. Ihalainen, Janne: Spectroscopic studies on light-harvesting complexes of green plants and purple bacteria. (42 pp.) 2002
93. Kunttu, Henrik, Kiljunen, Toni (Eds.): 4th International Conference on Low Temperature Chemistry. (159 pp.) 2002
94. Väisänen, Ari: Development of methods for toxic element analysis in samples with environmental concern by ICP-AES and ETAAS. (54 pp.) 2002
95. Luostarinen, Minna: Synthesis and characterisation of novel resorcarene derivatives. (200 pp.) 2002
96. Louhelainen, Jarmo: Changes in the chemical composition and physical properties of wood and nonwood black liquors during heating. (68 pp.) 2003
97. Lahtinen, Tanja: Concave hydrocarbon cyclophane B-prismands. (65 pp.) 2003
98. Laihia, Katri (Ed.): NBC 2003, Symposium on Nuclear, Biological and Chemical Threats – A Crisis Management Challenge. (245 pp.) 2003
99. Oasmaa, Anja: Fuel oil quality properties of wood-based pyrolysis liquids. (32 pp.) 2003
100. Virtanen, Elina: Syntheses, structural characterisation, and cation/anion recognition properties of nano-sized bile acid-based host molecules and their precursors. (123 pp.) 2003
101. Nättinen, Kalle: Synthesis and X-ray structural studies of organic and metallo-organic supramolecular systems. (79 pp.) 2003
102. Lampiselkä, Jarkko: Demonstraatio lukion kemian opetuksessa. (285 pp.) 2003
103. Kallioinen, Jani: Photoinduced dynamics of $Ru(dcbpy)_2(NCS)_2$ – in solution and on nanocrystalline titanium dioxide thin films. (47 pp.) 2004
104. Valkonen, Arto (Ed.): VII Synthetic Chemistry Meeting and XXVI Finnish NMR Symposium. (103 pp.) 2004

105. Vaskonen, Kari: Spectroscopic studies on atoms and small molecules isolated in low temperature rare gas matrices. (65 pp.) 2004
106. Lehtovuori, Viivi: Ultrafast light induced dissociation of $Ru(dcbpy)(CO)_2I_2$ in solution. (49 pp.) 2004
107. Saarenketo, Pauli: Structural studies of metal complexing schiff bases , Schiff base derived *N*-glycosides and cyclophane π-prismands. (95 pp.) 2004
108. Paasivirta, Jaakko (Ed.): CEOEC'2004, Sixth Finnish-Russian Seminar: Chemistry and Ecology of Organo-Element Compounds. (147 pp.) 2004
109. Suontamo, Tuula: Development of a test method for evaluating the cleaning efficiency of hard-surface cleaning agents. (96 pp.) 2004
110. Güneş, Minna: Studies of thiocyanates of silver for nonlinear optics. (48 pp.) 2004
111. Ropponen, Jarmo: Aliphatic polyester dendrimers and dendrons. (81 pp.) 2004
112. Vu, Mân Thi Hong: Alkaline pulping and the subsequent elemental chlorine-free bleaching of bamboo (*Bambusa procera*). (69 pp.) 2004
113. Mansikkamäki, Heidi: Self-assembly of resorcinarenes. (77 pp.) 2006
114. Tuononen, Heikki M.: EPR spectroscopic and quantum chemical studies of some inorganic main group radicals. (79 pp.) 2005
115. Kaski, Saara: Development of methods and applications of laser-induced plasma spectroscopy in vacuum ultraviolet. (44 pp.) 2005
116. Mäkinen, Riika-Mari: Synthesis, crystal structure and thermal decomposition of certain metal thiocyanates and organic thiocyanates. (119 pp.) 2006
117. Ahokas, Jussi: Spectroscopic studies of atoms and small molecules isolated in rare gas solids: photodissociation and thermal reactions. (53 pp.) 2006
118. Busi, Sara: Synthesis, characterization and thermal properties of new quaternary ammonium compounds: new materials for electrolytes, ionic liquids and complexation studies. (102 pp.) 2006
119. Mäntykoski, Keijo: PCBs in processes, products and environment of paper mills using wastepaper as their raw material. (73 pp.) 2006
120. Laamanen, Pirkko-Leena: Simultaneous determination of industrially and environmentally relevant aminopolycarboxylic and hydroxycarboxylic acids by capillary zone electrophoresis. (54 pp.) 2007
121. Salmela, Maria: Description of oxygen-alkali delignification of kraft pulp using analysis of dissolved material. (71 pp.) 2007
122. Lehtovaara, Lauri: Theoretical studies of atomic scale impurities in superfluid ^{4}He. (87 pp.) 2007
123. Rautiainen, J. Mikko: Quantum chemical calculations of structures, bonding, and spectroscopic properties of some sulphur and selenium iodine cations. (71 pp.) 2007
124. Nummelin, Sami: Synthesis, characterization, structural and

retrostructural analysis of self-assembling pore forming dendrimers. (286 pp.) 2008

125. Sopo, Harri: Uranyl(VI) ion complexes of some organic aminobisphenolate ligands: syntheses, structures and extraction studies. (57 pp.) 2008
126. Valkonen, Arto: Structural characteristics and properties of substituted cholanoates and *N*-substituted cholanamides. (80 pp.) 2008
127. Lähde, Anna: Production and surface modification of pharmaceutical nano- and microparticles with the aerosol flow reactor. (43 pp.) 2008
128. Beyeh, Ngong Kodiah: Resorcinarenes and their derivatives: synthesis, characterization and complexation in gas phase and in solution. (75 pp.) 2008
129. Välisaari, Jouni, Lundell, Jan (Eds.): Kemian opetuksen päivät 2008: uusia oppimisympäristöjä ja ongelmalähtöistä opetusta. (118 pp.) 2008
130. Myllyperkiö, Pasi: Ultrafast electron transfer from potential organic and metal containing solar cell sensitizers. (69 pp.) 2009
131. Käkölä, Jaana: Fast chromatographic methods for determining aliphatic carboxylic acids in black liquors. (82 pp.) 2009
132. Koivukorpi, Juha: Bile acid-arene conjugates: from photoswitchability to cancer cell detection. (67 pp.) 2009
133. Tuuttila, Tero: Functional dendritic polyester compounds: synthesis and characterization of small bifunctional dendrimers and dyes. (74 pp.) 2009
134. Salorinne, Kirsi: Tetramethoxy resorcinarene based cation and anion receptors: synthesis, characterization and binding properties. (79 pp.) 2009
135. Rautiainen, Riikka: The use of first-thinning Scots pine (*Pinus sylvestris*) as fiber raw material for the kraft pulp and paper industry. (73 pp.) 2010
136. Ilander, Laura: Uranyl salophens: synthesis and use as ditopic receptors. (199 pp.) 2010
137. Kiviniemi, Tiina: Vibrational dynamics of iodine molecule and its complexes in solid krypton - Towards coherent control of bimolecular reactions? (73 pp.) 2010
138. Ikonen, Satu: Synthesis, characterization and structural properties of various covalent and non-covalent bile acid derivatives of N/O-heterocycles and their precursors. (105 pp.) 2010
139. Siitonen, Anni: Spectroscopic studies of semiconducting single-walled carbon nanotubes. (56 pp.) 2010
140. Raatikainen, Kari: Synthesis and structural studies of piperazine cyclophanes – Supramolecular systems through Halogen and Hydrogen bonding and metal ion coordination. (69 pp.) 2010
141. Leivo, Kimmo: Gelation and gel properties of two- and three-component Pyrene based low molecular weight organogelators. (116 pp.) 2011
142. Martiskainen, Jari: Electronic energy transfer in light-harvesting complexes isolated from *Spinacia oleracea* and from three

photosynthetic green bacteria *Chloroflexus aurantiacus*, *Chlorobium tepidum*, and *Prosthecochloris aestuarii*.(55 pp.) 2011

143. Wichmann, Oula: Syntheses, characterization and structural properties of [O,N,O,X´] aminobisphenolate metal complexes. (101 pp.) 2011
144. Ilander, Aki: Development of ultrasound-assisted digestion methods for the determination of toxic element concentrations in ash samples by ICP-OES. (58 pp.) 2011
145. The Combined XII Spring Meeting of the Division of Synthetic Chemistry and XXXIII Finnish NMR Symposium. Book of Abstracts. (90 pp.) 2011
146. Valto, Piia: Development of fast analysis methods for extractives in papermaking process waters. (73 pp.) 2011
147. Andersin, Jenni: Catalytic activity of palladium-based nanostructures in the conversion of simple olefinic hydro- and chlorohydrocarbons from first principles. (78 pp.) 2011
148. Aumanen, Jukka: Photophysical properties of dansylated poly(propylene amine) dendrimers. (55 pp.) 2011
149. Kärnä, Minna: Ether-functionalized quaternary ammonium ionic liquids – synthesis, characterization and physicochemical properties. (76 pp.) 2011
150. Jurček, Ondřej: Steroid conjugates for applications in pharmacology and biology. (57 pp.) 2011
151. Nauha, Elisa: Crystalline forms of selected Agrochemical actives: design and synthesis of cocrystals. (77 pp.) 2012
152. Ahkola, Heidi: Passive sampling in monitoring of nonylphenol ethoxylates and nonylphenol in aquatic environments. (92 pp.) 2012
153. Helttunen, Kaisa: Exploring the self-assembly of resorcinarenes: from molecular level interactions to mesoscopic structures. (78 pp.) 2012
154. Linnanto, Juha: Light excitation transfer in photosynthesis revealed by quantum chemical calculations and exiton theory. (179 pp.) 2012
155. Roiko-Jokela, Veikko: Digital imaging and infrared measurements of soil adhesion and cleanability of semihard and hard surfaces. (122 pp.) 2012
156. Noponen, Virpi: Amides of bile acids and biologically important small molecules: properties and applications. (85 pp.) 2012
157. Hulkko, Eero: Spectroscopic signatures as a probe of structure and dynamics in condensed-phase systems – studies of iodine and gold ranging from isolated molecules to nanoclusters. (69 pp.) 2012
158. Lappi, Hanna: Production of Hydrocarbon-rich biofuels from extractives-derived materials. (95 pp.) 2012
159. Nykänen, Lauri: Computational studies of Carbon chemistry on transition metal surfaces. (76 pp.) 2012
160. Ahonen, Kari: Solid state studies of pharmaceutically important molecules and their derivatives. (65 pp.) 2012

161. Pakkanen, Hannu: Characterization of organic material dissolved during alkaline pulping of wood and non-wood feedstocks (76 pp.) 2012
162. Moilanen, Jani: Theoretical and experimental studies of some main group compounds: from closed shell interactions to singlet diradicals and stable radicals. (80 pp.) 2012
163. Himanen, Jatta: Stereoselective synthesis of Oligosaccharides by *De Novo* Saccharide welding. (133 pp.) 2012
164. Bunzen, Hana: Steroidal derivatives of nitrogen containing compounds as potential gelators.(76 pp.) 2013
165. Seppälä, Petri: Structural diversity of copper(II) amino alcohol complexes. Syntheses, structural and magnetic properties of bidentate amino alcohol copper(II) complexes. (67 pp.) 2013
166. Lindgren, Johan: Computational investigations on rotational and vibrational spectroscopies of some diatomics in solid environment. (77 pp.) 2013
167. Giri, Chandan: Sub-component self-assembly of linear and non-linear diamines and diacylhydrazines, formulpyridine and transition metal cations. (145 pp.) 2013
168. Riisiö, Antti: Synthesis, Characterization and Properties of Cu(II)-, Mo(VI)- and U(VI) Complexes With Diaminotetraphenolate Ligands. (51 pp.) 2013
169. Kiljunen, Toni (Ed.): Chemistry and Physics at Low Temperatures. Book of Abstracts. (103 pp.) 2013
170. Hänninen, Mikko: Experimental and Computational Studies of Transition Metal Complexes with Polydentate Amino- and Aminophenolate Ligands: Synthesis, Structure, Reactivity and Magnetic Properties. (66 pp.) 2013
171. Antila, Liisa: Spectroscopic studies of electron transfer reactions at the photoactive electrode of dye-sensitized solar cells. (53 pp.) 2013
172. Kemppainen, Eeva: Mukaiyama-Michael reactions with α-substituted acroleins – a useful tool for the synthesis of the pectenotoxins and other natural product targets. (190 pp.) 2013
173. Virtanen, Suvi: Structural Studies Of Dielectric Polymer Nanocomposites. (49 pp.) 2013
174. Yliniemelä-Sipari, Sanna: Understanding The Structural Requirements for Optimal Hydrogen Bond Catalyzed Enolization – A Biomimetic Approach.(160 pp.) 2013
175. Leskinen, Mikko V: Remote β-functionalization of β'-keto esters (105 pp.) 2014
176. 12th European Conference on Research in Chemistry Education (ECRICE2014). Book of Abstracts. (166 pp.) 2014
177. Peuronen, Anssi: N-Monoalkylated DABCO-Based N-Donors as Versatile Building Blocks in Crystal Engineering and Supramolecular Chemistry. (54 pp.) 2014
178. Perämäki, Siiri: Method development for determination and recovery of rare earth elements from industrial fly ash. (88 pp.) 2014

179. Chernyshev, Alexander, N.: Nitrogen-containing ligands and their platinum(IV) and gold(III) complexes: investigation and basicity and nucleophilicity, luminescence, and aurophilic interactions. (64 pp.) 2014
180. Lehto, Joni: Advanced Biorefinery Concepts Integrated to Chemical Pulping. (142 pp.) 2015
181. Tero, Tiia-Riikka: Tetramethoxy resorcinarenes as platforms for fluorescent and halogen bonding systems. (61 pp.) 2015
182. Löfman, Miika: Bile acid amides as components of microcrystalline organogels. (62 pp.) 2015
183. Selin, Jukka: Adsorption of softwood-derived organic material onto various fillers during papermaking. (169 pp.) 2015
184. Piisola, Antti: Challenges in the stereoselective synthesis of allylic alcohols. (210 pp.) 2015
185. Bonakdarzadeh, Pia: Supramolecular coordination polyhedra based on achiral and chiral pyridyl ligands: design, preparation, and characterization. (65 pp.) 2015
186. Vasko, Petra: Synthesis, characterization, and reactivity of heavier group 13 and 14 metallylenes and metalloid clusters: small molecule activation and more. (66 pp.) 2015
187. Topić, Filip: Structural Studies of Nano-sized Supramolecular Assemblies. (79 pp.) 2015
188. Mustalahti, Satu: Photodynamics Studies of Ligand-Protected Gold Nanoclusters by using Ultrafast Transient Infrared Spectroscopy. (58 pp.) 2015
189. Koivisto, Jaakko: Electronic and vibrational spectroscopic studies of gold-nanoclusters. (63pp.) 2015
190. Suhonen, Aku: Solid state conformational behavior and interactions of series of aromatis oligoamide foldamers. (68 pp.) 2016
191. Soikkeli, Ville: Hydrometallurgical recovery and leaching studies for selected valuable metals from fly ash samples by ultrasound-assisted extraction followed by ICP-OES determination. (107 pp.) 2016
192. XXXVIII Finnish NMR Symposium. Book of Abstracts. (51 pp.) 2016
193. Mäkelä, Toni: Ion Pair Recognition by Ditopic Crown Ether Based bis-Urea and Uranyl Salophen Receptors. (75 pp.) 2016
194. Lindholm-Lehto, Petra: Occurrence of pharmaceuticals in municipal wastewater treatment plants and receiving surface waters in Central and Southern Finland. (98 pp.) 2016
195. Härkönen, Ville: Computational and Theoretical studies on Lattice Thermal conductivity and Thermal properties of Silicon Clathrates (89 pp.) 2016
196. Tuokko, Sakari: Understanding selective reduction reactions with heterogeneous Pd and Pt:climbing out of the black box (85 pp.) 2016
197. Nuora, Piia: Monitapaustutkimus LUMA-Toimintaan liittyvissä oppimisympäristöissä tapahtuvista kemian oppimiskokemuksista (171 pp.) 2016

198. Kumar, Hemanathan: Novel Concepts on The Recovery of By-Products from Alkaline Pulping (61 pp.) 2016
199. Arnedo-Sánchez, Leticia: Lanthanide and Transition Metal Complexes as Building Blocks for Supramolecular Functional Materials (227 pp.) 2016
200. Gell, Lars: Theoretical Investigations of Ligand Protected Silver Nanoclusters (134 pp.) 2016
201. Vaskuri, Juhani: Oppiennätyksistä opetussuunnitelman perusteisiin - lukion kemian kansallisen opetussuunnitelman kehittyminen Suomessa vuosina 1918-2016 (314 pp.) 2017
202. Lundell Jan, Kiljunen Toni (Eds.): 22nd Horizons in Hydrogen Bond Research. Book of Abstracts. 2017
203. Turunen, Lotta: Design and construction of halogen-bonded capsules and cages. (61 pp.) 2017
204. Hurmalainen, Juha: Experimental and computational studies of unconventional main group compounds: stable radicals and reactive intermediates. (88 pp.) 2017
205. Koivistoinen Juha: Non-linear interactions of femtosecond laser pulses with graphene: photo-oxidation, imaging and photodynamics. (68 pp.) 2017
206. Chen, Chengcong: Combustion behavior of black liquors : droplet swelling and influence of liquor composition. (39 pp.) 2017
207. Mansikkamäki, Akseli: Theoretical and Computational Studies of Magnetic Anisotropy and Exchange Coupling in Molecular Systems. 2018, 190 p. (+included articles)